Translational repression and novel functions of Cth2 in the *Saccharomyces cerevisiae* response to iron deficiency

PhD Thesis

Lucía Ramos Alonso

May, 2020

Supervisors:

Dr. Sergi Puig Todolí and Dr. María Teresa Martínez Pastor

Dpto. de Bioquímica y Biología Molecular
Doctorado en Biomedicina y Biotecnología

SERGI PUIG TODOLÍ, Doctor en Ciencias Químicas y Científico Titular del Instituto de Agroquímica y Tecnología de los Alimentos (IATA) del Consejo Superior de Investigaciones Científicas (CSIC),

y MARÍA TERESA MARTÍNEZ PASTOR, Doctora en Ciencias Químicas y Profesora Contratada Doctora en el Departamento de Bioquímica y Biología Molecular de la Universitat de València

INFORMAN:

Que Lucía Ramos Alonso, graduada en Biotecnología por la Universitat de València ha realizado bajo su dirección el trabajo de Tesis Doctoral que lleva por título "Translational repression and novel functions of Cth2 in the *Saccharomyces cerevisiae* response to iron deficiency". Revisado el presente trabajo, expresan su conformidad para la presentación del mismo por considerar que reúne los requisitos necesarios para ser sometido a discusión ante el Tribunal correspondiente, para optar al título de Doctora en Biomedicina y Biotecnología por la Universitat de València.

En Paterna, a 21 de mayo del 2020

Director: Dr. Sergi Puig Todolí Directora: Dra. María Teresa Martínez Pastor

Agradecimientos

Si te paras a pensar, son muchas las personas que, sin querer o sin saberlo, han ayudado a que yo haya sido capaz de escribir esta tesis. Muchas personas cruzan mi mente, profesores del San Felices de Bilibio, IES Marqués de la Ensenada, de atletismo y el Conservatorio de mi pueblo Haro, con la genial forma ser de los jarreros de la que no te puedes deshacer por mucho que pase el tiempo. También mi familia y amigos de siempre, el "pequeño" viaje de 10 años a Valencia, mis Cholais de la carrera, "la Secta" del IATA, el Fluffy Team de Trondheim, el aprendizaje en Marburg, y finalmente mi nueva aventura en Oslo. Todas esas personas han influido en mí, y sin ellas no se hubiesen dado las circunstancias que me han llevado hasta esta tesis. Aunque todo el mundo lo dice, no me resulta tan difícil escribir estos agradecimientos tanto como lo complicado que va a ser no olvidarse de nadie, que no ocupen otras 200 páginas (o la vergüenza que pasaré cuando los leáis).

Gracias Maite y Sergi por esta oportunidad, por ser los directores de tesis y mentores "de libro". Gracias Maite por adaptarte a cualquier situación, por tu pasión por la ciencia, por ser una gran profesora y una persona excepcional, increíblemente generosa, luchadora y trabajadora. Gracias Sergi por estar cada día al pie del cañón, por ayudarme y guiarme siempre, por tu paciencia, por sacar tiempo para todos y ser un científico ejemplar. Gracias a los dos por dejarme vivir la experiencia investigadora, ayudándome y formándome para que pueda continuarla. Con vosotros, siempre hay respuesta y todo es más fácil de lo que parece.

Gracias a todas las personas que han pasado por el Iron Lab. A Raquel por adaptarte a todo, ser respetuosa, trabajadora y estar dispuesta a ayudar. A Ana, por estar siempre alegre y tener una canción de Vetusta Morla preparada. A Tania por abrirte a nosotros y dejarnos descubrir tu sentido del humor. A Pilar por tu ayuda, y a todos los estudiantes que han coincidido conmigo, especialmente Cristina, Rafa, Ana, Quique, Irene y Lidia, por ser tan trabajadores, humildes y una futura generación prometedora. Gracias a ti Anto, porque has sido una de las personas más importantes para mi durante mi tesis, y lo vas a seguir siendo. Por escucharme, ayudarme, compartir tu tiempo, tu casa, por ser divertida y buena persona, la mejor cortadora de fuet y por comprar olivas para tus invitados especiales.

Gracias a los muchos otros laboratorios con los que he tenido relación. Gracias al SBYBI del IATA, que incluyen los laboratorios de Amparo, Eladio,

Roberto y especialmente José Manuel por dejarme empezar con vosotros y apoyarme en mi búsqueda de doctorado. Gracias también a Julio, Vicenta y Carmela del IATA, y a todas las personas que han ido pasando por la tercera: Aurora, María, Clara, Eli, Bea, Bruno, Esther, Laura, David, Robertito, Little Alba, Marcos, Daniela, las dos Andreas, Ceci, Lainy, Thelma, Meli, Flor, Nubia, Vicky... A ti Abraham por tu paciencia y amistad. Gracias a las personas de la Universidad de Valencia, a Carlos por su ayuda con el oxímetro, del grupo de plantas a Lola por las buenas palabras en mis seminarios y a Amparo por la ayuda. También gracias al grupo GFL, especialmente a Paula por su ayuda imprescindible y sugerencias durante esta tesis, y también a José Enrique, Pepe, Fany, María, Adri y Marina, por hacerme siempre un sitio en la bancada y recordarme dónde están las cosas tras cada mudanza.

Thanks to the Iron/Sulfur cluster group of Prof. Roland Lill and the entire Cytobiology team of Marburg (Uli, Nadine, Debi, Marie, Marie-Claire, Martin, Thomas, Vinz, Steffi, Renate, Carina, Ralf, Oliver and Joseph, among others). The personal experience and the techniques learned are invaluable to me. I especially would like to mention Uli, thanks for your help, sincerity and sense of humor. Also, thank you Roland for your sensitivity and scientific advice as well as, together with Martin and Thomas, for your help in the difficult moments.

Como no podía faltar, aunque algunos ya han sido mencionados, quiero agradecer especialmente a "la Secta" todos estos años. Habéis hecho que esta sea una de las etapas más felices de mi vida. **Ojalá a cada sitio que vaya encuentre amigos la mitad de buenos y divertidos que vosotros, y así el lugar nunca importará. Porque os hacéis querer, ¡¡¡ os quiero un montón!!!**

A mi otro lab, el 303. Gracias Fani por estar desde el principio, por acogerme, enseñarme y enseñarme a enseñar, tener la paciencia que se necesita en los inicios y apostar por mí. Sin ti yo no tendría esta tesis. Gracias Sara por ser única, casi jarrera adoptiva (sólo te faltan un par de visitas más), sincera y buena amiga, por hacerme sentir que siempre podré contar contigo (¡y tú conmigo más!). Gracias Ric por tu sentido del humor, por abrirme las puertas de tu casa junto con Sara (y darme unas llaves, un batín, hacerme la cena, servirme más vino…), por no juzgar a nadie, tener esa calma y ser tan divertido. Gracias Ying por sonreír siempre, por aceptarnos y adaptarte tan rápido, por ser tan trabajadora y luchadora. De los laboratorios 307 y 309, el primer sevillano y defensor de Cruzcampo que conozco (seguramente no es casualidad), gracias Javi por tu amistad y por ser buena gente.

Gracias Jiri por los viajes en metro y la época del ron con limón. Adri, mi primera compi de congreso, gracias por animarme y estar conmigo (¿o era yo contigo?) en el lab hasta las tantas. Gracias a los más recientes, a Dolo y Seba, por adaptaros a todo y estar siempre dispuestos a ayudar, a Romain por tu sentido del humor y tus clases de vóley junto a Laura. También gracias Alba (Contreras) y Sonia, dignas sucesoras de las azúcar Romero, gracias Alba por tus visitas guiadas a Requena y por contagiarnos con tu alegría, gracias Sonia por traer aires nuevos, ¡sois geniales! Del único despacho con temperatura constante todo el año, a Laura por tu humor y generosidad, pero sobre todo por defenderme tan heroicamente en el camping, siempre estaré en deuda contigo. Gracias María por ser tan fallera, generosa y siempre acordarte del 302 para el café. Y Miguel, ¡eres único! Estoy esperando a que seas político para votarte en todo, gracias por estar ahí. También, gracias Alba (Yépez) por esa locura contagiosa, por ser tan amorosa y generosa con todos, eres genial. Gracias Ceci por ser la mejor, la mejor madre, la mejor carrot, la animadora de fiestas, gracias por entenderme y acudir siempre a "la llamada", tengo mucha suerte de tenerte. Gracias Walter por abrirte a nosotros, por sumergirnos en el mar y por los momentos divertidos.

Gracias a mis amigos de Haro, en especial a María, Esther, Marta y Nuria, por aguantarme y por acudir a Marburg cuando más lo necesitaba. Gracias a mis Cholais, Carol, Alba y en especial Elva, por convertiros en mi familia todos aquellos años juntas. *Thank you Fluffy Team for changing my life*.

Gracias Peris, por aparecer y añadirle un poco de ruido a mi vida. Gracias por ayudarme, entenderme durante esta tesis y en el *¿y ahora qué?* de después. Gracias por tu amor y tu paciencia, y por dejar que te cuente todo lo que hago en el lab nada más llegar a casa cada día. Contigo todo es más fácil, más divertido, el compañero de viaje perfecto. No podría haberlo hecho sin ti. Gracias por ser como eres. Te quiero.

Por último, gracias a mi familia, a mi abuela María por cuidarme siempre, a mis tíos, en especial Ernesto, mis hermanos Alberto y Mónica, a Kike y a mis sobrinos. Gracias a mi prima Iris y sus padres, por estar conmigo desde siempre. Pero sobre todo, gracias a mis padres (y mi hermana, casi una madre para mi) por todo vuestro apoyo, por darme educación y todo lo que hubieseis querido para vosotros, pero sin quitarme la libertad de tomar mis propias decisiones de qué hacer y dónde hacerlo.

A mis padres

Resumen amplio en castellano

El hierro (Fe) es un micronutriente y cofactor esencial para todos los organismos eucariotas. Las proteínas que incorporan hierro en su estructura lo hacen en forma de grupos hemo, centros Fe/S o centros de hierro y oxígeno, entre otros. Estos cofactores están implicados en numerosos procesos celulares como la respiración, la replicación y reparación del DNA, la biogénesis de ribosomas y la traducción de proteínas, la biosíntesis de ácidos nucleicos y lípidos, la fotosíntesis y el transporte de oxígeno. Pese a ser un metal abundante en la corteza terrestre, su forma oxidada Fe^{3+} es la más frecuente en un entorno oxidante y resulta insoluble a pH fisiológico. Esto hace de la deficiencia de hierro o anemia ferropénica el desorden nutricional más extendido del planeta. Alteraciones en la homeostasis del hierro también provocan hemocromatosis, o algunas enfermedades neurodegenerativas graves como la ataxia de Friedrich, y contribuyen al cáncer. Además, la deficiencia de hierro también provoca clorosis en los cultivos agrícolas, afectando tanto su producción como su valor nutricional. A pesar de ser un nutriente esencial, la presencia de hierro en exceso es tóxica para las células ya que participa en reacciones Fenton. Estas reacciones generan radicales hidroxilo (·OH) a partir del peróxido de hidrógeno (H_2O_2), los cuales pueden oxidar proteínas, DNA o lípidos si la maquinaria de detoxificación de especies reactivas del oxígeno (ROS) se ve sobrepasada. El estudio de los mecanismos que regulan la incorporación, almacenamiento y utilización del hierro en *Saccharomyces cerevisiae* resulta de gran importancia para entender la homeostasis del hierro en eucariotas. Éstos son el primer paso para el posterior desarrollo de tratamientos contra enfermedades relacionadas con el hierro o la mejora de cultivos causantes de graves pérdidas económicas.

El mecanismo de percepción de la deficiencia de hierro en eucariotas se sitúa en la síntesis de los centros Fe/S, que tiene lugar en la mitocondria. En la levadura *Saccharomyces cerevisiae*, utilizado como organismo modelo eucariota, la mutación de alguno de los componentes de la maquinaria mitocondrial de síntesis o exportación de centros Fe/S provoca, independientemente del hierro citosólico, la activación del regulón de hierro. En *S. cerevisiae* el regulón de hierro es un conjunto de unos 30 genes activados por los factores transcripcionales Aft1 y Aft2.

Aft1/Aft2 se unen específicamente a secuencias FeRE (*iron responsive elements*), PyPuCACCCPu (Py: pirimidina; Pu: purina), situadas en los promotores de los genes del regulón. Dichos genes codifican proteínas implicadas en la adquisición de hierro extracelular, la movilización y reciclaje del hierro intracelular y la remodelación metabólica de procesos dependientes de hierro. Esta última función, llevada a cabo principalmente por las proteínas Cth1 y Cth2, optimiza la utilización del hierro en aquellos procesos que son más esenciales en condiciones de baja biodisponibilidad de hierro.

Cth1 y Cth2 pertenecen a la familia de proteínas tipo tristetraprolina (TTP). Esta familia se caracteriza por tener un dominio conservado de dos dedos de zinc en tándem $Cx_8Cx_5Cx_3Hx_{18}Cx_8Cx_5Cx_3H$ (TZF, *Tandem Zinc-Finger*) que le permite unirse a secuencias ricas en adenina y uracilo (AREs, *AU-Rich Elements*) situadas en los extremos 3' no traducibles (3'-UTR, *3'-UnTranslated Region*) de algunos RNAs mensajeros (mRNAs). Tras la unión específica de mRNAs en el núcleo, Cth1/Cth2 promueven la degradación de éstos en el citoplasma. Éstos mRNAs diana de Cth1 y Cth2 codifican proteínas que contienen hierro o están implicadas en procesos que consumen hierro. Cth1 y Cth2 provocan la degradación de mRNAs que codifican proteínas de: la cadena de transporte de electrones (ETC, *Electron Transport Chain*), el ciclo de los ácidos tricarboxílicos (TCA, *Tricarboxylic acid cycle*), la ruta de biosíntesis de hemo, el metabolismo de lípidos, la síntesis de muchos aminoácidos, el transportador de hierro a la vacuola o la proteína Rli1 implicada en la biogénesis de ribosomas. Además, Cth1 y Cth2 se autorregulan, ya que sus mRNAs contienen secuencias ARE. A pesar de que Cth1 y Cth2 tienen funciones parcialmente solapantes, el mutante *cth2Δ*, y no el mutante *cth1Δ,* presenta un defecto de crecimiento en deficiencia de hierro, que es exacerbado en el doble mutante *cth1Δcth2Δ.* Además, mientras que *CTH1* se expresa de manera transitoria durante el inicio del crecimiento en deficiencia de hierro, *CTH2* se expresa en deficiencias más severas alcanzando niveles de expresión más elevados y constantes. Por ello, muchos procesos están principalmente regulados por Cth2, mientras que Cth1 tiene un papel secundario en la remodelación metabólica de procesos dependientes de hierro.

La degradación citoplasmática de mRNAs promovida por Cth2 se produce en los cuerpos de procesamiento (*P-bodies*) en sentido 5'-3'. Además, requiere de la RNA helicasa Dhh1, que activa la eliminación de la caperuza (*decapping*) a través de Dcp1 y Dcp2. También se requiere de la exonucleasa citoplasmática Xrn1. Dhh1 también está implicada en reclutar la maquinaria de deadenilación para el acortamiento de la cola 3' poli(A) y en la propia formación de los *P-bodies*. En mamíferos, las proteínas de la familia TTP además de promover la degradación de sus mRNAs diana, también reprimen la traducción de los mismos, incluido el propio mRNA de TTP. El homólogo de Dhh1 en mamíferos, RCK/p54, está implicado en la represión de la traducción de las dianas de TTP.

Uno de los procesos que requieren hierro es la traducción global de proteínas. Los genes implicados en la biosíntesis de varios aminoácidos y la proteína con centros Fe/S Rli1, esencial en la biogénesis y reciclado de ribosomas, son dianas de Cth2 a nivel de mRNA. Además, los niveles de rRNAs, tRNAs y otros mensajeros que codifican proteínas ribosómicas, disminuyen drásticamente durante la escasez de hierro debido a la inactivación de la ruta TOR. Por último, en deficiencia de hierro se produce un incremento en la fosforilación de la subunidad α del factor de inicio de la traducción eIF2, que ha sido descrito como una señal de bloqueo del inicio de la traducción global. Estos resultados previos indican que probablemente el inicio de la traducción global estaría afectado por la deficiencia de hierro.

La respiración mitocondrial es otro de los procesos que requieren un gran aporte de hierro a través de la ETC y del TCA y que no son esenciales en deficiencia de hierro en esta levadura. Además, la respiración mitocondrial es la responsable de generar niveles basales de ROS, principalmente a través de los complejos I y III de la cadena de transporte de electrones. Muchos de los mRNAs diana de Cth2 se encuentran en estas dos rutas. Sin embargo, otros procesos se encargan de disminuir la expresión de los genes implicados en respiración. Este es el caso de los factores transcripcionales Hap1 y el complejo Hap2-5. Éstos dependen de hemo y oxígeno para activar los genes de respiración, y también pueden verse negativamente afectados por el estrés oxidativo. Por otro lado, la expresión de *CTH2* ha sido descrita en condiciones de estrés por H_2O_2. El papel de Cth2 en estas

condiciones es la de regular la expresión de algunos miembros del regulón de hierro, además de reducir el potencial de membrana en la mitocondria, que a su vez indica un papel de Cth2 en el control de los niveles de ROS mitocondriales.

Por último, otro de los procesos esenciales que requiere hierro es la síntesis de dNTPs por parte de la enzima ribonucleótido reductasa (RNR). Su actividad está altamente regulada y restringida a situaciones en las que se requieren mayores niveles de dNTPs (fase S del ciclo celular, reparación del DNA o bajo condiciones de estrés genotóxico) para evitar el aumento de las tasas de mutación, los errores en la reparación del DNA o la aparición de tumores. La enzima RNR está formada por una subunidad grande con el sitio catalítico codificada por los genes *RNR1* y *RNR3*. Puede ser un homodímero Rnr1-Rnr1 o un heterodímero Rnr1-Rnr3. La subunidad pequeña, que es la que contiene el radical tirosilo oxo-dihierro, es un heterodímero codificado por los genes *RNR2* y *RNR4*. A pesar de que Rnr2 es la única subunidad que contiene el cofactor de hierro, todas las subunidades son reguladas en condiciones de deficiencia de hierro. En cuanto a la subunidad codificada por el gen *RNR3,* se expresa a muy bajos niveles en condiciones normales. Sin embargo, la expresión de *RNR3* se ve altamente inducida en condiciones de estrés replicativo o daños en el DNA, a pesar de que el mutante *rnr3Δ* no presenta un fenotipo afectado en estas condiciones. La inducción de dicho gen se produce a través de la ruta de quinasas Mec1–Rad53–Dun1. A pesar de los estudios sobre la regulación de la expresión de *RNR3* en condiciones de daños al DNA, pocos se han centrado en su regulación en deficiencia de hierro.

La finalidad de esta tesis doctoral es estudiar nuevos mecanismos moleculares implicados en la respuesta a la deficiencia de hierro en *S. cerevisiae*, centrándose en la identificación de rutas que promuevan la represión de la traducción global, así como el propio papel de Cth2 en la represión de la traducción, la respiración o la regulación de *RNR3* en deficiencia de hierro. Para ello, esta tesis ha sido dividida en cuatro capítulos que se corresponden con los siguientes objetivos propuestos:

1. Determinar las rutas y mecanismos moleculares implicados en la represión global de la traducción en respuesta a la deficiencia de hierro y cómo mRNAs específicos se ven afectados.

2. Dilucidar el papel de la proteína Cth2, de sus dominios conservados y de las secuencias ARE, en la represión de la traducción de mRNAs específicos durante la deficiencia de hierro.
3. Determinar la contribución de Cth2 en la respiración mitocondrial y en sus correspondientes actividades enzimáticas en suficiencia y deficiencia de hierro.
4. Caracterizar los mecanismos moleculares que inducen la expresión de *RNR3* en condiciones prolongadas de deficiencia de hierro.

La metodología empleada para llevar a cabo el estudio de estos objetivos propuestos incluye: (i) técnicas microbiológicas para la construcción de cepas y plásmidos específicos, así como su fenotipado en diferentes condiciones y medios de crecimiento; (ii) técnicas moleculares para el estudio y cuantificación del DNA, como la inmunoprecipitación de cromatina; para el estudio del RNA y su traducción (RT-qPCR y fraccionamiento de polisomas); y para el estudio de proteínas, como Western blot o inmunoblot; (iii) ensayos de actividad β-galactosidasa y de consumo de oxígeno; y (iv) determinación de actividades enzimáticas dependientes de hierro a partir de lisados celulares o mitocondrias purificadas.

Los resultados del capítulo 1 se centran en la respuesta traduccional global en condiciones de deficiencia de hierro. En este capítulo se vio mediante perfiles de polirribosomas como la traducción global se reprime gradualmente con el crecimiento bajo condiciones limitantes de hierro. La cepa W303 mostró una proporción polisomas/monosoma 80S (P/M) ligeramente disminuida después de 3 horas de crecimiento en deficiencia de hierro (-Fe), comparado con la situación de suficiencia de hierro (+Fe). Sin embargo, tras 6 horas de crecimiento en -Fe, la reducción P/M fue mucho más drástica. Dichos experimentos de fraccionamiento de polisomas empleando cicloheximida, junto con el aumento de la señal en la fracción correspondiente al pico 80S, indicaron que la represión global se produce al inicio de la traducción. El análisis de la distribución de mRNAs específicos en el perfil general de polirribosomas permitió diferenciar diferentes estados traduccionales pese a la represión global en -Fe. Mientras que la traducción del mRNA de *ACT1* apenas se vio afectada, los mRNAs de *RPS16B* y *RPL3* (proteínas

ribosómicas) se vieron desplazados a la fracción 80S, apoyando la represión traduccional global. Por otro lado, el mRNA de *GCN4* vio incrementada su presencia en fracciones de polisomas en -Fe. Esto sugirió una mayor traducción de *GCN4* en -Fe. Sin embargo, los resultados de la actividad β-galactosidasa utilizando el gen *lacZ* bajo el control del promotor *GCN4*, mostraron solamente una ligera inducción en -Fe comparada con la gran inducción en condiciones de deficiencia de aminoácidos. Resultados previos mostraron una mayor fosforilación del factor traduccional eIF2α en -Fe. En este trabajo se mostró cómo eIF2α se fosforila en -Fe de forma dependiente de Gcn2 y Gcn1. Una cepa mutante en la serina 51 de eIF2α mostró una significativa recuperación del ratio P/M durante la deficiencia de hierro. Además, los mutantes *gcn2Δ* y *gcn1Δ* también mostraron una gran recuperación de la traducción en deficiencia de hierro comparado con una cepa salvaje. Por otro lado, la represión global de la traducción dependiente de Gcn2 resultó ser transitoria ya que tiempos más prolongados de la deficiencia de hierro (12 horas en una cepa BY4741) mostraron ratios P/M disminuidos tanto en el mutante *gcn2Δ* como en la cepa salvaje. Con estos resultados, las conclusiones generales de este capítulo son las siguientes: (i) Durante el progreso de la deficiencia de hierro se reprime de manera gradual el inicio de traducción global; (ii) durante la deficiencia de hierro, la quinasa Gcn2 reprime el inicio de la traducción global fosforilando la serina 51 de eIF2α de manera dependiente de Gcn1, e induce la traducción de *GCN4*.

Los resultados del capítulo 2 demuestran el papel de Cth2 a través de sus TZFs en la represión traduccional de mRNAs específicos con secuencias ARE durante la deficiencia de hierro. Se realizaron perfiles de polirribosomas en los que se determinó la distribución de mRNAs concretos, además de llevarse a cabo cálculos de la eficiencia de traducción de ciertos mRNAs. La traducción del mRNA de *SDH4* disminuyó específicamente en deficiencia de hierro mientras que el mRNA de *ACT1* permaneció asociado a fracciones de polisomas. La represión traduccional de *SDH4* resultó ser dependiente de los AREs de su mensajero y de los TZFs de la proteína Cth2. Además, la propia traducción del mRNA de *CTH2* se vio reducida en deficiencia de hierro de forma dependiente a los AREs de su mRNA y los TZFs de su proteína. Mediante el análisis de la distribución en perfiles de

polirribosomas de otros mRNAs diana de Cth2 con AREs (*CCP1*, *HEM15* and *WTM1*), se mostró que Cth2 también reprime la traducción de éstos durante la escasez de hierro. Tras demostrarse la necesidad de tener intactos el dominio TZF de Cth2 y los AREs de los mRNAs diana para la represión de su traducción, se estudió la implicación de otros dominios de Cth2 menos conservados. Se estudió la implicación de dos regiones conservadas de Cth2 (CR1 y CR2), pertenecientes al extremo amino terminal, y una región del extremo carboxilo terminal (CR3), mediante diferentes construcciones truncadas de Cth2. Las construcciones de Cth2 truncadas en los 89 y 170 primeros aminoácidos (CR1 y CR2, respectivamente) del extremo amino mostraron, mediante la distribución del mRNA de *SDH4* en el perfil de polirribosomas y cálculos de eficiencia de traducción, que dicho extremo amino terminal de Cth2 está implicado tanto en la degradación de mRNAs como en la represión de la traducción. Sin embargo, la construcción de Cth2 truncada en los 52 últimos aminoácidos del extremo carboxilo no presentó defectos en la degradación de mensajeros, pero sí en la represión de la traducción. Además, dicho truncado *CTH2ΔC52* presentó un fenotipo negativamente afectado en el crecimiento en condiciones de deficiencia de hierro, y mayores niveles de proteínas Aco1, Hem15 y Bio2. Por último, la predicción de la estructura tridimensional de Cth2 mostró que el dominio carboxilo podría interaccionar directamente con el dominio TZF, diferenciándose así del dominio carboxilo no estructurado de TTP. Las conclusiones generales de este capítulo son las siguientes: (i) En respuesta a la deficiencia de hierro, Cth2 promueve la represión traduccional de mRNAs con secuencias ARE en un proceso que requiere de ambos, la integridad del dominio TZF y de los AREs; (ii) ambos dominios, amino y carboxilo terminal, de Cth2 contribuyen a la represión de la traducción de mRNAs, pero solo el dominio amino terminal es responsable de la degradación de mRNAs en respuesta a la deficiencia de hierro; (iii) el dominio carboxilo terminal de Cth2 es fisiológicamente relevante en condiciones de deficiencia de hierro.

Por otro lado, los resultados del capítulo 3 demuestran el papel de Cth2 en la regulación de la respiración celular en respuesta a la deficiencia de hierro. Mediante medidas del consumo de oxígeno, se vio que éste era significativamente menor en respuesta tanto a la deficiencia de hierro nutricional como genética, esta última observada en la cepa *fet3Δfet4Δ* mutante para los sistemas de transporte de

hierro de alta y baja afinidad. Sin embargo, esta disminución en la velocidad del consumo de oxígeno en deficiencia de hierro, y por tanto de la respiración celular, se produjo independientemente de Cth2. A pesar de ello, tanto la sobreexpresión de Cth2 como de Cth1, fueron capaces de reprimir el consumo de oxígeno de manera dependiente de sus TZFs en condiciones de suficiencia de hierro. En la misma línea, la expresión constitutiva del regulón de hierro mediante la mutación de la cisteína 291 de Aft1 (alelo *AFT1-1UP*) también reprimió el consumo de oxígeno en suficiencia de hierro, además de disminuir la capacidad de crecimiento en un medio con etanol y glicerol como fuentes de carbono no fermentables. En ambos casos, la eliminación del gen *CTH2* rescató tanto el consumo de oxígeno como el fenotipo de crecimiento. Estos resultados confirmaron la capacidad de la proteína Cth2 de participar en la represión de la respiración mitocondrial, aunque probablemente en deficiencia de hierro varios mecanismos redundantes repriman la respiración, y por ello se enmascare el efecto específico de Cth2. Varias actividades enzimáticas mitocondriales dependientes de hierro fueron determinadas con el fin de indagar más en la función de Cth2 de reprimir la respiración. Además de esto, también se determinó la actividad de la proteína Leu1 de la ruta de biosíntesis de leucina, la cual contiene centros Fe/S. Se confirmó la capacidad de Cth2 de inducir la degradación del mRNA de *LEU1* tanto en suficiencia de hierro (tras la sobreexpresión de Cth2) como en deficiencia de hierro. En cuanto a los niveles de proteína total de Leu1, se mostraron igualmente disminuidos tras sobreexpresar Cth2 en suficiencia de hierro como en condiciones de deficiencia. Este resultado se reflejó en la correspondiente bajada de actividad enzimática en +Fe. Sin embargo, la bajada de actividad en -Fe fue tal que se redujo más allá de los límites de sensibilidad del experimento, por tanto, no pudo determinarse el efecto de Cth2 en deficiencia de hierro sobre la actividad de Leu1. Respecto a las actividades enzimáticas relacionadas con la respiración mitocondrial, se determinó la actividad aconitasa, dependiente de hierro y perteneciente al ciclo de los ácidos tricarboxílicos. En este caso, el efecto de sobreexpresión de Cth2 en suficiencia de hierro mostró claramente la disminución tanto en niveles de mRNA de *ACO1*, como en cantidad de proteína Aco1 y su respectiva actividad. El papel de Cth2 en deficiencia de hierro se reflejó tanto a nivel de mRNA como de proteína. Sin embargo, la actividad enzimática aconitasa,

ya disminuida en deficiencia de hierro, sólo se vio ligeramente más reducida en células con *CTH2.* Los resultados obtenidos con las actividades enzimáticas de la cadena de transporte de electrones resultaron más determinantes. La actividad succinato deshidrogenasa, perteneciente al ciclo de los ácidos tricarboxílicos y complejo II de la cadena de transporte de electrones, se midió de manera individual y junto con la actividad citocromo *c* reductasa del complejo III. En ambos casos, los niveles de varios mRNAs con AREs que codifican algunas de las subunidades de los complejos se vieron claramente disminuidos, tanto por la sobreexpresión de Cth2 en +Fe como de manera dependiente de Cth2 en -Fe. Igualmente, dicho efecto se reflejó en las actividades enzimáticas del complejo II y de los complejos II+III, tanto en suficiencia como en deficiencia de hierro. Estos resultados demostraron el papel de Cth2 en la represión de los complejos II y III de la cadena de transporte de electrones. Sin embargo, los resultados relacionados con la actividad citocromo *c* oxidasa (complejo IV) fueron diferentes en ambos casos. La expresión constitutiva de Cth2 en suficiencia de hierro no afectó a la actividad del complejo IV, a pesar de los múltiples mRNAs diana de Cth2 que codifican algunas subunidades del complejo. Además, en deficiencia de hierro, aunque se apreció una bajada general en la actividad, ésta se vio respaldada por Cth2. Tras comprobarse que los niveles de mRNA de *COX4* y *COX6* efectivamente se correspondían con los resultados esperados, al tratarse de dianas de Cth2 con AREs, se determinaron los niveles de los mRNAs *COX1, COX2* y *COX3*. Estos tres genes codificados por el genoma mitocondrial constituyen el núcleo del complejo IV. En los tres casos se vieron incrementados sus niveles de mRNA en deficiencia de hierro independientemente de Cth2, y solamente en el caso del mRNA de *COX1* sus niveles fueron mayores en células que expresaban *CTH2* en deficiencia de hierro. En la misma línea, tras medir los niveles de proteína Cox1 en deficiencia de hierro, dichos niveles resultaron mayores en células con *CTH2* respecto a células *cth2Δ.* Las conclusiones generales de este capítulo son las siguientes: (i) La respiración mitocondrial se ve comprometida en deficiencia de hierro independientemente de Cth2, sin embargo, la expresión constitutiva del regulón de hierro reprime la respiración y disminuye la capacidad de crecimiento en fuentes de carbono no fermentables a través de Cth2; (ii) la sobreexpresión de Cth2 en suficiencia de hierro provoca la disminución, no solo del consumo de oxígeno, sino

también de varias actividades enzimáticas dependientes de hierro como Leu1, aconitasa y los complejos II y III de la cadena de transporte de electrones; (iii) Cth2 promueve la actividad del complejo IV de la cadena de transporte de electrones en respuesta a la deficiencia de hierro.

Los resultados del capítulo 4 demuestran que la inducción de la expresión del gen *RNR3* se produce a nivel transcripcional en condiciones prolongadas de deficiencia de hierro. Tras determinar el pico de expresión de *RNR3* a las 15 horas de deficiencia de hierro en condiciones de crecimiento exponencial, se comparó su expresión en -Fe con las condiciones de estrés replicativo y daños al DNA. El crecimiento en presencia de hidroxiurea, metil metanosulfonato o 4-nitroquinolina N-óxido produjo niveles similares de mRNA y proteína Rnr3 respecto a los producidos tras las 15 horas de deficiencia de hierro. De manera similar a estas condiciones de estrés replicativo o genotóxico, las quinasas Rad53 y Dun1 también resultaron implicadas en la inducción de *RNR3* en deficiencia de hierro. Además, se demostró que dicha inducción se produce a nivel transcripcional por la mayor unión de la RNA polimerasa II al promotor de *RNR3*. También se determinó que la presencia de Cth2 es necesaria para la inducción transcripcional del gen, solo en condiciones de deficiencia de hierro prolongadas y de manera independiente de la quinasa Dun1. Además, se vio que el papel de Cth2 en la inducción de *RNR3* en deficiencia de hierro se produce a través de sus TZFs y que es predominante respecto a la función de Cth1. Tras analizar los niveles de algunos mRNAs que codifican proteínas que son represoras directas o indirectas del promotor de *RNR3*, se determinó que los mRNAs de *CRT1* y *ROX1* están regulados por Cth2 en -Fe. Probablemente, el mRNA de *CRT1* sea una diana directa de Cth2 en deficiencia de hierro ya que posee un ARE casi completo. Por otro lado, el mRNA de *ROX1*, aunque se vio regulado de manera significativa por Cth2 tras 15 horas en deficiencia de hierro, no posee ningún ARE o similar y por tanto no sería una diana directa de Cth2. Además, el mRNA de *HOS1* con AREs resultó ser una diana clara de Cth2 en condiciones prolongadas de deficiencia de hierro. *HOS1* codifica para una histona deacetilasa empleada por el complejo represor de la transcripción Ssn6–Tup1. El complejo Ssn6–Tup1 es reclutado por Crt1 y Rox1 a los promotores de algunos genes, entre ellos *RNR3*. A pesar de esto, es probable que Cth2 también desreprima el promotor de *RNR3* independientemente de Rox1 y Crt1. La mutación

de *CTH2* en el triple mutante *rox1Δmot3Δcrt1Δ* aún provocó un defecto adicional en la inducción de *RNR3*. Por último, se determinó que Rnr3 es fisiológicamente relevante en deficiencia de hierro. Con estos resultados, las conclusiones generales de este capítulo son las siguientes: (i) *RNR3* es fisiológicamente relevante y se induce transcripcionalmente en respuesta a la deficiencia de hierro prolongada alcanzando niveles de mRNA y proteína comparables a aquellos alcanzados bajo condiciones de estrés genotóxico o replicativo; (ii) las quinasas Rad53 y Dun1 están implicadas en la inducción de *RNR3* bajo condiciones prolongadas de deficiencia de hierro. Además, Cth2 contribuye a la inducción de *RNR3* independientemente de Dun1, a través de sus TZF y sólo bajo condiciones prolongadas de deficiencia de hierro.

Table of contents

Abstract

Abstract

Iron is an essential micronutrient for all eukaryotes because of its redox properties. It participates as a cofactor in a wide range of biological processes, including protein translation, mitochondrial respiration (Krebs cycle and electron transport chain (ETC)) and DNA replication. The model organism *Saccharomyces cerevisiae* responds to iron deficiency by activating the iron acquisition and recycling systems, and by remodeling cellular metabolism to promote iron utilization in specific processes at the expense of others. The tandem zinc finger (TZF)-containing protein Cth2 plays an important role in prioritizing iron by promoting the degradation of multiple mRNAs containing A/U-rich elements (AREs), including the *CTH2* mRNA itself that is autoregulated. In this thesis, we identified and characterized new mechanisms involved in the global translational repression and novel functions of Cth2 in response to iron starvation. Our results with polysome fractionation experiments demonstrate that during the progress of iron deficiency the eIF2α/Gcn2 pathway is involved in the general repression of translational initiation. The Gcn2 kinase specifically phosphorylates serine 51 of eIF2α in a Gcn1-dependent manner, causing a slight induction of *GCN4* translation when iron is scarce. The Gcn2 activation by uncharged tRNAs and TORC1 inactivation during the iron deficiency is discussed. Besides, we show a role played by Cth2 in translational inhibition of several ARE-containing mRNAs during iron deficiency. Both the Cth2 TZF-domain as well as the AREs within *SDH4* (subunit of succinate dehydrogenase) and *CTH2* mRNAs are essential for translational repression. Besides, other mRNAs are translationally repressed by Cth2, suggesting a Cth2 general role on inhibition of translation of ARE-containing mRNAs. Our results also demonstrate that while the amino-terminal domain (NTD) of Cth2 is important for both mRNA turnover and translational inhibition functions, its carboxy-terminal domain (CTD) is only involved in translational repression. Importantly, Cth2 CTD is physiologically relevant during iron-deficient conditions. Two novel Cth2 functions under iron deficiency include the regulation of mitochondrial respiration and the *RNR3* catalytic subunit of the iron-dependent ribonucleotide reductase (RNR) enzyme responsible of dNTP synthesis. The overexpression of *CTH2* under iron sufficiency decreases respiration (measured by the oxygen consumption) as well as several iron-dependent enzymatic activities,

including Leu1, aconitase (from Krebs cycle) and complex II and III of the ETC, while the complex IV activity is unaffected. Under iron deficiency, oxygen consumption decreases regardless Cth2, despite the decrease in complex II and III activities of the ETC. Interestingly, under iron starvation Cth2 contributes to a better complex IV activity, probably by increasing Cox1 protein levels. Finally, *RNR3* has been described to be highly expressed under genotoxic or replication stress conditions by the Mec1–Rad53–Dun1 checkpoint kinase pathway. However, *RNR3* function is not clear as its paralog *RNR1* was described to be the major isoform of the catalytic subunit of RNR. Our results suggest a higher *RNR3* expression under long-term iron deficiency comparable to that observed under those stresses. Besides, we demonstrate the participation of Cth2 (through its TZF-domain) and Dun1 in the transcriptional induction of *RNR3* under long-term iron-deficient conditions. And importantly, unlike other stresses, *RNR3* is physiologically relevant when iron is scarce.

Glossary

+Fe – Iron-sufficient condition

-Fe – Iron-deficient condition

3-AT – 3-aminotriazole

4-NQO – 4-nitroquinoline N-oxide

AMD – ARE-mediated mRNA decay

AREs – Adenosine/Uridine Rich Elements

BPS – Bathophenanthrolinedisulfonic acid

CFUs – Colony Forming Units

ChIP – Chromatin immunoprecipitation

CHX – Cycloheximide

CIA – Cytosolic iron-sulfur protein assembly machinery

CR – Conserved Region

CTD – Carboxy-terminal domain

COX – Cytochrome *c* oxidase, complex IV

dNTPs – Deoxyribonucleoside triphosphates

eIF2 – Translation initiation factor

eIF2B – Guanine nucleotide exchange factor

ETC – Electron Transport Chain

ESR – Environmental Stress Response

FAC – Ferric ammonium citrate

FAS – Ferrous ammonium sulfate

FeRE – Iron Responsive Element

Fz – 3-(2-Pyridyl)-5,6-diphenyl-1,2,4-triazine-4′,4′′-disulfonic acid sodium (ferrozine)

gDNA – Genomic DNA

HU – Hydroxyurea

ISC – Iron-sulfur cluster assembly/export machinery

IREs – Iron-responsive elements

IRPs – Iron regulatory proteins

MMS – Methyl methanesulfonate

mRNA – messenger RNA

mtDNA – mitochondrial DNA

ND – Not Detectable

NTD – Amino-terminal domain

nts – Nucleotides

OD – Optical Density

OXPHOS – Oxidative phosphorylation

P-bodies – Processing bodies

PCR – Polymerase chain reaction

P/M – polysomes/monosome ratio

qPCR – Quantitative PCR

RiBis – Ribosome biogenesis

RNPs – Ribonucleoproteins

RNR – Ribonucleotide reductase

ROS – Reactive Oxygen Species

RPs – Ribosomal proteins

rpm – Revolutions per minute

RTG – Retrograde pathway

RT-qPCR – Quantitative reverse transcription PCR

SC – Synthetic Complete medium

SC minus – Synthetic Complete lacking specific requirements

SD – Minimum medium

TCA cycle– Tricarboxylic acid cycle

TNFα - Tumor necrosis factor alpha

TTP – Tristetraprolin

TZFs – Tandem Zinc Fingers

UTR – Untranslated region

uORF – Upstream open reading frame

WHO – World Health Organization

Introduction

Iron is an essential element for all eukaryotic organisms. Its redox activity and its ability to bind to multiple ligands makes iron an essential cofactor in numerous biological processes. Iron-containing proteins participate in many cellular processes including respiration, DNA replication and repair, ribosome biogenesis, translation, photosynthesis, biosynthesis of lipids and oxygen transport. Despite all of these iron-dependent processes, high iron concentrations can lead to cytotoxicity in living organisms

Iron is the fourth most abundant element of the Earth crust. The anoxic conditions of the primitive atmosphere made of the reduced ferrous iron form (Fe^{2+}) the main cofactor of many proteins. In fact, the oldest fossilized microorganisms (3.7-4.3 million years old and close to the Earth's formation) are thought to be iron-oxidizing bacteria (Dood et al., 2017). However, the Earth's change to an oxidizing atmosphere increased the ferric form (Fe^{3+}) that is highly insoluble at physiological pH. This low bioavailability of iron makes of the iron deficiency anemia the most common nutritional disorder worldwide according to the World Health Organization (WHO), affecting two billion people, particularly women and children (reviewed by Chaparro & Suchdev, 2019; Means, 2020). Iron deficiency anemia has several consequences for humans: reduced physical and growth capacity, fatigue, susceptibility to infections, impaired neurological development, premature birth or mortality. Besides, defects in human iron homeostasis have been related with severe disorders such as Friedreich's ataxia, myopathies and encephalomyopathies, hemochromatosis, multiple mitochondrial dysfunction syndromes, higher risk of pathogenesis and cancer (reviewed by Stehling et al., 2014; Muckenthaler et al., 2017). Iron deficiency in agriculture is also a concern with an important economic impact because it induces chlorosis and reduces photosynthesis, affecting both the yield and the nutritional value of crops (reviewed by Puig et al., 2007; Zhang et al., 2019a).

For these reasons, studying the molecular mechanisms that regulate iron metabolism is important for dealing with iron nutritional disorders, the development of medical treatments and the understanding of physiological alterations of significant economic impact.

1. The biological role of iron

As iron can easily oscillate between its two redox states (ferrous Fe^{2+} and ferric Fe^{3+} forms) it participates as cofactor in several oxido-reductase and electron transfer reactions. There are three main cofactors that contain iron centers:

- **Heme groups**: ferrous iron is coordinated with protoporphyrin IX. Heme forms the prosthetic group of many oxygen-related proteins such as hemoglobin (oxygen sensing and transport in vertebrates), myoglobin (oxygen transport and storage in muscle tissues), cytochromes (electron transfer reactions in respiratory and photosynthetic electron transport chains) or heme-containing catalases and peroxidases (catalyzing and diminishing the reactive oxygen species, ROS). In eukaryotes, the initial and final step in the biosynthesis of heme are located in mitochondria (reviewed by Mühlenhoff et al., 2015). The budding yeast *Saccharomyces cerevisiae* senses oxygen indirectly through the concentration of heme, and at the same time, heme-synthesis is oxygen-dependent as it requires oxygen as a substrate.

- **Iron-sulfur (Fe/S) clusters**: [2Fe-2S], [4Fe-4S] and [3Fe-4S] clusters are involved in the electron transport chain (ETC), the tricarboxylic acid (TCA) cycle, photosynthesis, protein translation and ribosome biogenesis (through the yeast Rli1 Fe/S-protein) (Kispal et al., 2005; Yarunin et al., 2005), DNA synthesis and repair (Puig et al., 2017), telomere length regulation as well as heme, biotin, lipoic acid and several amino acid biosynthetic pathways. Eukaryotic Fe/S cluster synthesis and assembly studies have been mainly performed in yeast. Fe/S clusters are synthetized by three well conserved, from yeast to human, machineries: the essential mitochondrial iron-sulfur cluster (ISC) assembly and export machineries, and cytosolic iron-sulfur protein assembly (CIA) machinery (reviewed by Lill et al., 2015). The synthesis starts in the mitochondria with the ISC assembly machinery. Then, an unknown sulfur-containing compound, named X-S, is exported to the cytoplasm by the Atm1 transporter (the main member of the ISC export machinery). Finally, the CIA machinery and the Grx3/4 glutaredoxins assemble the nuclear and cytosolic Fe/S proteins (Mühlenhoff et al., 2010).

- **Oxo-diiron (Fe-O-Fe) centers**: oxo-diiron proteins participate in the formation of biological membranes through the sterol metabolism and fatty acid metabolism. The essential fatty acid desaturase Ole1 in *S. cerevisiae* contains an Fe-O-Fe center. Also, the class Ia of ribonucleotide reductases that catalyze the rate-limiting step of dNTP synthesis use oxo-diiron centers as essential cofactors (see section 5).

2. Iron sensing and responses to changes in iron bioavailability in *Saccharomyces cerevisiae*

Despite iron is essential for all eukaryotes, it can participate in Fenton reactions and produce hydroxyl radicals (·OH) from hydrogen peroxide (H_2O_2). Therefore, high iron levels can generate ROS, and if the ROS detoxification machinery is not sufficient, cells can be damaged at DNA, lipid and protein levels. For these reasons, living organisms tightly regulate iron acquisition, storage and utilization. *S. cerevisiae* has been used as a model organism to study iron homeostasis regulation in eukaryotes in response to fluctuations in iron bioavailability.

ISC assembly and export machineries are directly involved in iron sensing in yeast and higher eukaryotes. The X-S molecule exported to the cytoplasm by the mitochondrial Atm1 (human ABCB7) transporter is crucial in communicating the iron status to cells and in regulating iron homeostasis. Cells with defective ISC machineries accumulate iron within mitochondria (Kispal et al., 1999) and induce the extracellular iron uptake systems (Chen et al., 2004; Rutherford et al., 2005; Hausmann et al., 2008). The X-S molecule is involved in post-transcriptional regulation of iron homeostasis in higher eukaryotes (through the iron regulatory proteins, IRPs) and transcriptional regulation of iron homeostasis in yeast (through Aft1/Aft2 and Yap5, see below) (reviewed by Mühlenhoff et al., 2015; Gupta & Outten, 2020).

Briefly, in mammals the IRP1 and IRP2 proteins bind the iron-responsive elements (IREs) in the untranslated regions (UTRs) of specific mRNAs related to iron homeostasis when iron is scarce. For example, when iron levels are low, the

IRP-IRE binding to the 5'UTR of ferritin mRNA (encoding the iron excess storage protein) inhibits its translation, and the binding to the 3'UTR of transferrin receptor-1 mRNA (encoding the receptor of the plasma iron transport protein) increases its mRNA stability and translation. In this manner, the iron storage is repressed and iron uptake increased under iron deficiency (reviewed by Anderson et al., 2012; Bayeva et al., 2013; Mühlenhoff et al., 2015). Under high iron conditions, IRP1 binds a [4Fe-4S] cluster and cannot adopt the conformation that allows IRE binding. In this way, in mammals the CIA machinery is also involved in iron homeostasis, as the CIA components are in charge of introducing the Fe/S cluster into IRP1. On the other hand, IRP2 does not bind any Fe/S cluster but it is also regulated in an iron-dependent manner and degraded by the proteasome under high iron conditions (Salahudeen et al., 2009; Vashisht et al, 2009; Thompson et al., 2012). However, not all the described IRP-dependent regulation in eukaryotes is at the post-transcriptional level. Recently, a remarkable study revealed a novel IRP1 transcriptional function in the iron homeostasis regulation in *Drosophila* (Huynh et al., 2019). The IRP1 protein containing the [4Fe-4S] cluster downregulated the transcription of iron- and heme-dependent processes once the peak iron demand was over (Huynh et al., 2019).

2.1. The regulation in response to iron excess in *S. cerevisiae*

Iron excess detoxification in *S. cerevisiae* involves the transcriptional activator Yap5. Yap5 binds its target promoters independently of the iron levels (Li et al., 2008) and only activates transcription when it directly binds two [2Fe-2S] clusters in an ISC (but not CIA)-dependent manner (Rietzschel et al., 2015). Yap5 activates the transcription of *CCC1*, *GRX4*, *TYW1* and *CUP1* (reviewed by Martínez-Pastor et al., 2017; Gupta & Outten, 2020). Ccc1 is the vacuolar iron importer, the main iron storage facilitator in yeast. The monothiol glutaredoxin Grx4 binds iron and inactivates the Aft1/2-dependent upregulation of the iron regulon (see below). The Tyw1 enzyme contains a [4Fe-4S] cluster and it was proposed to sequester cytosolic iron protecting cells from iron toxicity (Li et al., 2011). Finally, Cup1 is a cytosolic copper-binding protein important in the resistance to high copper concentrations. Cup1 also limits the copper availability to Fet3, component of the reductive iron uptake system (see below).

2.2. The regulation in response to iron deficiency in *S. cerevisiae*

It is a general pattern that the *S. cerevisiae* strains worse adapted to high iron concentrations are better adapted to iron starvation (Martínez-Garay et al., 2016). The iron deficiency regulation in *S. cerevisiae* involves the transcription factors Aft1 and Aft2. Aft1/2 activate the expression of ~30 genes collectively known as the iron regulon (reviewed by Martínez-Pastor et al., 2017). These genes are involved in: (i) acquisition of extracellular iron; (ii) mobilization and recycling of internal iron; and (iii) iron optimization due to a metabolic remodeling response (see section 2.2.1 and **Figure I-1**). Aft1 plays a predominant role in activating the cell surface iron uptake systems while Aft2 mainly activates genes of intracellular iron transport (Rutherford et al., 2001; Courel et al., 2005). Indeed, the *aft1Δ* mutant shows a growth defect under iron limitation that is more exacerbated in the *aft1Δaft2Δ* mutant (Blaiseau et al., 2001; Rutherford et al., 2001). Aft1 (and probably Aft2) shuttle between the nucleus and the cytoplasm and accumulate in the nucleus when iron is scarce (Yamaguchi-Iwai et al., 2002). Aft1 is imported to the nucleus by the Pse1 importin in an iron status-independent manner (Ueta et al., 2003). Then, Aft1/2 bind specific PyPuCACCCPu sequences (Py: pyrimidine; Pu: purine) called iron responsive elements (FeRE) in the promoters of the iron regulon members and activate their transcription (Yamaguchi-Iwai et al., 1996; Courel et al., 2005).

As previously mentioned, functional mitochondrial Fe/S cluster production by mitochondrial ISC (but not CIA) machineries are involved in the sensing of the iron deficiency (Chen et al., 2004; Rutherford et al., 2005; Hausmann et al, 2008). Two monothiol glutaredoxins Grx3 and Grx4 (Ojeda et al., 2006; Pujol-Carrión et al., 2006), the aminopeptidase P-like protein Fra1 and the BolA-like protein Fra2 (Kumanovics et al., 2008; Poor et al., 2014) are also required to deactivate the Aft1/2 transcriptional factors during iron sufficiency. A homodimer of Grx3 or Grx4 binds a [2Fe-2S] cluster with two glutathione molecules through the mitochondrial ISC systems but in a CIA-independent manner (Mühlenhoff et al., 2010). This step connects the mitochondrial iron status with Aft1/2 activity. Probably, the X-S molecule itself involves glutathione as it is present in the substrate binding pocket of the crystal structure of Atm1 (Lill et al., 2014;

Srinivasan et al., 2014). Besides, glutathione-deficient cells display Aft1/2-dependent activation of the iron regulon (Kumar et al., 2011; Sipos et al., 2002). Then, one Grx3/4 monomer and one glutathione are substituted by Fra2. Probably Fra1 is also involved in the latter complex as it interacts with Fra2 and Grx3/4 (Ueta et al., 2007; Kumanovics et al., 2008). This complex interacts with Aft1/2 transcriptional factors through their conserved CDC (Cys–Asp–Cys) motif and induces the dissociation of Aft1/2 from their promoters under iron sufficiency (Ueta et al., 2012; Poor et al., 2014; Li & Outen, 2019). Finally, Aft1/2 are exported from the nucleus via the nuclear export protein Msn5 (Ueta et al., 2012). This is the reason why Aft1/2 mutants in the CDC motif (*AFT1-1UP* and *AFT2-1UP* mutants) constitutively activate the iron regulon (Yamaguchi-lwai et al., 1995; Rutherford et al 2001). The Aft1 phosphorylation by Hog1 kinase in Ser210 and Ser224 is also necessary for its interaction with Msn5 (Ueta et al., 2007; Martins et al., 2018). However, the Msn5 mutation alone is not sufficient to constitutively activate the iron regulon, although Aft1/2 are maintained in the nucleus (Ueta et al., 2012).

2.2.1. The transcriptional response: the iron regulon

A list of ~30 genes transcriptionally activated by Aft1/2 are known as the iron regulon members (reviewed by Sanvisens & Puig, 2011; Martínez-Pastor et al., 2017). These genes encode proteins involved in several iron-related roles when iron is scarce (**Figure I-1**):

- (i) Acquisition of extracellular iron

The reductive iron uptake is transcriptionally activated by Aft1/2 when iron is scarce. It involves two heme-containing surface metalloreductases, Fre1 and Fre2, that convert Fe^{3+} from inorganic salts or Fe^{3+} chelates to reduced Fe^{2+}. Fre1/2 also reduce Cu^{2+} to Cu^{+}, important for the Fet3/Ftr1 high-affinity reductive iron uptake system (**Figure I-1**). Fet3 is a multicopper ferroxidase that oxidizes Fe^{2+} to Fe^{3+} reducing molecular oxygen to water for the subsequent Fe^{3+} transport by the Ftr1 transmembrane permease. Correct copper acquisition and delivery into Fet3 is essential for the Fet3/Ftr1 iron uptake system and for the iron deficiency adaptation.

The low-affinity reductive iron uptake system, transcriptionally activated by Aft1/2, is used under anaerobic conditions as its iron transporter Fet4 is oxygen-independent (**Figure I-1**). However, this system is less specific because it can bind other metals. The heme-dependent expression of Rox1 protein represses *FET4* promoter under aerobic conditions to prevent metal toxicity (Jensen & Culotta, 2002). In the same way, under anaerobic or heme-deficient conditions the general repressor complex Tup1–Ssn6 and Hda1 repress the Fet3/Frt1 high-affinity reductive iron uptake system (Crisp et al., 2006).

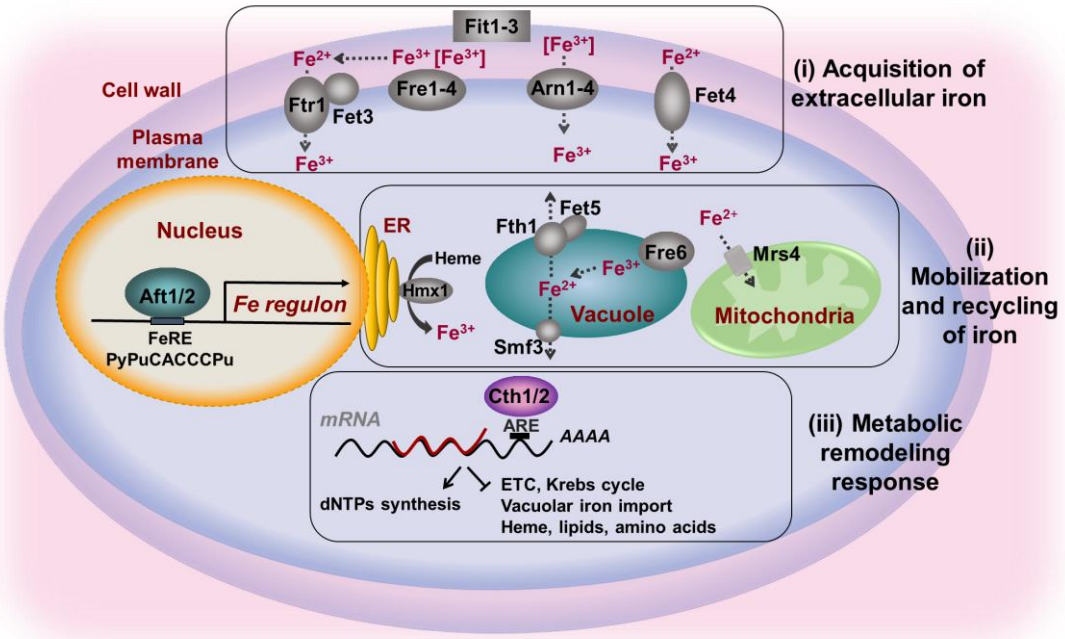

Figure I-1. The transcriptional factors Aft1 and Aft2 activate the iron regulon under iron starvation in *S. cerevisiae.* The iron regulon members include genes that encode proteins that enhance the (i) acquisition of extracellular iron; (ii) the mobilization and recycling of iron; and (iii) the metabolic remodeling response.

Siderophores are low molecular-mass Fe^{3+}-organic chelators that *S. cerevisiae* cannot produce but can specifically transport if produced by other organisms. The siderophore transport system is also transcriptionally activated by Aft1/2 under iron deficiency (**Figure I-1**). Fit1, Fit2 and Fit3 are cell wall mannoproteins that facilitate the iron-siderophore passage through the cell wall. Then, the Fre1/2, general metalloreductases, or Fre3/4, siderophore-specific metalloreductases,

reduce the Fe^{3+} from the siderophore and Fe^{2+} is released for its transport through the Fet3/Frt1 reductive system. Other nonreductive strategy involves the direct siderophore transport by Arn1-4 transporters, each specific for a group of fungal/bacterial siderophores. As this nonreductive system can operate independently of oxygen, Cti6, that is required for growth under iron starvation (Puig et al., 2004), derepresses *ARN1* and *FIT1* in anaerobiosis or in the absence of heme overcoming Tup1-repression (Crisp et al., 2006). In the same line of promoting the nonreductive system, when oxidative stress activates the iron regulon through Aft1, sets the iron assimilation through the nonreductive pathway to minimize the ferrous iron oxidative damage (Castells-Roca et al., 2011).

- (ii) Mobilization and recycling of internal iron

The vacuole is the main iron storage compartment in yeast. Aft1/2 activates several genes for the iron mobilization from the vacuole when iron is scarce (**Figure I-1**). The Fre6 metalloreductase converts the vacuolar Fe^{3+} to Fe^{2+} as well as it also reduces copper. Then, the Fet5/Fth1 transport system (paralog of Fet3/Ftr1) or the Smf3 transporter export vacuolar iron to the cytosol. The *SMF3* promoter, as *FET4*, is repressed by Rox1 under aerobic conditions (Jensen & Culotta, 2002), and then derepressed in anaerobiosis or under heme-deficient conditions.

On the other hand, heme is recycled by the heme oxygenase Hmx1 located in the cytosolic face of the endoplasmic reticulum. Cytoplasmic iron is introduced into the mitochondria by Mrs4. Both *HMX1* and *MRS4* genes are transcriptionally activated by Aft1/2 (**Figure I-1**).

- (iii) The metabolic remodeling response

Cth1 and Cth2 are two iron regulon members with FeRE sequences in their promoters that are transcriptionally activated by Aft1/2 when iron is scarce. These proteins are the main responsible for the metabolic remodeling response taking place in *S. cerevisiae* under iron limitation. By promoting the decay of some mRNAs, Cth1 and Cth2 help to prioritize the iron utilization in some iron-dependent processes at the expense of others (see below and in **Figure I-1**).

Besides Cth1/2 proteins, other Aft1/2 activated members promote a metabolic reorganization when iron is scarce. The synthesis of biotin in *S. cerevisiae* is iron-dependent. It lacks the first two steps of the pathway since it starts with the 7-keto, 8-amino-pelargonic acid (KAPA) precursor. The pathway depends on *BIO3*, *BIO4* and *BIO2* genes, containing the biotin synthase Bio2 protein a [4Fe-4S] cluster. All three genes are downregulated in low iron (Shakoury-Elizeh et al., 2004). Besides, under iron deficiency Aft1 activates the transcription of *VHT1*, transporter of extracellular biotin, and *BIO5,* the cell surface transporter of some precursors (KAPA and DAPA) of the pathway (Shakoury-Elizeh et al., 2004; Bellí et al., 2004). The transcriptional factor Vhr1 also transcriptionally activates *VHT1* and *BIO5* when biotin levels are low, condition that occurs under iron deficient-conditions (Weider et al., 2006).

2.2.2. The post-transcriptional response to iron deficiency: Cth1 and Cth2

Cth1 and Cth2 display very low expression levels under iron sufficiency and are transcriptionally activated by Aft1/2 under iron deficiency (Foury & Talibi, 2001; Rutherford et al., 2003; Shakoury-Elizeh et al., 2004; Puig et al., 2005; Puig et al., 2008). The *cth2Δ* mutant (but not *cth1Δ*) produces a growth defect only under iron deficiency that is exacerbated in the *cth1Δcth2Δ* double mutant (Puig et al., 2005). Despite some differences, both Cth1 and Cth2 proteins have an important role in prioritizing the iron utilization in the adaptation of yeast cells to iron scarcity.

- Structure and function

Cth1 and Cth2 belong to the eukaryotic tristetraprolin family of proteins (TTP family). This family specifically interacts through its highly conserved tandem zinc-fingers (TZFs), $Cx_8Cx_5Cx_3Hx_{18}Cx_8Cx_5Cx_3H$ (x being a variable amino acid), with adenosine/uridine-rich elements (AREs) within the 3'-untranslated region (3'-UTR) of multiple mRNAs to promote their degradation in the cytoplasm (**Figure I-2**). Humans express three TTP members: TTP or TIS11, TIS11d and TIS11b. The tridimensional structure of human TIS11d TZFs bound to single-stranded RNA was solved and demonstrated that each zinc finger binds adjacent

5′-UAUU-3′ motifs (Hudson et al., 2004). Because of these results, the 5′-UAUUUAUU-3′ and 5′-UUAUUUAU-3′ sequences are accepted as consensus AREs even though some variations still would maintain moderate TTP-binding affinity (Brewer et al., 2004).

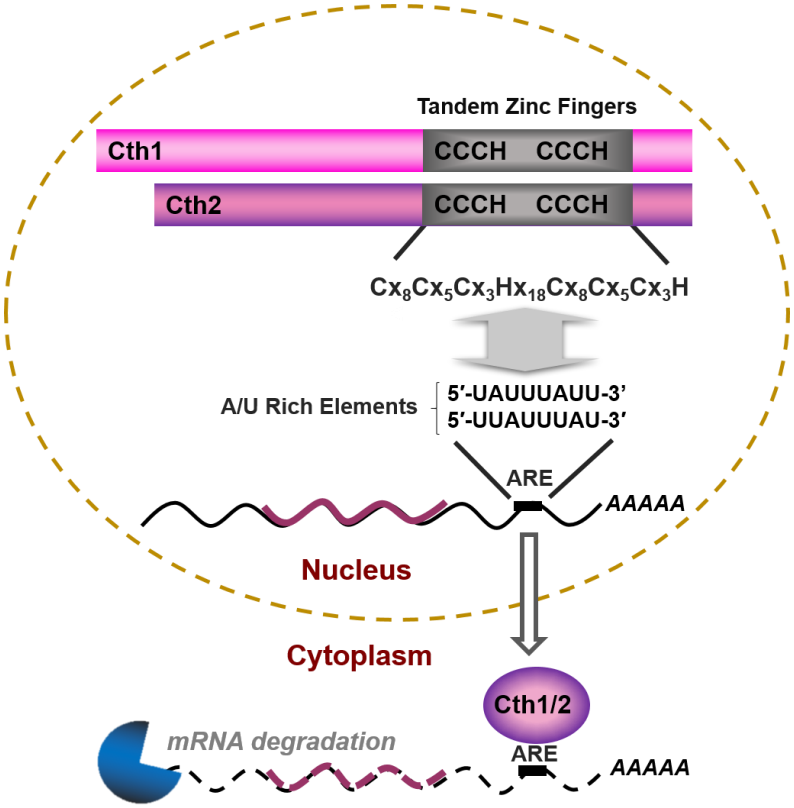

Figure I-2. The Cth1 and Cth2 post-transcriptional response carries out a metabolic remodeling under iron deficiency. The conserved tandem zinc-fingers (TZFs) specifically bind adenosine/uridine-rich elements (AREs) within the 3'-untranslated region (3'-UTR) of multiple mRNAs to promote their degradation in the cytoplasm.

The kind of mRNA targets downregulated by the TTP family members can vary between different species. Briefly, mammalian TTP, the most studied family member, is involved in the regulation of anti-inflammatory and immune responses. TTP physiological roles were initially pointed out by Taylor et al. in 1996, that described growth retardation, cachexia, arthritis, inflammation and autoimmunity in TTP mutant mice. This phenotype was suppressed by the use of anti-TNF

antibodies. Indeed, TTP is induced in response to inflammation or growth factors and promotes the mRNA decay of the tumor necrosis factor alpha (TNFα) (Carballo et al., 1998) and other cytokines (reviewed by Brooks & Blackshear, 2013; Wells et al., 2017). More recently, mammalian TTP has also been involved in the regulation of iron metabolism as (i) TTP levels are increased under iron deficiency, (ii) it promotes the decay of mRNAs encoding iron-containing proteins, and (iii) human TTP complements the Cth1/2 function in *S. cerevisiae* (Bayeva et al., 2012; Bayeva et al., 2013; Sato et al., 2018). Interestingly, an iron-related physiological role of TTP has been reported as TTP mutant mice display cardiac dysfunction when iron is scarce (Sato et al., 2018).

In *S. cerevisiae* the downregulation of the Cth1/2 mRNA targets prioritizes the utilization of iron. While *CTH1* is rapidly and transiently activated in the early iron deficiency, *CTH2* expression starts when the iron deficiency is more severe reaching higher and more constant levels and prevailing over Cth1 role (Puig et al., 2005; Puig et al., 2008). Despite they have redundant functions and common iron-dependent targets, Cth1 preferentially downregulates mitochondrial respiration or amino acid biosynthetic pathways in the early iron deficiency adaptation. On the contrary, when the iron deficiency is more severe, Cth2 is the main responsible of downregulating mitochondrial respiration, iron storage, heme or lipid biosynthetic pathways (Puig et al., 2008 and see below in "cell processes regulated by Cth1 and Cth2"). For these reasons, there are more Cth2-related studies compared to Cth1, especially those associated with the mechanism of mRNA turnover and protein destabilization.

- Mechanism of Cth2-mediated mRNA turnover

Cth2, as the rest of the TTP family members, is a nucleocytoplasmic shuttling protein (Vergara et al., 2011). While the nuclear import sequence of Cth2 is within its TZFs, its nuclear export depends on its mRNA binding capacity (Vergara et al., 2011). In fact, the nucleocytoplasmic shuttling is necessary for its ARE-mediated mRNA decay (AMD) function that takes place in the cytoplasm. Stopping the nuclear transcription with thiolutin or the mRNAs nuclear export (through *xpo1-1* or *mex67-5* thermosensitive mutants) (Vergara et al., 2011), as well as directly

mutating the Cth2-TZF domain, prevents the Cth2 nuclear export and therefore its AMD function (Puig et al., 2005). The TZF domain is the only highly conserved motif in Cth2 within the TTP family, but there are other three less conserved regions, present in the Cth2 paralogs of other *Saccharomyces* species: CR1 and CR2 in the amino-terminal domain (NTD) and CR3 after the TZFs in the carboxyl-terminal domain (CTD) (Prouteau et al., 2008). While the full integrity of the TZFs and the AREs are essential for AMD (Puig et al., 2005), the CR1 is partly involved in the AMD function of Cth2 (Prouteau et al., 2008).

The Cth2-dependent AMD involves the RNA helicase Dhh1 and the 5' to 3' cytoplasmic exonuclease Xrn1 (Pedro-Segura et al., 2008). The Dhh1 DEAD-box ATPase protein activates 5' mRNA decapping (completed by Dcp1/Dcp2) for the later 5' to 3' mRNA degradation by Xrn1 in the processing bodies (P-bodies) (reviewed by Coller & Parker, 2004; Decker & Parker, 2012). Interestingly, the formation of P-bodies is controlled by the ATPase activity of Dhh1 and its interaction with the deadenylation complex (Carroll et al., 2011; Mugler et al., 2016). Although P-bodies are not detected under iron deficiency, Cth2 is found in the P-bodies observed in *xrn1Δ*, *dcp1Δ* and *dcp2Δ* mutant strains (Pedro-Segura et al., 2008). Indeed, Cth2 (and also Cth1) interacts with the carboxyl-terminal domain of Dhh1 and fails to promote the degradation of the ARE-containing *SDH4* mRNA in a *dhh1Δ* mutant strain (Pedro-Segura et al., 2008). These results suggested a model for the Cth2-dependent post-transcriptional regulation when iron is scarce: Cth2 goes into the nucleus and binds its target-mRNAs, probably cotranscriptionally, then it is exported to the cytoplasm where it recruits deadenylation and decapping proteins, and finally the exonuclease Xrn1 degrades the ARE-containing mRNAs from 5' to 3' (Martínez-Pastor et al., 2013b).

Similarly, mammalian TTP-dependent AMD starts with the deadenylation or poly(A) shortening by the Ccr4-Not complex followed by either (i) 5' decapping by the Dhh1 homolog RCK/p54 and Dcp1/Dcp2 decapping enzymes plus final 5' to 3' degradation by Xrn1 or (ii) 3' to 5' mRNA decay via the exosome (Chen et al., 2001; Fenger-Grøn et al., 2005; Lykke-Andersen & Wagner, 2005). Importantly, it is known that mammalian TTP also can repress translation through interactions with the Dhh1 homolog RCK/p54, which acts as both a promoter of decapping and

repressor of translation initiation (Coller & Parker, 2005; Qi et al., 2012; Tiedje et al., 2012). Additionally, Dhh1 senses the mRNAs with non-optimal codons (with reduced ribosome speed) and promotes their translational repression and decay (Radhakrishnan et al., 2016).

- Cell processes regulated by Cth1 and Cth2

In response to iron-deficient conditions, Cth1 and Cth2 promote the decay of numerous mRNAs, most of them containing AREs, that encode proteins that directly bind iron or are involved in iron-consuming pathways (Puig et al., 2005; Puig et al., 2008):

- Mitochondrial respiration (see section 4.2)
- Heme biosynthesis: *COX10*, *HEM13* and the ferrochelatase *HEM15*
- Lipid metabolism: synthesis of sterols (*ERG1*, *ERG3*, *ERG5*, *ERG11*, *ERG25*), sphingolipids (*SCS7*) and unsaturated fatty acids (fatty acid desaturase *OLE1*). Besides being post-transcriptionally regulated by Cth2, *OLE1* is also transcriptionally induced under iron deprivation by Mga2 in an Aft1/2-independent manner (Puig et al., 2005; Romero et al., 2018a). Importantly, the sustaining of unsaturated fatty acids levels is essential under iron starvation as *mga2Δ* shows defects in activating the iron regulon when iron is scarce (Jordá et al., 2020)
- Synthesis of amino acids: leucine, isoleucine, valine (*LEU4*, *ILV3* and the isopropylmatale isomerase *LEU1*), lysine (homoaconitase *LYS4*), glutamate (glutamate synthase *GLT1*) and methionine (*MET7*). Besides the Cth1/2-dependent post-transcriptional downregulation, iron-dependent transcriptional downregulation can occur, for example, in the *GLT1* gene (Shakoury-Elizeh et al., 2004; Philpott et al., 2012) and in *LEU1* gene (Ihrig et al., 2010). In the latter case, the lack of the metabolite α-isopropylmalate under iron deficiency downregulates the transcription of *LEU1* (Ihrig et al., 2010)
- Iron storage: the vacuolar iron importer *CCC1*
- Ribosome biogenesis, recycling and translation initiation/termination: *RLI1*

- Some members of Fe/S mitochondrial cluster biogenesis: *ISA1* and *NFU1*

- Regulation of Cth1 and Cth2 protein levels

Overexpression of functional TZF-containing Cth2 protein is toxic for the cell (Pedro-Segura et al., 2008). However, *CTH1* and *CTH2* mRNAs contain AREs within their 3'-UTR. These AREs are important for their negative feedback regulation by AMD in a TZF-dependent manner that permits rapid recovery when yeast cells shift from iron-deficient to iron-sufficient conditions (Martínez-Pastor et al., 2013a). Similarly, feedback regulatory loops have been described for TTP, in this case at both the mRNA decay and translational levels (Brooks et al., 2004, Tchen et al., 2004; Pullmann et al., 2007; Tiedje et al., 2012). Cth2 protein levels are also controlled at the post-translational level. Cth2 protein stability is controlled by phosphorylation in several serine residues recognized by the SCF^{Grr1} ubiquitin ligase complex that accelerate the protein turnover by the proteasome (Romero et al., 2018b).

3. The global inhibition of translation in response to iron deficiency

Recently, iron deficiency has been added to the list of stresses or nutritional signals that inhibit the TORC1 pathway (Romero et al., 2019). Iron deficiency diminishes the RNA polymerase II transcription rate and decreases the abundance of many mRNAs. Besides, reduced activities of RNA polymerase I, showing subsequent decline in *18S* and *25S* rRNA levels, and RNA polymerase III, showing subsequent decrease in tRNAs, are probably due to the TORC1 inhibition under iron starvation (Romero et al., 2019). Also, the environmental stress response (ESR) and the retrograde response (RTG) would be activated under iron starvation (Romero et al., 2019). And finally, the reduced expression of ribosomal proteins (RPs) and ribosome biogenesis (RiBis) genes is achieved directly through TORC1 inhibition itself as well as through the ESR and the diminished RNA Pol II activity under iron limitation (Romero et al., 2019). On the other hand, protein synthesis is a highly energy consuming process in the cell and many stresses (heat shock, oxidative and osmotic stresses) and nutritional deficiencies (glucose and amino

acid limitation) inhibit bulk translation (Martínez-Pastor & Estruch, 1996; Ashe et al., 2000; Hinnebusch, 2005; Shenton et al., 2006; Yamamoto & Izawa, 2013; Crawford & Pavitt, 2019).

At this point, several evidences indicate that iron deficiency could impair the general translation activity of the cells: (i) decreased levels of several rRNAs, tRNAs, RPs and RiBis mRNAs are observed under iron deficiency (Romero et al., 2019); (ii) the *RLI1* ARE-containing mRNA (encoding the essential Fe/S protein involved in ribosome biogenesis and translation) is decreased in a Cth2-dependent manner as well as many mRNAs of amino acid biosynthesis pathways (Puig et al., 2005; Puig et al., 2008); and (iii) the alpha subunit of the translation initiation factor (eIF2α) is phosphorylated under iron deficiency (Romero, 2018; Romero et al., 2020; **Figure I-3: A and B**). Regarding the latter argument, translation initiation is the principal translational regulated point in eukaryotes (reviewed by Gebauer & Hentze, 2004; Sonnenberg & Hinnebusch, 2009; Jackson et al., 2010; Hershey et al., 2012; Dever et al., 2016; Crawford & Pavitt, 2019). Under optimal growing conditions, the translation initiation factor eIF2 (with three subunits α, β and γ), GTP and methionyl-tRNA form the ternary complex, the first step in forming the pre-initiation complex in translation. At the end of the initiation phase of translation, GTP hydrolyzes into GDP and the ternary complex disassembles. Then, the guanine nucleotide exchange factor eIF2B recycles the eIF2-GDP into eIF2-GTP and the subsequent addition of methionyl-tRNA forms the ternary complex again. However, when the growth conditions are not favorable (amino acid starvation or other stresses) uncharged tRNAs bind the histidyl-tRNA synthetase (HisRS)-like domain of the kinase Gcn2. The Gcn1–Gcn20 complex facilitates the transfer of the uncharged tRNA from the translating ribosome to Gcn2 and activates the Gcn2 kinase activity (Marton et al., 1997; Garcia-Barrio et al., 2000). However, Gcn2 activation can occur under stresses that not necessarily increase the levels of uncharged tRNAs, but it still depends on the HisRS domain, the tRNA binding and the Gcn1–Gcn20 complex. The current model proposes a Gcn2 activation in a Tap42–PP2A-dependent manner when TORC1 complex is inactivated. Under this situation, TORC1 cannot phosphorylate Tap42 and the protein phosphatase 2A (PP2A) complex dephosphorylates Ser-577 of Gcn2 activating its kinase function (Di Como & Arndt, 1996; Jiang & Broach, 1999; Valenzuela et al., 2001; Cherkasova

& Hinnebusch, 2003; Kubota et al., 2003; Narasimhan et al., 2004; Hinnebusch, 2005; Yan et al., 2006). Once Gcn2 kinase is active, it phosphorylates eIF2α in Ser-51 (Dever et al., 1992) and consequently inhibits the eIF2B function, decreasing the ternary complex levels and blocking the 5' cap-dependent translation initiation. On the other hand, and independently of the initial stress activating Gcn2, the *GCN4* mRNA translation is enhanced under low ternary complex levels due to its regulation by four short upstream open reading frames (uORFs) (Hinnebusch et al., 2005). Gcn4 is a transcriptional factor that activates amino acid biosynthetic pathways, especially necessary under amino acid starvation. Indeed, the polysomal distribution of the *GCN4* mRNA is more associated to polyribosome fractions after 6 hours of iron deficiency compared to iron sufficiency or earlier iron-deficient times (Romero, 2018; Romero et al., 2020; **Figure I-3: C**). This would indicate that the *GCN4* transcript is probably in a more active translation state under iron starvation.

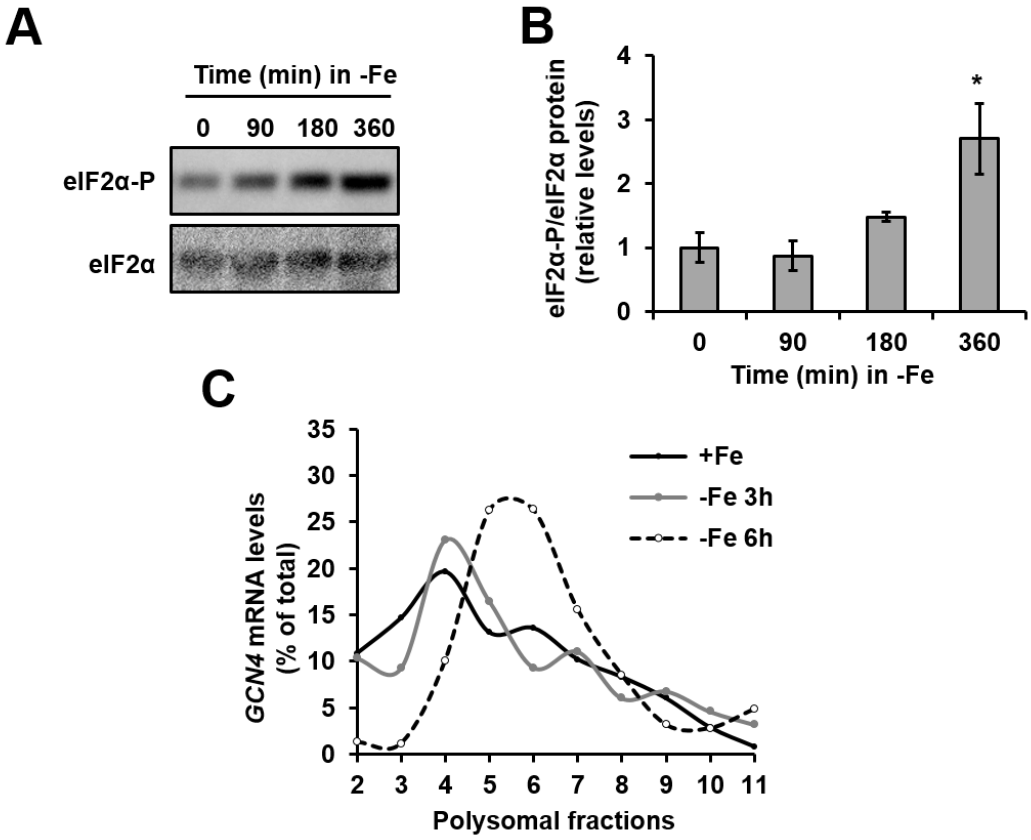

Figure I-3. Previous results (Romero, 2018; Romero et al., 2020) showed a higher eIF2α phosphorylation and enhanced translation of the *GCN4* mRNA under iron deficiency. The protein levels of eIF2α phosphorylated and total

eIF2α of wild-type W303 prototroph strain were analyzed by Western blot in SC cultures growing for 15 hours until early exponential phase. Then, cells were maintained in SC (+Fe, here indicated as 0 minutes in -Fe) or in SC with 100 μM BPS (-Fe) during 90, 180 or 360 minutes. **(A)** A representative result is shown. **(B)** Mean values and standard deviations from the quantification of three independent biological replicates are shown relative to the 0 minutes in -Fe. An asterisk (*) indicates a significant difference (*p*-value <0.05) from two-tailed student's t-test compared to the SC condition (0 hours in -Fe). **(C)** Polysome profile experiments were performed under the same growth conditions before described and the *GCN4* mRNA profile was analyzed by RT-qPCR.

Altogether, these results strongly suggest that if general translation initiation is compromised under iron starvation it is probably in a Gcn2/eIF2α-dependent manner.

4. Respiration in iron deficiency

Mitochondria produce energy from the aerobic metabolism that couples the ATP production (by the F_1F_0-ATP synthase, complex V) and the oxidative reactions of the TCA cycle and the ETC (complexes I-IV). This oxidative phosphorylation (OXPHOS) process is known as mitochondrial respiration. Mitochondria are also involved in other processes such as the amino acid metabolism, and the synthesis of Fe/S clusters, heme and lipoic acid. However, in yeast the only indispensable function of mitochondria is the biogenesis of Fe/S clusters. *S. cerevisiae* is a microorganism that can produce energy from fermentation or aerobic respiration. Although aerobic respiration could produce 17 times more ATP compared to fermentation, *S. cerevisiae* only respires a proportion of the total carbon source and this also depends on the carbon source available (Lagunas, 1986). Glucose is yeast's preferred carbon source, and although only 3 % is metabolized through respiration, 34 % of the total ATP is produced by respiration because of the higher ATP yield (Lagunas, 1986). This is due to the fact that glucose represses respiration in yeast cells despite the presence of oxygen. But, upon glucose deprivation, the Snf1 kinase complex is activated by phosphorylation and derepresses the respiratory genes (reviewed by Kayikci & Nielsen, 2015). On the

other hand, respiration is a highly iron-consuming process and there is no growth under non-fermentable carbon sources during iron starvation. Indeed, during the diauxic shift, the iron regulon is induced in a Snf1 kinase complex- and Aft1-dependent manner, suggesting the exceptional need of iron during respiration (Haurie et al., 2003). Moreover, during iron deficiency glycogen levels as well as mRNAs encoding glucose import and storage accumulate in a Cth1/2-dependent manner (Puig et al., 2008). Also Snf1 is phosphorylated under iron starvation although glucose is abundant (Puig et al., 2008). Thus, iron homeostasis, glucose sensing and respiration are highly connected processes.

4.1. The Hap complex regulation

The Hap complex is the master regulator of respiratory metabolism. It induces the expression of cytochromes and respiratory genes that contain the CCAAT box in their promoters (reviewed by Hortschansky et al., 2017; Mao & Chen, 2019). The DNA-binding domain of the Hap complex (Hap2/3/5) is constitutively expressed. The activation domain encoded by *HAP4* is the only one transcriptionally regulated (DeRisi et al., 1997; Forsburg & Guarente, 1989). The activity of the complex is heme- and oxygen-dependent as: (i) the transcriptional factor Hap1 depends on heme and activates the *HAP4* expression (Zhang & Guarente, 1995; Zhang & Hach., 1999); and (ii) heme directly binds Hap4 increasing the half-life of the protein (Bouchez et al., 2020). In addition to the heme-dependent activity, the Hap complex is sensitive to oxidative stress. Thus, increased levels of ROS from mitochondria or after a H_2O_2 treatment, produce lower Hap activity and lower Hap4 protein levels (Chevtzoff et al., 2010). In the same way, decreased levels of reduced glutathione, involved in many ROS detoxifying reactions, produce very low Hap4 protein levels (Yoboue et al., 2012). During iron deficiency, the synthesis of heme is compromised and this directly downregulates the transcription of *CYC1* (cytochrome *c*) dependently of both Hap1 and Hap4 transcriptional activators (Ihrig et al., 2010). In the same direction, under low iron concentrations the *hmx1Δ* mutant (with defects in heme degradation) shows increased transcription of the *CYC1* promoter (Protchenko & Philpott, 2003).

4.2. Cth2 mRNA targets in the Krebs cycle and the electron transport chain

Respiration is the main source of intracellular ROS under physiological conditions (reviewed by Herrero et al., 2008; Murray et al., 2011; Baccolo et al., 2018). Besides, the steady-state levels of Fe/S clusters are reduced in the presence of oxygen because of the formation of basal ROS (Ast et al., 2019). In this way, hypoxia rescues Fe/S cluster levels and their activity, and even rescues the frataxin mutant phenotype (member of the core ISC assembly machinery) (Ast et al., 2019). Additionally, a ROS-protective capacity of Cth2 during oxidative stress has been shown. Under oxidative stress, iron entrance is limited by downregulating the expression of some iron regulon members in a Cth2-dependent manner (Castells-Roca et al., 2016). Also, the expression of Cth2 decreases the mitochondrial membrane potential under non-stress conditions (Matsuo et al., 2017). Despite these interesting results, the role of Cth2 in respiration during iron starvation has not been studied beyond the observation of decreased mRNA levels of several components of the TCA and ETC in a Cth2-dependent manner (**Figure I-4**; Puig et al., 2005; Puig et al., 2008; Romero et al., 2019). However, this strongly suggest a Cth2 role in the downregulation of respiration during iron deficiency that could help in the ROS reduction and in the cofactor preserving.

- Krebs cycle or tricarboxylic acid (TCA) cycle

The Krebs or TCA cycle is the connection between glycolysis and the ETC as it oxidizes the acetyl-CoA to obtain NADH and $FADH_2$ later used in ETC. It takes place in the mitochondrial matrix with the exception of the succinate dehydrogenase activity (SDH, complex II in the ETC) that takes place in the inner mitochondria membrane. Ten mRNAs that encode enzymes of the TCA cycle show increased levels in a *cth2Δ* mutant during iron starvation, and eight of them are ARE-containing mRNAs (**Figure I-4: A**). Importantly, the aconitase enzyme (Aco1) contains a [4Fe-4S] cluster. On the other hand, the Sdh2 subunit from the SDH enzyme contains three different Fe/S clusters ([4Fe-4S], [3Fe-4S] and [2Fe-2S]) and Sdh3-Sdh4 subunits share a heme center. The alpha-ketoglutarate dehydrogenase has three subunits encoded by *KGD1*, *KGD2* and *LPD1.* It does not contain iron but the Kgd2 subunit requires lipoic acid which synthesis requires the

lipoic acid synthase (encoded by *LIP5*). Lip5 contains two [4Fe-4S] clusters and its mRNA contains 3 AREs, putative targets for Cth2-dependent downregulation (Puig et al., 2005; Puig et al., 2008).

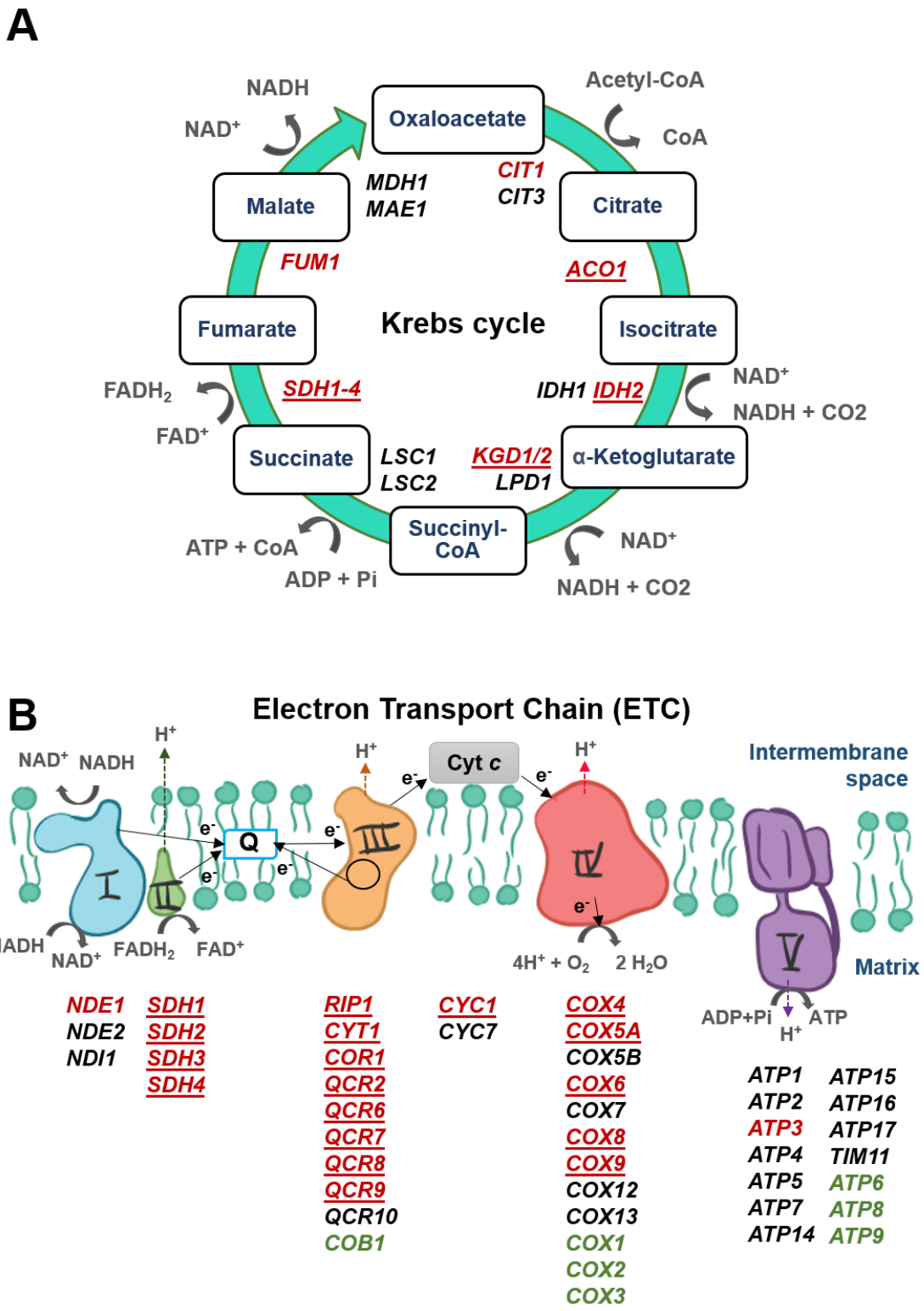

Figure I-4. The Cth2 mRNA-targets in the Krebs cycle (A) and Electron Transport Chain (B). The transcripts showing decreased mRNA levels in a Cth2-dependent manner (Puig et al., 2005; Puig et al., 2008) are shown in red and those with AREs in the 3'UTR are underlined. Genes of the ETC complexes encoded by the mitochondrial genome are shown in green.

- Complex I (NADH:ubiquinone oxidoreductase)

In yeast, there is no complex I as such, instead there are three NADH dehydrogenases in the inner mitochondria membrane that do not pump protons (**Figure I-4: B**). There is one internal NADH dehydrogenase (*NDI1*) facing the mitochondrial matrix, and two external (*NDE1* and *NDE2*) facing the intermembrane space. They transfer the electrons from NADH to ubiquinone (coenzyme Q) to reduce it to ubiquinol. Only the *NDE1* mRNA shows increased levels in a *cth2Δ* mutant during iron starvation, but it is not an ARE-containing mRNA.

- Complex II (succinate dehydrogenase, SDH)

As mentioned before, this tetrameric enzyme contains three Fe/S clusters and one heme and it is the link between the ETC and the TCA cycle. It oxidizes succinate to fumarate in the TCA cycle and transfers the electrons from $FADH_2$ to ubiquinone for reducing it to ubiquinol. The four subunits of the complex are ARE-containing mRNAs that show increased levels in a *cth2Δ* mutant during iron starvation (**Figure I-4: B**).

- Complex III (cytochrome *c* reductase or cytochrome bc_1)

This complex contains ten subunits (nine encoded by the nuclear genome and one, cytochrome *b COB1*, by the mitochondrial genome). All but one of the nuclear genes encode ARE-containing mRNAs with increased transcript levels in a *cth2Δ* mutant during iron starvation (**Figure I-4: B**). The complex III, together with the external NADH dehydrogenases, are the main sources of superoxide anions in the ETC (reviewed by Herrero et al., 2008; Murray et al., 2011; Baccolo et al.,

2018). Complex III receives two electrons from ubiquinol. One electron passes through the [2Fe-2S] cluster of Rieske protein (encoded by *RIP1*), then through the cytochrome c_1 (encoded by *CYT1*) and finally reduces the cytochrome *c* (encoded by *CYC1* and *CYC7*). The other electron passes through the b_L and b_H heme groups of cytochrome *b* (encoded by the mitochondrial gene *COB1*) and returns to ubiquinone forming a semi-reduced ubiquinone. This semi-reduced ubiquinone would need another electron to be completely reduced and start a new cycle. The semi-reduced ubiquinone is highly reactive and, if the ETC is slow, it can react with oxygen leading to superoxide formation and subsequent H_2O_2.

- Complex IV (cytochrome *c* oxidase, COX)

This complex of eleven subunits transfers the electrons from the reduced cytochrome *c* to molecular oxygen. The three subunits encoded by the mitochondrial genome (*COX1, COX2* and *COX3*) form the catalytic core of the complex, in which only Cox1 contains iron (and copper) in form of heme centers. Five of the nuclear genes encode ARE-containing mRNAs with increased transcript levels in a *cth2Δ* mutant during iron starvation (**Figure I-4: B**).

- Complex V (F_1F_0-ATP synthase)

The named complex V is not part of the ETC, but uses the protons pumped by the complexes II, III and IV in the synthesis of ATP. Only one subunit with no AREs in its mRNA shows increased transcript levels in a *cth2Δ* mutant during iron starvation (**Figure I-4: B**).

5. Ribonucleotide reductase (RNR) in *Saccharomyces cerevisiae*

Iron is closely related to the DNA metabolism. Several DNA repair enzymes (Pri2, Dna2, Rad3, Chl1, Ntg2, Tpa1), DNA polymerases (DNA Pol α, ε, δ and ζ) and the ribonucleotide reductase use iron as cofactor from yeast to humans (reviewed by Puig et al., 2017). Besides, defects in some ISC and CIA machineries members cause nuclear genome instability (Stehling et al., 2012; Gari et al., 2012; Pijuan et al., 2015). The RNR enzyme constitutes the limiting step in the *de novo* synthesis of deoxyribonucleoside triphosphates (dNTPs). The class I RNR is found in almost all

eukaryotic organisms, including yeast and humans, and contains an oxo-diiron cofactor. A poor control of the dNTP levels could cause DNA replication and repair problems and subsequent high mutation rates, genome instability and cancer. Indeed, human RNR activity is increased in some tumor types, and therefore it is a common target for anti-tumor therapies including iron chelators (reviewed by Richardson et al., 2009; Aye et al., 2015; Mannargudi & Deb, 2017; Knighton et al., 2019).

5.1. Structure and function

The class Ia RNR of *S. cerevisiae* contains the large R1 (α_2) and the small R2 ($\beta\beta'$) subunits in a quaternary structure $R1_3R2_{n\ (n=1\ or\ 3)}$. Besides, the unique aspect of *S. cerevisiae* is that R2 is a heterodimer (reviewed by Kolberg et al., 2004; Nordlund & Reichard, 2006; Cotruvo & Stubbe, 2011; Sanvisens et al., 2013; Puig et al., 2017). RNR enzyme catalyzes the synthesis of deoxyribonucleotides (dNDPs) reducing the corresponding ribonucleotides (NDPs) in the cytoplasm. Briefly, the large R1 subunit is usually an Rnr1 homodimer and sometimes an Rnr1–Rnr3 heterodimer, however, *RNR3* is usually expressed at very low levels (see below section 5.3). Each R1 component contains one catalytic and two allosteric effector sites. The latter are the specificity S and activity A sites that balance the four dNTP pools and control the general enzymatic activity, respectively. The A site is controlled by the dATP (inhibitor)/ATP (activator) ratio. On the other hand, the R2 small subunit is an Rnr2–Rnr4 heterodimer with the essential diferric tyrosyl radical [$(Fe^{3+})_2$-Y·] cofactor in Rnr2. Despite Rnr4 does not contain cofactor, it is essential for the cofactor assembly into Rnr2 as well as for R1–R2 assembly. Besides Rnr4, the cytosolic monothiol glutaredoxins Grx3 and Grx4 (Muhlenhoff et al., 2010) as well as Dre2–Tah18 members of the CIA machinery (Zhang et al., 2011; Zhang et al., 2014) were described to be involved in the iron delivery to Rnr2. A few years later, Dre2 was described to be required for the RNR cofactor formation but to be dispensable for the Grx3/4-dependent iron loading (Li et al., 2017). Thioredoxin or glutaredoxin systems are in charge of reducing two conserved cysteines in R1 catalytic site, then the electron is transferred to the cofactor in R2 and the NDP is reduced to dNDP.

5.2. Regulatory aspects

RNR function is tightly regulated and its enzymatic activity is restricted to periods when dNTPs are required (DNA damage, DNA replication stress or entering the S phase) to avoid elevated mutation rates. The Mec1–Rad53–Dun1 checkpoint kinase pathway controls the RNR activity under these conditions, and also under iron-deficient conditions (**Figure I-5** and Sanvisens et al., 2013; Puig et al., 2017). Also, different mechanisms limit the RNR activity under non-stress conditions. These are deactivated under iron deficiency, in some cases similarly to DNA damage and replication stress (**Figure I-5**):

- (i) Sml1 protein inhibits RNR catalytic activity by directly binding to the Rnr1 protein. Under iron deficiency or in strains defective in the ISC assembly machinery, Sml1 is phosphorylated by Dun1 and its levels decrease, leading to an increase in RNR function (Sanvisens et al., 2014; Pijuan et al., 2015). Subsequent Sml1 degradation occurs in a vacuolar/proteasomal-dependent manner under iron-deficient conditions (Sanvisens et al., 2014).

- (ii) Dif1 promotes the nuclear localization of R2 while R1 stays in the cytoplasm. Under iron starvation, Dun1 phosphorylates Dif1 and promotes the R2 cytoplasmic-localization and subsequent RNR activity (Sanvisens et al., 2016). Besides, there are reduced levels of Dif1 in defective strains of the ISC assembly machinery promoting the R2-cytoplasmatic localization (Pijuan et al., 2015). Also, Dif1 is more phosphorylated in a *DRE2*-defective (component of CIA machinery) strain in a Dun1-dependent manner (Zhang et al., 2014).

- (iii) *RNR2/3/4* genes are repressed by the transcriptional repressor Crt1. The expression of *RNR2/3/4* increases in the *DRE2*-defective (component of CIA machinery) strain (that also induces the expression of *CTH2*) because of the phosphorylation and subsequent removal of the Crt1 repressor from their promoters (Zhang et al., 2014). Besides, there is an increased Rad53-

phosphorylation and higher expression of *RNR3*, also in a Dun1-dependent manner, in strains defective in ISC and CIA machineries (Stehling et al., 2012; Zhang et al., 2014).

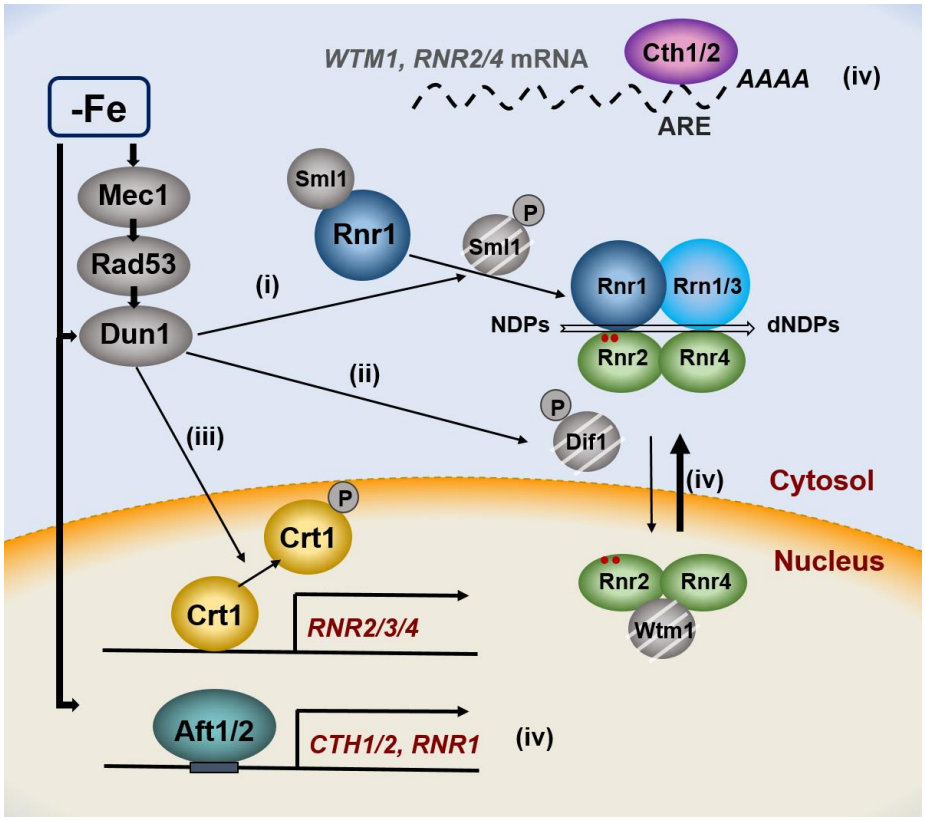

Figure I-5. Mechanisms of activation of *S. cerevisiae* ribonucleotide reductase enzyme under Fe/S cluster and iron deficient-conditions. (i) Sml1, **(ii)** Dif1 and **(iii)** Crt1 are phosphorylated by Dun1 promoting the Rnr1 protein activity, avoiding the Rnr2–Rnr4 transport to the nucleus and derepressing the *RNR2/3/4* transcription, respectively. **(iv)** Transcriptional factors Aft1/2 activate the transcription of *CTH1, CTH2* and *RNR1*. The Cth1/2 proteins promote the degradation of the ARE-containing *WTM1* mRNA triggering the subsequent Rnr2–Rnr4 cytoplasmic-localization.

- (iv) The connection of the iron regulon with the iron-dependent RNR activity is remarkable as cells treated with hydroxyurea (HU), a specific RNR inhibitor, activate the iron regulon, and the *aft1Δaft2Δ* mutant is hypersensitive to HU (Dubacq et al., 2006). Wtm1 anchors R2 in the nucleus

while R1 stays in the cytoplasm. Cth1/2 downregulate the ARE-containing *WTM1*, *RNR2* and *RNR4* mRNAs (Sanvisens et al., 2011) in response to iron deficiency (and in ISC-CIA defective strains that activate the iron regulon). This happens in a Mec1–Rad53–Dun1 checkpoint pathway-independent manner. The downregulation of the *RNR2* and *RNR4* mRNA levels plus the redistribution of R2 to the cytoplasm increases the dNTP levels (Sanvisens et al., 2011). On the other hand, *RNR1* was recently considered as a new member of the iron regulon. Aft1/2 enhance the *RNR1* expression under iron limitation through two FeRE sites in the *RNR1* promoter with a subsequent increase in the synthesis of dNTPs (Ros-Carrero et al., 2020).

5.3. The *RNR3* subunit

Unlike *RNR1*, *RNR3* is expressed at very low levels under non-stress conditions. No negative phenotype has been described in the *rnr3Δ* mutant under the stresses typically defined to strongly upregulate its expression (DNA damage, genotoxic stress, replication stress). However, *RNR3* overexpression rescues the *rnr1Δ* mutant lethality (Elledge & Davis, 1990; Domkin et al., 2002). Indeed, Rnr1 and Rnr3 proteins share 80 % amino acid sequence identity, and both maintain the amino acids for the catalytic and allosteric activities of RNR. All R1 combinations (Rnr1–Rnr1, Rnr1–Rnr3, Rnr3–Rnr3) are active, but the specific activity of Rnr3 is very low (Domkin et al., 2002). However, there is a strong synergism between Rnr1 and Rnr3 that probably increases the Rnr3 incorporation into the holoenzyme when *RNR3* gene is expressed (Domkin et al., 2002).

Despite the necessity of more efforts to elucidate the physiological function of Rnr3, some studies have described various differences between Rnr1 and Rnr3. Rnr3 lacks the dATP-dependent inhibition and this could be advantageous in the dNTP synthesis (Domkin et al., 2002). However, the *rnr3Δ* mutation does not cause lower dNTP levels in response to DNA damage (Chabes et al., 2003; Maicher et al., 2017). More recently, it has been described that Rnr3 is not involved in the Rnr1 function facilitating the elongation of short telomeres by telomerase (Maicher et al., 2017; Maicher & Kupiec, 2018). However, these authors showed that the deletion of *CRT1*, that causes the Rnr3 upregulation, was sufficient to increase the

dNTP levels compared to the dNTP levels in the wild-type. Also, the dNTP (except dGTP) levels were still higher than in the wild-type in the *rnr1Δcrt1Δ* mutant (Maicher et al., 2017). These results demonstrate a possible advantageous role of Rnr3 in the synthesis of dNTPs (except dGTP) compared to Rnr1. Finally, a recent study showed that Rnr3 is upregulated in a Mec1-dependent manner under non-fermentable carbon sources or limiting concentrations of glucose, while Rnr1 is downregulated (Corcoles-Saez et al., 2019). Importantly, these authors show that the *rnr3Δ* mutant has a negative phenotype growing in glycerol and suggest a dNTP-independent role of Rnr3 in mitochondrial function (Corcoles-Saez et al., 2019).

Rnr3 is almost undetectable under non-stress conditions. But its property of being highly induced (or derepressed) under DNA damage or replication stress has been used as a sensor of genome instability, replication stress responses or chemical-genotoxicity in several studies, some at genome-wide level (Ochi et al., 2011; Wei et al., 2013; Hendry et al., 2015). Several proteins are involved in the *RNR3*-promoter repression. As above mentioned, Crt1 is a transcriptional repressor of *RNR2/3/4*. Crt1 binds motives known as X-box. These are *cis*-regulatory elements of 13 nucleotides present in the promoter of *RNR2/3/4* damage-inducible genes and also the *CRT1* promoter (Huang et al., 1998). Crt1 represses the *RNR3* transcription by recruiting the general repressor complex Tup1–Ssn6, that positions nucleosomes through the chromatin remodeling complex ISW2 and recruits several histone deacetylases (Huang et al., 1998; Li & Reese, 2001; Zhang & Reese, 2004a; Zhang & Reese, 2004b; Zhang & Reese, 2005; Sharma et al., 2007). Under DNA damage, Crt1 is phosphorylated in a Mec1–Rad53–Dun1-dependent manner and dissociates from the *RNR3* promoter (Huang et al., 1998). But, before dissociating the *RNR3* promoter, Crt1 binds the general transcription factor TFIID and the chromatin remodeling complex SWI/SNF, that promotes nucleosome remodeling, for the derepression of *RNR3* (Li & Reese, 2000; Sharma et al., 2003; Zhang & Reese, 2005). Interestingly, the chromatin remodeling complexes ISW2 and SWI/SNF repress and activate *RNR3*, respectively, antagonistically (Tomar et al., 2009). Also, the multifunctional protein Rap1 involved in transcription is required for the activation of *RNR3* in a Mec1–Rad53–Dun1, TFIID and SWI/SNF-dependent manner, probably preventing the

repositioning of nucleosomes and stabilizing the TFIID binding (Tomar et al., 2008). Besides TFIID, the full transcriptional activation of *RNR3* requires Gcn5, the catalytic subunit of the SAGA histone acetyltransferase complex (Zhang et al., 2008; Ghosh & Pugh, 2011). Other mechanisms regulate the expression of *RNR3*. In response to DNA damage, the Hrr25 kinase phosphorylates Swi6 and this is required for the *RNR3* transcriptional upregulation via the cell cycle regulator SBF complex (Swi6–Swi4) (Ho et al., 1997).

Rox1 and Mot3 are also Ssn6–Tup1-recruiting transcriptional repressors, but in this case, of hypoxic genes. Mot3 enhances the repression function of Rox1 by helping it in the recruitment of Ssn6–Tup1 (Klinkenberg et al., 2005). Besides, Rox1 and Mot3 bind the promoters of *RNR2/3/4*. The repression of *RNR3* by Crt1 together with the Rox1 and Mot3 repression works synergistically under non-stress conditions (Klinkenberg et al., 2006). Additionally, under DNA damage or genotoxic stress, Rox1 and Mot3 still repress *RNR3*, but in a weaker manner compared to when Crt1 is also attached (Klinkenberg et al., 2006).

Objectives

In the context of the model eukaryotic organism *Saccharomyces cerevisiae*, the present doctoral thesis aims to characterize the general translational repression and novel functions of Cth2 during the progress of iron starvation. For these purposes, this thesis has been divided in four chapters corresponding to the following objectives:

1. To decipher the molecular pathways involved in the general translational repression that occurs in response to iron deficiency, and how it affects particular transcripts.

2. To elucidate the role of Cth2 protein, its conserved domains, and AREs in the selective translational repression of specific mRNAs in response to iron deficiency.

3. To determine the contribution of Cth2 to mitochondrial respiration activities under iron-sufficient and iron-deficient conditions.

4. To characterize the molecular mechanisms that induce the expression of *RNR3* upon long-term iron deficiency.

Materials and Methods

Materials and Methods

1. Microbiological techniques in *Saccharomyces cerevisiae*

1.1. List of *Saccharomyces cerevisiae* strains

SPY number	Strain	Genotype	Source
SPY382	W303a prototroph	HTLU-2832-1B *MATa*, *HIS3, TRP1, LEU2, URA3, ADE2, can1*	Frederick R. Cross Lab
SPY1159	*ura3Δ*	W303a prototroph *ura3::hphB*	Romero et al., 2020.
SPY1160	*gcn2Δura3Δ*	W303a prototroph (SPY1159) *gcn2::KanMX4*	Romero et al., 2020.
SPY1012	*SUI2*	RS86 *MATa, ura3-52, leu2-3,-112, trp1-Δ63, Δsui2, Δp919*, [*SUI2, URA3*] pRS-65 [pRS414 *SUI2-TRP1]*	Hueso et al., 2012.
SPY1013	*SUI2-S51A*	RS88 *MATa ura3-52, leu2-3,-112, trp1-Δ63, Δsui2, Δp919*, [*SUI2, URA3*] pRS-67 [pRS414 *SUI2*-S51A-*TRP1*]	Hueso et al., 2012.
SPY17	BY4741	*MATa, his3Δ1, leu2Δ0, met15Δ0, ura3Δ0*	Research Genetics
SPY999	*gcn2Δ*	BY4741 *gcn2::KanMX4*	Research Genetics
SPY1146	*gcn1Δ*	BY4741 *gcn1::KanMX4*	Research Genetics
SPY245	*sdh4Δ*	BY4741 *sdh4::KanMX4*	Research Genetics
SPY122	*cth1Δcth2Δ*	BY4741 *cth1::KanMX4, cth2::His3MX6*	Puig et al., 2005.
SPY251	*cth1Δcth2Δsdh4Δ*	BY4741 *cth1::KanMX4, cth2::HisMX6, sdh4::hphB*	Puig et al., 2005.
SPY386	*fet3Δfet4Δ*	BY4741 *fet3::URA3, fet4::KanMX4*	Sanvisens et al., 2011.
SPY28	*aft1Δ*	BY4741 *aft1::KanMX4*	Research Genetics
SPY904	*aft1Δcth2Δ*	BY4741 (SPY25) *aft1::hphB, cth2::KanMX4*	Ramos-Alonso et al., 2018b.
SPY325	*cth1Δcth2Δ*	BY4741 (SPY25) *cth1::hphB, cth2::KanMX4*	Sanvisens et al., 2011.

SPY number	Strain	Genotype	Source
SPY387	W303-1a	*MATa, ade2-1, trp1-1, leu2-3,112, his3-11,15, ura3, can1-100, GAL+, psi+*	Seiko Ishida Lab
SPY391	*sml1Δ*	W303-1a *sml1::HIS3*	Yao et al., 2003.
SPY388	*dun1Δ*	W303-1a *dun1::HIS3*	Yao et al., 2003.
SPY390	*rad53Δsml1Δ*	W303-1a *rad53::HIS3, sml1::HIS3*	Yao et al., 2003.
SPY131	*cth1Δ*	BY4741 *cth1::KanMX6*	Puig et al., 2005
SPY25	*cth2Δ*	BY4741 *cth2::KanMX4*	Research Genetics
SPY556	*dun1Δ*	BY4741 *dun1::KanMX4*	Research Genetics
SPY452	*cth1Δcth2Δ*	BY4741 *cth1::hphB, cth2::His3MX6*	Fe homeostasis Lab
SPY454	*dun1Δcth1Δcth2Δ*	BY4741 (SPY556) *cth1::hphB, cth2::His3MX6*	Fe homeostasis Lab
SPY814	*crt1Δ*	BY4741 *crt1::KanMX4*	Research Genetics
SPY805	*cth1Δcth2Δcrt1Δ*	BY4741 (SPY452) *crt1::KanMX4*	This study
SPY813	*rox1Δmot3Δ*	BY4741 rox*1::KanMX4, mot3::His3MX6*	Markus Proft Lab
SPY818	*rox1Δmot3Δcth1Δ cth2Δ*	BY4741 (SPY813) *cth1::hphB, cth2::loxP*	This study
SPY819	*rox1Δmot3Δcrt1Δ*	BY4741 (SPY813) *crt1::loxP*	This study
SPY820	*rox1Δmot3Δcrt1Δ cth1Δcth2Δ*	BY4741 (SPY818) *crt1::loxP-LEU2-loxP*	This study
SPY998	*rnr3Δ*	BY4741 *rnr3::His3MX6*	This study

1.2. Liquid growth media

- Complete medium for yeast growth (YPD) was prepared with yeast extract 1 % (w/v), bacteriological peptone 2 % (w/v) and glucose 2 % (w/v). In the YPEG medium ethanol 2 % and glycerol 3 % were added instead of glucose.

- Synthetic complete medium (SC) and synthetic complete lacking specific requirements (SC minus) for selection of auxotrophic markers were prepared using specific amino acid drop-out supplements at 0.2 % (w/v) (Kaiser, Formedium). Besides, in both cases, they were prepared with yeast nitrogen base without amino acids and ammonium sulfate (Condalab) 0.17 % (w/v), $(NH_4)_2SO_4$ 0.5 % (w/v) and glucose 2 % (w/v). In some cases, galactose 2 % (w/v) was added instead of glucose.

- For iron-sufficient (+Fe) conditions with SC or SC minus media, ferrous ammonium sulfate (FAS, Sigma) was added in the indicated cases to a final concentration of 10 μM.

- For iron-deficient (-Fe) conditions with SC or SC minus media, bathophenanthrolinedisulfonic acid (BPS, Sigma), a specific Fe^{2+} chelator, was always added to a final concentration of 100 μM. Only in the analysis of cell growth experiments (section 1.4 of Materials and Methods) different BPS concentrations or another Fe^{2+} specific chelator, 3-(2-Pyridyl)-5,6-diphenyl-1,2,4-triazine-4′,4′′-disulfonic acid sodium (ferrozine, Fz, Sigma), were used as indicated in each case.

- For genotoxic stress conditions, SC medium was supplemented during 1 hour with hydroxyurea (HU, Sigma) to a final concentration of 0.2 M, methyl methanesulfonate (MMS, Sigma) at 0.04 %, or 4-nitroquinoline N-oxide (4-NQO, Sigma) at 0.2 mg/L.

- Minimal medium (SD) was mostly used in the determination of iron-dependent enzymatic activities (section 4.6 of Materials and Methods). The medium was prepared as SC, but without drop-out supplementation. Only requirements corresponding to the auxotrophic mutations were added if necessary, at the concentrations of the Kaiser (Formedium) drop-out (histidine 76 mg/L, leucine 380 mg/L, methionine 76 mg/L and uracil 76 mg/L). In the SD +Fe condition, 50 μM of ferric ammonium citrate (FAC) was added to the SD medium, whereas the SD -Fe condition corresponded to an iron-free SD medium (yeast nitrogen base without amino acids, ammonium sulphate and iron, Formedium) without the addition of any metal chelator.

- SD with 3-aminotriazole (3-AT) was used as control treatment to trigger amino acid starvation, since it inhibits the product of the *HIS3* gene and therefore, histidine biosynthesis. Times and concentrations used are indicated in each case.

1.3. Solid growth media

Solid media were obtained by adding bacteriological agar to a final concentration of 1.5 % (w/v) to the liquid media before autoclave sterilization. BPS, ferrozine and 3-AT were added before pouring the solution. For antibiotic resistance selection, Geneticin (G418, Gibco Life Technologies) was added to a final concentration of 200 µg/mL and Hygromycin B (Invivogen) to a final concentration of 300 µg/mL. SC-Ura plates with 5-Fluoroorotic Acid (5-FOA) were used for selection of *ura3Δ* cells (5-FOA 0.1 % (w/v) and uracil 12 mg/L).

1.4. Analysis of cell growth

Individual colonies were cultivated at 30 °C overnight in 3 mL of the appropriate SC minus medium for selection of auxotrophic markers. Later on, cells were reinoculated in 3 mL of fresh medium to an OD_{600} of 0.2 for 4-6 hours at 30 °C, allowing 2-3 yeast duplications events. At least three biological replicates were used to study yeast cell growth in different liquid and solid media.

In liquid media, cells were washed and the OD_{600} was adjusted to 1.0 with sterile distilled water. 10 µL of cells were inoculated per well in a 96-well plate, previously filled with 260 µL of the liquid medium indicated in each case. The OD_{600} was monitored in a SPECTROstar Omega instrument (BMG Labtech, Offenburg, Germany) every 30 min during 3-4 days at 30 °C, with 20 sec of shaking at 500 rpm before each measurement. Mean values of the growth curves (OD_{600} vs. time) were represented and the maximum OD_{600} mean values were determined. Besides, the μ_{max} (maximum specific growth rate, h^{-1}) parameter was calculated from each well using the reparameterized Gompertz equation (Zwietering et al., 1990),

$$\ln (OD_t/OD_0) = D * e^{\wedge} \{-e^{\wedge}[((\mu_{max}*e)/D)*(\lambda - t) + 1]\}$$

where OD_0 is the initial OD_{600} and OD_t is the OD_{600} at time t; $D = \ln(OD_\infty/OD_0)$ is the OD_{600} value reached with OD_∞ as the asymptotic maximum, and λ is the lag phase period (h).

In solid media, cell cultures were diluted to an OD_{600} of 0.1 and then two 10-fold serial dilutions were performed (1:10, 1:100). Approximate volumes of 3 µL were plated onto the agar media with the replicate plater for 96-well plate (Sigma). Plates were incubated at 30 °C for 4-10 days and images of the plates were taken every 2-3 days.

1.5. Cell viability

Cell viability was determined by counting in YPD agar plates the number of Colony Forming Units (CFUs) of a strain that was previously subjected to iron deficiency. Three independent exponential phase cultures were cultivated in both iron-sufficient and iron-deficient conditions. The OD_{600} was measured, and 10-fold serial dilutions were performed for plating and counting between 30-300 CFUs after 2-3 days of incubation at 30 °C. Then, cell viability was calculated as (CFUs x dilution) / OD_{600}. Relative viabilities at the different times of the iron deficiency were represented compared to the iron-sufficient condition.

2. Microbiological and molecular techniques in *Escherichia coli*

2.1. *E. coli* strains

Subcloning Efficiency™ DH5α Competent Cells (Invitrogen, ThermoFisher Scientific). Genotype: F^- φ80*lac*ZΔM15 Δ(*lac*ZYA-*arg*F)U169 *rec*A1 *end*A1 *hsd*R17(r_k^-, m_k^+) *pho*A *sup*E44 *thi*-1 *gyr*A96 *rel*A1 λ-

One Shot® TOP10 Chemically Competent *E. coli* (Invitrogen, ThermoFisher Scientific). Genotype: F^- *mcr*A Δ(*mrr-hsd*RMS-*mcr*BC) φ80*lac*ZΔM15 Δ*lac*X74 *rec*A1 *ara*D139 Δ(*ara-leu*) 7697 *gal*U *gal*K *rps*L (Str^R) *end*A1 *nup*G λ-

2.2. Growth conditions

The Lysogeny Broth (LB) medium was used to grow *E. coli*: NaCl 1 % (w/v), tryptone 1 % (w/v) and yeast extract 0.5 % (w/v). For LB agar plates, 1.5 % (w/v) of agar was added. In both cases, ampicillin (50 µg/mL) was used to select the bacteria with the plasmids containing the antibiotic-resistance gene.

2.3. Plasmid construction

The DNA sequences for cloning (insert) were amplified by the polymerase chain reaction (see section 3.1 of Materials and Methods) using oligonucleotides with restriction sites that flanked the insert. After PCR product purification (Illustra GFX PCR DNA and Gel Band Purification Kit, GE Healthcare) the plasmid and the insert were digested with restriction enzymes according to manufacturer's instructions. Then, the removal of the 5' phosphate from the plasmid was made for preventing recircularization (FastAP Thermosensitive Alkaline Phosphatase, Thermo Scientific). Finally, both digested DNAs were isolated by gel purification (Illustra GFX PCR DNA and Gel Band Purification Kit, GE Healthcare) to subsequent ligation (Rapid DNA Ligation Kit, Roche).

2.4. *E. coli* transformation and plasmid extraction

The competent *E. coli* strains One Shot® TOP10 and DH5α (see section 2.1 of Materials and Methods) were used for propagation of newly ligated and already verified plasmids, respectively. Transformation was made according to manufacturer's instructions. For posterior plasmid extraction, the GeneJET Plasmid Miniprep Kit (Thermo Scientific) was used. In the case of new constructs, plasmids coming from several individual colonies were analyzed by PCR and/or restriction enzyme digestion followed by DNA sequencing to check the position and sequence of the insert.

2.5. List of plasmids

pSP number	Plasmid description	Source
pSP1116	p180: pRS416-*GCN4-lacZ*	Hinnebusch, 1985.
P37	pRS413	Sikorski & Hieter, 1989.
P127	pFA6-pAG32-hphMX4	Goldstein & McCusker, 1999.
pSP888	pRS416-Flag$_2$-*SDH4*	Ramos-Alonso et al., 2018a.
pSP527	pRS416-*SDH4*	Puig et al., 2005.
pSP889	pRS416-Flag$_2$-*SDH4-AREmt*	Ramos-Alonso et al., 2018a.
pSP528	pRS416-*SDH4-AREmt*	Puig et al., 2005.
pSP419	pRS415-*CTH2*	Puig et al., 2005.
P39	pRS415	Sikorski & Hieter, 1989.

pSP number	Plasmid description	Source
pSP571	pRS415-*CTH2-C190R*	Puig et al., 2005.
pSP414	pRS416-Flag$_2$-*CTH2*	Puig et al., 2005.
pSP760	pRS416-Flag$_2$-*CTH2-AREmt*	Martínez-Pastor et al., 2013a.
pSP410	pRS416-*CTH2*	Puig et al., 2005.
pSP758	pRS416-*CTH2-AREmt*	Puig et al., 2005.
pSP429	pRS416-Flag$_2$-*CTH2-C190R*	Martínez-Pastor et al., 2013a.
pSP427	pRS416-*CTH2-C190R*	Puig et al., 2005.
pSP457	pRS416-*GFP-CTH2*	Vergara et al., 2011.
pSP724	pRS416-*GFP-ΔN89-CTH2*	Vergara et al., 2011.
pSP464	pRS416-*GFP-ΔN170-CTH2*	Ramos-Alonso et al., 2018a.
pSP465	pRS416-*GFP-ΔC52-CTH2*	Ramos-Alonso et al., 2018a.
pSP949	pRS415-Flag$_2$-*SDH4*	Ramos-Alonso et al., 2018a.
pSP569	pRS415-*SDH4*	Puig et al., 2005.
pSP529	pRS415-*GAL1-SDH4*	Puig et al., 2005.
P40	pRS416	Sikorski & Hieter, 1989.
pSP449	p416-*TEF*-Flag$_2$-*CTH2*	Sato et al., 2018.
pSP450	p416-*TEF*-Flag$_2$-*CTH2-C190R*	Sato et al., 2018.
pSP486	p416-*TEF-CTH1*	Puig et al., 2008.
pSP487	p416-*TEF-CTH1-C225R*	Fe homeostasis Lab
P175	pRS316-*AFT1-1UP(C291F)*	Rutherford et al., 2001.
pSP425	p416-*TEF-CTH2*	Puig et al., 2008.
P139	pUG73 (*LEU2, Kluyveromyces lactis*)	Gueldener et al., 2002.
P140	pSH47 (*GAL1-cre*)	Güldener et al., 1996.
P3	pFA6a-His3MX6	Wach et al., 1997.
pSP638	pRS416-*RNR3-lacZ*	Klinkenberg et al., 2006.

3. General molecular biology techniques

3.1. Polymerase chain reaction (PCR)

PCR was used to amplify DNA fragments and generate deletion cassettes, cloning inserts and to test yeast transformants and constructed plasmids. The DNA polymerases Expand High Fidelity (Roche) or Phusion High-Fidelity (Finnzymes) were used when 3'-5' exonuclease activity was needed. When the proofreading

activity was not required, the DNA polymerase Biotaq (Bioline) was used. The list of oligonucleotides used in PCR are listed in the section 3.2 of Materials and Methods. The PCR was performed in a thermocycler (Mastercycler personal, Eppendorf). PCR cycles consisted of an initial denaturing step at 95 °C, several amplification cycles divided in 3 steps (denaturation, annealing and elongation) and a final extension step. Durations and temperatures depended on the DNA polymerase used and the size to amplify. Manufacturer's instructions were followed.

3.2. List of oligonucleotides for PCR

SPO number	Primer	Primer sequence 5'-3'	Use
SPO2077	*URA3-pAG-F*	TCTTAACCCAACTGCACAGAAC AAAAACCTGCAGGAAACGAAGA TAAATCATG**GTACGCTGCAGGT CGACA**	SPY1159 construction (*ura3::hphB* from pAG32)
SPO2078	*URA3-pAG-R*	GCTCTAATTTGTGAGTTTAGTA TACATGCATTTACTTATAATAC AGTTTT **ACTAGTGGATCTGAT ATC**	SPY1159 construction (*ura3::hphB* from pAG32)
SPO2041	*GCN2-294 F*	GGACTATAGTGATGTAGGTAG	SPY1160 construction (*gcn2::KanMX4* from SPY999)
SPO2043	*GCN2+124 R*	GGTGACCTACCCCCTTTACA	SPY1160 construction (*gcn2::KanMX4* from SPY999)
SPO2040	*GCN2-383 F*	GACGTGCAAGGGCCTGCTTG	SPY1160 *gcn2::KanMX4* verification
SPO1318	*CRT1-193-F*	CTCGTGGCTCACCTATGGAT	SPY805 construction (*crt1::KanMX4* from SPY814)
SPO1320	*CRT1+209-R*	CTCATCACTCCATCTCATCCTAT	SPY805 construction (*crt1::KanMX4* from SPY814) and SPY819 *crt1::loxP* verification
SPO1319	*CRT1-251-F*	GTAGCGCCACTCCACGATAT	SPY805 *crt1::KanMX4*, SPY819 *crt1::LEU2-loxP* and SPY819 *crt1::loxP* verifications
SPO1104	*Kan-R-atg*	GTGAGTCTTTTCCTTACCCAT	SPY805 *crt1::KanMX4* verification
SPO1200	*CTH1-300-F*	GTCTGTGCCAATGGCACCCAA	SPY818 construction (*cth1::hphB* from SPY325)
SPO1201	*CTH1+300-R*	ACAAAGCCGATCATTTGGCAA	SPY818 construction (*cth1::hphB* from SPY325)

SPO number	Primer	Primer sequence 5'-3'	Use
SPO1199	*CTH1-500-F*	CGCGGATCCATACCAACCGACAG CATGGGAAA	SPY818 *cth1::hphB* verification
SPO1148	*hphB:500-R*	GGTCGGAGACGCTGTCGAACT	SPY818 *cth1::hphB* verification
SPO1094	*CTH2-43-pUG-F*	GTTGTTGGGACTTGGAGGCTCT TGGTAGGTCGTATTTGTGCATC TTGAGAGAAA**CAGCTGAAGCTT CGTACGC**	SPY818 construction (*cth2::LEU2-loxP* from PUG73)
SPO1095	*CTH2-pUG-R*	TGTTTAGTTGAGACGCCGGTCT TCGCCAGGCCAGGAATTGTTT**C ATAGGCCACTAGTGGATCTG**	SPY818 construction (*cth2::LEU2-loxP* from PUG73)
SPO1205	*CTH2-340-F*	CGCGGATCCAGCCCATTTGCGTC TTC	SPY818 *cth2::LEU2-loxP* verification
SPO1016	*LEU2-B-R*	AGTTATCCTTGGATTTGG	SPY818 *cth2::LEU2-loxP* and SPY819 *crt1::LEU2-loxP* verifications
SPO1204	*CTH2-500-F*	CGCGGATCCCCAGCCCAGAGGGT TCAAACGTT	SPY818 *cth2::loxP* verification
SPO1214	*CTH2+300-R*	TGGGCCGATGTTCAAGGAATA	SPY818 *cth2::loxP* verification
SPO1328	*CRT1-pUG-F*	TGTCATGGCGATTTGGGAAAAA GTTGAAAAAAAAAATAGCAGTA A**CAGCTGAAGCTTCGTACGC**	SPY819 construction (*crt1::LEU2-loxP* from pUG73)
SPO1329	*CRT1-pUG-R*	GTTATATTCTTTTTTAAATATC CCCATATACTAATGATAGAACT T**GCATAGGCCACTAGTGGATC TG**	SPY819 construction (*crt1::LEU2-loxP* from pUG73)
SPO1852	*RNR3-F1*	CAAGAATAGCAGCAGCAATAAA TCAAATACTCCCACACAA**CGGA TCCCCGGGTTAATTAA**	SPY998 construction (*rnr3::His3MX6* from pFA6a-His3MX6)
SPO1853	*RNR3-R1*	CCAAGTTAGATAAGGAAAGGGA AAAATGCCACCAGAAAGA**GAAT TCGAGCTCGTTTAAAC**	SPY998 construction (*rnr3::His3MX6* from pFA6a-His3MX6)
SPO1854	*RNR3-269-F*	TGCCATGGCGAGGACCAAAC	SPY998 *rnr3::His3MX6* verification
SPO1014	*TEFprom-R*	GGGCGACAGTCACATCAT	SPY998 *rnr3::His3MX6* and SPY1160 *gcn2::KanMX4* verifications

3.3. Agarose gel electrophoresis

DNA size determination and separation, as well as the RNA quality control, were carried out in 1.0 or 1.5 % (w/v) agarose gels. Agarose was dissolved in the electrophoresis buffer TAE 1x (Tris Base 40 mM, glacial acetic acid 20 mM, EDTA pH 8.0 1 mM). When the solution was tempered, 2 µL of GreenSafe Premium nucleic acid stain (Nzytech) were added per 100 mL. The 1 Kb Plus DNA Ladder (Invitrogen, ThermoFisher Scientific) or the FastGene 50 bp DNA Ladder (NIPPON Genetics) were used for estimating the size of large and small DNA products, respectively. Nucleic acids were resuspended in DNA Gel Loading Dye (Thermo Scientific) and visualized under UV illumination.

4. Molecular biology techniques in *Saccharomyces cerevisiae*

4.1. DNA-related molecular techniques

4.1.1. Genomic DNA extraction

Genomic DNA (gDNA) was obtained from a 10 mL yeast overnight culture grown in YPD at 30 °C. The culture was centrifuged at 4000 rpm for 2 min and washed with sterile distilled water. Then, cells were resuspended in 200 µL of lysis buffer (Triton X-100 2 %, SDS 1 %, NaCl 100 mM, Tris-HCl pH 8.0 10 mM) and transferred into a screw-cap tube already containing 300 µL of sterile glass beads and 200 µL of phenol:chloroform:isoamyl alcohol (25:24:1) saturated with 10 mM Tris-HCl pH 8.0 and 1 mM EDTA (Sigma). Cells were broken using the Millmix 20 bead beater (Tehtnica) with 3 shaking cycles of 30 sec each. A volume of 200 µL of TE 1x buffer (Tris-HCl pH 8.0 10 mM, EDTA 1 mM) was added to each tube and they were centrifuged at 12000 rpm for 5 min. The aqueous layer was transferred into a fresh tube, and nucleic acids were precipitated with 1 mL of 96 % ethanol. Each sample was again centrifuged at 12000 rpm for 5 min and the pellet was resuspended in 400 µL of TE 1x buffer. A volume of 30 µL of RNase A (1 mg/mL) was added to eliminate the RNA contaminants during 1 hour at 37 °C. DNA was then precipitated by adding 10 µL of ammonium acetate 4 M and 1 mL of 96 %

ethanol. Finally, after centrifuging at 12000 rpm for 5 min and washing with 96 % ethanol, the dried DNA pellet was resuspended in 100 µL of TE 1x buffer.

4.1.2. Obtention of new strains by gene disruption

The disruption of genes was carried out with deletion cassettes generated by PCR (see section 3.1 of Materials and Methods) that allowed auxotrophic or antibiotic resistance selection. The PCR products were concentrated by precipitation with 2.5 volumes of 96 % ethanol and 0.1 volumes of sodium acetate 3 M, washed with 70 % ethanol, dried and resuspended in sterile water before yeast transformation. In some cases, *loxP*-flanked gene disruption cassettes were generated from the pUG73 plasmid (Gueldener et al., 2002). This allowed the later marker rescue using the *cre* expression plasmid pSH47 (see the list of plasmids in section 2.5 of Materials and Methods). The expression of the Cre recombinase was induced by cultivating the transformants 2 hours in galactose-containing medium, as detailed in Güldener et al. (1996). The loss of the marker gene was verified by PCR and by plating in selective and non-selective media. The later selection of mutants without the *cre* plasmid was performed by plating in 5-FOA (see section 1.3 of Materials and Methods)

4.1.3. Yeast transformation

Yeast transformation with plasmids or with deletion cassettes was carried out following the lithium acetate-based method (Gietz & Woods, 2002). After thermal shock, transformants selected by antibiotic resistance were incubated 2 hours in YPD at 30 °C before plating in the selective medium. Selection plates were incubated at 30 °C for 2-3 days.

4.1.4. Chromatin immunoprecipitation (ChIP)

To perform chromatin immunoprecipitation (chIP) analysis, 25 OD_{600} units (in a total volume of 50 mL) were collected for each exponential phase culture. The protein-chromatin cross-linking was made by adding 1.35 mL of formaldehyde 37 % and incubating 15 min at room temperature with occasional mixing. Then, a volume of 2.5 mL of glycine 2.5 M was added to each sample and, after 5 min, the samples were placed on ice. After centrifuging at 4000 rpm for 5 min at 4 °C, cells

were washed 4 times with 20 mL of TBS pH 7.5 (Tris Base 25 mM, NaCl 15 mM) and snap frozen in liquid nitrogen.

Pelleted cells were then resuspended in 300 µL of lysis buffer (HEPES pH 7.5 50 mM, NaCl 140 mM, EDTA pH 8.0 1 mM, Triton X-100 1 %, sodium deoxycholate 0.1 %, PMSF 1 mM, benzamidine 1 mM and cOmplete™ Protease Inhibitor Cocktail) and transferred into screw-cap tubes containing 300 µL of glass beads. Cells were broken using the Precellys 24 homogeniser (Bertin Technologies) in two rounds of 20 sec at 6500 rpm. Then, 150 µL of lysis buffer were added and glass beads were eliminated by centrifugation at 2000 rpm for 1 min at 4 °C. Cell lysates were then sonicated in a chilled water bath using Bioruptor (Diagenode) to generate chromatin fragments between 300-600 base pairs. After a centrifugation at 12000 rpm for 5 min at 4 °C, 10 µL of each supernatant were transferred into new tubes and maintained on ice (INPUT samples). The rest of supernatants (IP samples) were incubated (2 h and 30 min at 4 °C) with magnetic beads Dynabeads™ Pan Mouse IgG (Invitrogen, ThermoFisher Scientific) previously overnight combined with the monoclonal antibody that recognizes Rpb1, the largest subunit of the RNA polymerase II (8WG16, BioLegend).

Once the incubation finished, samples were centrifuged at 3000 rpm for 1 min at 4 °C and supernatants were removed using a magnetic rack. Then, successive washes were performed: twice with 1 mL of lysis buffer, twice with 1 mL of lysis buffer containing NaCl 360 mM, twice with 1 mL of wash buffer (Tris-HCl pH 8.0 10 mM, LiCl 250 mM, NP-40 0.5 %, sodium deoxycholate 0.5 %, EDTA pH 8.0 1 mM) and once with 1 mL of TE buffer (Tris-HCl pH 8.0 10 mM, EDTA 1 mM).

Following washing, 50 µL of elution buffer (Tris-HCl pH 8.0 50 mM, EDTA pH 8.0 10 mM, SDS 1 %) were added to elute the samples from the Dynabeads during 10 min at 600 rpm at 65 °C (Thermomixer, Eppendorf). A volume of 40 µL of supernatant was transferred into a new tube, and the elution process was repeated again with 30 µL more of elution buffer. Finally, additional elution buffer was added to all supernatants (IP and INPUT samples) to a final volume of 150 µL. A posterior 15 h incubation at 600 rpm at 65 °C was performed to reverse cross-linking.

To finally obtain the DNA, each sample was treated with 7.5 µL of Proteinase K (Roche) and 142.5 µL of TE buffer at 600 rpm at 37 °C during 1 h 30 min. Next, DNA was purified using the GeneJet PCR Purification kit #K0702 (Fermentas) according to the manufacturer's instructions. Specific binding of Rbp1 protein (RNA polymerase II) to DNA fragments was analyzed by quantitative PCR (qPCR, end of section 4.2.1 of Materials and Methods). IP samples were tested undiluted and INPUT samples were tested at 1/100 dilution.

4.2. RNA related molecular techniques

4.2.1. Quantitative reverse transcription PCR (RT-qPCR)

- RNA extraction

A volume of an exponential phase culture corresponding to 5.0 OD_{600} units was centrifuged at 4000 rpm for 2 min. The cell pellet was washed with cold distilled water, snap frozen and stored at -80 °C. Then, cells were resuspended in 500 µL of cold LETS buffer (LiCl 0.1 M, EDTA pH 8.0 10 mM, Tris-HCl pH 7.4 10 mM, SDS 0.2 %) and transferred into a screw-cap tube already containing 500 µL of sterile glass beads and 400 µL of phenol:chloroform (5:1). Then, cells were broken using the Millmix 20 bead beater (Tehtnica) with 3 shaking cycles of 30 sec each, and 30 sec of incubation on ice in between. After centrifugation at 13000 rpm for 5 min at 4 °C, the supernatant was transferred into a new tube containing 400 µL of phenol:chloroform (5:1) and then to a tube containing 400 µL of chloroform:isoamyl alcohol (25:1). The RNA from the top phase was precipitated, with 2.5 volumes of cold 96 % ethanol and 0.1 volumes of LiCl 5 M, during 3 hours at -80 °C or overnight at -20 °C. After 15 min of centrifugation and rinsing with cold 70 % ethanol, the pellet was dried and resuspended in RNase-free milliQ water. A second step of RNA precipitation was performed adding 2.5 volumes of cold 96 % ethanol and 0.1 volumes of sodium acetate 3 M. Once pelleted, washed and dried as before, the RNA of each sample was resuspended again in RNase-free milliQ water for later RNA quantification and quality control with NanoDrop and agarose gel electrophoresis, respectively.

- Treatment with DNase I

The DNA of each sample was removed from 1 µg of RNA using the DNase I RNase-free (Roche) for 15 min at 25 °C in a final volume of 10 µL. To inactivate the DNase I, a volume of 0.625 µL of EDTA 2 mM was added and incubated 10 min at 65 °C.

- cDNA synthesis

The RNA retrotranscription into cDNA was performed with 2.5 µL of DNA-free RNA in a final volume of 10 µL using the Thermo Scientific Maxima Reverse Transcriptase (200 U/µL). The manufacturer's instructions were followed for both oligo dT and random primers application scenarios.

- Quantitative PCR (qPCR)

The qPCR is the last step in the RT-qPCR and ChIP protocols. In both cases, the qPCR was carried out using the LightCycler® 480 Instrument II and 5 µL of SYBR Green Premix Ex Taq (Tli RNase H Plus, TaKaRa) for a total reaction volume of 10 µL. A cDNA pool with all samples was made and serial dilutions (1/5, 1/10, 1/50, 1/100, 1/500 and 1/1000) were used to generate a calibration curve for each primer pair in each experiment. A volume of 2.5 µL of cDNA (1/40 dilution) and 0.2 µL of each 10 µM primer were added to a final volume of 10 µL for RT-qPCR; and 2 µL of DNA and 0.4 µL of each 10 µM primer were added for ChIP experiments. The list of oligonucleotides used in qPCR are listed in the section 4.3 of Materials and Methods. For amplification, the PCR conditions consisted of an initial denaturing cycle (95 °C for 10 sec) and 40 amplification cycles (annealing at 55 °C for 10 sec and extension at 95 °C for 15 sec). Then, the melting curves generated with each primer pair confirmed the specificity of the PCR reaction. The cycle threshold (Ct) value of each sample was used to determine the amount of cDNA or DNA in each case by interpolation to respective calibration curves.

4.2.2. mRNA stability determination

The *SDH4* mRNA half-life determination was performed using a fusion of the *GAL1* promoter with *SDH4* coding sequence (pSP529, list of plasmids in section 2.5 of Materials and Methods). Cells were grown overnight in SC-Ura-Leu, for selection of auxotrophic markers, with raffinose 2 % (w/v) at 30 °C. Later on, cells were reinoculated to an OD_{600} of 0.2 in fresh SC-Ura-Leu -Fe (BPS 100 µM) medium with

galactose 2 % (w/v) at 30 °C during 4 hours. Then, glucose was added to a final concentration of 4 % (w/v) to inhibit the *GAL1* promoter transcription. Aliquots of cells at 0, 5, 10 and 15 min were taken for RT-qPCR experiments using random primers for cDNA synthesis (see section 4.2.1 of Materials and Methods). The *SDH4/PGK1* mRNA relative half-life was determined as follows: $t_{½} = \ln 2/k_D$

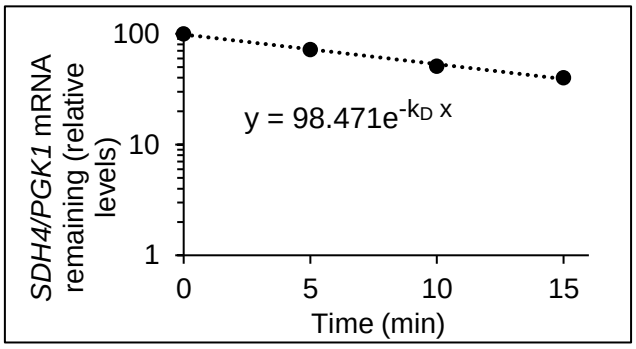

4.2.3. Polysome fractionation

- Sample preparation

To perform polyribosome profile analyses, a volume of an exponential phase culture (OD_{600} between 0.6-1.0) corresponding to 60 OD_{600} units was separated into two equal volumes in 50 mL conical tubes. Then, 100 µL of cycloheximide (10 mg/mL) were added per 10 mL of the cell culture, to a final concentration 0.1 mg/mL. These tubes were incubated 5 min on ice with occasional mixing to block translational elongation. After centrifugation at 4000 rpm for 5 min at 4 °C, cells from the same sample were unified and resuspended in 2 mL of cold lysis buffer (Tris-HCl pH 8.0 20 mM, KCl 140 mM, $MgCl_2$ 5 mM, DTT 0.5 mM, cycloheximide 0.1 mg/mL, heparin 0.5 mg/mL, Triton X-100 1 %). Cells were again washed and centrifuged in the same conditions, for later being resuspended in 700 µL of lysis buffer. The entire volume was transferred into a 2 mL screw-cap tube containing 500 µL of glass beads. Cells were broken by vortexing 8 times during 30 sec, with 30 sec of incubation on ice in between. After centrifugation at 5000 rpm for 5 min at 4 °C, the supernatant was transferred into a new tube and centrifuged again at 8000 rpm for 5 min at 4 °C. RNA from the supernatant was quantified, verifying

that the ratio A_{260nm}/A_{280nm} is higher than 2. Glycerol was added to a final concentration of 5 % and samples were snap frozen and stored at -80 °C.

- Preparation and detection of sucrose gradients

For the preparation of 6 sucrose gradients, 50 mL of sucrose 10 % (solution A) and 55 mL of sucrose 50 % (solution B) were prepared from a 70 % (w/v) sucrose stock and, in both cases, Tris-HCl pH 8.0 20 mM, KCl 140 mM, $MgCl_2$ 5 mM, DTT 0.5 mM, cycloheximide 0.1 mg/mL and heparin 1 mg/mL. The polysome fractioner was used for the gradients preparation and posterior detection (Density Gradient Fractionation System; Teledyne Isco, Lincoln, NE). Then, 8.5 A_{260nm} units of each sample were loaded onto the gradients. The solution A was used to balance the tubes for the ultracentrifuge (Beckman SW41 Rotor) that ran at 35000 rpm for 2 h 40 min at 4 °C. For the detection of gradients, sucrose 60 % was used as pump solution. The ultraviolet detection at A_{260nm} generated the general polyribosome profiles and the outgoing gradient fractions were collected in aliquots that were snap frozen and stored at -80 °C (outline of the process in **Figure M-1**).

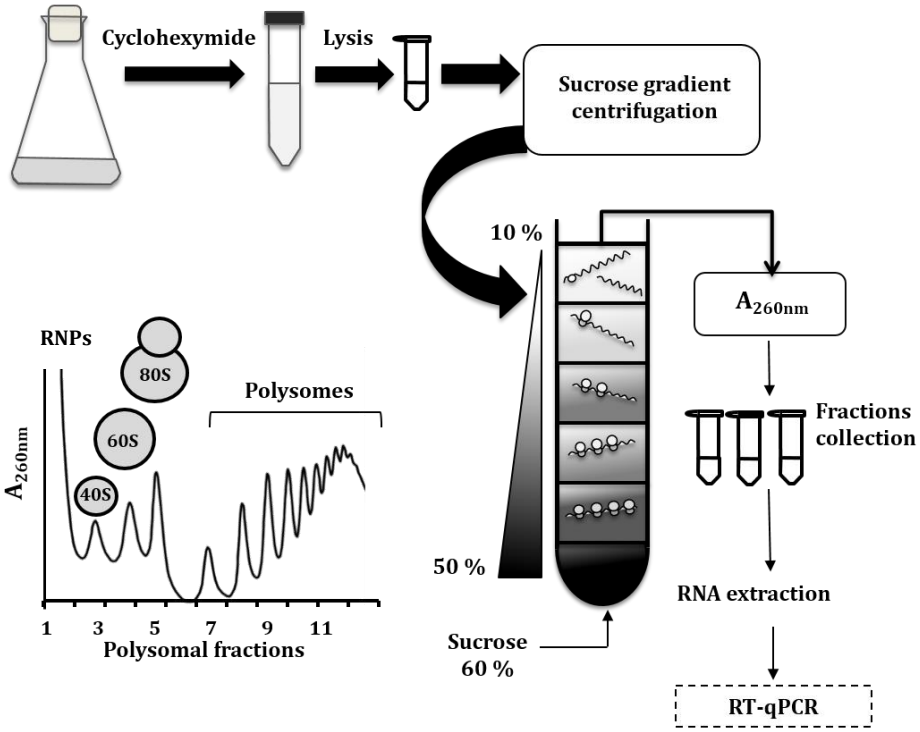

Figure M-1. Schematic representation of the polysome fractionation protocol explained in section 4.2.3 of Materials and Methods. The general polysome profile represented shows, from lighter to heavier fractions, the ribonucleoproteins (RNPs), the total mRNAs bound to ribosomal subunits (40S and

60S), monosomes (80S) and polysomes. The ratio polysomes/(ribosomal subunits + monosome 80S) or polysomes/monosome 80S is associated with the mRNAs translational state as higher polysome abundance is usually correlated with greater translation efficiency.

- RNA extraction of polysome fractionation samples

The RNA extraction was performed from 200 µL of each fraction, to which 8 µL of the mRNAs *phe* and *lys* (6 ng/µL each) from *Bacillus subtilis* were added as control of the RNA extraction. The SpeedTools Total RNA Extraction kit (Biotools B&M Labs) was used according to manufacturer's instructions (following the alternative protocol of DNA digestion post-elution and ethanol precipitation for salts removal). The distribution of specific mRNAs in general polyribosome profiles was analyzed by RT-qPCR (see section 4.2.1 of Materials and Methods from cDNA synthesis) using 3.5 µL of DNA-free RNA (instead of 2.5 µL) in a final volume of 10 µL.

4.3. List of oligonucleotides for qPCR

SPO number	qPCR Primer	Primer sequence 5'-3'
SPO1119	*Oligo dT*	TTTTTTTTTTTTTTTVN
SPO1120	*ACT1-qPCR-F*	TCGTTCCAATTTACGCTGGTT
SPO1121	*ACT1-qPCR-R*	CGGCCAAATCGATTCTCAA
SPO1338	*RPS16B-qPCR-F*	GACGAACAATCCAAGAACGA
SPO1339	*RPS16B-qPCR-R*	AGAACGAGCACCCTTACCAC
SPO1699	*RPL3-qPCR-F*	CGAAGCTGTCACCGTTGTTG
SPO1700	*RPL3-qPCR-R*	AAATGTTCAGCCCAGACGGT
SPO2083	*phe-qPCR-F*	CATGGATGCTGTTTTTCCAT
SPO2084	*phe-qPCR-R*	GCACCTGACCTATCCTCCAA
SPO2085	*lys-qPCR-F*	CGAGCAAAGCATTCTCATCA
SPO2086	*lys-qPCR-R*	AGCTCTCTCCGGATACGACA
SPO1299	$Flag_2$-*SDH4*-qPCR-F	TTGATCTTTCCTACGCTTTCG
SPO1300	$Flag_2$-*SDH4*-qPCR-R	TCGTCCTTGTAGTCGCCTTT
SPO1149	*PGK1-qPCR-F*	AAGCGTGTCTTCATCAGAGTTG
SPO1150	*PGK1-qPCR-R*	CGTATCTTGGGTGGTGTTCC
SPO1134	*SDH4-qPCR-F*	GCACTCCCAATGATGCCTAC
SPO1135	*SDH4-qPCR-R*	AATGGAACGACGGACAAGG
SPO1130	*CTH2-qPCR-F*	GCAGTTTCATTCTCTCCAC

SPO number	qPCR Primer	Primer sequence 5'-3'
SPO1131	*CTH2-qPCR-R*	TAGGTGCCGTGCTATTCAGG
SPO1310	*CCP1-qPCR-F*	ACTCGCAATCCCAAAAGAGA
SPO1311	*CCP1-qPCR-R*	CGGTGTAGTGGAAGCCAAAG
SPO1156	*HEM15-qPCR-F*	CCAAAGTTGATGGCCTAATG
SPO1157	*HEM15-qPCR-R*	TATTCCGATTCCCCAATGAC
SPO1132	*WTM1-qPCR-F*	TCCTGACGATACCATTGCTC
SPO1133	*WTM1-qPCR-R*	TCTTCTGCTTCCACCCTTGT
SPO1306	*ACO1-qPCR-F*	GCCATCAAGAGACCCATTGT
SPO1307	*ACO1-qPCR-R*	ATCCAGCGTTTCCACATTCT
SPO1178	*LEU1-qPCR-F*	GCCAGACAAGGTATCGTCCA
SPO1179	*LEU1-qPCR-R*	TGAGTAGAGGTATGAGAGTCACCA
SPO2015	*COX1-qPCR-F*	GTATGGCAGGAACAGCAATGT
SPO2016	*COX1-qPCR-R*	ATGCTGTATCTGTAGCTCCA
SPO1663	*COX2-qPCR-F*	AGTTGATGCTACTCCTGGTAGA
SPO1664	*COX2-qPCR-R*	CATGACCTGTCCCACACAAC
SPO2017	*COX3-qPCR-F*	TCTTTGCTGGTTTATTCTGAGC
SPO2018	*COX3-qPCR-R*	TCAATACCTACGGGTGGTCAA
SPO2013	*COX4-qPCR-F*	TCAAGCCAGCCACAAGAAC
SPO2014	*COX4-qPCR-R*	AGCACCAGGACCAATCAAAG
SPO1736	*COX6-qPCR-F*	CGCAAGATACGAAAAGGAGT
SPO1737	*COX6-qPCR-R*	TCAATAACAGCAGGAGCAG
SPO1747	*SDH1-qPCR-F*	GCCAATTCCTTGTTGGATCTTG
SPO1748	*SDH1-qPCR-R*	TGGCAACCCAGGCTGTAAAG
SPO1182	*SDH2-qPCR-F*	CGAAGAAGGGTATGGCTACTG
SPO1183	*SDH2-qPCR-R*	CACTTGGCTCGTCTGGATT
SPO1726	*SDH3-qPCR-F*	CTCTTCGGAGTCTCTGGTTT
SPO1727	*SDH3-qPCR-R*	CGGTATCCCAGATCAAGTGT
SPO1227	*RIP1-qPCR-F*	GGTCGGTGCTATGGGTCTTT
SPO1228	*RIP1-qPCR-R*	CAAAACATCGGCAGTAGCGG
SPO1180	*CYC1-qPCR-F*	AGATGTCTACAATGCCACACC
SPO1181	*CYC1-qPCR-R*	CCCTTCAGCTTGACCAGAGT
SPO1885	*CYT1-qPCR-F*	CTTGACAGAGTTGCTTGGAG
SPO1886	*CYT1-qPCR-R*	CCTTGTTCATCAGGTTCGTC
SPO1186	*RNR3-qPCR-F*	CTGAACAAAAGGCGGCATC
SPO1187	*RNR3-qPCR-R*	GGGGCAACACTATCTTCCAA
SPO1541	*ACT1-qPCR-chIP-prom-282-F*	AAACTCGCCTCTCTCTCTC
SPO1542	*ACT1-qPCR-1-chIP-prom-134-R*	GGGGAAGGAAGAATACAAG
SPO1537	*FET3-qPCR-chIP-prom-388-F*	TACTTTCCGGGTGCGAAT
SPO1538	*FET3-qPCR-chIP-prom-217-R*	TGGCGAGAATAAGAGCAC

SPO number	qPCR Primer	Primer sequence 5'-3'
SPO1412	*RNR3-qPCR-chIP-prom-260-F*	AGGACCAAACGACAAGATGG
SPO1413	*RNR3-qPCR-chIP-prom-131-R*	TTTGCAGCAGAACACGAAAC
SPO1865	*CRT1-qPCR-F*	ATCCTCCTACTGCTGCCAAA
SPO1866	*CRT1-qPCR-R*	TCTTGCGTGTTTCTCCTTGA
SPO1330	*ROX1-qPCR-F*	CAACAGAAAGAACAGCAGCA
SPO1331	*ROX1-qPCR-R*	CCGAGGAAGATGGTGAAAGA
SPO1332	*MOT3-qPCR-F*	CCCCATCATCAGACCATAAA
SPO1333	*MOT3-qPCR-R*	CACCAAGGGCATAGAAAATG
SPO1824	*YOX1-qPCR-F*	TCTCGTTCTTCCTCTTCTTCAC
SPO1825	*YOX1-qPCR-R*	CCTGGCTTCTCTTTATGCTTG
SPO1826	*YPH1-qPCR-F*	CCAAAAAGGAAAAGTCCACAGG
SPO1827	*YPH1-qPCR-R*	GCGTGAATGGTGAATGAGAG
SPO1834	*IRA2-qPCR-F*	GGATACACAGCAGAGCAACA
SPO1835	*IRA2-qPCR-R*	TCCAAACGAGTGACAGACAA
SPO1685	*RPA190-qPCR-F*	GATAAAGACACGCCAGCAGA
SPO1686	*RPA190-qPCR-R*	GCATTGACCTTGGAGGATGT
SPO1828	*HAP4-qPCR-F*	ATTCTTCTGCCTCCTCCA
SPO1829	*HAP4-qPCR-R*	CAGCAATGGTTTCCACATC
SPO1830	*CWP1-qPCR-F*	TTCTCCACTGCTTTGTCTGTC
SPO1831	*CWP1-qPCR-R*	CGGAACGGATACTCACCA
SPO1822	*HOS1-qPCR-F*	GACTACAATCCATCGCAAG
SPO1823	*HOS1-qPCR-R*	TGGGCACCTCACTGTTATT
SPO1832	*DIA2-qPCR-F*	CGATAAGTGGTTCTGCGTTG
SPO1833	*DIA2-qPCR-R*	CCTTGCTGTATGAGCGTGA

4.4. Protein related molecular techniques

4.4.1. Western blot assay

- Protein extraction

To identify and quantify specific proteins, first, protein extraction was performed in cells from exponential phase cultures. After centrifuge a volume corresponding to 5-10 OD_{600} units, cell pellets were washed with distilled water and then resuspended in 200 µL of NaOH 0.2 M. The tubes were incubated at room temperature for 5 min for posterior centrifugation at 12000 rpm for 1 min. Then, samples were resuspended in 100 µL of 2X-SDS protein loading buffer (Tris-HCl

pH 6.8 24 mM, Glycerol 10 %, SDS 0.8 %, β-mercaptoehtanol 5.76 mM, bromophenol blue 0.04 %) and boiled 5 min at 95 °C. After, samples were centrifuged at 3000 rpm for 10 min at 4 °C, supernatants transferred into fresh tubes and finally stored at -20 °C.

- Electrophoresis and protein immunodetection

To load equal protein amounts per sample, these were quantified using the Protein Assay Dye Reagent (BioRad) at A_{595nm}. After boiling the samples at 65 °C, the microliters corresponding to the ratio $1.2/A_{595nm}$ of each sample (which approximately correspond to 30 μg of protein) were separated by molecular weight in denaturing polyacrylamide gel electrophoresis (SDS-PAGE). The percentage of acrylamide:bis-acrylamide 37.5:1 (PanReac AppliChem) of the gels was adjusted (8-15 %) depending on the molecular weight of the proteins analyzed. The MiniProtean 3 (BioRad) system was used with protein SDS Running buffer (Tris Base 25 mM, glycine 192 mM, SDS 0.1 %, pH: 8.1-8.5) at 100 V during 3-4 hours at room temperature. Once proteins were resolved together with 5 μL of protein ladder per gel (PageRuler Prestained, Thermo Scientific), they were transferred onto a nitrocellulose membrane (Amersham Protran 0.45 μm NC, GE Healthcare). Transfer buffer (Tris Base 25 mM, glycine 192 mM, SDS 0.1 %, methanol 20 %, pH: 8.1-8.5) was used in the Mini Trans-Blot Electrophoretic Transfer Cell (BioRad) system at 400 mA during 1 hour with refrigeration. Then, the membranes were stained during 5 min with Ponceau S staining solution (Sigma) 0.5 % (w/v in acetic acid 1 %) to check that the same load of proteins was made in each sample. After eliminating the rests of Ponceau S with TBS-T pH 7.5 (Tris Base 25 mM, NaCl 15 mM, Tween 20 0.05 %), the blocking was made with 5 % skim milk powder (Oxoid, Thermo Scientific) in TBS-T at 4 °C overnight. The primary, and corresponding secondary antibodies (see the list and dilutions used for each antibody in section 4.4.2 of Materials and Methods), were incubated during 1-2 hours at room temperature in 5 % milk blocking solution. The washing with TBS-T between antibodies and after the secondary antibody was made 5 times.

- Protein exposure and quantification

For the final protein exposure, the ECL Advance Western blotting Detection Kit (GE Healthcare) was used according to manufacturer's instructions in the chemiluminescence image analyzer ImageQuant LAS 4000 mini (GE Healthcare). Several exposure times per membrane were quantified using the ImageQuant TL 1D gel analysis (GE Healthcare).

4.4.2. List of antibodies used in Western Blot

Primary Antibody	Secondary Antibody
α-eIF2α	α-rabbit
(John M. Zaborske Lab)	(Santa Cruz Biotechnology)
1:2000	1:10000
α-eIF2α-phosphorylated (Ser51/52)	α-rabbit
(Santa Cruz Biotechnology)	(Santa Cruz Biotechnology)
1:2000	1:10000
α- Flag M2 Peroxidase-conjugated	
(Sigma)	-
1:10000	
α-Pgk1	α-mouse
(Invitrogen)	(Amersham)
1:10000	1:50000
α-Aco1	α-rabbit
(Roland Lill Lab)	(Santa Cruz Biotechnology)
1:20000-1:50000	1:10000
α-Bio2	α-rabbit
(Roland Lill Lab)	(Santa Cruz Biotechnology)
1:2500-1:5000	1:10000
α-Hem15	α-rabbit
(Roland Lill Lab)	(Santa Cruz Biotechnology)
1:2500-1:5000	1:10000
α-Leu1	α-rabbit
(Roland Lill Lab)	(Santa Cruz Biotechnology)
1:2500-1:5000	1:10000
α-Por1	α-rabbit
(Roland Lill Lab)	(Santa Cruz Biotechnology)
1:2500-1:5000	1:10000

Primary Antibody	Secondary Antibody
α-Cox1	α-mouse
(Abcam)	(Amersham)
1:500-1:1000	1:5000
α-Cox2	α-rabbit
(Roland Lill Lab)	(Santa Cruz Biotechnology)
1:500-1:1000	1:5000
α-Cox4	α-rabbit
(Roland Lill Lab)	(Santa Cruz Biotechnology)
1:1000	1:5000
α-Rnr3	α-rabbit
(Mingxia Huang Lab)	(Santa Cruz Biotechnology)
1:100000	1:10000
α-Act1	α-mouse
(MP Biomedicals)	(Amersham)
1:2500-1:5000	1:10000

4.4.3. Protein stability determination

Protein half-life determination experiments were performed adding cycloheximide (final concentration 50 μg/mL) to exponential phase cultures to stop translation. Aliquots of cells at different times during the first 60 minutes were taken for posterior protein disappearance determination by Western Blot. The protein relative half-life was determined as explained in section 4.2.2 of Materials and Methods for mRNA stability calculations.

4.5. Determination of β-galactosidase activity

Several yeast strains containing an *URA3* plasmid with the *RNR3* or the *GCN4* promoter fused to *lacZ* (pSP638 and pSP1116, list of plasmids in section 2.5 of Materials and Methods) were used to perform the β-galactosidase assays. The *lacZ* gene encodes the β-galactosidase enzyme. This enzyme hydrolyzes a lactose analog (Ortho-Nitrophenyl-β-D-galactopyranoside, ONPG) resulting in the formation of yellow ortho-nitrophenol, spectrophotometrically detectable at $A_{420nm.}$ This allows the study of the regulation of expression of the corresponding *lacZ* fused promoters.

At least three individual colonies were grown at 30 °C overnight in the appropriate SC minus medium for plasmid/s maintenance. Next day, cells were reinoculated in fresh medium under different growth conditions. In some cases, cells were co-transformed with two plasmids: one with a gene of interest in a plasmid with *LEU2* or *HIS3* as auxotrophic marker, and the other the *URA3* plasmid containing the *RNR3-lacZ* fusion. In these cases, the β-galactosidase activity in -Fe in SC-Ura-Leu or SC-Ura-His did not reach levels as high as in SC-Ura (**Figure M-2**). For this reason, SC-Ura-Leu and SC-Ura-His media were only used in the overnight cultures for both plasmid maintenance, and SC-Ura was used for the exponential growth in the *RNR3-lacZ* assays.

After exponential cell growth, a volume corresponding to 1-5 OD_{600} units was pelleted and stored at -80 °C. Cells were then resuspended in 1 mL of buffer Z (Na_2HPO_4 60 mM, NaH_2PO_4 40 mM, KCl 10 mM, MgSO4 1 mM, β–mercaptoethanol 50 mM) and 700 µL were transferred into a new tube already containing 50 µL of SDS 0.1 % and 50 µL of chloroform. Cells were permeabilized by vortexing during 10 sec. The assay started by adding 200 µL of ONPG (4 mg/mL) to each sample and incubating in a Thermomixer (Eppendorf) at 30 °C with maximum shaking. The reaction was stopped after 5-30 minutes adding 350 µL of Na_2CO_3 1 M and incubating the tubes on ice. Samples were centrifuged at high speed during 2 minutes and A_{420nm} was determined, as well as the OD_{600} using the original cell suspension in buffer Z. The β-galactosidase activity was calculated in Miller Units (one unit corresponds to 1 nmol of ONPG hydrolyzed per min at 30 °C and pH 7.0):

Miller Units = (A_{420nm} *1000) / (OD_{600} *cell volume (mL)*assay time (min))

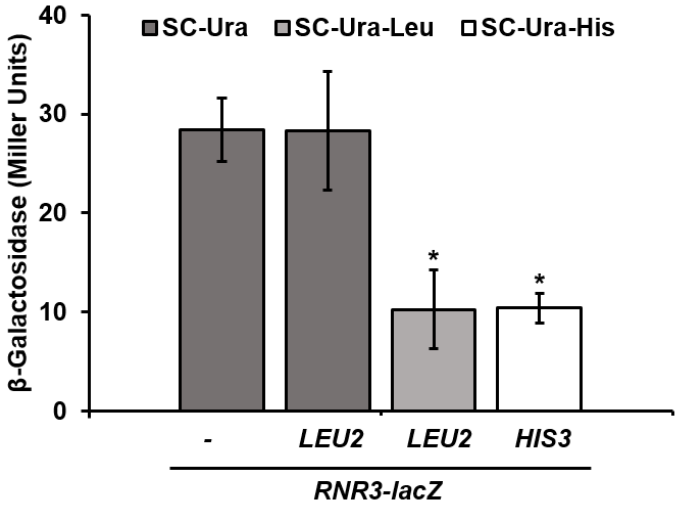

Figure M-2. The *RNR3-lacZ* β-galactosidase activity in iron deficiency is lower in SC-Ura-Leu and SC-Ura-His compared to SC-Ura. BY4741 cells with *RNR3-lacZ* (*URA3* plasmid) and, in the cases indicated, an empty plasmid with the *LEU2* or *HIS3* gene were grown in the SC medium specified with 100 μM of BPS (-Fe) during 18 hours for β-galactosidase assays. The asterisk (*) indicates a significant *p*-value (≤ 0.05) from two-tailed student's *t*-test compared with cells grown in SC-Ura only with *RNR3-lacZ* plasmid.

4.6. Determination of iron-dependent enzymatic activities

The iron-dependent enzymatic activities isopropylmalate isomerase (Leu1), aconitase (ACO), complex II succinate dehydrogenase, complex III cytochrome *c* reductase and complex IV cytochrome *c* oxidase were measured using the protocols and resources from the laboratory of Dr. Roland Lill (Philipps-Universität, Marburg) as described below. All cell cultures were performed in minimal media (see section 1.2 of Materials and Methods) and all activities were normalized to malate-dehydrogenase (MDH) activity, whose levels remained constant.

4.6.1. From cellular lysates

Whole-cell lysates were obtained to determine isopropylmalate isomerase (Leu1), aconitase (ACO) and cytochrome *c* oxidase (complex IV, CIV) enzymatic activities. A volume corresponding to 100-150 OD_{600} units was pelleted for each cell culture at 3500 rpm for 3 min at 4 °C. After washing with 15 mL of cold water in 15 mL conical tubes, pelleted cells were weighed. Approximately 100 μL of lysis buffer (TNEG + Triton: Tris-HCl pH pH 7.4 25 mM, NaCl 150 mM, EDTA 2.5 mM, Glycerol 10 % and Triton X-100 0.5 %) were added per 100 mg of cells and resuspended by vortexing. Then, 2 μL of saturated PMSF, 2 μL of cOmplete™ Protease Inhibitor Cocktail diluted in 1 mL of water, and approximately 50 μL of glass beads were added for each 100 μL of lysis buffer. With tubes upside down, cells were broken by vortexing 4 times during 1 min, with 1 min of incubation on ice in between. Next, samples were centrifuged at 3500 rpm for 5 min at 4 °C and supernatant centrifuged at 13000 rpm for 5 min at 4 °C. The collected cellular supernatants were maintained on ice and immediately used for enzymatic

activities through spectrophotometric determination in 1 cm cuvettes. In all cases, the absolute value of ΔAbs/min was calculated in the linear zone of each kinetics, and represented relative to the mg of total protein in each assay, as follows:

$$\frac{\text{Specific enzymatic activity (U)}}{\text{Total protein (mg)}} = 10^6 \frac{|\Delta\text{Abs/min}|}{\varepsilon\ (\text{M}^{-1}\text{cm}^{-1}) \times \text{total protein (mg)}}$$

where enzymatic activity units are U= μmol/min and ε is the molar absorption coefficient (M^{-1} cm^{-1}). The total protein concentration was calculated using the Protein Assay Dye Reagent (BioRad) and a protein calibration curve.

- Isopropylmalate isomerase (Leu1)

The A_{235nm} of isopropyl-malate (ε_{235}: 4950 M^{-1} cm^{-1}) was measured during 3 min in 1 cm quartz cuvettes.

	Sample cuvette
Buffer (Tris-HCl pH 8.0 50 mM, NaCl 50 mM)	980 μL
100 mM 3-isopropylmalic acid	10 μL
Cellular lysate	5-10 μL

- Aconitase (ACO) IDH-coupled

The A_{340nm} of NADPH (ε_{340}: 6200 M^{-1} cm^{-1}) was measured during 2 min in 1 cm quartz cuvettes.

	Sample cuvette	Reference cuvette
Buffer (Triethanolamine pH 8.0 50 mM, NaCl 50 mM, $MgCl_2$ 1.5 mM)	960 μL	960 μL
20 mM cis-aconitic acid	12 μL	-
40 mU/μl Isocitrate Dehydrogenase	10 μL	-
0.1 M $NADP^+$	12 μL	12 μL
Cellular lysate	5-10 μL	5-10 μL

- Cytochrome *c* oxidase (complex IV, CIV)

The A_{550nm} of reduced cytochrome *c* (ε_{550}: 20000 M^{-1} cm^{-1}) was measured during 2 min in 1 cm plastic cuvettes.

	Sample cuvette
COX buffer (MES pH 6.5 50 mM, NaCl 50 mM)	950 µL
20 mg/mL Reduced cytochrome *c*	50 µL
Cellular lysate	5-20 µL

When the assay finished, 10 µL of KCN 100 mM were added to confirm a flat activity. Before the assay, cytochrome *c* was reduced on ice by incubation with sodium dithionite to a final concentration of 10 mM during 5 min. Then, desalting of the reduced cytochrome *c* was performed using a PD-10 column with COX buffer. Aliquots were snap frozen and stored at -80 °C.

- Malate-dehydrogenase (MDH)

The A_{340nm} of NADH (ε_{340}: 6200 M^{-1} cm^{-1}) was measured during 2 min in 1 cm quartz cuvettes.

	Sample cuvette
Buffer (Tris-HCl pH 8.0 50 mM, NaCl 50 mM)	950 µL
10 mg/mL NADH	20 µL
5 mg/mL Oxalacetate	20 µL
Cellular lysate	2-5 µL

4.6.2. From isolated mitochondria

Yeast mitochondria isolation was performed as described by Daum et al. (1982) with modifications, to determine succinate dehydrogenase (complex II), cytochrome *c* reductase (complex III) and cytochrome *c* oxidase (complex IV) enzymatic activities. Briefly, individual colonies were grown at 30 °C overnight either in 50 mL of iron-sufficient (+Fe with 50 µM ferric ammonium citrate, FAC) or in 100 mL of iron-free media (-Fe). Next day, cells were reinoculated in 200 mL and 400 mL, +Fe and -Fe respectively, of fresh media to an OD_{600} of 0.2. When

OD_{600} was around 1.0, cultures were inoculated overnight in 2 L and 4 L, +Fe and -Fe respectively.

- Harvesting and washing of cells

After centrifuging each culture at 3500 rpm for 5 min, supernatant was removed by decanting. Cells were gently resuspended in 200 mL of water, centrifuged again and the supernatant completely removed. Pelleted cells were weighed, estimating 10 g of wet cells per sample (the following indicated volumes correspond for each 10 g of wet cells). Then, 30 mL of Tris-SO_4 pH 9.4 0.1 M and DTT 10 mM were added to the cells, gently resuspended and incubated at 150 rpm for 15 min at 30 °C. After centrifuging at 3000 rpm for 5 min, pellets were washed in 40 mL of sorbitol buffer (sorbitol 1.2 M, potassium phosphate buffer KPi pH 7.4 20 mM), centrifuged and resuspended again in 40 mL of sorbitol buffer.

- Spheroplasting

The amount of 7 mg of Zymolyase 100T (Seikagaku Corp.) was resuspended in 1 mL of sorbitol buffer and added to each cell sample for incubation at 30 °C and 150 rpm for 45 min. Next, spheroplast formation was tested checking the rapid drop of the OD_{600} of 25 µL of cells in 1 mL of water, and not in 1 mL of sorbitol buffer. After centrifuging at 3000 rpm for 5 min at 4 °C, spheroplasts were gently resuspended in 40 mL of cold sorbitol buffer, centrifuged and washed again as indicated. Then, spheroplasts were resuspended in 30 mL of cold BB buffer (sorbitol 0.6 M, HEPES-KOH pH 7.4 20 mM, PMSF 1 mM).

- Dounce homogenization and isolation of mitochondria

The homogenization was performed with 25 strokes using a pre-chilled Douncer. Then, samples were centrifuged at 4000 rpm for 5 min at 4 °C. The supernatant of each sample was again centrifuged at 10000 rpm for 12 min at 4 °C. Each pellet was resuspended in 30 mL of BB buffer without PMSF and transferred into 50 mL corning tubes. After centrifuging at 4000 rpm for 5 min at 4 °C, supernatants were centrifuged again at 10000 rpm for 12 min at 4 °C as before. Between 100-200 µL of BB buffer without PMSF were used for gently resuspension of the pelleted mitochondria. Smaller aliquots were snap frozen and stored at -80 °C. The total protein concentration was calculated using the Protein Assay Dye

Reagent (BioRad) and a protein calibration curve. Enzymatic activities assays were performed as follows, and calculations were performed using the previously explained formula.

- Succinate dehydrogenase (complex II)

The A_{600nm} of dichlorphenol-indophenol, DCIP (ε_{600}: 21000 M^{-1} cm^{-1}) was measured during 2 min in 1 cm plastic cuvettes.

	Sample cuvette	Reference cuvette
Buffer (Tris-HCl pH 8.0 50 mM, NaCl 50 mM, KCN 1 mM, Triton 0.1 %)	920 µL	920 µL
20 % Sodium succinate	12 µL	12 µL
20 % Sodium malonate (inhibitor)	-	12 µL
20 mg/mL Phenazine methosulfate	12 µL	12 µL
2.9 mg/mL Dichlorphenol-indophenol	20 µL	20 µL
Isolated Mitochondria (total protein)	25 µg	25 µg

- Succinate dehydrogenase-Cytochrome *c* reductase (complex II+III)

The A_{550nm} of reduced cytochrome *c* (ε_{550}: 20000 M^{-1} cm^{-1}) was measured during 2 min in 1 cm plastic cuvettes. With this assay, both complex II and III enzymatic activities were measured at the same time.

	Sample cuvette	Reference cuvette
Buffer (Tris-HCl pH 8.0 50 mM, NaCl 50 mM, KCN 1 mM)	920 µL	920 µL
20 % Sodium succinate	12 µL	12 µL
20 % Sodium malonate (inhibitor)	-	12 µL
20 mg/mL Oxidized cytochrome *c*	50 µL	50 µL
Isolated Mitochondria (total protein)	25 µg	25 µg

- Cytochrome *c* oxidase (complex IV)

The A_{550nm} of reduced cytochrome *c* (ε_{550}: 20000 M^{-1} cm^{-1}) was measured during 2 min in 1 cm plastic cuvettes.

	Sample cuvette
COX buffer (MES pH 6.5 50 mM, NaCl 50 mM)	950 µL
20 mg/mL Reduced cytochrome *c*	50 µL
Isolated Mitochondria (total protein)	5-10 µg

When the assay finished, 10 µL of KCN 100 mM were added to confirm a flat activity. Reduced cytochrome *c* was prepared as above explained.

- Malate-dehydrogenase (MDH)

The A_{340nm} of NADH (ε_{340}: 6200 M^{-1} cm^{-1}) was measured during 2 min in 1 cm quartz cuvettes. First, the lysis of 20 µg of isolated mitochondria was performed adding 4 µL of dodecylmaltoside 3 % in a final volume of 50 µL using the buffer below indicated.

	Sample cuvette
Buffer (Tris-HCl pH 8.0 50 mM, NaCl 50 mM)	910 µL
10 mg/mL NADH	20 µL
5 mg/mL Oxalacetate	20 µL
Total lysate of 20 µg of mitochondria	50 µL

4.7. Determination of oxygen consumption rate

Individual colonies were grown at 30 °C overnight in 3 mL of the appropriate SC minus medium for selection of auxotrophic markers. Later on, cells reinoculated to an OD_{600} of 0.1-0.2 were grown during 6 hours at 30 °C in 10 mL under iron-sufficient or -deficient conditions. A volume corresponding to 2.0 OD_{600} units was collected and washed with distilled water, resuspended in 1 mL of YPEG medium (yeast extract 1 %, bacteriological peptone 2 %, ethanol 2 %, glycerol 3 %) and transferred into an air-tight chamber. The oxygen content decline was monitored during 15 min using the Oxyview 1 System (Hansatech) with a S1 Clark-type O_2 electrode.

The system consists of a platinum cathode (-) in contact with both the silver anode (+), through KCl 3 M, and the chamber on the top where cells were placed. A basal 0.7 V voltage difference occurs between the cathode and the anode, and when O_2 is present in the chamber it is reduced and the voltage difference increases proportionally. First, the maximum voltage was established at 0.9 V using oxygen-saturated distilled water (0.28 μmol O_2 per mL at 20 °C). This maximum value was registered on a graph paper at the 180 mm horizontal division, and the minimum value, 0 μmol O_2 per mL, was situated at the 20 mm division. Second, vertical output speed of the register graph paper was established in 5 mm/min. Thereby, the horizontal changes in the recording corresponded to a decrease in the O_2 content of the solution in the chamber, and vertical changes corresponded to the time elapsed. In this way, it was possible to calculate the oxygen consumption rate per minute and per OD_{600}. Between 2 and 4 nmol O_2/(min x OD_{600}) were measured to be consumed by a wild-type strain after growing 6 hours with glucose 2 % under iron-sufficient conditions.

5. Structural modeling of the Cth2 protein domains

The structural model of the Cth2 protein (from amino acid 160 to 285) has been performed by Dr. Julio Polaina (IATA-CSIC) using the I-TASSER server for protein structure and function prediction (Yang et al., 2015). PDB structures 1RGO (Hudson et al., 2004) and 2CQE, which corresponds to the zinc-finger domain of human protein KIA1046, were used as templates. The IUPred2A software (http://iupre d2a.elte. hu) was used to predict potential intrinsically unstructured protein regions (Meszaros et al., 2018).

Chapter 1
Results

Chapter 1. Global translational repression under iron deficiency depends on the eIF2α/Gcn2 pathway

This work was published in the *Scientific Reports* journal, volume 10 (Romero et al., 2020). The authors are Antonia María Romero*, Lucía Ramos-Alonso*, Paula Alepuz, Sergi Puig and María Teresa Martínez-Pastor

**These authors contributed equally to this work.*

As previously introduced, bulk translation is a highly energy consuming cellular process that is inhibited in response to several environmental and nutritional stresses. Translation is an iron-dependent process because ribosome biogenesis and recycling require the essential Fe-S protein Rli1. Moreover, in yeast, the biosynthesis of multiple amino acids, including leucine, isoleucine, valine, lysine, glutamate, methionine and cysteine depends on iron. Despite all the existing studies on iron homeostasis regulation, there is no evidence for translation alterations during the adaptation to iron-deficient conditions in yeast. This work provides new indications of the global translational repression that takes place in *S. cerevisiae* under iron starvation.

C1.1. General translation decreases in response to iron limitation

To explore whether iron deficiency modifies the bulk of mRNA translation, we performed polysome profile experiments with a wild-type W303 prototroph strain cultivated in iron sufficiency (+Fe) or iron deficiency (-Fe). No statistically significant differences were observed in the polysomes/monosome 80S (P/M) ratio between 3 and 6 hours of iron sufficiency (**Figure C1-1: A, B and E**). However, after 3 hours of iron deficiency, there was a significant decrease in polysome abundance compared to both +Fe times (**Figure C1-1: C and E**). After 6 hours in -Fe conditions, the repression of translation became more evident, with the observation of an increased 80S monosomal peak compared to the polysome area, and the consequent reduction in the P/M ratio (**Figure C1-1: D and E**). These results indicate that a general repression of translation initiation occurs during the progress of iron limitation.

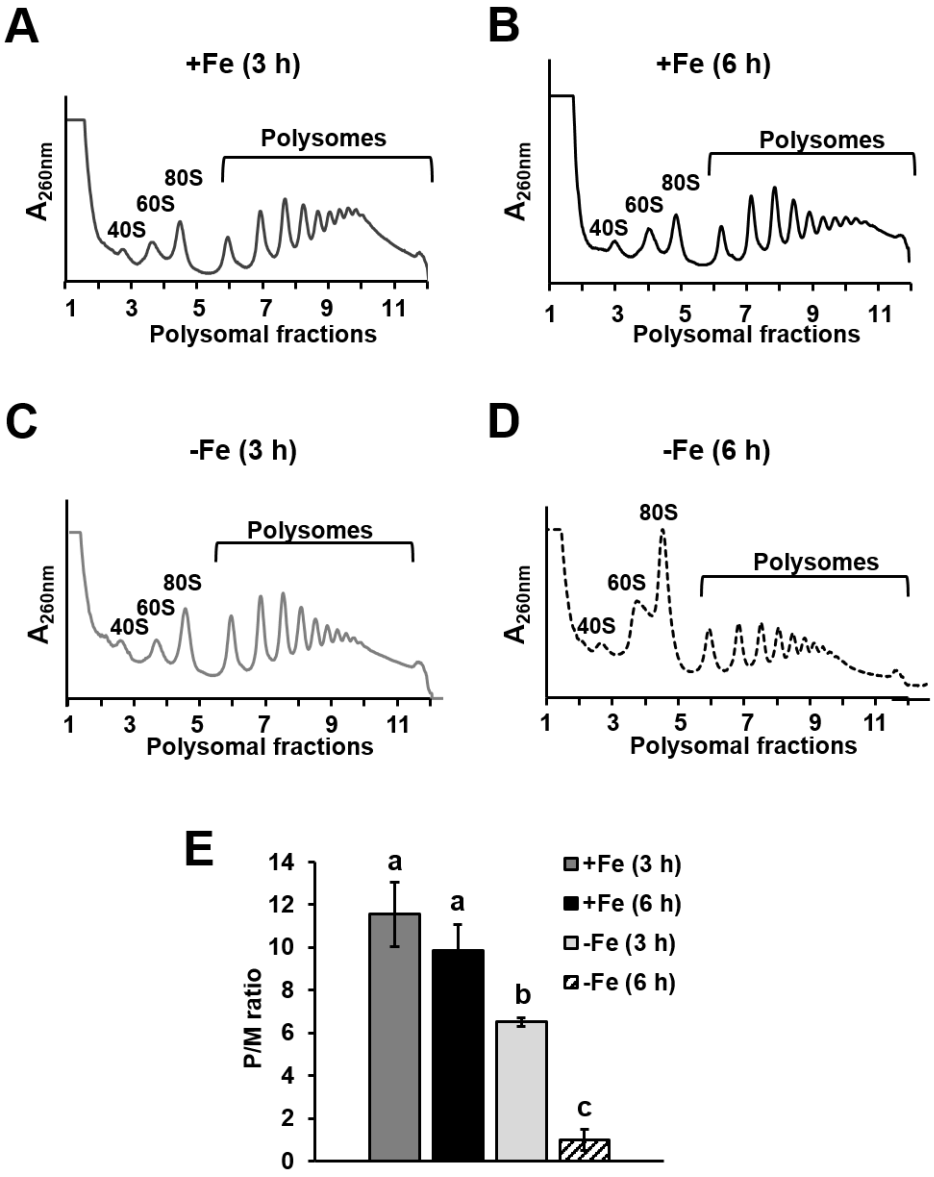

Figure C1-1. A general repression of translation occurs during iron deficiency. Polysome profile experiments of a W303 prototroph strain were performed in SC cultures growing for at least 15 hours until early exponential phase (OD_{600} 0.05 and 0.2 for the experiments at 3 and 6 hours, respectively). Then, the cells were maintained in SC (+Fe) **(A and B)** or in SC with 100 μM BPS (-Fe) **(C and D)**. A representative A_{260nm} polysome profile of three biologically independent replicates is shown. The ribosomal subunits (40S and 60S), monosome (80S) and polysome fractions are indicated, and the average of polysomes/monosome 80S (P/M) ratio represented with standard deviations **(E)**. Different letters over the bars indicate statistically significant differences (*p*-value<0.05) from two-tailed student's *t*-test.

C1.2. The polysome profile of specific transcripts responds differently to the iron limitation progress

To study how the global repression of translation during iron deficiency is affecting specific transcripts, we studied the translational state of different mRNAs by determining their distribution on the polysome profiles. The total RNA of the different fractions was extracted and the levels of specific transcripts were analyzed by RT-qPCR. The profiles of *RPS16B* and *RPL3* (mRNAs encoding the corresponding ribosomal proteins, RPs) showed an enriched association to the 80S fraction, which decreased or shifted to lighter polysomal fractions in the progression of iron deficiency (**Figure C1-2: A and B**). This result was interpreted as a decrease in the specific translation of these RP transcripts, which was consistent with the repression of general translation during iron starvation. Regarding the translation profile of a housekeeping gene, such as *ACT1*, its pattern of elevated association to polysomes indicated a constant level of translation, with only a slight shift to lighter polyribosome fractions after 6 hours of iron deficiency (**Figure C1-2: C**). Therefore, the *ACT1* translation profile was mostly unaffected in the conditions of iron deficiency used in this study. On the contrary, the previously observed shift in the distribution of *GCN4* mRNA to polysomal fractions after 6 hours of iron deficiency (Romero, 2018; Romero et al., 2020; **Figure I-3: C**) suggested a higher translation efficiency of the *GCN4* mRNA. This result was supported by the higher eIF2α phosphorylation observed in -Fe conditions (Romero, 2018; Romero et al., 2020; **Figure I-3: A and B**), as active *GCN4* mRNA translation has been described to occur when eIF2α is phosphorylated and eIF2 function is limited (reviewed by Hinnebusch, 2005). To further investigate *GCN4* mRNA translation in iron deficiency, we analyzed the β-galactosidase activity of W303 cells expressing a construct containing the wild-type *GCN4* promoter (with its four uORFs) fused to the *lacZ* reporter coding sequence. Only a slight, but statistically significant, increase in the β-galactosidase activity was observed in -Fe compared to +Fe conditions (**Figure C1-2: D**). However, the increase in β-galactosidase activity observed after the treatment with 3-aminotriazole (3-AT), used as control as it causes amino acid starvation, was more pronounced that the change observed upon iron deficiency (**Figure C1-2: D**). Taken together, these results suggest that, despite the global repression of translation that occurs when

iron is scarce, the translation of specific mRNAs is differentially regulated under iron deficiency.

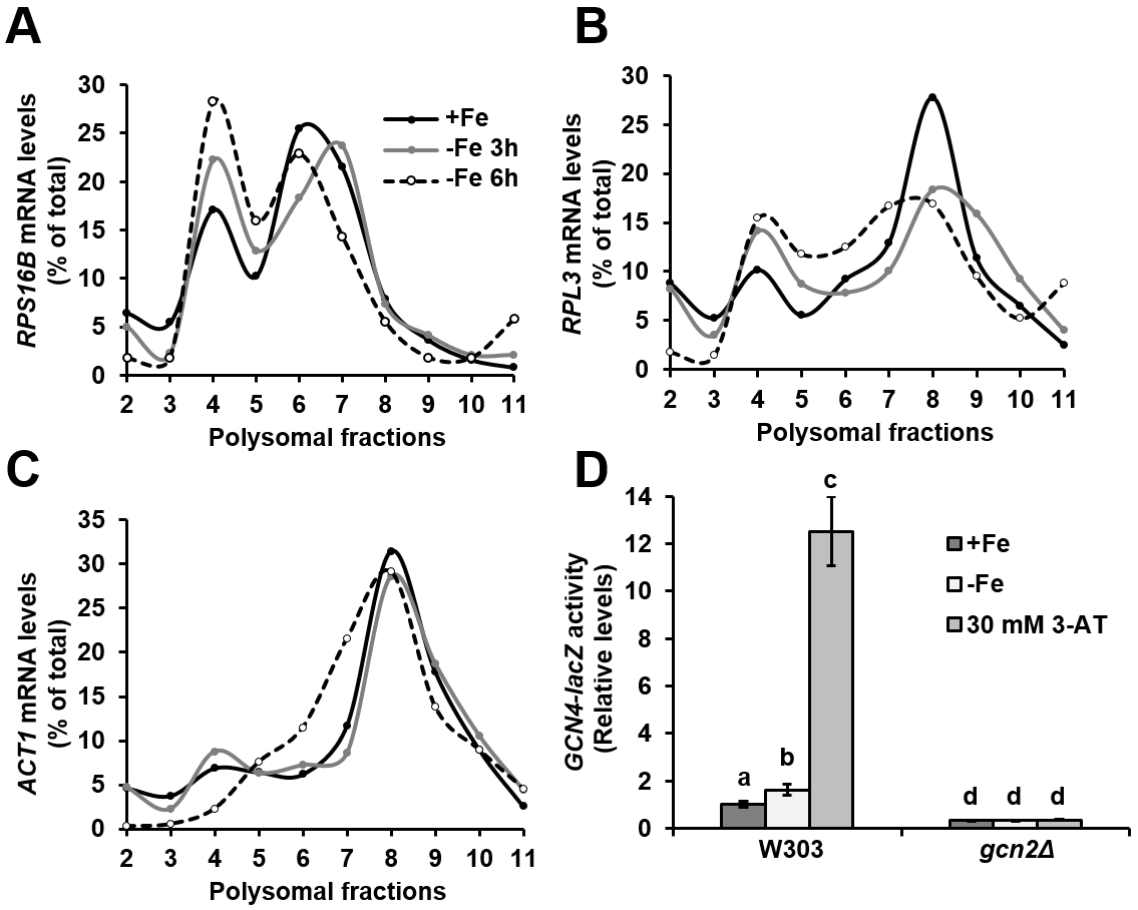

Figure C1-2. Specific mRNAs are differentially translated under iron deficiency. The RNA from the different fractions of the polyribosome profiles shown in Figure C1-1 was extracted and the *RPS16B* **(A)**, *RPL3* **(B)** and *ACT1* **(C)** mRNA profiles were analyzed by RT-qPCR as described in Materials and Methods. **(D)** The *ura3Δ* and *gcn2Δura3Δ* strains (W303 prototroph background) transformed with pRS416-*GCN4-lacZ* plasmid were grown in SD (+Fe) and in SD supplemented with 100 μM BPS (-Fe) during 6 hours, and in SD with 30 mM 3-aminotriazole (3-AT) during 5 hours. Then, the β-galactosidase activities were determined and represented relative to W303 in +Fe. Mean values and standard deviations from three biologically independent experiments are shown. Different letters over the bars indicate statistically significant differences (p-value<0.05) from two-tailed student's t-test.

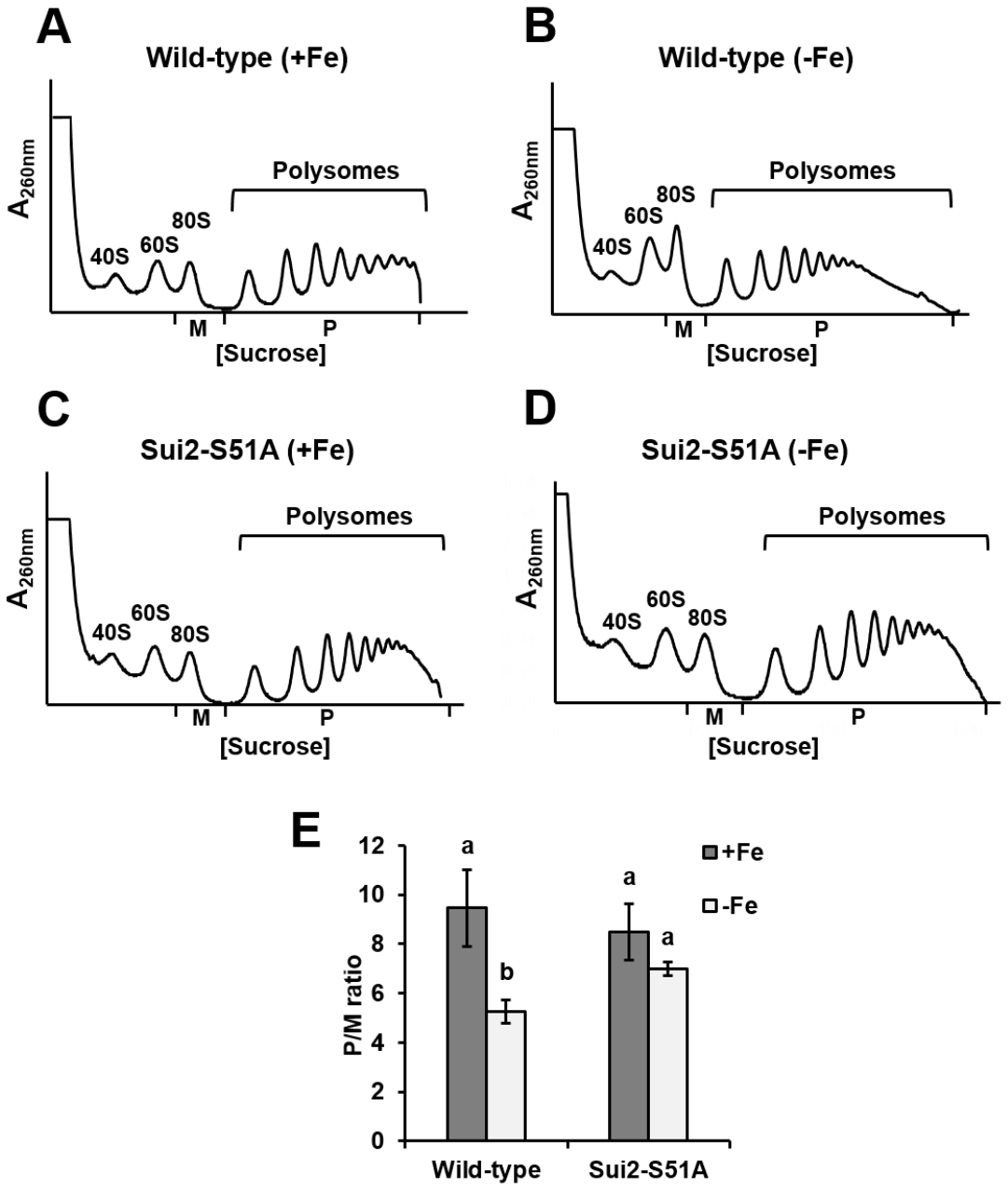

Figure C1-3. The phosphorylation of eIF2α (Sui2) in Ser51 is involved in the global translational repression under iron deficiency. Polysome profile experiments of wild-type *SUI2* (RS-86) and *SUI2-S51A* mutant (RS-88) cells (Hueso et al., 2012) were performed from overnight cultures reinoculated in SC (+Fe) **(A and C)** and SC with 100 μM BPS (-Fe) **(B and D)** for 9 hours. A representative A_{260nm} polysome profile of three biologically independent replicates is shown. The average of polysomes/monosome 80S (P/M) ratio is represented with standard deviations **(E)**. Different letters over the bars indicate statistically significant differences (p-value<0.05) from two-tailed student's t-test.

C1.3. The eIF2α-Gcn2 pathway is involved in the global translational repression that occurs under iron deficiency

As previously mentioned in the introduction, under amino acid starvation or different stress conditions, the Gcn2 kinase is activated and phosphorylates eIF2α, which downregulates general translation initiation and increases the translation of *GCN4*. The observation that during iron deficiency the translation of *GCN4* mRNA was slightly increased, together with the higher eIF2α phosphorylation, suggested a possible implication of the eIF2α-Gcn2 pathway in the global repression of translation under iron limitation. This hypothesis is consistent with the low *GCN4-lacZ* activity observed when *GCN2* was deleted under all the conditions tested (+Fe, -Fe and amino acid starvation) (**Figure C1-2: D**). Besides, the increased 80S monosomal peak in the global profile under prolonged iron deficiency (**Figure C1-1: D**) is usually indicative of repression of translation initiation. These results suggest a potential role for the eIF2α-Gcn2 pathway in global translational control under iron starvation.

Further polysome profile experiments were performed to evaluate the implication of the eIF2α (encoded by the *SUI2* gene) phosphorylation in the global translational repression under iron deficiency. Given that the phosphorylation in serine 51 of eIF2α by Gcn2 kinase has been previously reported to inhibit protein synthesis under amino acid starvation (Dever et al., 1992), we analyzed the polysome profile of a *SUI2-S51A* mutant (non-phosphorylatable eIF2α strain). The P/M ratio observed in iron sufficiency was similar between the wild-type and the *SUI2-S51A* strains (**Figure C1-3: A, C and E**), and, as expected, the wild-type P/M ratio decreased under iron starvation (**Figure C1-3: B and E**). And importantly, the P/M ratio of the *SUI2-S51A* mutant did not decrease during iron deficiency compared to the wild-type (**Figure C1-3: B, D and E**). For this reason, we conclude that the phosphorylation of eIF2α in serine 51 is involved in the repression of global translation initiation when iron bioavailability is limited.

Following these observations, we proceeded to test the role of the Gcn2 kinase in repressing general translation during iron deficiency as it directly phosphorylates the serine 51 of eIF2α. As mentioned in the literature (Hinnebusch & Fink 1983; Garcia-Barrio et al., 2000), the *gcn2Δ* mutant exhibited the expected

growth defect in the absence of amino acids achieved by adding 3-AT (**Figure C1-4**). In the same way, this mutant could not phosphorylate eIF2α in any of the tested conditions (+Fe, -Fe or 3-AT) (**Figure C1-5**). When polysome profile experiments were performed, similar results were obtained with the *gcn2Δ* and *SUI2-S51A* mutants. Very similar P/M ratios were obtained for the wild-type (BY4741) and *gcn2Δ* strains under iron sufficiency (**Figure C1-6: A, C and E**). However, while the wild-type decreased the P/M ratio upon iron starvation, *gcn2Δ* did not (**Figure C1-6: B, D and E**). Together, these results highlight the importance of the Gcn2 kinase in repressing the global translation initiation during iron deficiency. Despite of this, it should be remarked that the translational derepression caused by *gcn2Δ* in -Fe is transient, since at prolonged times of iron deficiency, the P/M ratios between the wild-type and the *gcn2Δ* were equally lowered (**Figure C1-7**). Taken together, these results demonstrate the importance of the eIF2α-Gcn2 pathway in the inhibition of global translation under iron starvation.

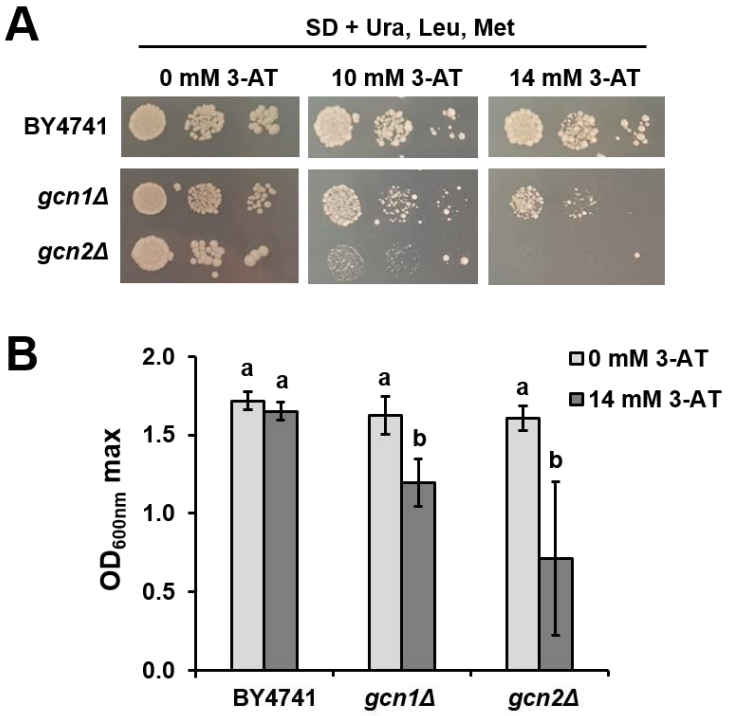

Figure C1-4. The *gcn1Δ* and *gcn2Δ* mutants displayed the expected growth defect in the presence of 3-aminotriazole. Analyses of the cell growth of wild-type BY4741, *gcn1Δ* and *gcn2Δ* cells, transformed with the pRS413 plasmid

containing the *HIS3* gene, were performed in triplicate in SD (+ Ura 20 mg/L + Leu 60 mg/L + Met 20 mg/L) in solid **(A)** and liquid **(B)** media, with or without 3-AT, as explained in section 1.4 of Materials and Methods. Mean values and standard deviations of maximum OD_{600nm} are shown **(B)**. Different letters over the bars indicate statistically significant differences (*p*-value<0.05) from two-tailed student's *t*-test.

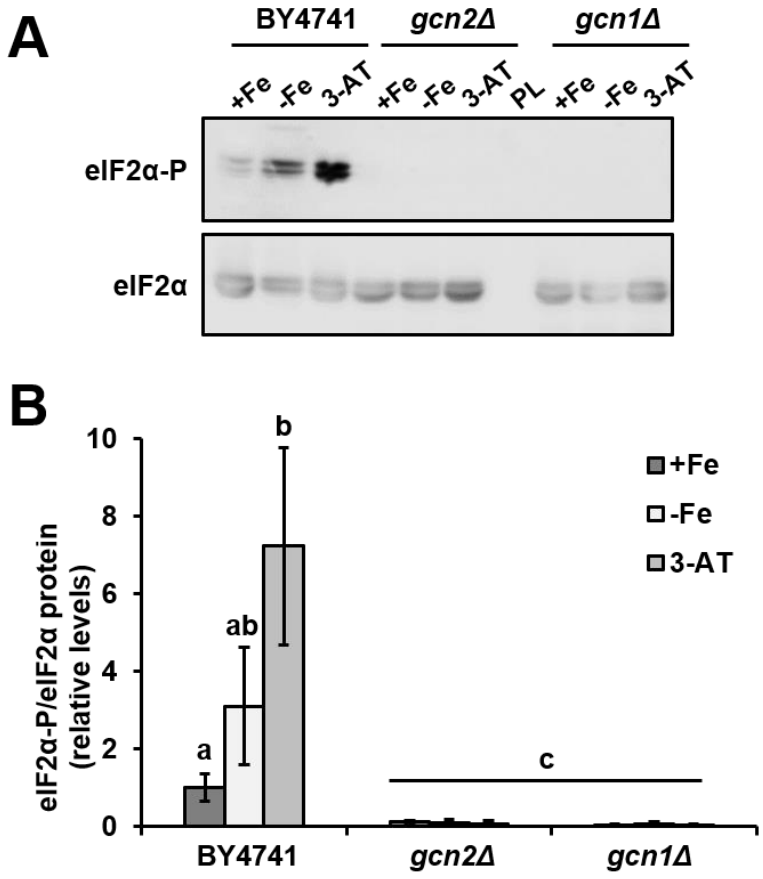

Figure C1-5. The eIF2α phosphorylation was absent in the *gcn1Δ* and *gcn2Δ* mutants in the three tested conditions: +Fe, -Fe and 3-aminotriazole. The protein levels of eIF2α phosphorylated and total eIF2α of wild-type BY4741, *gcn1Δ* and *gcn2Δ* cells, transformed with the pRS413 plasmid containing the *HIS3* gene, were analyzed by Western blot from overnight precultures reinoculated in SC-His (+Fe, 6 hours), SC-His with 100 μM BPS (-Fe, 9 hours) and SC-His with 30 mM 3-AT (5 hours). **(A)** A representative result is shown. PL: Protein ladder. **(B)** Mean values and standard deviations from the quantification of three independent biological replicates are shown. Different letters over the bars indicate statistically significant differences (*p*-value<0.05) from two-tailed student's *t*-test.

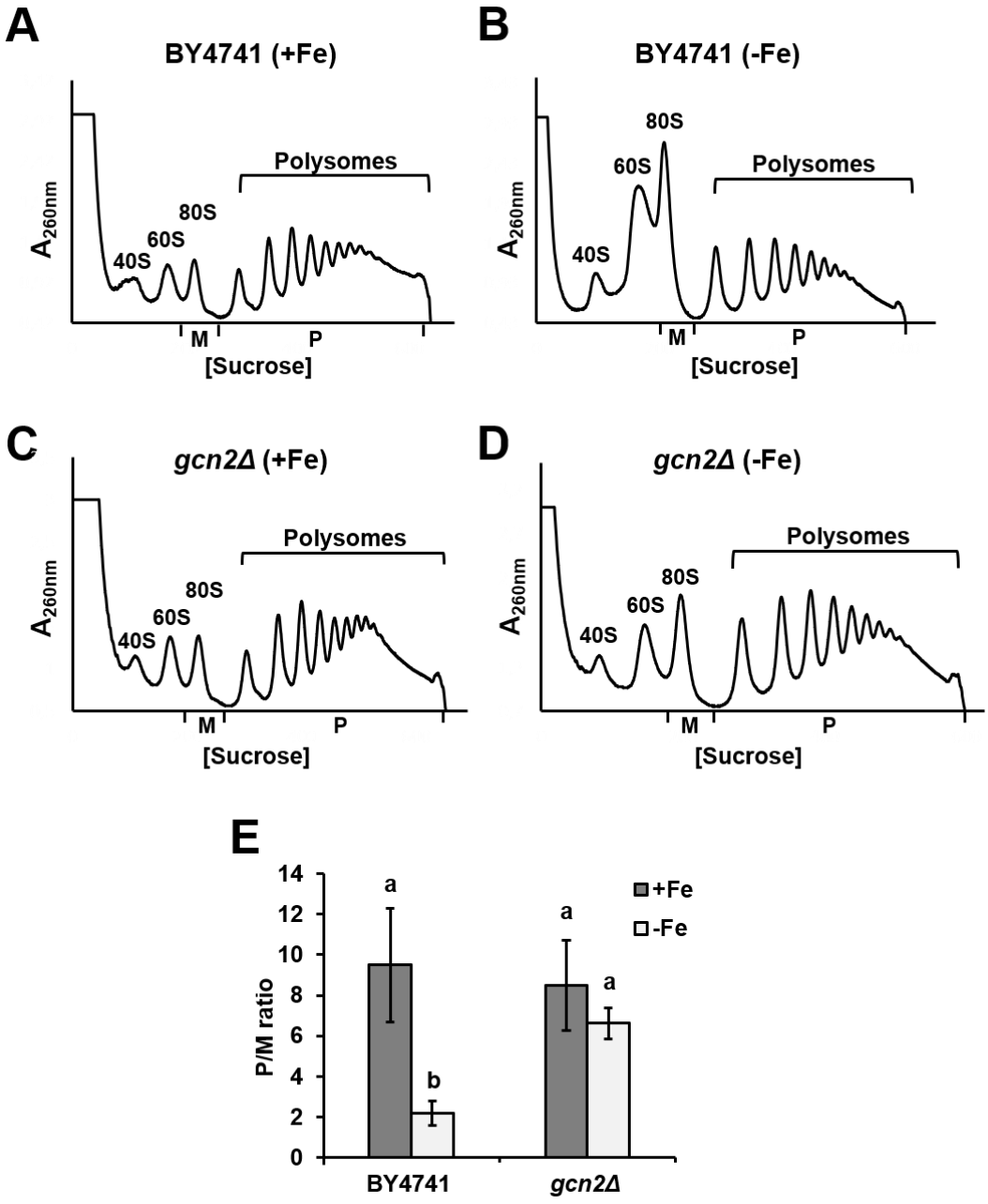

Figure C1-6. Gcn2 is involved in the global translational repression under iron deficiency. Polysome profile experiments of wild-type BY4741 and *gcn2Δ* cells were performed from overnight cultures reinoculated in SC (+Fe) **(A and C)** and SC with 100 µM BPS (-Fe) **(B and D)** for 9 hours. A representative A_{260nm} polysome profile of at least three biologically independent replicates is shown. **(E)** The average of polysomes/monosome 80S (P/M) ratio is represented with standard deviations. Different letters over the bars indicate statistically significant differences (p-value<0.05) from two-tailed student's t-test.

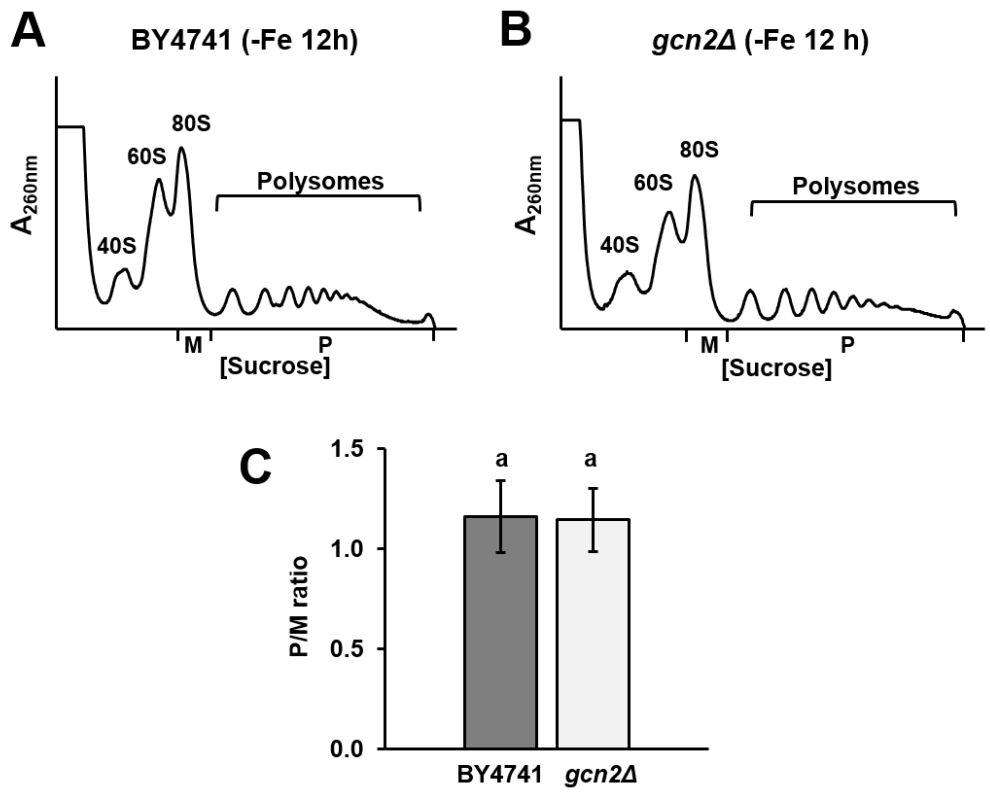

Figure C1-7. The derepression of global translational observed in *gcn2Δ* cells during the iron deficiency is temporary. Polysome profile experiments of wild-type BY4741 **(A)** and *gcn2Δ* **(B)** cells were performed at 12 hours as explained in Figure C1-6. The P/M ratios are represented **(C)** and analyzed as previously mentioned.

C1.4. Gcn1 is involved in global translational repression under iron deficiency

The phosphorylation of eIF2α requires the previous activation of Gcn2 kinase through the binding of uncharged tRNAs to the histidyl-tRNA synthetase (HisRS)-like domain of Gcn2. Moreover, the Gcn1–Gcn20 complex is required for the activation of Gcn2 by amino acid starvation (Marton et al., 1997; García-Barrio et al., 2000), oxidative stress and UV irradiation (Shenton et al., 2006; Anda et al., 2017). We decided to investigate the implication of this mechanism in the repression of global translation mediated by eIF2α-Gcn2 under iron starvation. Similar to *gcn2Δ*, the *gcn1Δ* mutant exhibited a minor but significant growth defect under amino acid starvation (**Figure C1-4**). Importantly, the *gcn1Δ* mutant did not phosphorylate eIF2α in any of the tested conditions (+Fe, -Fe or 3-AT) (**Figure C1-**

5). Regarding the polyribosome profile experiments, no differences were observed between the wild-type and the *gcn1Δ* mutant in iron sufficiency (**Figure C1-8: A, C and E**). On the other hand, the global repression of translation observed in the wild-type under iron deficiency was somewhat limited in the *gcn1Δ* mutant (**Figure C1-8: B, D and E**). Therefore, Gcn1 is involved in the global translational repression when iron is limited, most likely in the specific activation of Gcn2 kinase.

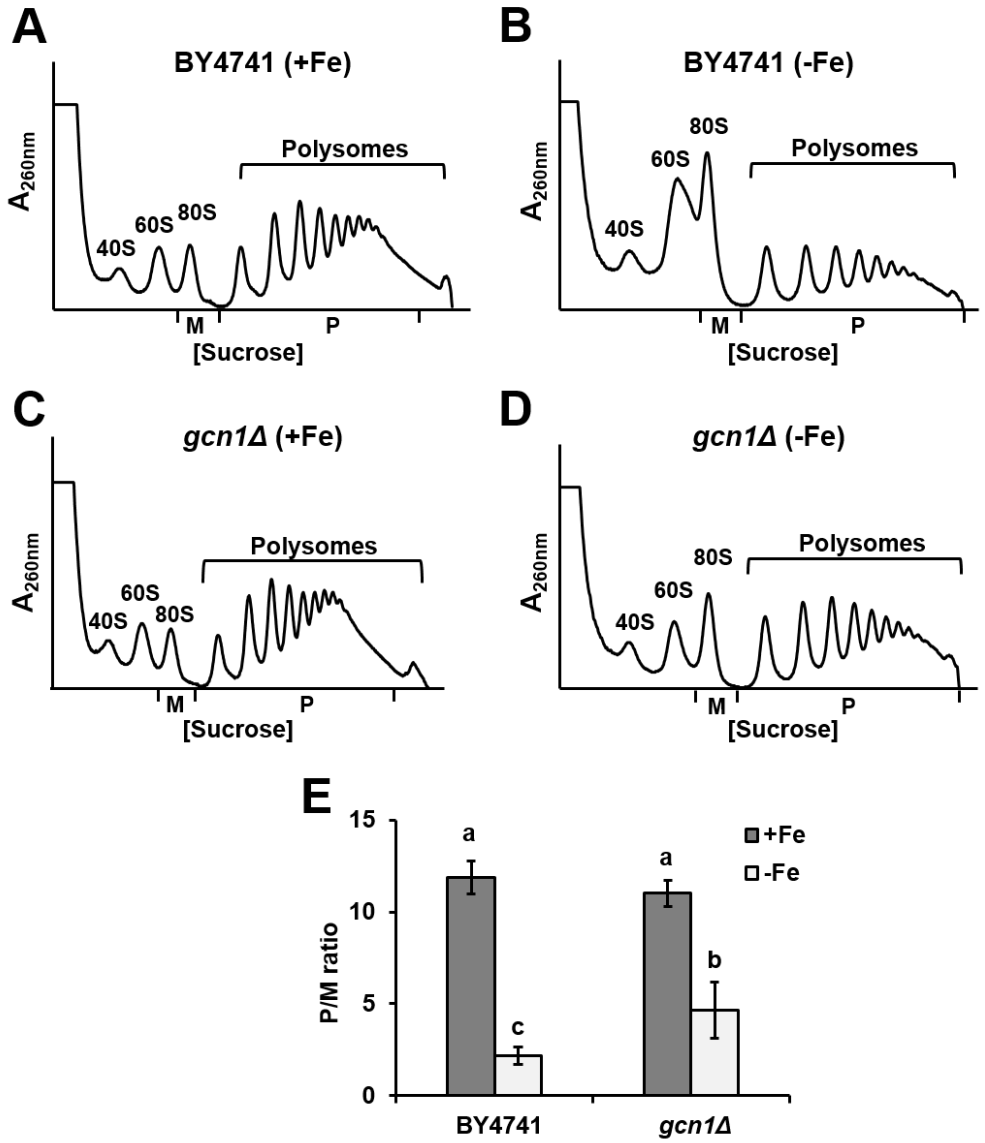

Figure C1-8. Gcn1 is involved in the global translational repression under iron deficiency. Polysome profile experiments of wild-type BY4741 **(A and B)** and *gcn1Δ* **(C and D)** cells were performed as explained in Figure C1-6. **(E)** The P/M ratios are represented with standard deviations. Different letters over the bars

indicate statistically significant differences (p-value<0.05) from two-tailed student's t-test.

Discussion

Chapter 1

Discussion of Chapter 1

As protein synthesis is a highly energy consuming process, it is common that prokaryotic and eukaryotic cells repress global translation when exposed to stress conditions. Besides, cells need to adapt its proteome to respond and survive to these stresses. Nutritional deficiencies like glucose or amino acid limitation, and several stresses like heat shock, oxidative and osmotic stress rapidly arrest general translation (Martínez-Pastor & Estruch, 1996; Ashe et al., 2000; Shenton et al., 2006; Yamamoto & Izawa, 2013). Indeed, the repression of translation initiation usually is observed fast (within the first 30 minutes of the stress) being sometimes a temporary response that relaxes when the transcriptional response arrives (reviewed by Crawford & Pavitt, 2019). However, we have seen that the translational response is not immediate during the progress of the iron deficiency. Moreover, translation is even supported by the robust homeostasis of amino acid levels during iron starvation (Shakoury-Elizeh et al., 2010; Philpott et al., 2012). The arrest of translation is not the first response as it is not significantly reduced within the first 3 hours of -Fe (**Figure C1-1**). The fastest response of yeast cells to iron starvation is the activation of the iron regulon. TORC1 inhibition (reducing all RNA polymerases levels) occurs later in the iron deficiency (6 hours and 9-11 hours in the W303 and BY4741 yeast backgrounds, respectively) (Romero et al., 2019). Under these conditions, the RP and RiBi mRNA levels drop (Romero et al., 2019). These results strongly suggested a global translation inhibition, which we have confirmed taking place at longer times of iron deficiency. The global translation observed by polysome profiles in the W303 background was slightly decreased during short-term iron deficiency (3 hours) but dramatically decreased at longer times of the iron starvation (6 hours) (**Figure C1-1: C, D and E**). Importantly, the global translational arrest observed is specific of the iron deficiency as same cultures in iron sufficiency (with similar OD_{600}) did not show translational inhibition (**Figure C1-1: A, B and E**). Therefore, the global inhibition of translation initiation occurs at long times during the iron deficiency.

Despite the general mRNA translation arrest that occurs during the response to stresses, certain mRNAs can be upregulated contrary to the global response (Shenton et al., 2006; Melamed et al., 2008; Warringer et al., 2010; Garre et al., 2012; Garre et al., 2018). This can be achieved (i) through mRNA modifications, (ii)

because of specific regulation of mRNA-binding proteins, (iii) internal ribosome entry sites or (iv) through upstream ORFs (reviewed by Spriggs et al., 2008; Hinnebusch et al., 2016; Crawford & Pavitt, 2019). The latter is the case of the *GCN4* mRNA that contains four uORFs. *GCN4* translation increases when the ternary complex levels (eIF2–GTP–methionyl-tRNA) are low, and therefore the general translation initiation is repressed. This counter is well characterized under amino acid limitation as the transcriptional factor Gcn4 activates genes for the amino acid biosynthetic pathways (Hinnebusch et al., 2005). Previous results support that this would be also the case during iron deficiency (Romero, 2018; Romero et al., 2020; **Figure I-3: C**). However, the *GCN4-lacZ* results (**Figure C1-2: D**) do not fully correlate with the polysome presence of the *GCN4* transcript after 6 hours in -Fe, especially if compared to the β-galactosidase in the amino acid starvation situation. Moreover, we currently do not know the function and relevance of *GCN4* translation under iron-deficient conditions. The slight *GCN4-lacZ* induction during the iron deficiency supports a mild drop in ternary complex levels compared to amino acid limitation, or additional translational problems posterior to initiation. However, the shift to monosomal fractions of the *RPS16B* and *RPL3* mRNAs encoding ribosomal proteins corroborates the general translational repression (**Figure C1-2: A and B**).

The phosphorylation of eIF2α in serine 51 turns eIF2–GDP into a competitive inhibitor of eIF2B and decreases the ternary complex levels. The eIF2α phosphorylation under iron deficiency (Romero, 2018; Romero et al., 2020; **Figure I-3: A and B**) and the increased 80S peak observed in this work when translation is arrested (**Figure C1-1: D**) suggest that translation is being inhibited at the initiation step. Gcn2 is the only kinase in *S. cerevisiae* that phosphorylates serine 51 of eIF2α. We have determined that Gcn2 is activated and phosphorylates eIF2α in -Fe: (i) eIF2α is not phosphorylated in the *gcn2Δ* mutant (**Figure C1-5**), (ii) this phosphorylation is important for the inhibition of the translation initiation (**Figure C1-3**), and (iii) *gcn2Δ* mutant lacks the *GCN4-lacZ* induction (**Figure C1-2: D**). Consistent with this, the *gcn2Δ* mutant, which shows the expected phenotype under amino acid limitation (**Figure C1-4**), does not exhibit repression of the translation initiation in -Fe (**Figure C1-6**). However, when the iron deficiency

persists longer (12 hours), the *GCN2* deletion does not rescue anymore the translational state (**Figure C1-7**). Perhaps the role of Gcn2 is transient and other mechanisms are involved in the repression of translation initiation at longer times (12 hours in -Fe). For instance, after 12 hours in -Fe the levels of rRNAs, mRNAs, especially RPs and RiBis, and tRNAs, could be dramatically low. Besides, the recycling of amino acids and ribosomes, the latter especially dependent of the Fe/S-dependent Rli1 protein, would be more compromised with the progression of the iron deficiency. As a consequence, removing Gcn2 activity would not be enough to recover bulk translation.

Unlike *S. cerevisiae*, with only one eIF2α kinase, in mammals there are four eIF2α kinases. These are expressed in different tissues and activated by different stresses: GCN2 is activated under nutrient limitation (Sood et al., 2000), PKR under viral infections (Clemens, 1997), PERK/PEK by endoplasmic reticulum stress (Shi et al., 1998; Harding, 1999) and HRI is the heme-regulated eIF2α kinase activated under iron deficiency in erythroid cells (Ranu & London, 1976; Kramer et al., 1976; Levin et al., 1976). All these kinases phosphorylate eIF2α when activated, repress general translation and activate the translation of the *ATF4* mRNA (*GCN4* in yeast) also regulated by uORFs. This has been termed the Integrated Stress Response (ISR) (reviewed by Pakos-Zebrucka et al., 2016; Pavitt, 2018). The global inhibition of translation under iron deficiency in mammals seems to be conserved in yeast. Iron starvation limits heme synthesis and the heme-regulated eIF2α kinase (HRI) phosphorylates eIF2α in erythroid cells. This decreases bulk translation, downregulates the translation of globins and increases the synthesis of specific transcripts like HbF (fetal hemoglobin) (Han et al., 2001; Hahn & Lowrey, 2013; Hahn & Lowrey, 2014; Zhang et al., 2019b). When HRI is disrupted, global translation and especially the synthesis of globins in mice is improved, similarly to *GCN2* deletion in yeast (Han et al., 2001). Interestingly, iron deficiency decreases the translation of mRNAs encoding cytosolic and mitochondrial ribosomal proteins in an HRI-dependent manner (Zhang et al., 2019b). In the same way, we have observed the shift to monosomal fractions of two mRNAs encoding cytosolic RPs during the iron deficiency (**Figure C1-2: A and B**).

The ISR pathway was initially outlined in yeast as the General Amino Acid Control (GAAC) as it was first described to induce the amino acid biosynthetic genes in response to amino acid depletion (Hinnebusch & Fink, 1983). Since then, Gcn2 in yeast has been described to be activated under several stresses like purine starvation, glucose limitation, salt stress, membrane stress, oxidative stress and intracellular acid stress (Rolfes & Hinnebusch, 1993; Yang et al., 2000; Goosens et al., 2001; Deloche et al., 2004; Shenton et al., 2006; Hueso et al., 2012). We are adding iron deficiency to the list of conditions activating Gcn2 in yeast. Our proposed model of Gcn2 activation in iron deficiency (**Figure D1-1**) would be similar to the amino acid limitation condition. During iron deficiency uncharged tRNAs would bind the A site of the ribosome. Gcn1 is the protein of the Gcn1–Gcn20 complex that directly binds the ribosome and directly transfers the tRNA to the HisRS-like domain of Gcn2, promoting its kinase activity as in amino acid starvation (Marton et al., 1997; Garcia-Barrio et al., 2000). In fact, under iron deficiency, as in amino acid limitation, eIF2α is not phosphorylated in the *gcn1Δ* mutant (**Figure C1-5**) and this mutant shows a significant recovery of the translation initiation in -Fe (**Figure C1-8**). Then, Gcn2 would phosphorylate eIF2α in Ser-51 decreasing the ternary complex levels, repressing the general translation initiation but increasing the translation in the main ORF of *GCN4* (**Figure D1-1**). Further studies would be necessary to elucidate whether other mRNAs in addition to *GCN4* are preferentially translated during the progress of iron deficiency via Gcn2.

We cannot ignore other hypothesis about the Gcn2 activation under iron starvation. Other stresses that activate Gcn2, different from amino acid limitation or glucose depletion, do not show clear reduced amino acid levels. Instead, higher levels of uncharged tRNAs could be consequence of defects in the aminoacyl tRNA synthase, like in oxidative stress or acidic intracellular pH (Shenton et al., 2006; Hueso et al., 2012). It could even be possible that Gcn2 is being activated independently of the uncharged tRNA pool. This hypothesis would still require Gcn1 and the binding of a tRNA (uncharged or not) to the HisRS-like domain of Gcn2 (Kubota et al., 2003; Narasimhan et al., 2004; Hinnebusch et al., 2005; Anda et al., 2017). The Ser-577 of Gcn2 could be involved in this last hypothesis. When

this residue is phosphorylated, the Gcn2 kinase is inactivated. The kinase/s involved in this phosphorylation are not known, but the protein phosphatase 2A (PP2A) complex is known to dephosphorylate Ser-577. The Ser-577 dephosphorylation is believed to increase the tRNA binding affinity of Gcn2, and once the tRNA is bound in a Gcn1-dependent manner, the Gcn2-kinase activity increases (Cherkasova & Hinnebusch, 2003; Kubota et al., 2003). The PP2A complex is regulated by TORC1. Inactivation of TORC1 promotes the dephosphorylated state of Tap42 that cannot bind and deactivate the PP2A complex (Jiang & Broach, 1999).

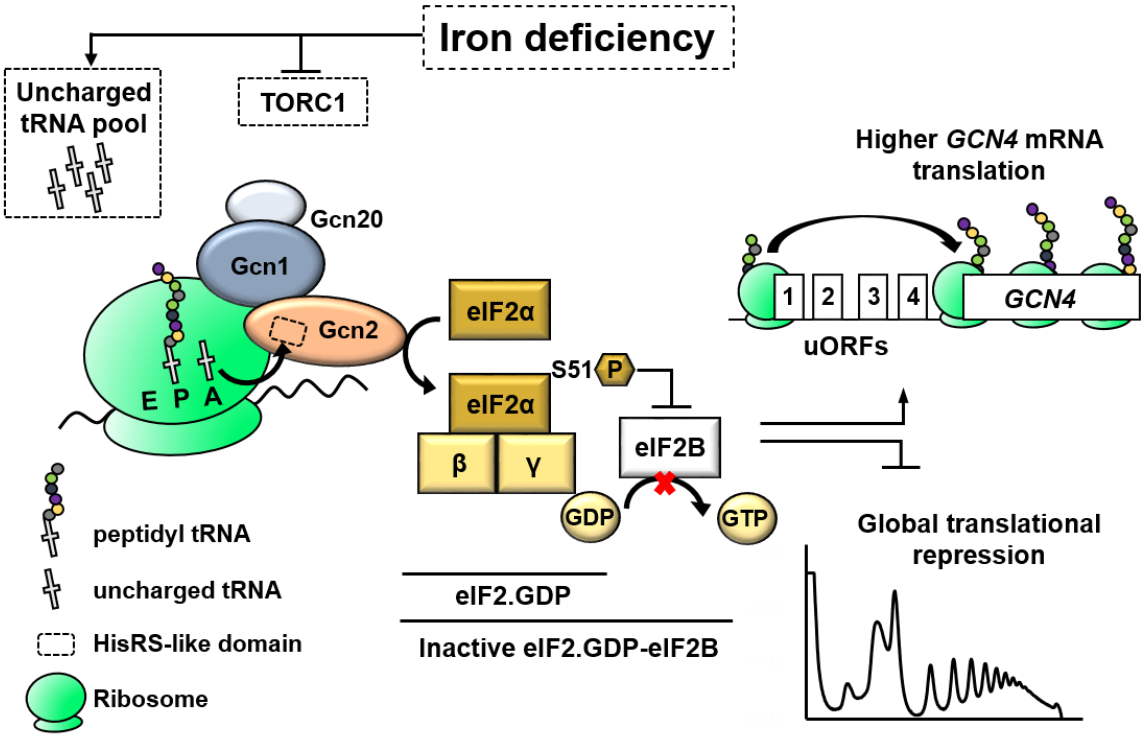

Figure D1-1. Proposed model for the eIF2α-Gcn2 pathway-dependent regulation of translation under iron deficiency.

Therefore, during iron-deficient conditions both hypotheses of Gcn2 activation could coexist (**Figure D1-1**): (i) limited amino acid levels would increase the uncharged tRNAs, and (ii) TORC1 inactivation could activate Gcn2 in a Tap42/PP2A-dependent manner. The first hypothesis is supported by the fact that the synthesis of several amino acids requires iron-containing proteins whose

mRNAs are downregulated in a Cth1/2-dependent manner (Puig et al., 2005; Puig et al., 2008). At our severe iron-deficient conditions it is likely that amino acids are scarce and this could promote the subsequent increment of uncharged tRNAs. On the other hand, the second hypothesis is supported by the observed decrease in rRNAs, tRNAs, RP and RiBi mRNAs during iron deficiency because of the reduced activity of all RNA polymerases due to the TORC1 inhibition (Romero et al., 2019). Bulk translation is probably limited because of reduced ribosome levels as a consequence of TORC1 inactivation. However, the phosphorylation state of Tap42 or Ser-577 of Gcn2 during iron deficiency has not been addressed and would require further studies.

Chapter 2

Results

Chapter 2. Cth2 represses the translation of ARE-containing mRNAs in response to iron deficiency

This work was published in:

- *PLoS Genetics* journal, volume 14 (Ramos-Alonso et al., 2018a). The authors are Lucía Ramos-Alonso, Antonia María Romero, Maria Àngel Soler, Ana Perea-García, Paula Alepuz, Sergi Puig and María Teresa Martínez-Pastor

- *Current Genetics* journal, volume 65, mini-review (Ramos-Alonso et al., 2019). The authors are Lucía Ramos-Alonso, Antonia María Romero, Julio Polaina, Sergi Puig and María Teresa Martínez-Pastor

As previously introduced, Cth2 promotes the metabolic remodeling of several cellular processes in order to optimize iron utilization (Puig et al., 2005; Puig et al., 2008). The role of Cth2 and of the TTP family of proteins is to promote ARE-mediated mRNA decay (AMD), including their own transcripts whose AREs are important for negative feedback regulation (Brooks et al., 2004; Tchen et al., 2004; Pullmann et al., 2007; Tiedje et al., 2012; Martínez-Pastor et al., 2013a). Besides, it is known that mammalian TTP can also repress translation of its ARE-containing targets, including again its own transcript (Coller & Parker, 2005; Qi et al., 2012; Tiedje et al., 2012). Because of these studies and because of the observation of a poor correlation between *CTH2* mRNA and Cth2 protein levels in an ARE mutant allele of *CTH2* (Martínez-Pastor et al., 2013a), we decided to investigate a potential role of Cth2 in ARE-dependent translational regulation during iron starvation.

C2.1. *SDH4* mRNA translation decreases under iron deficiency

SDH4 mRNA, which encodes the subunit 4 of succinate dehydrogenase, exhibited one of the most down-regulated transcript patterns in a wild-type strain compared to the *cth2Δ* mutant during iron deficiency (Puig et al., 2005). Therefore, *SDH4* mRNA has been widely used as a model for an ARE-containing Cth2 target in response to iron starvation (Puig et al., 2005; Pedro-Segura et al., 2008; Prouteau et al., 2008; Puig et al., 2008; Vergara et al., 2011). We decided to explore whether

the down-regulation of *SDH4* expression was also controlled at the translational level, as TTP represses the translation of its targets in mammals (Qi et al., 2012; Tiedje et al., 2012). Therefore, *SDH4* mRNA translation was analyzed in a wild-type strain cultivated in iron sufficiency (+Fe) or iron deficiency (-Fe) using two different approaches. First, *SDH4* translation efficiency, defined as the Sdh4 protein/*SDH4* mRNA ratio, was normalized to the translation efficiency of 3-phosphoglycerate kinase *PGK1*, whose levels were not altered by changes in the iron availability. As expected, in response to iron starvation, the *SDH4/PGK1* mRNA levels dropped to the third of those in iron sufficiency (**Figure C2-1: A**). However, the corresponding protein levels lowered to a greater extent, a tenth of the iron sufficiency levels, reducing the translation efficiency of *SDH4* to the third of the translation efficiency in +Fe (**Figure C2-1: A**). However, a potential explanation for this reduced translation efficiency of *SDH4* in -Fe could be a different Sdh4 protein half-life. For this reason, we analyzed the protein half-life of $Flag_2$-Sdh4 protein as explained in Materials and Methods. The result showed that the $Flag_2$-Sdh4 protein half-life during iron limitation was not diminished but increased (**Figure C2-1: B**). Therefore, the decreased Sdh4 protein levels observed during the iron deficiency were not due to the protein destabilization, but probably to a decrease in translation efficiency.

The second experimental approach used to study the translation of *SDH4* in iron deficiency was by polysome fractionation experiments. Polysome profiles in -Fe conditions showed a general decrease in the polysome/80S abundance compared to the +Fe condition (**Figure C2-2: C and D**), as expected from the results of Chapter 1. The specific distribution of the *SDH4* transcript among the fractions showed a greater monosomal 80S peak association during iron starvation compared to the heavy polysomal distribution during iron sufficiency (**Figure C2-2: A**). On the contrary, the polysomal profile of *ACT1* mRNA, a housekeeping gene non-iron regulated, showed a constant and high polyribosome association under both +Fe and -Fe conditions (**Figure C2-2: B**). Taken together, these results suggest that the *SDH4* mRNA translation is inhibited under iron deficiency.

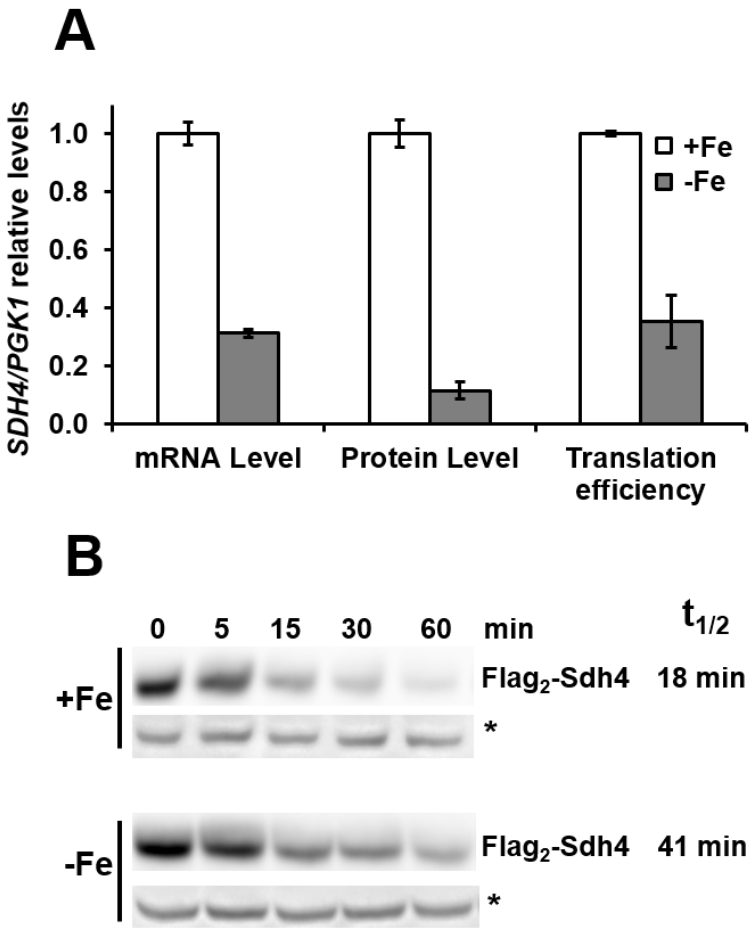

Figure C2-1. The *SDH4* mRNA translation efficiency is decreased under iron deficiency. (A) Analyses of the translation efficiency of *SDH4/PGK1* of wild-type BY4741 cells transformed with the pRS416-Flag$_2$-*SDH4* (*SDH4*) plasmid were performed in three independent biological replicates from overnight cultures reinoculated in SC-Ura with 10 μM FAS (+Fe) and SC-Ura with 100 μM BPS (-Fe) for 7 hours. Flag$_2$-*SDH4* and *PGK1* mRNA levels were determined by RT-qPCR using specific primers, and Flag$_2$-Sdh4 and Pgk1 protein levels were determined by Western blot with anti-Flag and anti-Pgk1 antibodies. The translation efficiency was calculated as: (Flag$_2$-Sdh4 protein / Flag$_2$-*SDH4* mRNA) / (Pgk1 protein / *PGK1* mRNA). Mean values and standard deviations are shown and referred to those in +Fe. **(B)** Flag$_2$-Sdh4 expressing cells were grown as in (A) and protein levels were determined at the indicated times after adding cycloheximide (50 μg/mL). Mean values of the Flag$_2$-Sdh4 protein half-life ($t_{1/2}$) from two independent biological replicates are indicated and were calculated as explained in section 4.4.3 of

Materials and Methods. One of the Western blot results is shown. A non-specific anti-Flag band (*) was used as loading control.

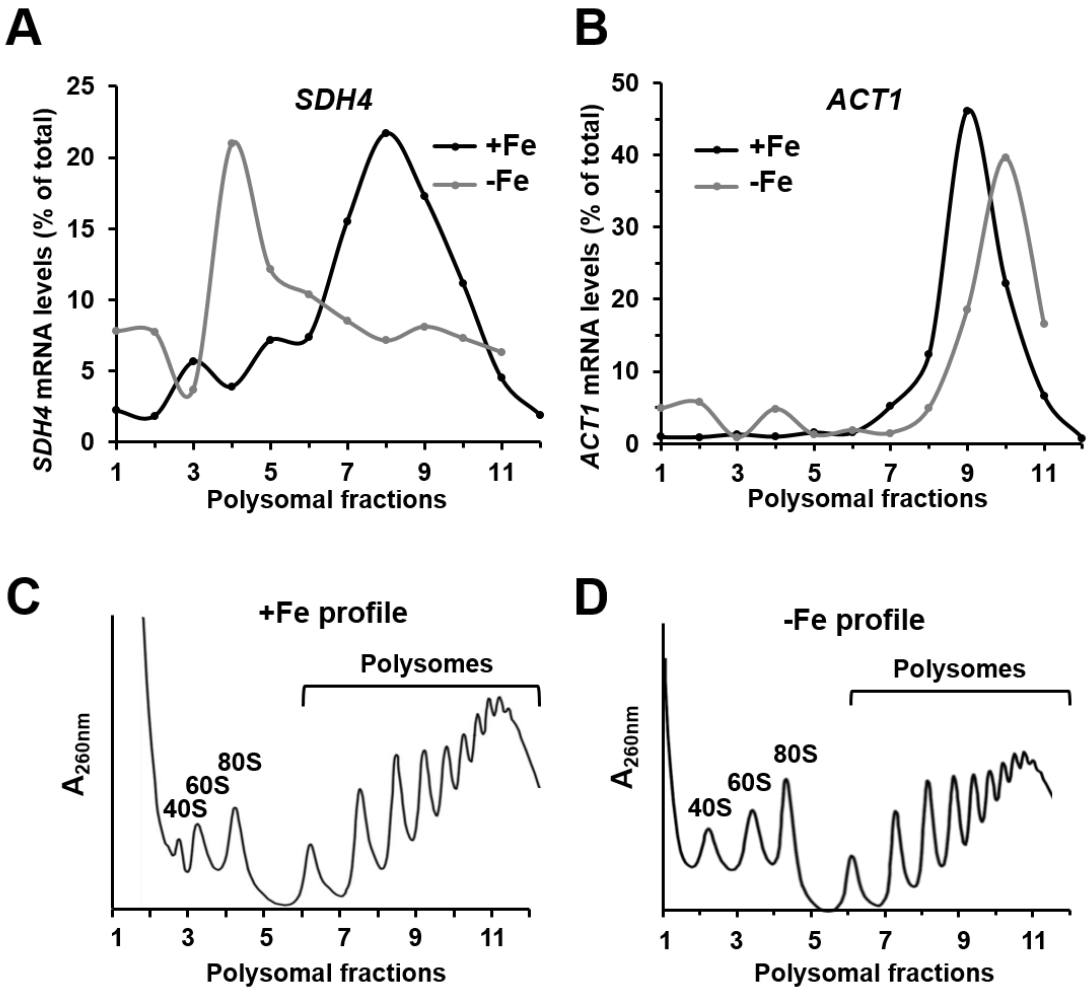

Figure C2-2. The *SDH4* mRNA is more associated to the 80S peak in iron deficiency. Polysome profile experiments of *sdh4Δ* cells transformed with the pRS416-*SDH4* (*SDH4*) plasmid were performed from overnight cultures reinoculated in SC-Ura with 10 μM FAS (+Fe) and SC-Ura with 100 μM BPS (-Fe) for 7 hours. A representative A_{260nm} polysome profile of at least two biologically independent replicates is shown for +Fe **(C)** and -Fe **(D)** and the ribosomal subunits (40S and 60S), monosome (80S) and polysome fractions are indicated. The RNA from individual fractions was extracted and *SDH4* **(A)** and *ACT1* **(B)** mRNA levels were analyzed by RT-qPCR as described in Materials and Methods.

C2.2. AREs within *SDH4* mRNA are required for its translational inhibition under iron deficiency

The degradation of *SDH4* mRNA under iron deficiency depends on the two ARE motifs within its 3'-UTR (Puig et al., 2005). We wanted to test if the *SDH4* mRNA translational inhibition observed in -Fe was ARE-dependent. We used a wild-type (*SDH4*) and a mutated version of *SDH4* (*SDH4-AREmt*) with four adenine nucleotides mutated to cytosine (Puig et al., 2005). Consistent with previous work (Puig et al., 2005), *SDH4-AREmt* mRNA levels displayed a 5-fold increase upon iron deficiency when the AREs were mutated (**Figure C2-3: A**). But importantly, Sdh4 protein levels more than tripled the observed mRNA increase, from 5-fold to 16-fold, which resulted in a 3-fold increment of the *SDH4* translation efficiency when AREs were mutated during iron deficiency (**Figure C2-3: A**). This result was corroborated by polysome profile experiments (**Figure C2-3: B, C, D and E**). While the AREs mutation did not affect the high polyribosome association already observed for *SDH4* in +Fe (**Figure C2-2: A and Figure C2-3: D**), iron deficiency provoked a shift of the *SDH4-AREmt* transcript to polysomal fractions (**Figure C2-3: B**). Again, the high polyribosome association of *ACT1* mRNA was neither affected by the iron availability nor by the AREs of *SDH4* (**Figure C2-3: C and E**). Therefore, these results are indicative of an ARE-mediated *SDH4* mRNA translational inhibition specifically taking place during iron starvation.

C2.3. Cth2 is the responsible of the *SDH4* mRNA translational inhibition under iron deficiency

As previously mentioned, the presence of Cth2 during iron limitation is necessary for the ARE-dependent degradation of *SDH4* mRNA. This regulation requires the binding of the TZFs of Cth2 to the AREs in the 3'UTR of *SDH4* mRNA (Puig et al., 2005). As we already demonstrated that the AREs are the *cis* regulatory elements in the translational inhibition of *SDH4*, we decided to test the implication of Cth2 as *trans* regulatory element in *SDH4* translational repression during iron starvation. We performed *SDH4* translation efficiency and polysome profile experiments during iron deficiency either with a plasmid of the wild-type version of *CTH2*, a TZFs mutant (*CTH2-C190R*) or an empty vector (*cth2Δ*). In order to eliminate the secondary role played by Cth1, the experiments were performed in a

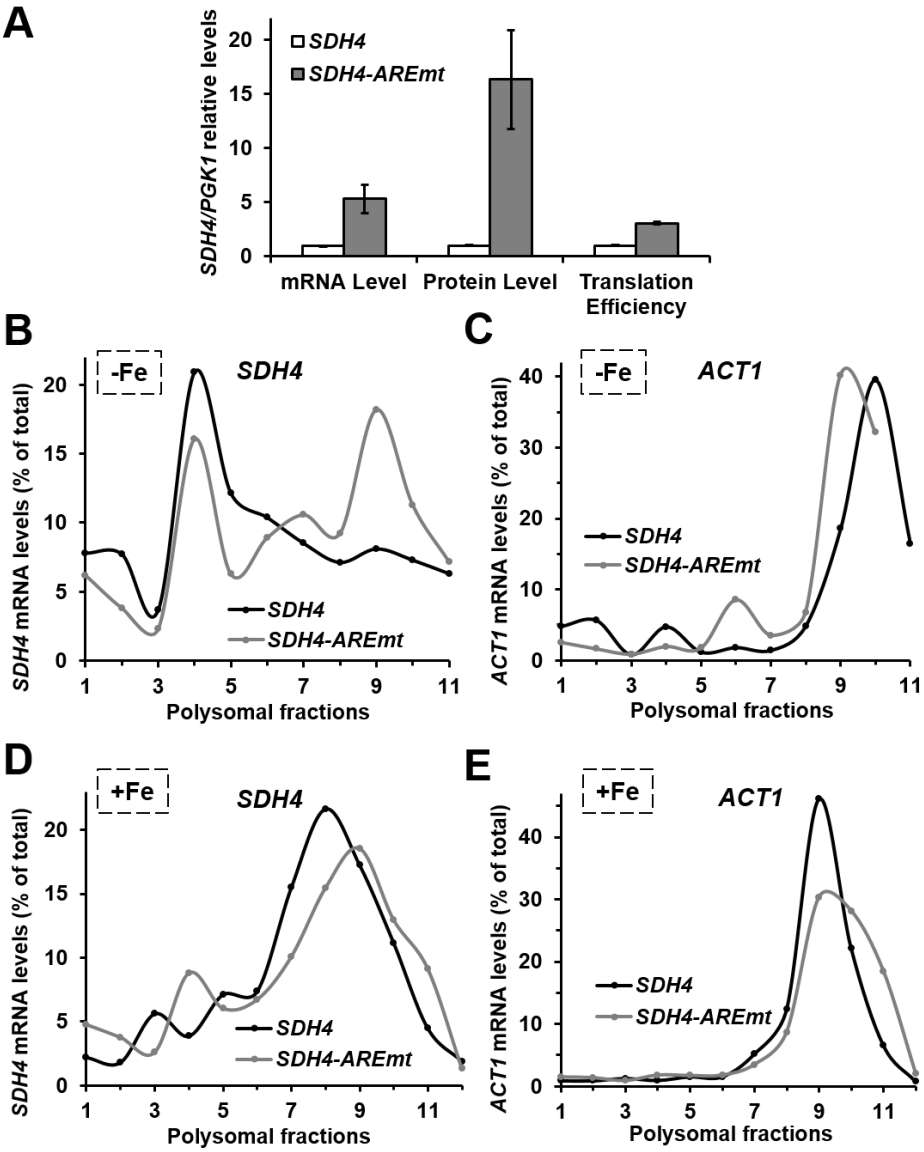

Figure C2-3. AREs within *SDH4* mRNA are required for its translational inhibition under iron deficiency. (A) Analyses of the translation efficiency of *SDH4/PGK1* were performed in *sdh4Δ* cells transformed with pRS416-Flag$_2$-*SDH4* (*SDH4*) or pRS416-Flag$_2$-*SDH4-AREmt* (*SDH4-AREmt*) in -Fe as explained in Figure C2-1 A. Mean values and standard deviations from two independent experiments are shown and referred to pRS416-Flag$_2$-*SDH4* (*SDH4*). **(B-E)** Polysome profile experiments of *sdh4Δ* cells transformed with pRS416-*SDH4* (*SDH4*) or pRS416-*SDH4-AREmt* (*SDH4-AREmt*) were performed in +Fe and -Fe as in Figure C2-2. The RNA from individual fractions was extracted and *SDH4* **(B, D)** and *ACT1* **(C, E)** mRNA levels were analyzed by RT-qPCR as described in Materials and Methods. A representative profile from at least two biologically independent replicates is shown in each case.

cth1Δcth2Δ background, as it was done in most Cth2-related investigations previously performed (Puig et al., 2005; Pedro-Segura et al., 2008; Puig et al., 2008; Vergara et al., 2011; Romero et al., 2018b). When Cth2 was absent (*cth2Δ*) or mutated in the TZFs (*CTH2-C190R*), *SDH4* mRNA levels increased by 1.5 to 1.8-fold during iron limitation (**Figure C2-4: A**), whereas the Sdh4 protein levels increment

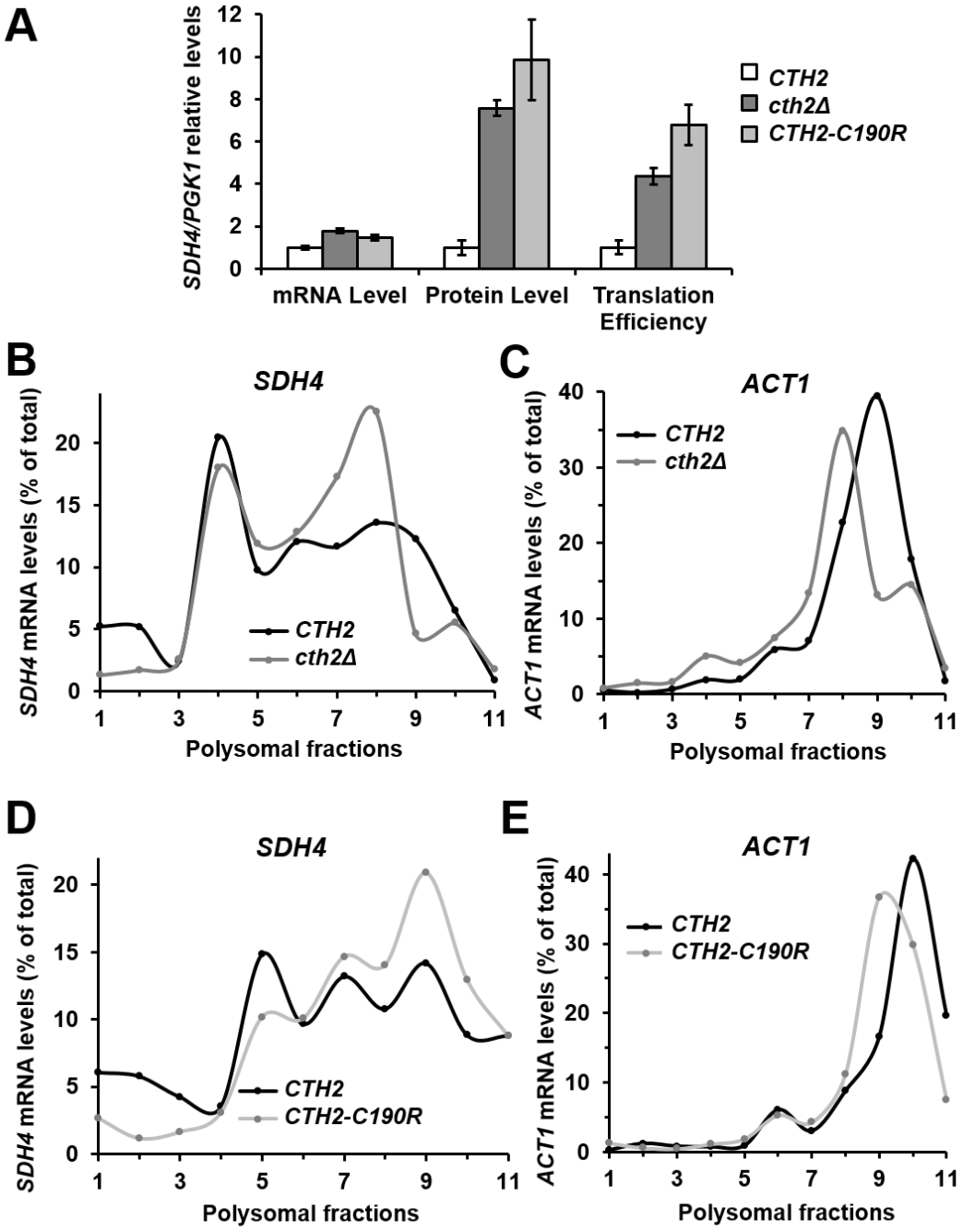

Figure C2-4. Cth2 represses *SDH4* mRNA translation in a Cth2-TZF-dependent manner when iron is scarce. (A) Analyses of the translation efficiency of

SDH4/PGK1 of *cth1Δcth2Δ* mutant cells co-transformed with pRS416-Flag$_2$-*SDH4* and either pRS415-*CTH2* (*CTH2*), pRS415 (*cth2Δ*) or pRS415-*CTH2-C190R* (*CTH2-C190R*) were performed in three independent biological replicates from overnight cultures reinoculated in SC-Ura-Leu with 100 μM BPS (-Fe) for 7 hours. Calculations were performed as explained in Figure C2-1 A. Mean values and standard deviations are shown and referred to pRS415-*CTH2* (*CTH2*). **(B-E)** Polysome profile experiments of *cth1Δcth2Δsdh4Δ* cells co-transformed with pRS416-*SDH4* and either pRS415-*CTH2* (*CTH2*), pRS415 (*cth2Δ*) or pRS415-*CTH2-C190R* (*CTH2-C190R*) were performed as mentioned above. The RNA from individual fractions was extracted and *SDH4* **(B, D)** and *ACT1* **(C, E)** mRNA levels analyzed by RT-qPCR as described in Materials and Methods. A representative profile from at least two biologically independent replicates is shown in each case.

was from 8 to 10-fold. With this result, the calculated *SDH4* translation efficiency increased by 5 to 7-fold during iron deficiency in a Cth2-dependent manner. This result was again corroborated by polysome profile experiments (**Figure C2-4: B, C, D and E**). Similar results to *SDH4-AREmt* cells were obtained (**Figure C2-3: B**), since a higher *SDH4* mRNA polysomal association was observed in *cth2Δ* and *CTH2-C190R* cells in -Fe (**Figure C2-4: B and D**). Again, *ACT1* mRNA distribution was not affected by Cth2 (**Figure C2-4: C and E**). These results demonstrate that *SDH4* translational repression under iron deficiency is mediated by the Cth2 protein through the binding of its TZFs to the AREs in the 3'-UTR of the *SDH4* mRNA.

C2.4. *CTH2* mRNA translation is also repressed by Cth2 protein under iron limitation

As before mentioned, Cth2 protein promotes its own mRNA decay in an ARE-dependent manner (Martínez-Pastor et al., 2013a). This is important for rapid Cth2 disappearance and the consequent recovery of cell respiration, among other iron-dependent processes, when iron availability is restored (Martínez-Pastor et al., 2013a). In this way, the Cth2 translational repression of its own mRNA would contribute to its negative feedback regulation. To test whether the ARE of *CTH2* mRNA was the *cis*-regulatory element in its translational inhibition, we assayed a

wild-type (*CTH2*) and an ARE mutated version of *CTH2* (*CTH2-AREmt*) in iron deficiency. While the *CTH2* mRNA levels suffered only a 1.3-fold increase in the *CTH2-AREmt* samples, the corresponding protein levels increased 4.8-fold (**Figure C2-5: A**). Consequently, *CTH2* translation efficiency was 3.6-fold higher in the *CTH2-AREmt* mutant than in the wild-type *CTH2* during the iron deficiency (**Figure C2-5: A**). Regarding the polysome profile experiments, *CTH2* mRNA was more associated to heavier polysomal fractions in the ARE mutated version of *CTH2* in -Fe (**Figure C2-5: B**), while *ACT1* mRNA was similar in both cases (**Figure C2-5: C**). Therefore, these results are indicative of an ARE-mediated *CTH2* mRNA translational repression.

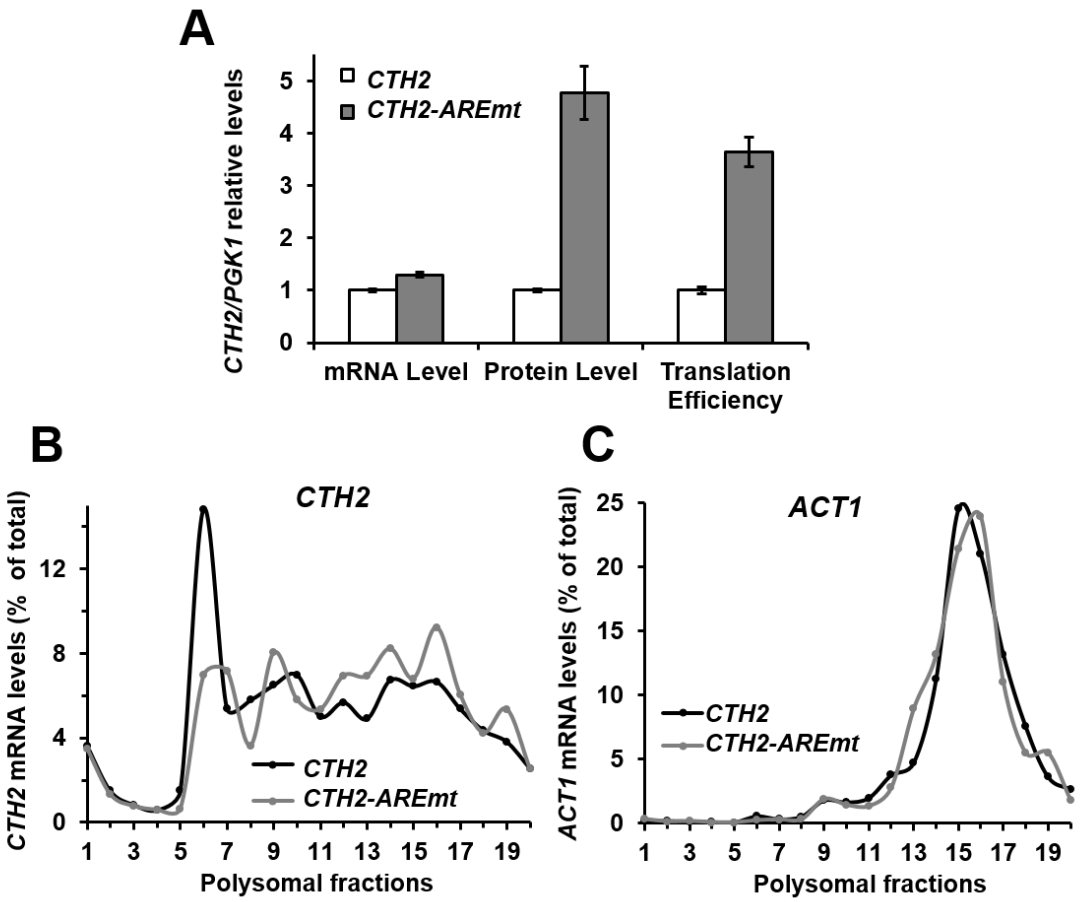

Figure C2-5. The ARE sequence of the *CTH2* mRNA represses its translation in low iron conditions. (A) Analyses of the translation efficiency of *CTH2/PGK1* of *cth1Δcth2Δ* mutant cells transformed with pRS416-Flag$_2$-*CTH2* (*CTH2*) or pRS416-Flag$_2$-*CTH2-AREmt* (*CTH2-AREmt*) were performed in at least two independent biological replicates from overnight cultures reinoculated in SC-Ura with 100 μM

BPS (-Fe) for 7 hours. Calculations were performed as explained in Figure C2-1 A with *CTH2* instead of *SDH4* data. Mean values and standard deviations are shown and referred to those of pRS416-Flag$_2$-*CTH2* (*CTH2*). **(B and C)** Polysome profile experiments of *cth1Δcth2Δ* mutant cells transformed with pRS416-*CTH2* (*CTH2*) or pRS416-*CTH2-AREmt* (*CTH2-AREmt*) were performed as mentioned above. The RNA from individual fractions was extracted and *CTH2* **(B)** and *ACT1* **(C)** mRNA levels were analyzed by RT-qPCR as described in Materials and Methods. A representative profile from at least two biologically independent replicates is shown in each case.

At this point, Cth2 protein seemed likely to be the *trans*-acting factor regulating the *CTH2* mRNA translational inhibition through its TZFs. To demonstrate it, we used the wild-type (*CTH2*) and the TZFs mutated version of *CTH2* (*CTH2-C190R*) in iron deficiency, since Cth2 protein stability was not affected by the *C190R* mutation (**Figure C2-6**). The *CTH2* mRNA levels were increased 2.8-fold in *CTH2-C190R* expressing cells, compared to *CTH2* wild-type cells, whereas the protein increased 4.5-fold (**Figure C2-7: A**). The result was a 1.6-fold increment in the translation efficiency of *CTH2* in the TZF mutant in -Fe (**Figure C2-7: A**). The results obtained with polysome profiles indicated similar conclusions. The *CTH2* transcript was more associated to heavier polysomal fractions in *CTH2-C190R* cells in -Fe, whereas *ACT1* mRNA did not (**Figure C2-7: B and C**, respectively). Taken together, we can conclude from these results that the Cth2 protein represses its own mRNA translation by the specific binding of its TZFs to the ARE in the 3'UTR of its transcript.

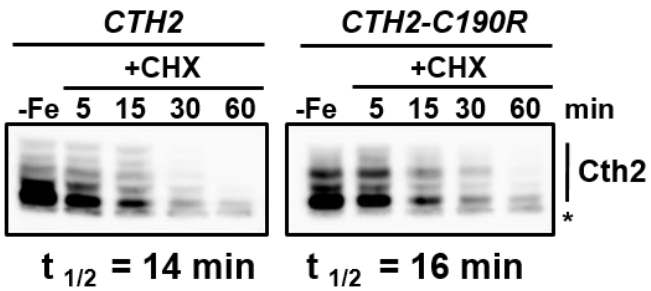

Figure C2-6. The Cth2 protein stability in iron deficiency is TZF-independent. Protein half-life ($t_{1/2}$) of *cth1Δcth2Δ* mutant cells transformed with pRS416-Flag$_2$-

CTH2 (*CTH2*) or pRS416-Flag$_2$-*CTH2-C190R* (*CTH2-C190R*) was determined from overnight cultures reinoculated in SC-Ura with 100 µM BPS (-Fe) for 7 hours. Protein levels were determined at the indicated times after adding cycloheximide (50 µg/mL). Mean values of the protein half-life ($t_{1/2}$) from two independent biological replicates are indicated, and one of the Western blot results is shown. A non-specific anti-Flag band (*) was used as loading control.

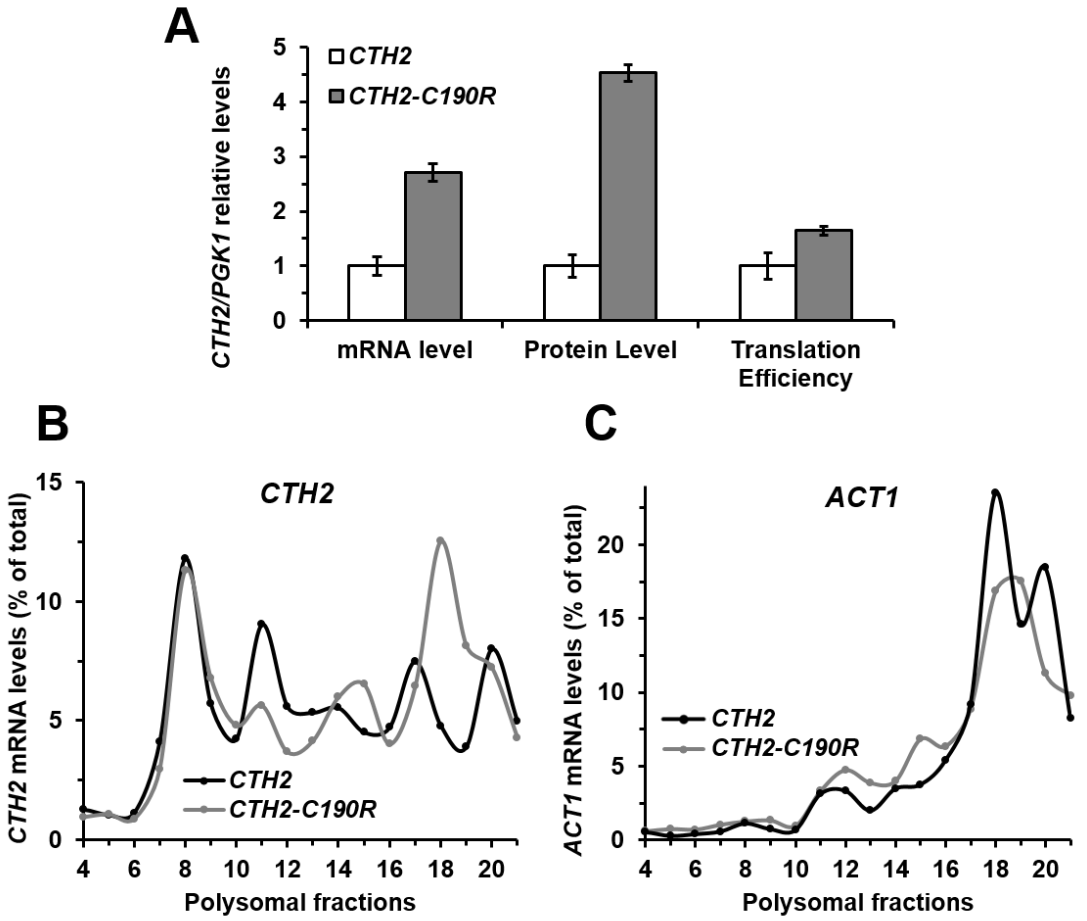

Figure C2-7. Cth2 represses its own mRNA translation in a Cth2-TZF-dependent manner under iron-limited conditions. (A) Analyses of the translation efficiency of *CTH2/PGK1* of *cth1Δcth2Δ* mutant cells transformed with pRS416-Flag$_2$-*CTH2* (*CTH2*) or pRS416-Flag$_2$-*CTH2-C190R* (*CTH2-C190R*) were performed in four independent biological replicates represented and normalized as in Figure C2-5 A. **(B and C)** Polysome profile experiments of *cth1Δcth2Δ* mutant

cells transformed with pRS416-*CTH2* (*CTH2*) or pRS416-*CTH2-C190R* (*CTH2-C190R*) were performed as mentioned above. The RNA from individual fractions was extracted and *CTH2* **(B)** and *ACT1* **(C)** mRNA levels were analyzed by RT-qPCR as described in Materials and Methods. A representative profile from at least two biologically independent replicates is shown in each case.

C2.5. Cth2 represses the translation of multiple ARE-containing mRNAs

Besides the above *SDH4* and *CTH2* mRNAs translational repression via Cth2-binding, we wondered if Cth2 was able to repress the translation of other ARE-containing mRNAs. For this purpose, we analyzed the polysome profiles of additional Cth2 mRNA-targets in cells expressing or lacking *CTH2* in iron deficiency. For a better quantification of the mRNAs distribution, the fractions of each replicate were grouped in two pools prior to RNA extraction: monosomal and polysomal (**Figure C2-8**), in addition to the analysis of individual fractions (**Figure C2-9**).

The analysis showed that the presence of cytochrome-*c* peroxidase (*CCP1*), ferrochelatase (*HEM15*) and the ribonucleotide reductase inhibitor (*WTM1*) mRNAs in the pooled polysomal *versus* monosomal fractions was higher in the *cth2Δ* cells compared to the wild-type *CTH2*-expressing cells (**Figure C2-8: A, B and C**). These results were also confirmed by the profile of individual fractions (**Figure C2-9: A, B and C**). This higher association to heavier polysomal fractions (and lower to monosomal fractions) in the *cth2Δ* mutant was similarly found in *SDH4* mRNA (**Figure C2-8: D and Figure C2-9: D**), which already was shown to be regulated at the translational level in a Cth2-dependent manner (**Figure C2-4: A, B and D**), while the control *ACT1* mRNA showed minimal differences (**Figure C2-8: E and Figure C2-9: E**). The polyribosome analyses of specific mRNAs in individual fractions, as well as in pooled fractions, confirmed that, in addition to *SDH4*, other Cth2 mRNA-targets (*CCP1*, *HEM15* and *WTM1*) were translationally inhibited by Cth2 during iron starvation.

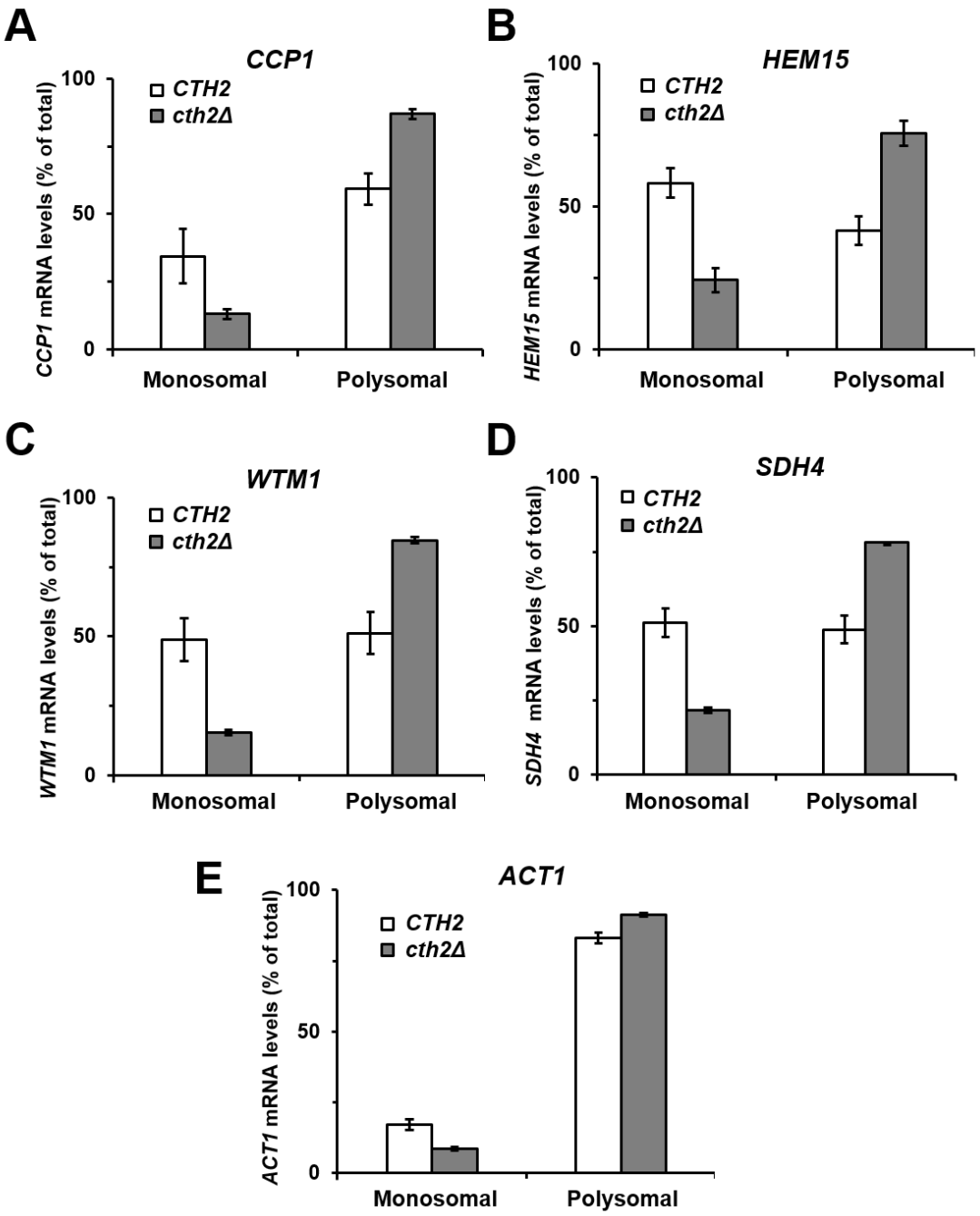

Figure C2-8. Cth2 represses the translation of several ARE-containing mRNAs under iron deficiency. Polysome profile experiments of *cth1Δcth2Δsdh4Δ* cells co-transformed with pRS416-*SDH4* and either pRS415-*CTH2* (*CTH2*) or pRS415 (*cth2Δ*) were performed in two independent biological replicates from overnight cultures reinoculated in SC-Ura-Leu with 100 μM BPS (-Fe) for 7 hours. The RNA from unified monosomal and polysomal fractions was extracted and *CCP1* **(A)**, *HEM15* **(B)**, *WTM1* **(C)**, *SDH4* **(D)** and *ACT1* **(E)** mRNA levels were analyzed by RT-qPCR as described in Materials and Methods. Mean values and standard deviations are shown.

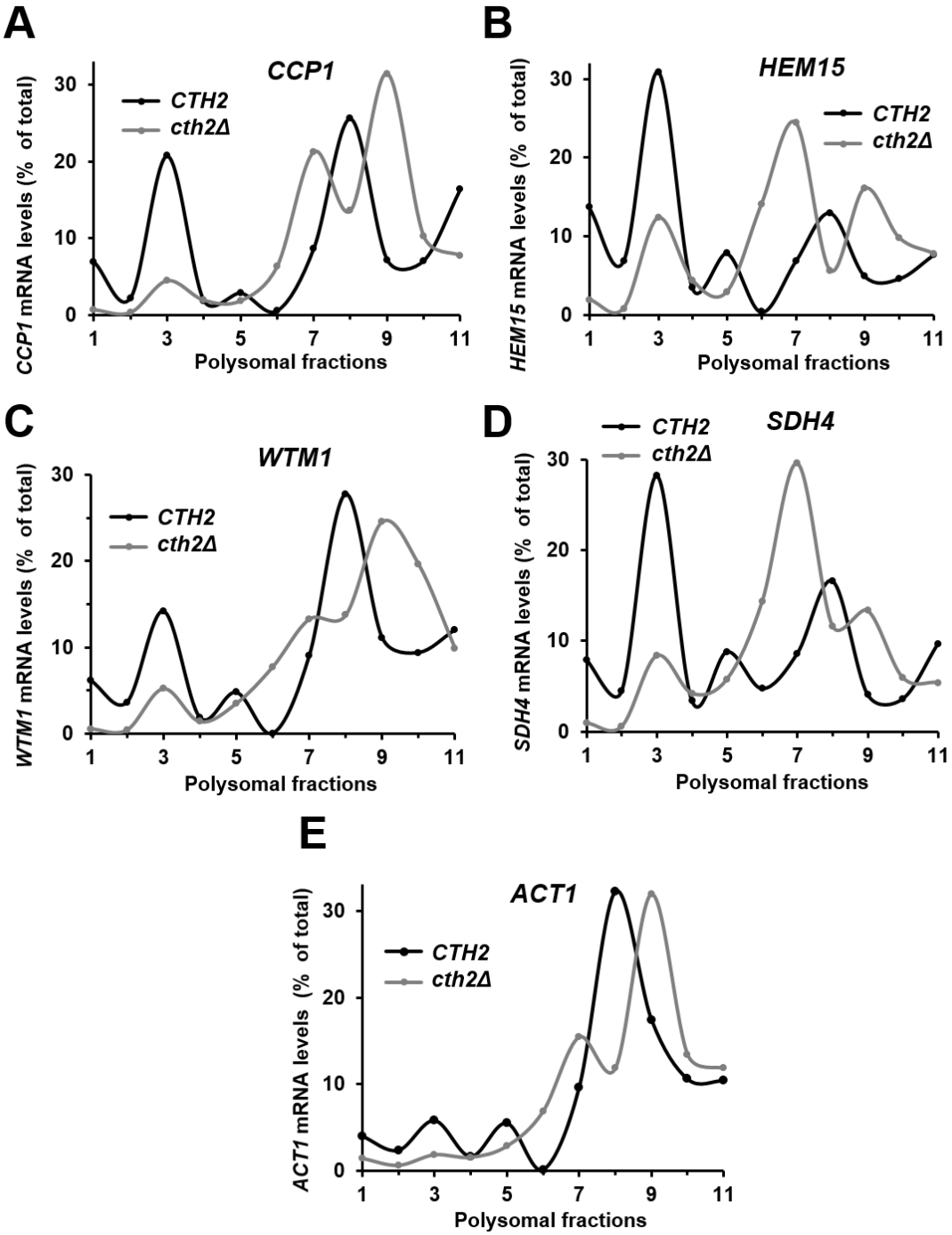

Figure C2-9. Cth2 represses the translation of several ARE-containing mRNAs under iron deficiency. The RNA from individual fractions of the polysome profile experiments from Figure C2-8 was extracted and *CCP1* **(A)**, *HEM15* **(B)**, *WTM1* **(C)**, *SDH4* **(D)** and *ACT1* **(E)** mRNA levels were analyzed by RT-qPCR as described in Materials and Methods. Mean values and standard deviations are shown. A representative profile from two biologically independent replicates is shown in each case.

C2.6. Both Cth2 amino and carboxy-terminal domains are involved in *SDH4* mRNA translational repression, but only the amino-terminal domain is responsible for mRNA decay

Previous studies have shown that the first 89 amino acids of the amino-terminal domain (NTD) of Cth2 are involved in its ability to promote targeted mRNA decay without affecting the protein shuttling between the nucleus and the cytoplasm (Prouteau et al., 2008; Vergara et al., 2011). These amino acids are within the conserved CR1 region of Cth2, probably involved in the recruitment of components of the mRNA degradation machinery. To decipher which Cth2 protein regions, besides the TZFs, were important for the Cth2-dependent mRNA translational repression, we studied the *SDH4* mRNA translational status with different truncated versions of Cth2 fused to GFP (**Figure C2-10: A**, *GFP-CTH2ΔN89* lacking CR1*, GFP-CTH2ΔN170* lacking CR1 and CR2, and *GFP-CTH2ΔC52* lacking CR3). The fusion of GFP to the amino-terminus of Cth2 did not affect its function in mRNA decay, -Fe growth or nucleus-cytoplasm shuttling (Vergara et al., 2011; Ramos-Alonso et al., 2018a). The translation efficiency experiments under iron starvation showed the expected increment in *SDH4* mRNA levels in the *cth2Δ* cells compared to the *GFP-CTH2* (*CTH2*) wild-type cells (**Figure C2-10: B**). The increment was more pronounced at the Sdh4 protein level, obtaining a 1.7-fold increment in *SDH4* translation efficiency in *cth2Δ* cells during iron deficiency compared to *CTH2* (**Figure C2-10: B**). The cells expressing the truncated versions of Cth2 in the NTD (*CTH2ΔN89* and *CTH2ΔN170*) showed an intermediate situation between wild-type and *cth2Δ* cells*. SDH4* translation efficiency slightly increased in *CTH2ΔN89* compared to wild-type. However, translation efficiency levels closer to those obtained with *cth2Δ* were reached in *CTH2ΔN170* expressing cells (**Figure C2-10: B**). To further address the Cth2 NTD contribution to *SDH4* translation, polysome profile experiments were performed with *CTH2ΔN170* expressing cells in -Fe (**Figure C2-10: C**). Again, the *SDH4* mRNA profile showed an intermediate situation between wild-type *CTH2* cells and the *cth2Δ* mutant (**Figure C2-10: C**). These results suggest that both CR1 and CR2 conserved NTDs of Cth2 are involved in *SDH4* mRNA decay as well as in the translational inhibition of *SDH4* that occurs during iron starvation.

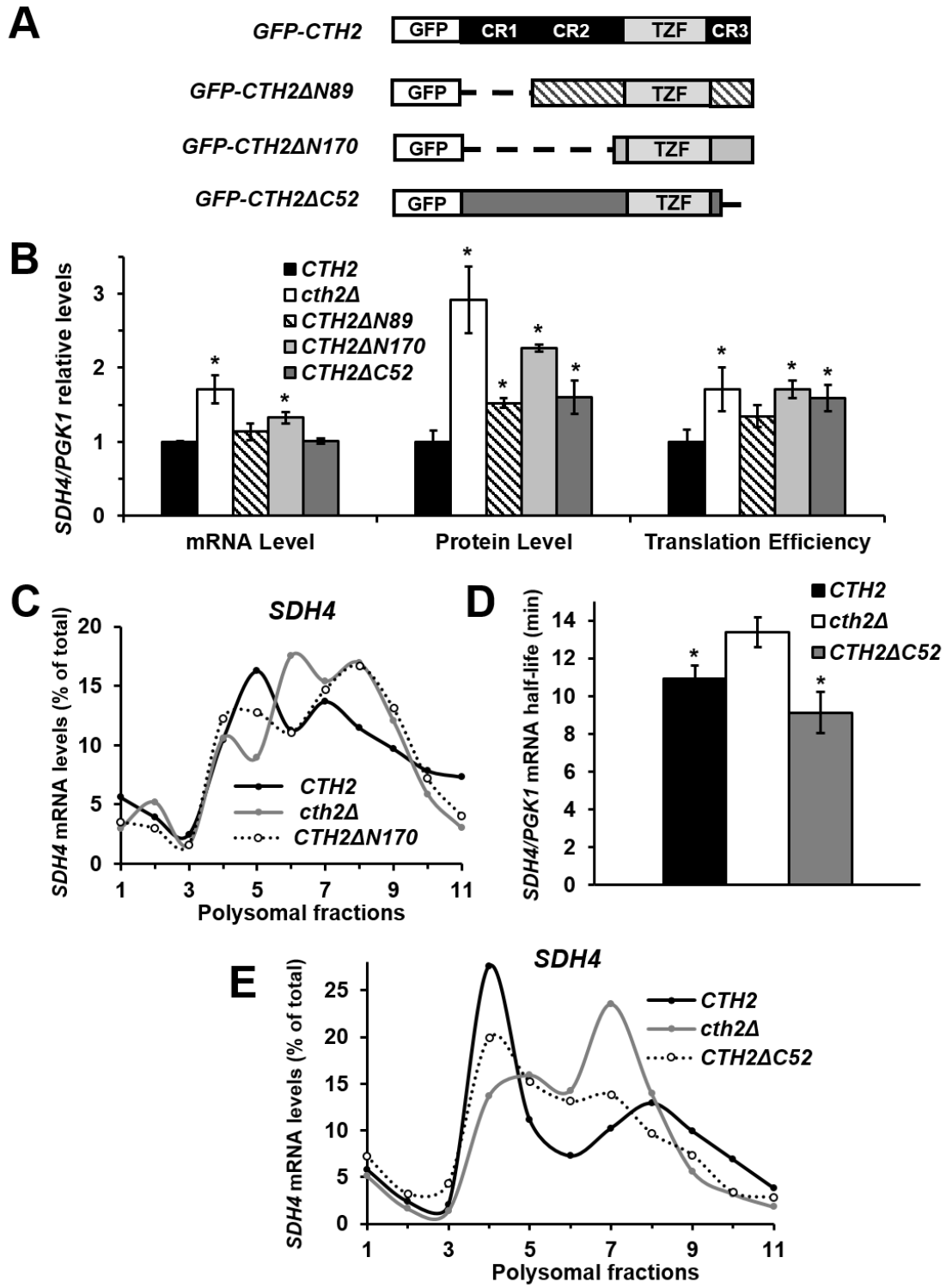

Figure C2-10. Both Cth2 NTD and CTD are necessary for *SDH4* mRNA translational repression, whereas only Cth2 NTD is involved in *SDH4* mRNA decay during iron deficiency. (A) Schematic representation of the pRS416-*GFP-CTH2* fusion truncated plasmids at the amino-terminal domain (NTD) and the carboxy-terminal domain (CTD). The number of amino acids truncated is indicated

(*ΔN89* and *ΔN170* in the NTD, and *ΔC52* in the CTD) as well as the situation of the conserved regions (CR) and the TZFs. **(B)** Analyses of the translation efficiency of *SDH4/PGK1* of *cth1Δcth2Δ* mutant cells co-transformed with pRS415-$Flag_2$-*SDH4* and either pRS416-*GFP-CTH2* (*CTH2*), pRS416 (*cth2Δ*), pRS416-*GFP-CTH2ΔN89* (*CTH2ΔN89*), pRS416-*GFP-CTH2ΔN170* (*CTH2ΔN170*) or pRS416-*GFP-CTH2ΔC52* (*CTH2ΔC52*) were performed in three independent biological replicates from overnight cultures reinoculated in SC-Ura-Leu with 100 μM BPS (-Fe) for 7 hours. Calculations were performed as explained in Figure C2-1 A. Mean values and standard deviations are shown and referred to pRS416-*GFP-CTH2* (*CTH2*). An asterisk (*) indicates a significant difference (*p*-value <0.03) from two-tailed student's t-test compared with pRS416-*GFP-CTH2* (*CTH2*). **(C and E)** Polysome profile experiments of *cth1Δcth2Δsdh4Δ* cells co-transformed with pRS415-*SDH4* and either pRS416-*GFP-CTH2* (*CTH2*), pRS416 (*cth2Δ*), pRS416-*GFP-CTH2ΔN170* (*CTH2ΔN170*, in panel **C**) or pRS416-*GFP-CTH2ΔC52* (*CTH2ΔC52*, in panel **E**) were performed as mentioned above. The RNA from individual fractions was extracted and *SDH4* mRNA levels were analyzed by RT-qPCR as described in Materials and Methods. A representative profile from at least two biologically independent replicates is shown in each case. **(D)** The *SDH4/PGK1* relative mRNA half-life was calculated in *cth1Δcth2Δsdh4Δ* cells co-transformed with pRS415-*GAL1-SDH4* and either pRS416-*GFP-CTH2* (*CTH2*), pRS416 (*cth2Δ*) or pRS416-*GFP-CTH2ΔC52* (*CTH2ΔC52*) as explained in section 4.2.2 of Materials and Methods. Mean values and standard deviations from three independent experiments are shown. An asterisk (*) indicates a significant difference (*p*-value <0.04) from two-tailed student's t-test compared with *cth2Δ*.

On the other hand, the experiments involving the conserved region CR3 in the carboxy-terminal domain (CTD) of Cth2, using the *CTH2ΔC52* truncated version, suggested that the steady-state *SDH4* mRNA levels were not altered by the CTD (**Figure C2-10: B**). This result was consistent with Prouteau et al. (2008), but to unequivocally determine whether Cth2 CTD contributed to *SDH4* mRNA stability, *SDH4* mRNA half-life was determined in *CTH2ΔC52*, wild-type *CTH2* and in *cth2Δ* mutant cells. *SDH4* mRNA half-life in *CTH2ΔC52* was similar to the one

obtained in wild-type *CTH2* cells, and both lower than in *cth2Δ* (**Figure C2-10: D**). With these results, we can conclude that the Cth2 CTD is not involved in the decay of *SDH4* mRNA. However, Sdh4 protein levels and *SDH4* translation efficiency in *CTH2ΔC52* were significantly higher than in cells expressing wild-type *CTH2* (**Figure C2-10: B**). In the same way, polysome profile experiments with *CTH2ΔC52* showed an intermediate *SDH4* mRNA distribution between wild-type *CTH2* and *cth2Δ* cells in the 80S peak and in polysome fractions (**Figure C2-10: E**). Taken together, these results suggest that Cth2 NTD is important for both *SDH4* mRNA decay and translational repression, whereas CTD is only involved in translational inhibition during iron deficiency.

C2.7. The deletion of Cth2 CTD alters the levels of various iron-dependent proteins under iron starvation

After the observation that the CTD of Cth2 was significantly involved in the translational repression of *SDH4* but not in its mRNA degradation, we wanted to test if there were increased protein levels of other Cth2-targets in *CTH2ΔC52* cells during the iron deficiency. We determined the protein levels of three iron-dependent proteins: aconitase (Aco1), biotin synthase (Bio2) and ferrochelatase (Hem15) under iron starvation in wild-type *CTH2*, *CTH2ΔC52* and *cth2Δ* mutant cells (**Figure C2-11: A**). Hem15, Bio2 and, to a minor extent, Aco1 protein levels were increased in *cth2Δ* cells in -Fe, as observed with Sdh4 protein (**Figure C2-4: A and Figure C2-10: B**) and previously shown with Sdh2 (Martínez-Pastor et al., 2013a). However, *CTH2ΔC52* expressing cells, which only lack the CR3, displayed similar or more increased protein levels of these Cth2 targets. (**Figure C2-11: A**). This result reinforces the previous suggestion of the Cth2 CTD involvement in the translational repression of Cth2 mRNA-targets during iron starvation.

Following these results, we wondered how the NTD and CTD of Cth2 were structured when the TZF domain was binding the mRNA, probably exposing some motifs for the recruitment of components of mRNA decay and/or translational repressive machineries. Using as template the solved TZFs structure of the human homologue TIS11d associated with a single-stranded RNA (Hudson et al., 2004), Dr. Julio Polaina predicted Cth2 protein structure (**Figure C2-11: B**). On the one hand, the prediction suggested an NTD unstructured conformation, not showed in

the figure. On the other hand, the model interestingly predicted the CTD folding back into the TZFs of Cth2 (**Figure C2-11: B**). This is in agreement with previous observations about the lack of functionality of any CTD-tagged Cth2 protein, as it could be interfering with the ARE-binding function of the TZFs (Puig et al., 2005; Prouteau et al., 2008; Vergara et al., 2011). Together, these results suggest that the unstructured Cth2 NTD could be recruiting both mRNA decay and translational repressive machineries, whereas the CTD, that could be interacting with the TZF domain, would be dispensable for the *SDH4* mRNA decay but would contribute to the translational repression of several iron-dependent proteins.

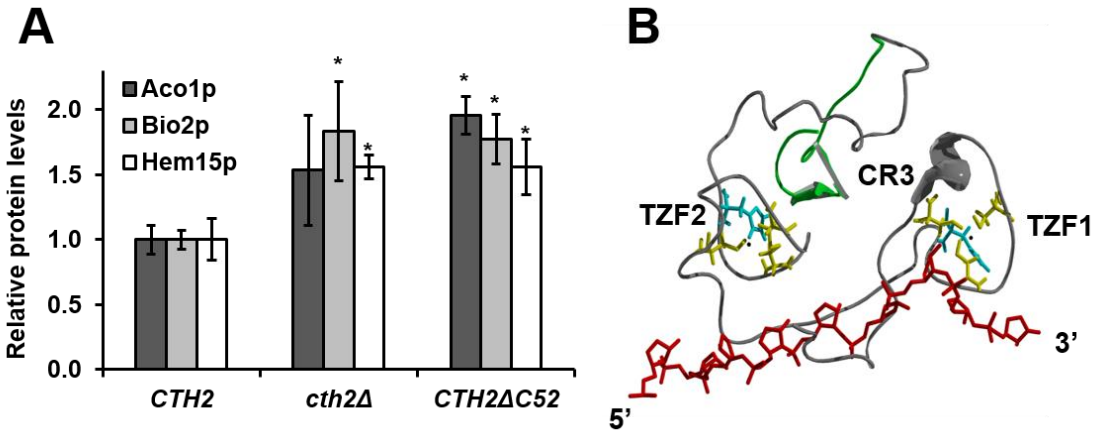

Figure C2-11. The Cth2 CTD deletion increases the abundance of various iron-dependent proteins. (A) Western blot experiments of *cth1Δcth2Δ* mutant cells transformed with pRS416-*GFP-CTH2* (*CTH2*), pRS416 (*cth2Δ*) or pRS416-*GFP-CTH2ΔC52* (*CTH2ΔC52*) were performed from overnight cultures reinoculated in SC-Ura with 100 µM BPS (-Fe) for 7 hours. Total protein levels of aconitase (Aco1p), biotin synthase (Bio2p) and ferrochelatase (Hem15p) were determined. Relative mean values and standard deviations from three independent experiments are shown. An asterisk (*) indicates a significant difference (*p*-value <0.05) from two-tailed student's t-test compared to *CTH2*. **(B)** The structural model for Cth2 CTD and TZFs was performed as explained in section 5 of Materials and Methods. The structure from amino acid 160 to 285 bound to single-stranded RNA (in red) is represented. The protein back-bone is indicated in gray except the CR3 (from amino acid 263 to 285), which is indicated in green. The histidine and cysteine residues that coordinate the two Zn^{2+} ions (symbolized by black small

spheres) are displayed in blue and yellow colors, respectively. TZF1: TZF on the NTD side; TZF2: TZF on the CTD side.

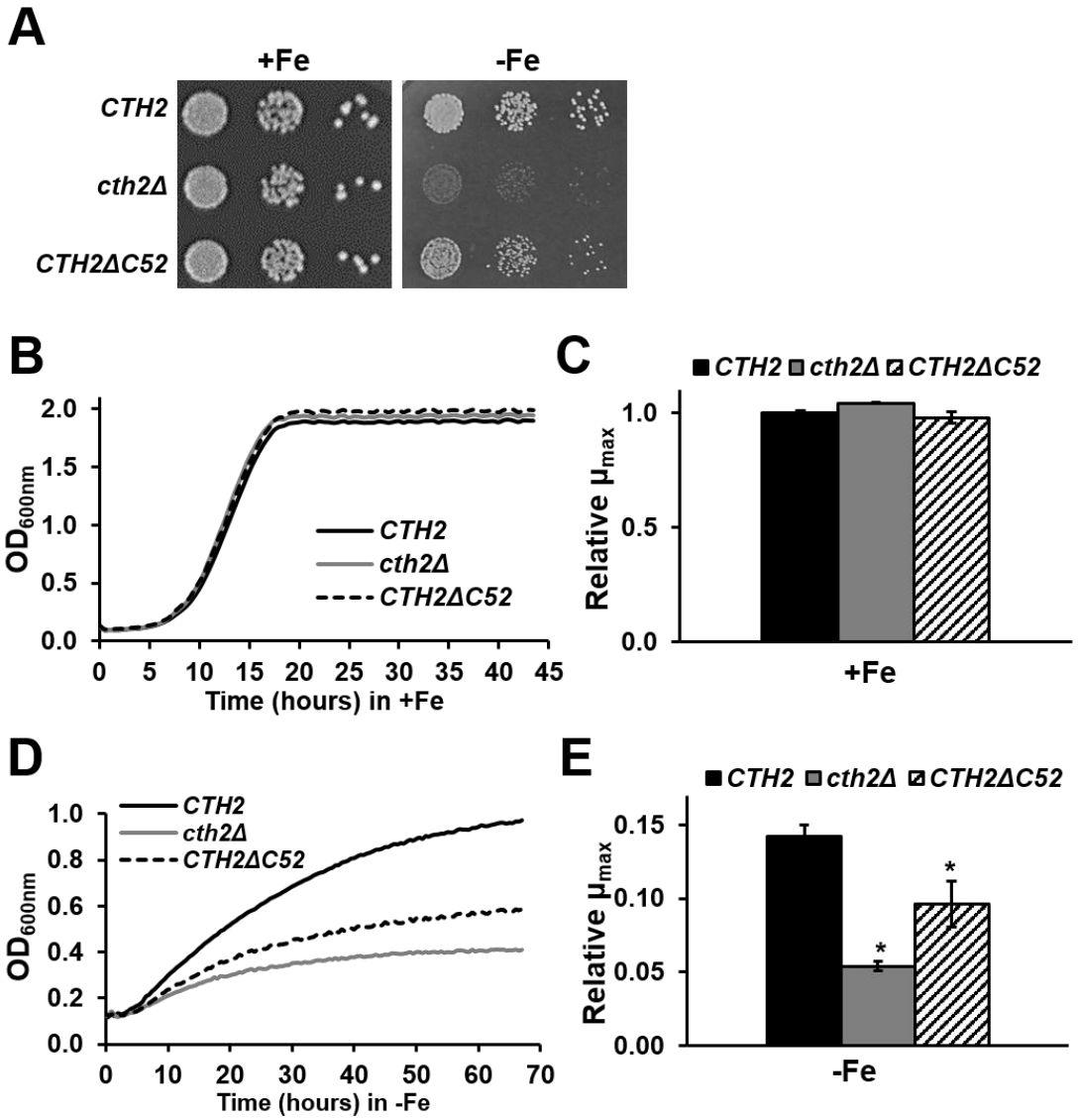

Figure C2-12. The Cth2 CTD mutant shows growth defects under iron-deficient conditions. Cell growth analyses of *cth1Δcth2Δ* mutant cells transformed with pRS416-*GFP-CTH2* (*CTH2*), pRS416 (*cth2Δ*) or pRS416-*GFP-CTH2ΔC52* (*CTH2ΔC52*) were performed from overnight cultures in SC-Ura (+Fe) and SC-Ura with 700 μM Ferrozine (-Fe) as explained in section 1.4 of Materials and Methods in solid media **(A)** and in liquid media **(B-E)**. At least three independent biological replicates are shown in each case. Mean values of the growth curves (OD_{600} vs. time) were represented **(B and D)** and relative mean μ_{max} (maximum specific growth rate, h^{-1}) values referred to *CTH2* in +Fe are shown with

standard deviations **(C and E)**. An asterisk (*) indicates a significant difference (*p*-value <0.05) from two-tailed student's t-test compared to *CTH2* value in -Fe.

C2.8. The Cth2 CTD is physiologically relevant under iron deficiency

The specific role of Cth2 CTD in translational repression of Cth2-mRNA targets, together with the predicted CTD interaction with the TZF domain, suggest an implication of the Cth2 CTD in the yeast adaptation to iron-deficient conditions. As expected, neither the cell growth of *CTH2ΔC52* nor *cth2Δ* mutant cells was affected compared to the wild-type *CTH2* in solid or in liquid iron-sufficient media (**Figure C2-12: A, B and C**). However, the Cth2 CTD mutant showed a slight growth defect in iron-deficient solid medium (**Figure C2-12: A**). Remarkably, this growth defect was more prominent under iron deficiency in liquid media, with maximum OD_{600} mean values (**Figure C2-12: D**) and maximum specific growth rate (μ_{max}) (**Figure C2-12: E**) of *CTH2ΔC52* cells significantly decreased in comparison with *CTH2*. Taken together, these results support a physiologically relevant role of Cth2 CTD under iron starvation.

Discussion

Chapter 2

Discussion of Chapter 2

The expression of *CTH2* in response to iron deficiency is known to be necessary to optimize iron utilization. Cth2 protein promotes a metabolic remodeling of iron-dependent processes via ARE-mediated mRNA decay that is essential for the physiological fitness of cells under iron starvation (Puig et al., 2005). In the nucleus, Cth2 binds through its TZFs to ARE-containing mRNAs encoding proteins involved in iron-consuming pathways (Puig et al., 2005; Puig et al., 2008). Then, the mRNA-bound to Cth2 is exported to the cytoplasm where mRNA degradation occurs preferentially via the 5' to 3' pathway in a Dhh1- and Xrn1-dependent manner (Pedro-Segura et al., 2008). Occasionally, Cth2 can also interfere in the nucleus with the choice of the polyadenylation site and promote extended transcripts of its target mRNAs, which are rapidly degraded in the nucleus by the 5' to 3' exonuclease Rat1 or in the cytoplasm by Xrn1 (Ciais et al., 2008; Prouteau et al., 2008; Vergara et al., 2011; Martínez-Pastor et al., 2013b). Besides the role of Cth2 in promoting AMD, several observations suggested that Cth2 could have a role in the translation status of its mRNA targets: (i) an ARE mutant allele of *CTH2* mRNA shows a poor correlation between *CTH2* transcript and Cth2 protein levels in -Fe (Martínez-Pastor et al., 2013a), (ii) Cth2 physically interacts with the RNA helicase Dhh1 (Pedro-Segura et al., 2008), homolog of human RCK/p54 involved in the repression of translation initiation of TTP mRNA targets (Coller & Parker, 2005; Qi et al., 2012; Tiedje et al., 2012), and (iii) in *xrn1Δ*, *dcp1Δ* and *dcp2Δ* strains Cth2 localizes into P-bodies (Pedro-Segura et al., 2008), which contain transcripts that are temporarily not being translated (Parker & Sheth et al., 2007; Decker & Parker, 2012).

The polyribosome experiments under iron-sufficient and -deficient conditions confirmed the results of Chapter 1 related to the mild repression of general translation observed here in Chapter 2 after 7 hours in -Fe in the BY4741 background (**Figure C2-2: C and D**), with only a slight shift to monosomal fractions in *ACT1* mRNA in -Fe compared to +Fe (**Figure C2-2: B; Figure C2-3: C and E**). Besides, the translation of *SDH4* mRNA was specifically repressed under iron deficiency compared to iron sufficiency, by measuring both the translation efficiency of *SDH4* mRNA (**Figure C2-1**) and the *SDH4* mRNA association to the

different polyribosome fractions (**Figure C2-2: A; Figure C2-3: B and D**). Also, the strong association to the 80S monosomal peak of the *SDH4* mRNA in -Fe suggests a repression of translation taking place at the initiation step. On the other hand, the global arrest of translation initiation observed under iron starvation (**Figure C2-2: C and D**), reproduced by the mild change in the *ACT1* mRNA profile (**Figure C2-2: B**), was only partially responsible of the strong arrest of *SDH4* mRNA in -Fe (**Figure C2-2: A**) that was 3 times more associated to monosomal fractions than the global profile. Therefore, the *SDH4* mRNA translation initiation is repressed specifically under iron starvation.

In mammals, the AREs were the first 3'-UTR motifs of mRNAs described to lead to rapid mRNA decay of certain lymphokines, cytokines and proto-oncogenes (Shaw & Kamen, 1986). Later, they were described to participate also in translational control. The TIA-1 RNA-binding protein acts as a translational repressor binding the ARE of the 3'-UTR of TNFα mRNA and cyclooxygenase-2 mRNA (Piecyk et al., 2000; Dixon et al., 2003). On the other hand, the HuR RNA-binding protein acts as a translational enhancer binding the ARE of the 3'-UTR of p53 (Galbán et al., 2003; Mazan-Mamczarz et al., 2003). More recently, the mammalian TTP was included in the list of proteins repressing the translation of ARE-containing mRNAs in a DEAD-box RNA helicase RCK/p54-dependent manner (Qi et al., 2012) or by competition with the HuR translational activator (Tiedje et al., 2012). Here, we have demonstrated that ARE motifs of *SDH4* and *CTH2* transcripts (**Figure C2-3 and Figure C2-5,** respectively) are the *cis* regulatory elements responsible of their translational repression occurring specifically during iron starvation. Moreover, as in the mRNA targets of mammalian TTP, the Cth2 protein was demonstrated to be the *trans* regulatory element repressing the translation of *SDH4* and *CTH2* ARE-containing mRNAs in -Fe in a TZFs-dependent manner (**Figure C2-4 and Figure C2-7,** respectively). Accordingly, the *SDH4* ARE dependency in the association to polyribosome fractions was not observed in +Fe due to the lack of *CTH2* expression (**Figure C2-3: D**). However, the sustained presence of the *SDH4* and *CTH2* mRNAs in the 80S peak of polyribosome experiments in -Fe despite the ARE motif (**Figure C2-3: B and Figure C2-5: B**, respectively) or Cth1/2 proteins (**Figure C2-4: B and D; and Figure C2-7: B**, respectively) still cannot be completely explained by the mild repression of general

translation (**Figure C2-2: C and D**). Probably, additional unknown regulatory factors and/or additional *cis* regulatory elements different from the AREs could be involved in the translational repression of *SDH4* and *CTH2* mRNAs in -Fe.

The fact that Cth2 represses the translation of its own mRNA reinforces the importance of the *CTH2* negative feedback regulation already described at the mRNA decay level (Martínez-Pastor et al., 2013a). This autoregulation is important for a rapid Cth2 removal when cells shift from iron-deficient to iron-sufficient conditions, allowing the reactivation of the iron-dependent processes downregulated by Cth2 that are important for cell growth, like mitochondrial respiration (Martínez-Pastor et al., 2013a). Similar feedback regulation at both mRNA decay and translational levels have been described for TTP (Brooks et al., 2004, Tchen et al., 2004; Tiedje et al., 2012). In both cases, other family members (TIS11b and TIS11d in mammalian cells and Cth1 in yeast) contain AREs and auto- and cross-regulate their expression (Tan & Elowitz, 2014; Martínez-Pastor et al., 2013a). The Cth2 translational inhibition of its own mRNA adds an extra step of control in the regulation of Cth2, supporting the cells requirement of carefully restrict Cth2 presence to specific iron-deficient conditions.

Other Cth2 mRNA-targets that participate in iron-dependent processes (*CCP1*, *HEM15* and *WTM1*) were here described to be translationally inhibited by Cth2 in -Fe (**Figure C2-8 and Figure C2-9**). These results suggest that Cth2 has a role in both, mRNA decay and translational repression of the set of ARE-containing mRNAs that facilitate the adaptation to iron starvation. However, very little is known about the mechanism by which Cth2 regulates both processes. The conserved CR1 of Cth2 in the NTD is important for the mRNA decay, and its lack leads to higher presence of extended Cth2 target transcripts (Prouteau et al., 2008). This Cth2 NTD is believed to be involved in recruiting the components of the mRNA decay machinery (Prouteau et al., 2008). Therefore, we further investigated the Cth2 domains involved in both mRNA decay and translational repression. While Cth2 NTD was important for both *SDH4* mRNA degradation and *SDH4* translational inhibition, the CTD was involved in translation regulation, but was dispensable for *SDH4* mRNA decay (**Figure C2-10**). Besides, the lack of Cth2 CTD increased other iron-proteins (Aco1, Bio2 and Hem15) encoded by ARE-

containing mRNAs (**Figure C2-11: A**). These results, together with the fact that the Cth2 CTD has a physiological relevant role in -Fe (**Figure C2-12**), supports the importance of Cth2 as translational regulator of its mRNA targets when iron is scarce.

The mammalian and the *Drosophila melanogaster* TTP protein structure prediction showed the lack of tertiary structure for TTP beyond its TZFs, with unstructured NTD and CTD domains (Ngoc et al., 2014), both necessary for its function (Rigby et al., 2005). We thought that predicting the structure of the yeast Cth2 could support the functional differences described here for both CTD and NTD domains. The predicted TZF and CTD structure binding an ARE-containing mRNA suggested that the CTD (mainly the CR3 domain) folds back into the TZFs (**Figure C2-11: B**). Interestingly, this difference compared to TTP could be the reason why Cth2 CTD is not involved in mRNA decay and also explains the lack of functionality of any CTD-tagged Cth2 protein (Puig et al. 2005; Prouteau et al., 2008; Vergara et al. 2011). On the other hand, Cth2 NTD acquires the unstructured conformation already described for TTP that could more easily facilitate the exposure of motifs involved in the recruitment of proteins. We currently do not know which Cth2-dependent process takes place first, activation of decay or translational repression. Generally, the mRNA decay occurs as a consequence of translational repression (reviewed by Roy & Jacobson, 2013; Huch & Nissan, 2014). Prior to decapping and transcript degradation, mRNAs usually need to be first in a low translational state. In this way, the decapping activator Dhh1 also functions in the inhibition of translation initiation and elongation. Dhh1 inhibits the production of a stable 48S preinitiation complex *in vitro* and binds slow elongating ribosomes in mRNAs with non-optimal codons (Coller & Parker, 2005; Carroll et al., 2011; Sweet et al., 2012; Radhakrishnan et al., 2016). However, not always both mRNA decay and translation processes are connected. For example, a distinct role of some ARE-binding proteins in translation inhibition, but not in mRNA decay, has been established (Bell et al., 2006). In the same way, the effect of TTP in TNFα mRNA translational repression is more pronounced than the mRNA decay, with TNFα mRNA levels showing a marginal change (Qi et al., 2012). This could indicate a TTP dominant role in the translational downregulation of its target mRNAs compared to their mRNA degradation, emphasizing the importance

of TTP in translational control. In the case of Cth2, its role in translational repression is important as both CTD and NTD domains are involved, and probably it is physiologically relevant under iron starvation. Cth2 CTD would preferentially interact with factors that control translation, while proteins involved in both mRNA turnover and translation would associate with its NTD.

Chapter 3
Results

Chapter 3. Study of the role of Cth2 in the regulation of cellular respiration during iron deficiency

Part of this work was published in:

- *Proceedings of the National Academy of Sciences* journal, volume 115 (Sato et al., 2018). The authors are Tatsuya Sato*, Hsiang-Chun Chang*, Marina Bayeva, Jason S. Shapiro, Lucía Ramos-Alonso, Hidemichi Kouzu, Xinghang Jiang, Ting Liu, Sumeyye Yar, Konrad T. Sawicki, Chunlei Chen, María Teresa Martínez-Pastor, Deborah J. Stumpo, Paul T. Schumacker, Perry J. Blackshear, Issam Ben-Sahra, Sergi Puig, and Hossein Ardehali
- *Metallomics* journal, volume 10 (Ramos-Alonso et al., 2018b). The authors are Lucía Ramos-Alonso, Nadine Wittmaack, Isabel Mulet, Carlos A. Martínez-Garay, Josep Fita-Torró, María Jesús Lozano, Antonia M. Romero, Carlos García-Ferris, María Teresa Martínez-Pastor and Sergi Puig

**These authors contributed equally to this work.*

As previously introduced, mitochondrial respiration is a highly iron-consuming process particularly important for energy production. Both the Krebs cycle, also called tricarboxylic acid cycle, and the electron transport chain require iron and heme in multiple steps. Because of this, a shift from respiration to fermentation occurs during iron-deficient conditions. Interestingly, multiple potential Cth2 mRNA-targets encode components of the TCA cycle and the ETC (**Figure I-4**; Puig et al., 2005; Puig et al., 2008). Moreover, most Cth2 studies have been focused on the degradation and translational repression of its mRNA targets (Puig et al., 2005; Puig et al., 2008; Pedro-Segura et al., 2008; Prouteau et al., 2008; Ihrig et al., 2010; Vergara et al., 2011; Martínez-Pastor et al., 2013a; Ramos-Alonso et al., 2018a; Ramos-Alonso et al., 2019). However, little is known about the corresponding protein levels and enzymatic activities, and how Cth2 impacts respiration and oxygen consumption. For this reason, the aim of this chapter is to investigate the role of Cth2 in the control of cellular respiration beyond mRNA regulation.

C3.1. Mitochondrial respiration is repressed under iron deficiency independently of Cth2

To explore the requirement of iron in mitochondrial respiration, we decided to measure the oxygen consumption rate in cells growing in iron sufficiency (+Fe) or iron deficiency (-Fe) as explained in section 4.7 of Materials and Methods. The relative oxygen consumption rate of a wild-type BY4741 strain in -Fe was significantly reduced compared to the +Fe condition (**Figure C3-1: A**). To further confirm that this reduction of the respiratory capacity was due to the low availability of iron, and not to a secondary effect of the iron chelator BPS, we determined the oxygen consumption in a *fet3Δfet4Δ* mutant strain, with the high- and low-affinity Fe transport systems knocked out. Again, an important decrease in oxygen consumption was observed in the *fet3Δfet4Δ* mutant in +Fe compared to the wild-type BY4741 in +Fe (**Figure C3-1: A**). These results suggest that mitochondrial respiration is compromised under both nutritional and genetic iron deficiencies.

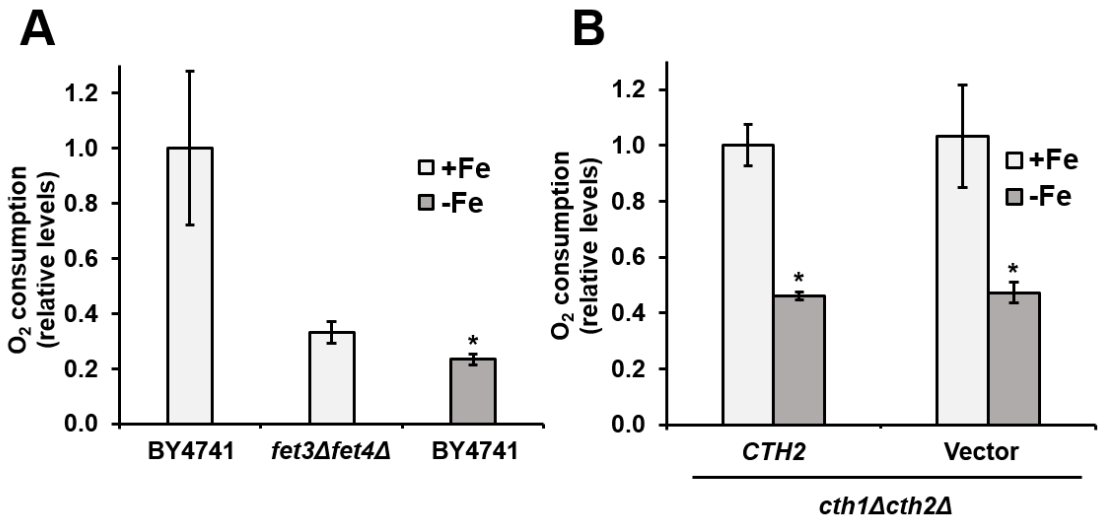

Figure C3-1. Iron deficiency causes a decreased oxygen consumption independently of Cth2. Analyses of the oxygen consumption rate were performed as described in section 4.7 of Materials and Methods. **(A)** Wild-type BY4741 overnight cultures were reinoculated in SC with 10 µM FAS (+Fe) and SC with 100 µM BPS (-Fe), and *fet3Δfet4Δ* cultures in SC (+Fe) during 6 hours. Oxygen consumption rates were determined and represented relative to BY4741 in +Fe. **(B)** Overnight cultures of *cth1Δcth2Δ* mutant cells transformed with pRS416-*CTH2* (*CTH2*) or pRS416 (Vector) were reinoculated in SC-Ura with 10 µM FAS (+Fe) and SC-Ura with 100 µM BPS (-Fe) for 6 hours. Oxygen consumption rates were

represented relative to *CTH2* in +Fe. In both panels, mean values and standard deviations from at least two biologically independent experiments are shown. An asterisk (*) indicates a significant difference (*p*-value <0.05) from two-tailed student's t-test compared with BY4741 in +Fe **(A)** and *CTH2* in +Fe. **(B)**

Next, we investigated the implication of Cth2 in the inhibition of the respiratory capacity under iron deficiency, probably by promoting the mRNA degradation and translational repression of several of the components of both the Krebs cycle and the ETC. As in chapter 2, all the experiments were performed in a *cth1Δcth2Δ* background. As *CTH2* is only expressed under iron-deficient conditions, there were no differences in the oxygen consumption in +Fe between *cth1Δcth2Δ* cells transformed with the *CTH2* plasmid (*CTH2*) or empty vector (Vector) (**Figure C3-1: B**). As expected, a diminished respiration was observed in both cases under iron deficiency, but it occurred in a Cth2-independent manner (**Figure C3-1: B**). Together, these results indicate that iron deficiency can inhibit mitochondrial respiration regardless of Cth2.

C3.2. *CTH1* or *CTH2* overexpression decreases respiration in a TZF-dependent manner under iron sufficiency

Despite that the lack of *CTH2* expression seemed to be dispensable in the repression of respiration observed under iron deficiency, we wondered if it was also the case in cells constitutively expressing *CTH2* in iron sufficiency. The oxygen consumption analyses were performed in +Fe in *cth1Δcth2Δ* cells transformed with an empty vector (Vector), or constitutively expressing *CTH2* by the *TEF2* promoter fusion with either the *CTH2* coding sequence (*TEF-CTH2*) or with the TZF-mutated version (*TEF-CTH2-C190R*). An important decrease in oxygen consumption was observed in *TEF-CTH2*-expressing cells in +Fe compared to *cth1Δcth2Δ* cells (Vector), which was completely recovered in the *TEF-CTH2-C190R* mutant (**Figure C3-2: A**). Similar results were obtained with *CTH1* overexpression in +Fe. The decreased oxygen consumption measured in *TEF-CTH1* compared to *cth1Δcth2Δ* cells (Vector) in +Fe, was recovered in the corresponding TZF mutant (**Figure C3-2: B**). These results demonstrate that either *CTH1* or *CTH2* can repress

the mitochondrial respiration in a TZF-dependent manner if overexpressed under iron-sufficient conditions.

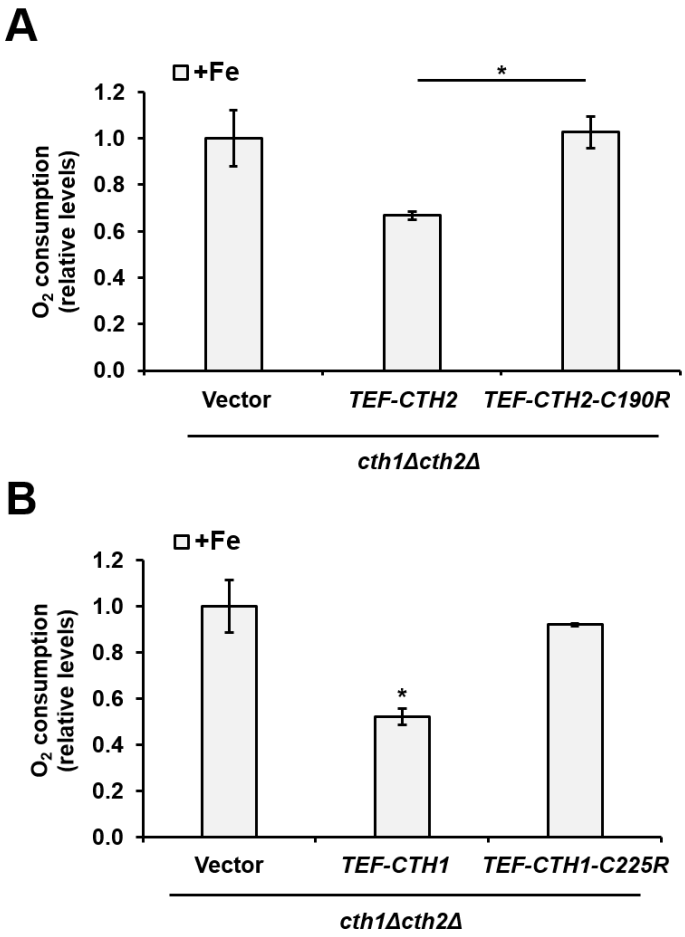

Figure C3-2. *CTH1* and *CTH2* overexpressing cells reduce oxygen consumption in a TZF-dependent manner in iron-sufficient conditions. Analyses of oxygen consumption rate were performed as described in section 4.7 of Materials and Methods. **(A)** Analyses of *cth1Δcth2Δ* mutant cells transformed with pRS416 (Vector), p416-*TEF*-Flag$_2$-*CTH2* (*TEF-CTH2*) or p416-*TEF*-Flag$_2$-*CTH2-C190R* (*TEF-CTH2-C190R*) were performed from overnight cultures reinoculated in SC-Ura with 10 μM FAS (+Fe) during 6 hours. **(B)** Analyses of *cth1Δcth2Δ* mutant cells transformed with pRS416 (Vector), p416-*TEF-CTH1* (*TEF-CTH1*) or p416-*TEF-CTH1-C225R* (*TEF-CTH1-C225R*) were performed as explained in panel A. In both panels, mean values and standard deviations from at least two biologically independent experiments were determined and represented relative to Vector. An asterisk (*) indicates a significant difference (*p*-value <0.05) from two-tailed student's t-test comparing the indicated samples **(A)** or compared to Vector **(B)**.

C3.3. The constitutive activation of the iron regulon in iron sufficiency decreases respiration in a *CTH2*-dependent manner

Next, we wanted to test if the constitutive activation of the entire iron regulon triggered an oxygen consumption reduction under iron sufficiency. The single *C291F* mutation in the *AFT1* gene (called *AFT1-1UP* allele) retains Aft1 in the nucleus (Yamaguchi-Iwai et al., 2002) and promotes the constitutive transcriptional activation of the iron regulon (Rutherford et al., 2001) by preventing the Aft1 dissociation from its target promoters (Ojeda et al; 2006; Ueta et al., 2012). We used the *AFT1-1UP* allele to determine the oxygen consumption rate. The *AFT1-1UP* expressing cells in +Fe showed a significant decrease in respiration compared to a wild-type strain, which was partially recovered by the deletion of *CTH2* (**Figure C3-3: A**). In the same way, the growth capacity of the *AFT1-1UP* cells in the non-fermentable ethanol-glycerol medium (YPEG) was decreased compared to the wild-type, and partially rescued by the *CTH2* deletion (**Figure C3-3: B**). These results strongly suggest that the constitutive activation of the iron regulon represses mitochondrial respiration mainly through Cth2.

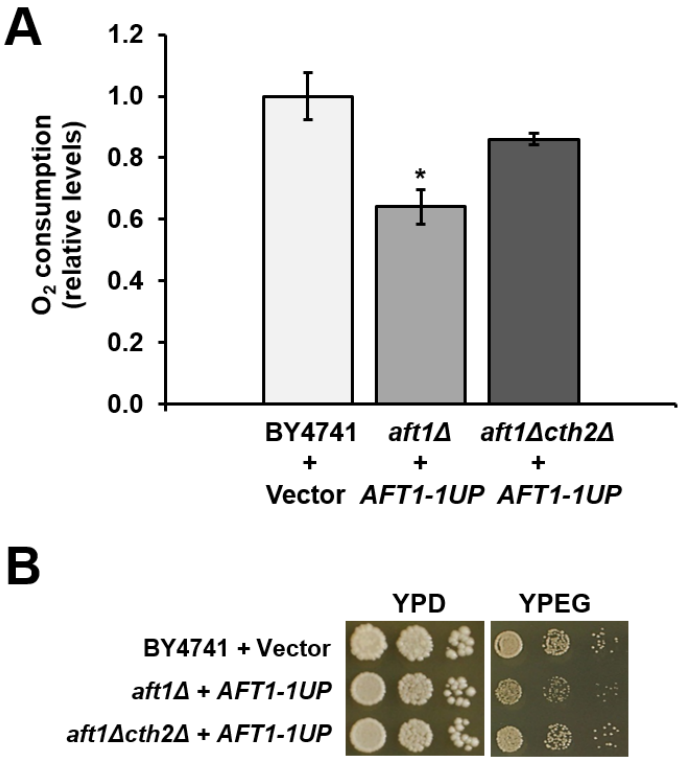

Figure C3-3. *AFT1-1UP* expressing cells inhibit respiration in a *CTH2*-dependent manner in iron sufficiency. (A) Analyses of the oxygen consumption

rate of wild-type BY4741 cells transformed with pRS416 (Vector) and *aft1Δ* mutant cells and *aft1Δcth2Δ* transformed with pRS316-*AFT1-1UP-C291F* (*AFT1-1UP*) were performed from overnight cultures reinoculated in SC-Ura with 10 μM FAS (+Fe) during 6 hours. Mean values and standard deviations from at least two biologically independent experiments were determined and represented relative to BY4741 + Vector. An asterisk (*) indicates a significant difference (*p*-value <0.05) from two-tailed student's t-test compared with BY4741 + Vector. **(B)** Analyses of the cell growth in solid media of cells transformed as explained in panel A were performed in triplicate in YPD (glucose 2 %) and YPEG (ethanol 2 % and glycerol 3 %) as explained in section 1.4 of Materials and Methods.

C3.4. The Fe-dependent activity of Leu1 decreases upon *CTH2* overexpression or iron deficiency

Before testing mitochondrial enzymatic activities that contribute to cellular respiration, we decided to test the iron-dependent activity of Leu1, which takes place in the cytoplasm. *LEU1* encodes the Fe/S protein isopropylmalate isomerase, which catalyzes the second step in the leucine biosynthesis pathway. The *LEU1* mRNA is strongly downregulated under iron-deficiency through a mechanism partially dependent on its ARE sites and Cth2 protein (Puig et al., 2005; Ihrig et al., 2010). Besides, Leu1 is considered one of the most abundant Fe/S proteins in *S. cerevisiae* (Ghaemmaghami et al., 2003). Leu1 enzymatic activity is easily detected on whole cellular lysates, whereas most of the respiration-related activities require a previous step of mitochondria isolation.

We determined the mRNA, enzymatic activity and protein levels of *LEU1* in *cth1Δcth2Δ* cells carrying the *CTH2* plasmid (*CTH2*), under iron sufficiency and deficiency. As the wild-type version of *CTH2* is only activated in -Fe, the plasmid constitutively expressing *CTH2* (*TEF-CTH2*) was used in +Fe, and *CTH2* wild-type cells were the negative control under iron sufficiency. In -Fe, the negative control of *CTH2* expression was the empty vector (Vector). In +Fe, the *LEU1* mRNA was reduced in *TEF-CTH2* expressing cells compared to *CTH2* wild-type cells (**Figure C3-4: A**). And, under iron deficiency, the *LEU1* mRNA was drastically decreased with slightly recovered levels in Vector cells compared to *CTH2* cells (**Figure C3-4:**

A). In fact, in addition to its Cth2-dependent post-transcriptional mRNA degradation, *LEU1* is also strongly downregulated at the transcriptional level in -Fe (Puig et al., 2005; Ihrig et al., 2010). To better study the outcome of Cth2-dependent regulation beyond the mRNA levels, we determined Leu1 enzymatic activity. Importantly, lower Leu1 activity levels were detected in *TEF-CTH2* expressing cells compared to the *CTH2* situation in both exponentially growing (**Figure C3-4: B**) and saturated cultures (**Figure C3-4: C**) in +Fe. The determination of Leu1 enzymatic activity under iron deficiency was exclusively tested in saturated cultures, due to the elevated number of cells required for activity detection under iron starvation. Despite this, no detectable Leu1 activity was measured under iron deficiency (**Figure C3-4: C**).

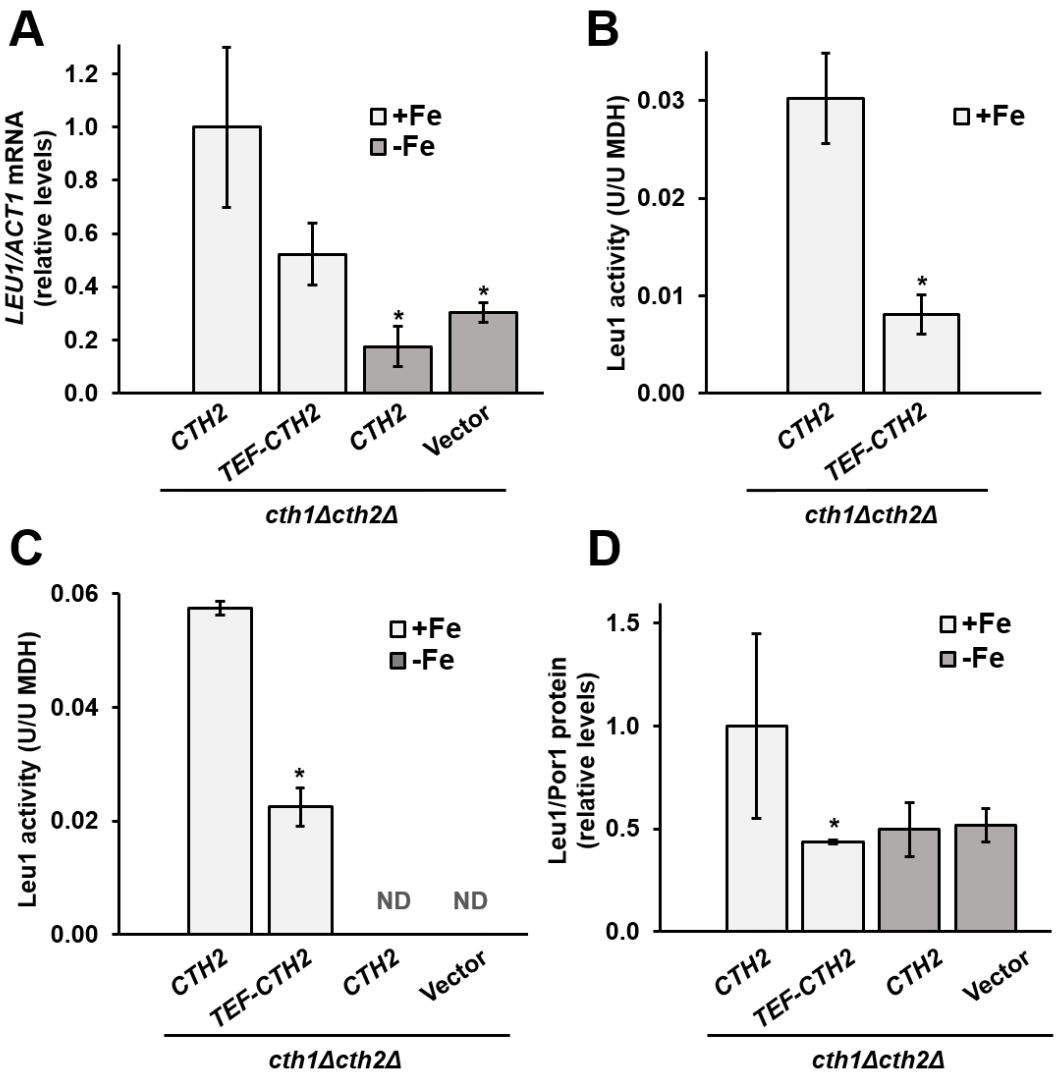

Figure C3-4. *LEU1* mRNA, activity and protein levels are downregulated by both Cth2 overexpression and iron deficiency. (A) The *LEU1/ACT1* mRNA

levels of *cth1Δcth2Δ* mutant cells transformed with pRS416-*CTH2* (*CTH2*), p416-*TEF-CTH2* (*TEF-CTH2*) or pRS416 (Vector) were determined from overnight cultures reinoculated in SC-Ura with 10 μM FAS (+Fe, 6 hours) and/or in SC-Ura with 100 μM BPS (-Fe, 10 hours) by RT-qPCR as described in Materials and Methods. **(B)** Leu1 enzymatic activity was determined relative to malate dehydrogenase (MDH) from cellular lysates of *cth1Δcth2Δ* mutant cells transformed with p416-$Flag_2$-*CTH2* (*CTH2*) or p416-*TEF*-$Flag_2$-*CTH2* (*TEF-CTH2*) as explained in Materials and Methods. Overnight cultures were reinoculated in SD with 50 μM FAC (+Fe, 7 hours). **(C)** Leu1 enzymatic activity was also determined from cellular lysates of *cth1Δcth2Δ* mutant cells transformed with pRS416-$Flag_2$-*CTH2* (*CTH2*), p416-*TEF*-$Flag_2$-*CTH2* (*TEF-CTH2*) or pRS416 (Vector). Overnight cultures in SD with 50 μM FAC (+Fe) and 50 μM BPS (-Fe) were reinoculated overnight in SD with 50 μM FAC (+Fe) and in iron-free SD (-Fe), respectively. ND: not detectable activity. **(D)** The Leu1/Por1 protein levels were determined from the cell lysates of panel A and panel B (+Fe, 6-7 hours; -Fe, 10 hours) by Western blot. In all cases, mean values and standard deviations from at least two independent biological replicates are shown. An asterisk (*) indicates a significant difference (*p*-value <0.05) from two-tailed student's t-test compared with *CTH2* cells in +Fe.

Regarding Leu1 protein levels, a significant decrease was detected in *TEF-CTH2* cells compared to *CTH2* cells in +Fe (**Figure C3-4: D**). Also, an important reduction in Leu1 protein levels was observed in both *CTH2* and Vector cells in -Fe, but unlike mRNA levels, no recovered Leu1 protein levels were observed in Vector cells compared to *CTH2* cells (**Figure C3-4: D**). Taken together, these results suggest that *CTH2* overexpression under iron-sufficient conditions is able to reduce *LEU1* mRNA levels as well as its enzymatic activity, possibly as a consequence of the diminished Leu1 protein levels. On the other hand, the Cth2-dependent regulation of Leu1 under iron deficiency is only observed at the mRNA level. The undetectable Leu1 enzymatic activity in -Fe was probably due to the lack of cofactor in the Leu1 protein.

C3.5. The Fe-dependent aconitase activity decreases upon *CTH2* overexpression or iron deficiency

Aconitase is a respiration-related activity easily detectable as no previous mitochondria isolation step is needed in the enzymatic assay. *ACO1* encodes the Fe/S protein aconitase that catalyzes the conversion of citrate to isocitrate, second step in the TCA cycle. As *LEU1*, the *ACO1* mRNA also contains several AREs in its 3'UTR and is a target of the Cth2-dependent regulation (**Figure I-4: A**; Puig et al., 2005; Puig et al., 2008). The mRNA, enzymatic activity and protein levels of *ACO1* were determined in the aforementioned cellular lysates. Although in +Fe the *ACO1* mRNA was not significantly reduced in *TEF-CTH2* expressing cells compared to *CTH2* cells (**Figure C3-5: A**), the aconitase enzymatic activity was drastically reduced in *TEF-CTH2* cells in both exponentially growing (**Figure C3-5: B**) and saturated cultures (**Figure C3-5: C**). Under iron deficiency, as previously described (Puig et al., 2005; Puig et al., 2008), the Cth2-dependent *ACO1* mRNA downregulation was evident comparing *CTH2* and Vector expressing cells (**Figure C3-5: A**). However, an important increment in *ACO1* mRNA levels was displayed in -Fe regardless of Cth2 (**Figure C3-5: A**), due to the transcriptional activation of the mitochondrial retrograde pathway under iron starvation (Romero et al., 2019). On the other hand, the corresponding aconitase enzymatic activity was drastically reduced under iron starvation compared to the iron sufficiency in a Cth2-independent manner (**Figure C3-5: C**). The decreased Aco1 protein levels in *TEF-CTH2* cells in +Fe (**Figure C3-5: D**) were well suited with the decreased aconitase activities of *TEF-CTH2* cells in this condition (**Figure C3-5: B and C**). However, under iron limitation, the Cth2-dependent downregulation of the *ACO1* mRNA, although also observed at the Aco1 protein level (**Figure C3-5: D**), was not maintained at the enzymatic activity level (**Figure C3-5: C**). In the same way, the aforementioned transcriptional activation of *ACO1* through the RTG pathway in -Fe was not reflected beyond the mRNA levels. Taken together, these results show a decrease in aconitase activity due to diminished Aco1 protein levels when *CTH2* is overexpressed under iron-sufficient conditions. However, the aconitase activity under iron-deficiency shows a Cth2-independent reduction despite of the increased Aco1 protein levels when *CTH2* is not present.

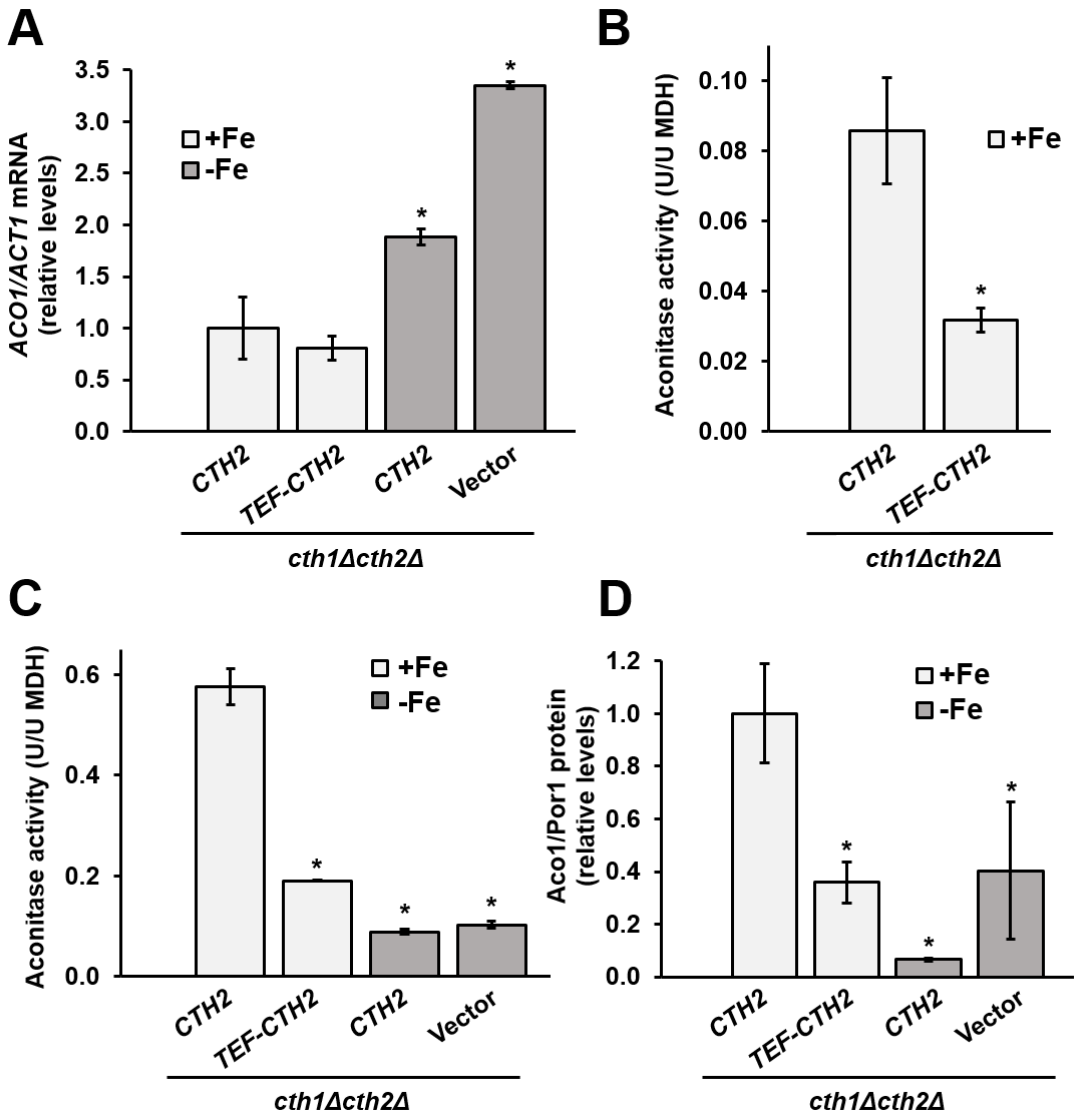

Figure C3-5. Aconitase activity is downregulated by both Cth2 overexpression and iron deficiency. The *ACO1/ACT1* mRNA levels **(A)**, the aconitase enzymatic activities from cellular lysates in exponential phase (+Fe, 7 hours) **(B)** and overnight in SD with 50 µM FAC (+Fe) and iron-free SD (-Fe) **(C)** were determined as explained in Figure C3-4 panels A-C, respectively. **(D)** The Aco1/Por1 protein levels were determined from the cell lysates of panel B (+Fe, 7 hours) and from *cth1Δcth2Δ* mutant cells transformed with pRS416-Flag$_2$-*CTH2* (*CTH2*), p416*TEF*-Flag$_2$-*CTH2* (*TEF-CTH2*) or pRS416 (Vector) grown in SD with 50 µM FAC (+Fe, 6 hours) and/or SD with 50 µM BPS (-Fe, 9 hours) by Western blot. In all cases, mean values and standard deviations from at least two independent biological replicates are shown. An asterisk (*) indicates a significant difference (*p*-value <0.05) from two-tailed student's t-test compared with *CTH2* cells in +Fe.

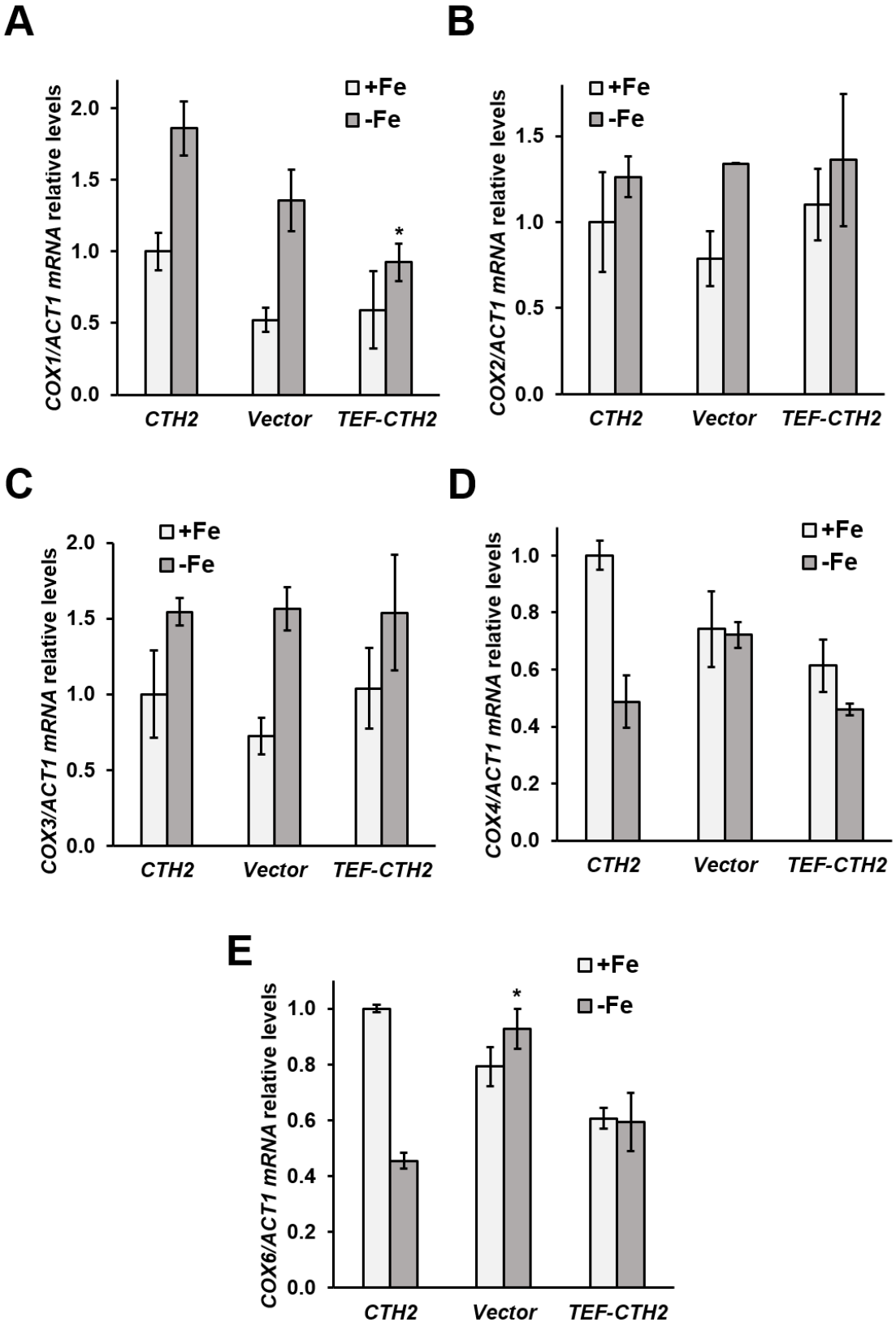

Figure C3-6. mRNA levels of several components of the cytochrome *c* oxidase (COX, complex IV). The *COX1* **(A)**, *COX2* **(B)**, *COX3* **(C)**, *COX4* **(D)** and *COX6* **(E)** mRNA levels relative to *ACT1* mRNA in *cth1Δcth2Δ* mutant cells transformed with

pRS416-*CTH2* (*CTH2*), p416-*TEF-CTH2* (*TEF-CTH2*) or pRS416 (Vector) were determined from overnight cultures reinoculated in SC-Ura with 10 μM FAS (+Fe, 6 hours) and in SC-Ura with 100 μM BPS (-Fe, 10 hours) by RT-qPCR using random primers for reverse transcription as described in Materials and Methods. Mean values and standard deviations from at least three independent biological replicates are shown. An asterisk (*) indicates a significant difference (*p*-value <0.05) in -Fe from two-tailed student's t-test compared with *CTH2* cells in -Fe.

C3.6. The mitochondrial respiratory Complex IV activity is affected only under iron deficiency in a Cth2-dependent manner

The cytochrome *c* oxidase (COX) constitutes the complex IV and terminal electron acceptor of the ETC involved in the reduction of molecular oxygen to water. As previously introduced, complex IV is encoded by twelve genes, with the three catalytic core subunits encoded in the mitochondrial DNA (*COX1*, *COX2* and *COX3*). Besides, five of the nuclear encoded genes (**Figure I-4: B**) are Cth2 mRNA-targets containing ARE motifs (Puig et al., 2005; Puig et al., 2008). Again, before carrying out the enzymatic activity assay, we determined the role of Cth2 in the mRNA fluctuations of some of the COX components under iron sufficiency and deficiency. *COX1* showed an increment in its mRNA levels under iron deficiency compared to iron sufficiency in both *CTH2* and Vector cells (**Figure C3-6: A**). The highest levels of *COX1* mRNA were reached in *CTH2* cells in -Fe, and were significantly decreased in *TEF-CTH2* cells only in this condition (**Figure C3-6: A**). Regarding *COX2* and *COX3* mRNAs, their levels were slightly incremented in -Fe compared to +Fe, but remained unaltered under iron deficiency independently of Cth2 (**Figure C3-6: B and C**). *COX4* and *COX6* mRNAs are ARE-containing Cth2 targets, and thus showed the expected behavior, with decreased mRNA levels in *CTH2* cells in -Fe compared to +Fe, recovered in Vector cells in -Fe (**Figure C3-6: D and E**). And finally, *TEF-CTH2* expressing cells diminished *COX4* and *COX6* mRNA levels both in +Fe and -Fe, compared to cells or conditions not expressing *CTH2* (**Figure C3-6: D and E**). In summary, these results confirm the expected regulation of the Cth2 targets within the ETC complex IV in -Fe, and show increased *COX1* mRNA levels when *CTH2* is expressed in -Fe under the control of its own promoter.

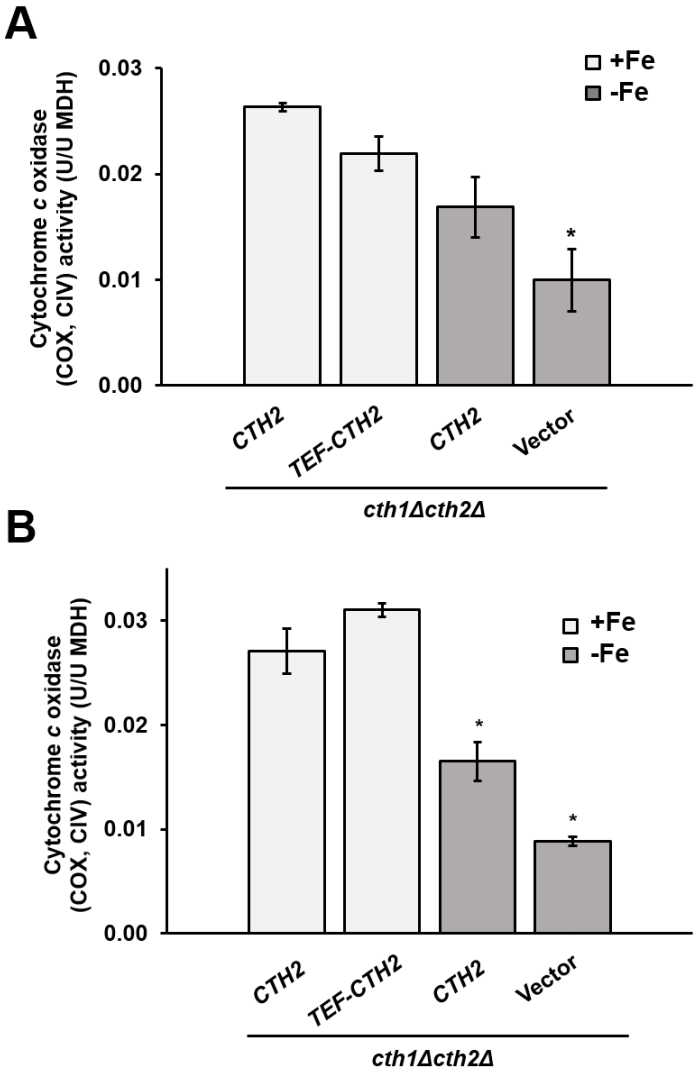

Figure C3-7. COX activity is affected under iron deficiency in a Cth2-dependent manner. COX enzymatic activity was determined as described in Materials and Methods in *cth1Δcth2Δ* mutant cells transformed with pRS416-Flag$_2$-*CTH2* (*CTH2*), p416-*TEF*-Flag$_2$-*CTH2* (*TEF-CTH2*) or pRS416 (Vector). **(A)** The assay was performed from cellular lysates of overnight cultures in SD with 50 µM FAC (+Fe) and 50 µM BPS (-Fe) reinoculated overnight in SD with 50 µM FAC (+Fe) and in iron-free SD (-Fe), respectively. **(B)** Experiments were also performed from isolated mitochondria of overnight cultures in SD with 50 µM FAC (+Fe) and iron-free SD (-Fe) reinoculated again overnight in fresh media. Mean values and standard deviations from two independent biological replicates **(A)** and three technical replicates **(B)** are shown. An asterisk (*) indicates a significant difference (p-value <0.05) from two-tailed student's t-test compared with *CTH2* cells in +Fe.

The enzymatic activity of complex IV was measured to test the involvement of Cth2 in mitochondrial respiration. Experiments were performed with both cellular lysates and isolated mitochondria (**Figure C3-7: A and B**, respectively). Surprisingly, in spite of the multiple Cth2 mRNA-targets within the COX complex, the enzymatic activity was unaltered in *TEF-CTH2* expressing cells in +Fe compared to *CTH2* cells (**Figure C3-7: A and B**). In the same way, iron starvation decreased COX activity, a decline that was more pronounced in Vector cells (**Figure C3-7: A and B**). After this observation, we contemplated a possible role of Cth2 in the maintenance of COX activity under iron starvation. This could happen by increasing Cox1, the catalytic core subunit of the complex responsible of the reduction of oxygen and the only COX component containing iron (heme centers) as well as copper. As mentioned above, *COX1* mRNA levels increased in *CTH2* cells compared to Vector cells in -Fe (**Figure C3-6: A**). This seemed also to be the case in Cox1 and, to a lesser extent, in Cox2 protein levels (**Figure C3-8**). On the other hand, the Cox4 protein levels were lower in *CTH2* cells compared to Vector cells as *COX4* mRNA is a Cth2 mRNA-target (**Figure C3-6: D and Figure C3-8**). Altogether, these results suggest a new role of Cth2 in maintaining a better complex IV activity during iron starvation compared to Vector cells.

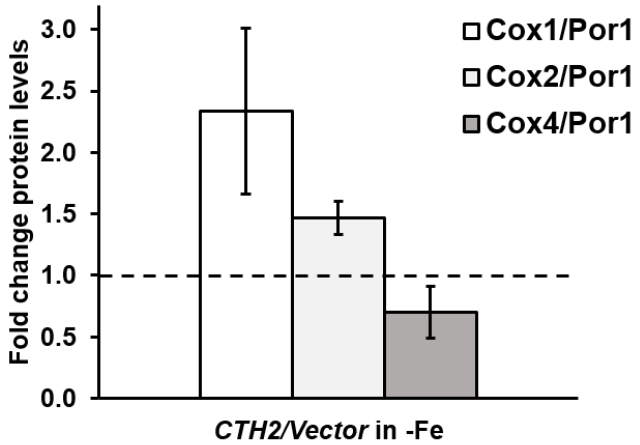

Figure C3-8. Cox1 and Cox2 protein levels increase under iron-deficient conditions in a Cth2-dependent manner. The protein levels of Cox1, Cox2 and Cox4 relative to Por1 protein were analyzed by Western blot from the isolated mitochondria in iron-free SD (-Fe) of Figure C3-7 B. Mean values and standard deviations of each protein fold change (*CTH2*/Vector cells) are shown. Two independent biological replicates were analyzed.

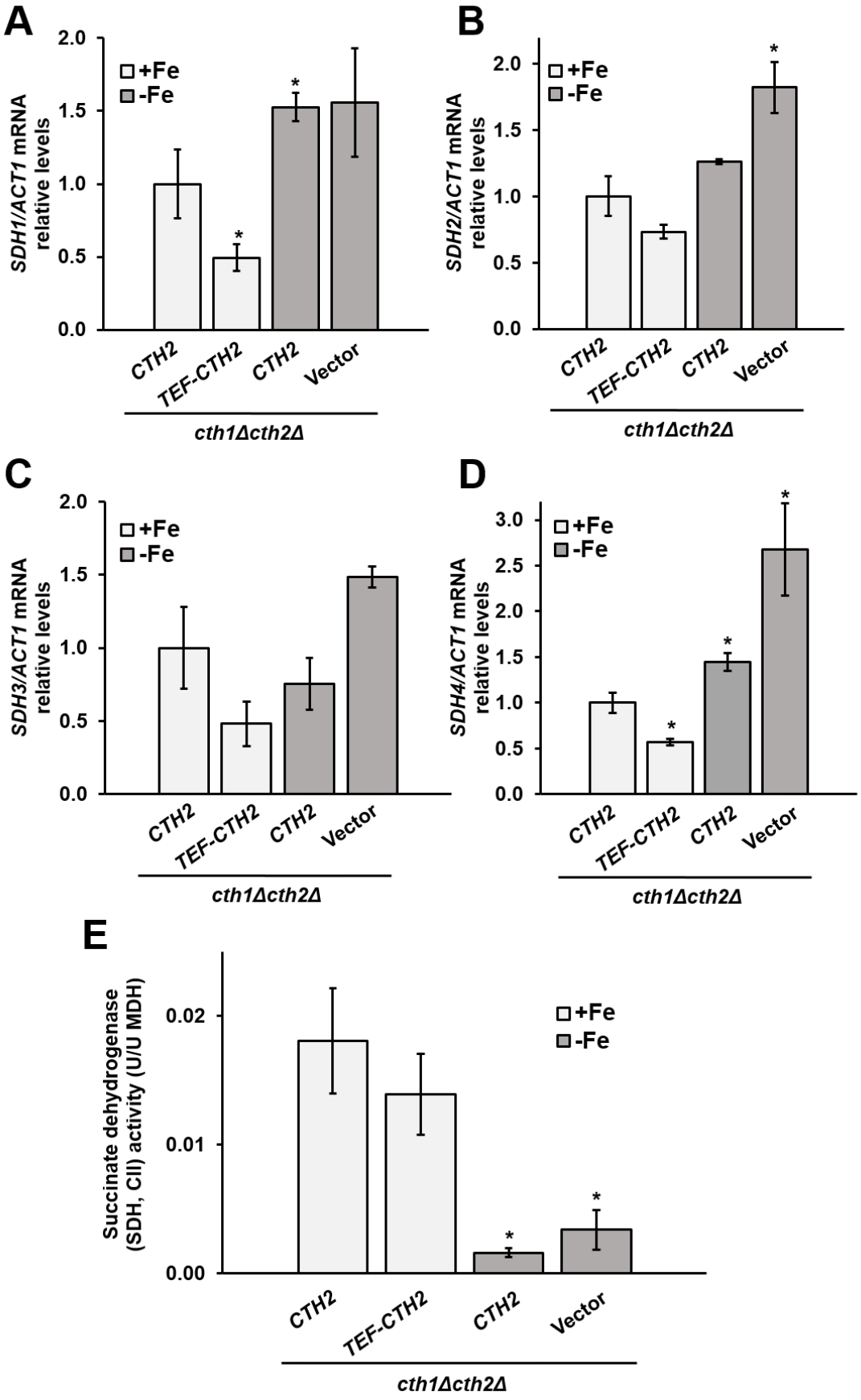

Figure C3-9. Succinate dehydrogenase activity is slightly downregulated by Cth2 overexpression and iron deficiency. The *SDH1* **(A)**, *SDH2* **(B)**, *SDH3* **(C)**

and *SDH4* **(D)** mRNA levels relative to *ACT1* mRNA were determined from cultures and conditions as explained in Figure C3-4 A. **(E)** SDH enzymatic activity was determined from isolated mitochondria as described in Materials and Methods and in Figure C3-7 B. An asterisk (*) indicates a significant difference (*p*-value <0.05) from two-tailed student's t-test compared with *CTH2* cells in +Fe.

C3.7. The activity of mitochondrial respiratory Complexes II+III is negatively affected by either *CTH2* overexpression or iron deficiency

Succinate dehydrogenase (SDH) constitutes the complex II in the ETC. The SDH complex oxidizes succinate to fumarate as part of the Krebs cycle and reduces co-enzyme Q or ubiquinone in the ETC. As previously introduced, the SDH complex is encoded by four genes (*SDH1*, *SDH2*, *SDH3* and *SDH4*). The Sdh2 subunit contains 3 Fe/S clusters, and Sdh3 and Sdh4 share a heme center. Despite these differences, all of them seemed to be coregulated at the mRNA level in a Cth2-dependent manner under iron starvation (**Figure I-4: B**; Puig et al., 2005; Puig et al., 2008). In all cases, these genes also showed decreased mRNA levels in *TEF-CTH2* expressing cells compared to *CTH2* cells in +Fe (**Figure C3-9: A, B, C and D**). On the other hand, higher levels of *SDH2*, *SDH3* and *SDH4* mRNAs were here observed in Vector cells compared to *CTH2* cells in -Fe (**Figure C3-9: B, C and D**, respectively). Only *SDH1* did not show the expected result in -Fe (**Figure C3-9: A**), probably because of the different times in exponential phase used in previous studies (Puig et al., 2005; Puig et al., 2008). The enzymatic activity of SDH under iron starvation was hardly detectable (**Figure C3-9: E**), but unlike aconitase (**Figure C3-5: C**), in this case reflected the Cth2-dependent regulation observed at the mRNA level in -Fe. Also, the decreased *SDH1-4* mRNA levels of *TEF-CTH2*-expressing cells was corresponded to the slight decrease in SDH activity in *TEF-CTH2* compared to *CTH2* cells in +Fe (**Figure C3-9**). Moreover, when the enzymatic activities of both complex II and III of the mitochondrial ETC were determined together, the results showed more drastic reductions of activity levels in *TEF-CTH2* cells in +Fe (**Figure C3-10: D**). Finally, very low enzymatic activity levels of complex II and III together were detected under iron deficiency, but these were even lower in the presence of Cth2 (**Figure C3-10: D**).

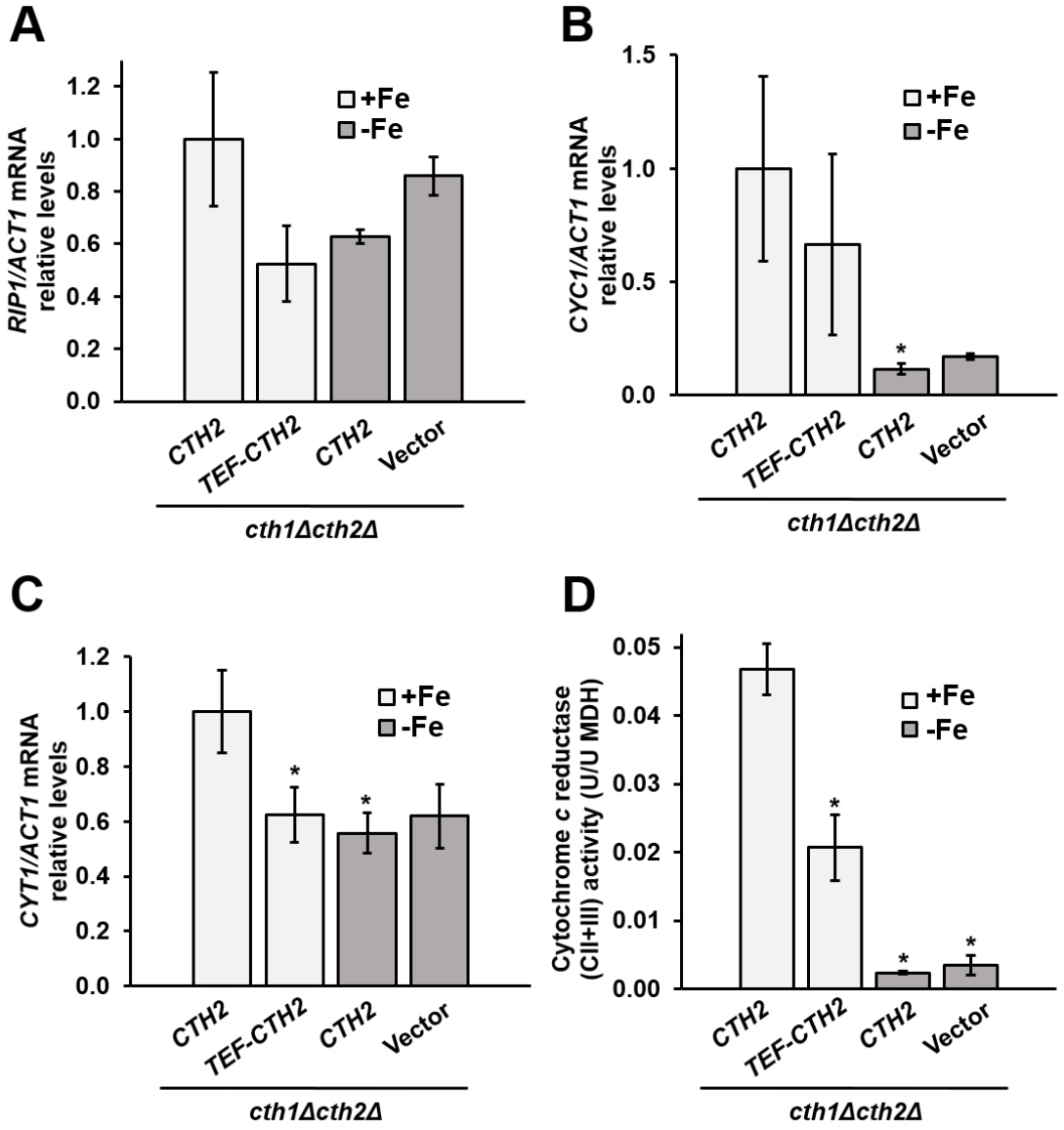

Figure C3-10. Succinate dehydrogenase and cytochrome *c* reductase activities are downregulated by Cth2-overexpression and iron deficiency. The *RIP1* **(A)**, *CYC1* **(B)**, *CYT1* **(C)** mRNA levels relative to *ACT1* mRNA were determined from cultures and conditions as explained in Figure C3-4 A. **(D)** SDH and cytochrome *c* reductase enzymatic activities were determined from isolated mitochondria as described in Materials and Methods and in Figure C3-7 B. An asterisk (*) indicates a significant difference (*p*-value <0.05) from two-tailed student's t-test compared with *CTH2* cells in +Fe.

The cytochrome *c* reductase (complex III) of the ETC catalyzes the oxidation of ubiquinol and reduction of the cytochrome *c* (encoded by *CYC1*). Complex III

contains ten subunits. The cytochrome *b* (*COB1*) is the only one encoded by the mitochondrial DNA, and together with Cyt1 (cytochrome c_1) and Rip1 (Rieske protein) form the redox center of the complex with an Fe/S cluster and several heme groups. Both *CYC1* and eight subunits of the complex (**Figure I-4: B**) contain ARE motifs in their mRNAs that are Cth2 targets (Puig et al., 2005; Puig et al., 2008). The *RIP1*, *CYC1* and *CYT1* mRNA levels decreased in *TEF-CTH2*-expressing cells compared to *CTH2* cells in +Fe (**Figure C3-10: A, B and C**, respectively). Under iron starvation, minor Cth2-dependent mRNA regulation was detected with *CYC1* and *CYT1* mRNA levels (**Figure C3-10: B and C**), but *RIP1* mRNA levels were clearly affected by Cth2 (**Figure C3-10: A**). Importantly, the *CYC1* mRNA levels were almost undetectable (**Figure C3-10: B**) under iron starvation with a very scarce Cth2-dependent regulation. This is consistent with a previous work (Ihrig et al., 2010) in which Hap1 and Hap4 were shown to downregulate the transcription of *CYC1,* due to the reduction in heme levels when iron is scarce. Altogether, these results show an inhibition of complexes II+III activities when *CTH2* was overexpressed under iron-sufficient conditions, and drastically reduced activities under iron starvation, even more reduced in a Cth2-dependent manner.

Discussion

Chapter 3

Discussion of Chapter 3

Mitochondrial respiration is a highly iron-consuming process controlled by the carbon source, oxygen and heme levels. Yeast cells growing in glucose, their preferred carbon source, repress respiration in a Mig1-dependent manner due to the inactivation of the Snf1 kinase complex (reviewed by Kayikci & Nielsen, 2015). However, despite the presence of glucose we could detect differences in mitochondrial respiration related to the variations in iron availability. We observed a decreased oxygen consumption rate under both nutritional and genetic iron deficiencies, in a Cth2-independent manner (**Figure C3-1**). Under iron deficiency, respiration is downregulated both transcriptionally (via Hap1 and the Hap2-5 complex) and post-transcriptionally (via Cth1/2). The fact that under iron starvation two independent pathways downregulate (or fail to induce) respiration would explain the reduced oxygen consumption regardless of Cth2. In fact, under iron starvation, *CYC1* transcription is drastically decreased due to lack of activity of the heme-dependent Hap1 and Hap4 transcription factors (Ihrig et al., 2010) and if the degradation of heme is impaired, using a *hmx1Δ* mutant, the transcription of *CYC1* increases again (Protchenko & Philpott, 2003). However, previous evidences, as well as new ones presented here, support a role for Cth2 in the repression of respiration: (i) Cth2 promotes the AMD of twenty-two components of the TCA cycle and ETC (**Figure I-4**; Puig et al., 2005; Puig et al., 2008; Romero et al., 2019); (ii) mammalian TTP is induced during iron starvation and downregulates NDUFS1 and UQCRFS1 (Rieske/Rip1 in yeast) of the complex I and III of the ETC, respectively (Bayeva et al., 2012; Bayeva et al., 2013; Sato et al., 2018); (iii) Cth2 (and Cth1) can reduce oxygen consumption in a TZF-dependent manner if overexpressed in +Fe conditions (**Figure C3-2**); and (iv) the constitutive activation of the iron regulon decreases respiration and growth in non-fermentable carbon sources through Cth2 (**Figure C3-3**). These last two points are in agreement with a Cth2 predominant role over Cth1 when expressed under the control of their own promoters, despite both proteins having partially redundant functions (Puig et al., 2008). However, to observe the specific Cth2-dependent downregulation of respiration in -Fe, by measuring oxygen consumption, it is probably necessary to eliminate the additional respiratory repression by glucose.

During iron deficiency, *S. cerevisiae* needs to regulate the uptake and intracellular storage of iron as well as the iron-dependent pathways and machineries involved in the synthesis of its cofactors. However, it is not currently known if cells have a direct mechanism to preferentially guide and incorporate the iron into certain iron-proteins over others. Against this idea, it has been shown during low and sufficient iron conditions that the amount of iron bound to several proteins is proportional to the amount of total protein (Shakoury-Elizeh et al., 2010). Due to these results, the authors suggested that iron incorporation into proteins is determined by the amount of apo-protein available (Shakoury-Elizeh et al., 2010). Interestingly, in the case of the essential Fe/S Rli1 protein, little amount of protein accumulates without iron, even under low iron. However, the decrease in the Rli1 protein levels when iron is scarce probably reduces its overall activity. Therefore, probably yeast cells do not possess a specific mechanism that preferentially allocates iron into essential pathways (Shakoury-Elizeh et al., 2010). Instead, cells transcriptionally and/or post-transcriptionally downregulate certain iron-dependent pathways to control their final protein levels, and therefore the iron delivery.

We have described in Chapter 2 that Cth2 not only promotes AMD but also represses the translation of its targets. This fact, together with the high number of Cth2 mRNA targets in the Krebs cycle and ETC (**Figure I-4**; Puig et al., 2005; Puig et al., 2008; Romero et al., 2019) and the reduced oxygen consumption, strongly suggest a Cth2 role in downregulating the apo-protein levels of respiratory subunits. This could mean a Cth2 indirect function in the iron distribution under iron limitation. We measured several mRNA, protein and enzymatic activity levels of mitochondrial respiratory steps (aconitase from TCA cycle and complex IV, complex II and complex II+III of ETC), as well as the cytosolic Leu1 activity. The clearest result observed was the reduction in all levels (mRNA, protein and activities) in *TEF-CTH2*-expressing cells under iron sufficiency (**Figure C3-4; Figure C3-5; Figure C3-9; Figure C3-10**), with the only exception of complex IV activity (**Figure C3-7**). These results clearly confirm the Cth2 capacity of inhibiting mitochondrial respiration when overexpressed in +Fe conditions. Probably this situation also diminishes more iron-dependent cytosolic activities besides the

Leu1 activity by reducing the respective apo-proteins levels (see the summarized activities results in **Figure D3-1**).

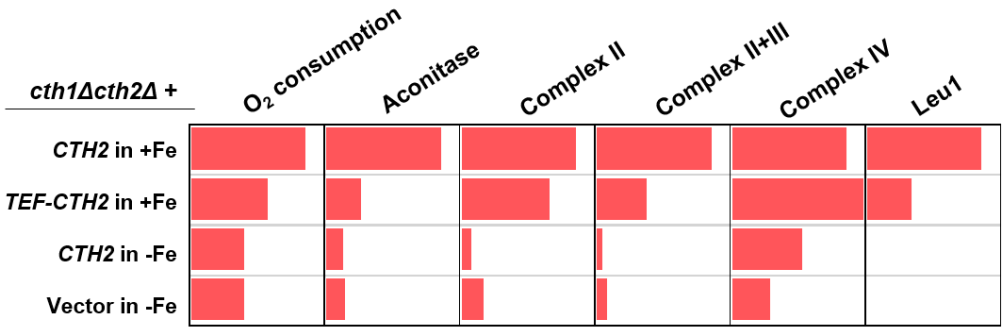

Figure D3-1. Outline of relative levels of O_2 consumption and enzymatic activities assays from this chapter.

On the other hand, under low iron conditions, there is a dramatic decrease in all enzymatic activities measured (**Figure D3-1**), in most cases with little or no obvious Cth2 dependency (**Figure C3-4; Figure C3-5; Figure C3-9; Figure C3-10**), again with the only exception of complex IV activity (**Figure C3-7**), which will be discussed below. In the case of the cytoplasmic Leu1, despite being one of the most abundant iron-dependent enzymes in the cell (Ghaemmaghami et al., 2003) and maintaining relatively abundant protein levels (**Figure C3-4: D**), its activity was undetectable in -Fe (**Figure C3-4: C;** Ihrig et al., 2010). The *leu2Δ* background of the BY4741 strain used, significantly increases *LEU1* expression (Ihrig et al., 2010). Regarding the hypothesis of iron incorporation according to the amount of apo-protein available (Shakoury-Elizeh et al., 2010), we could expect that Leu1 protein incorporates significant amounts of the iron available and this could be detrimental in -Fe. However, the increased *LEU1* expression of the *leu2Δ* background has been described not to significantly change its iron-responsive downregulation of activity (Ihrig et al., 2010). Accordingly, Leu1 activity levels are without doubt reduced in -Fe, but as they are below the detection levels, it is impossible to observe a Cth2 dependency (**Figure C3-4: C**). However, the Cth2-dependent downregulation can still be observed at the mRNA level (**Figure C3-4: A**; Ihrig et al., 2010). Regarding aconitase, the increased *ACO1* mRNA levels in -Fe

(**Figure C3-5: A**) are explained by the activation of the RTG response that upregulates the first steps of the TCA cycle (Romero et al., 2019). The Cth2-dependent regulation of *ACO1* in -Fe was clearly observed at mRNA and protein levels (**Figure C3-5: A and D**). Besides, Aco1 protein levels are also dependent on Cth2 CTD as shown in Chapter 2 (**Figure C2-11: A**). On the other hand, aconitase activity was extremely decreased in -Fe and in a Cth2-independent manner (**Figure C3-5: C**). In general, the extremely low enzymatic activities detected in -Fe forced us to work with high volumes of cell cultures to perform these measurements. This situation made difficult working with exponential phase cultures when using cell lysates, and impossible when mitochondria isolation was needed. However, the decreased Leu1 and aconitase activities of *TEF-CTH2* in +Fe in exponential phase cultures (**Figure C3-4: B; Figure C3-5: B**) were maintained in overnight cultures (**Figure C3-4: C; Figure C3-5: C**).

Regarding ETC complexes, *SDH1-4* mRNA levels of complex II showed a tendency to be coordinately regulated in a Cth2-dependent manner (**Figure C3-9: A, B, C and D**). Probably, as shown in Chapter 2 with Sdh4, the protein levels would be affected by the Cth2-dependent translational repression in -Fe, and this is reflected by the SDH activity, drastically decreased in -Fe, especially in *CTH2* expressing cells (**Figure C3-9: E**). The complex II+III activity also showed a significant Cth2 dependency in +Fe (when overexpressed) and lighter in -Fe (**Figure C3-10: D**). Among the three ARE-containing mRNA levels measured (**Figure C3-10: A, B and C**), the best Cth2 AMD effect was observed with *RIP1* mRNA, the only one downregulated by mammalian TTP in complex III (Sato et al., 2018). Importantly, the incorporation of Rip1 into the complex is one of the final steps in both yeast and mammalian cells, and it is required for the complex stability (Atkinson et al., 2011; Diaz et al., 2012; Sánchez et al., 2013). On the other hand, *CYC1* mRNA radically decreases in -Fe with a slight Cth2 dependency, as previously described (Ihrig et al., 2010). Altogether, these results suggest a Cth2 role in downregulating both the mRNA and the corresponding protein levels of Aco1 and some subunits of complex II and III, which supports: (i) the Cth2 capacity of repressing respiration when overexpressed in +Fe and (ii) a role of Cth2 in inhibiting even more the already dramatic decay of respiration in -Fe.

On the contrary, the complex IV activity is not affected by the Cth2 overexpression in +Fe (**Figure C3-7**). Even in -Fe, it is unexpectedly supported by *CTH2* compared to Vector cells (**Figure C3-7**). This happens despite the downregulation of the ARE-containing *COX4* and *COX6* mRNAs occurring in a Cth2-dependent manner (**Figure C3-6: D and E**). On the contrary, the mRNA levels of the mitochondrial encoded subunits *COX1*, *COX2* and *COX3* were always increased in -Fe (**Figure C3-6: A, B and C**). Among the three, *COX1* mRNA was the only one showing a Cth2-dependent regulation. *COX1* mRNA levels were higher in -Fe in a Cth2-dependent manner, but lower in *TEF-CTH2* cells in -Fe (**Figure C3-6: A**). Accordingly, Cox1 protein levels, and to a lesser extent Cox2, were increased in *CTH2*-expressing cells in -Fe, while, as expected, Cox4 slightly decreased (**Figure C3-8**). It is important to remind that in the determination of enzymatic activities, all needed substrates are added in excess into each spectrophotometric test to ensure that maximum activities can be reached. Particularly, in the determination of complex II+III and complex IV activities, oxidized and reduced amounts of cytochrome *c* are added, respectively to each assay (see section 4.6 of Materials and Methods). This would mean that the diminished complex II+III activity is due to the lack of stability of the complexes. In the case of complex IV, the results suggest that cells expressing *CTH2* in -Fe would have better complex IV functionality if sufficient cytochrome *c* were reduced in the mitochondrial ETC. However, this situation in cells under iron starvation is unlikely due to the lack of complex II+III activity (**Figure C3-9: E; Figure C3-10: D**) and the drastically reduced levels of *CYC1* mRNA and protein (**Figure C3-10: B;** Ihrig et al., 2010). Then, why do cells maintain complex IV functionality better than that of complex II-III in -Fe? In the ETC, the complex I and complex III are the main source of ROS under physiological conditions (reviewed by Herrero et al., 2008; Murray et al., 2011; Baccolo et al., 2018). Accordingly, mammalian TTP reduces the apo-protein levels of two ETC components in -Fe, one from complex I and the other one from complex III (Sato et al., 2018). The absence of TTP in -Fe does not result in a higher ETC activity, on the contrary, it leads to the accumulation of nonfunctional apo-protein forms of ETC subunits, reduces respiration and increases electron leakage and ROS, finally promoting cardiac disfunction in mice (Sato et al., 2018). In this line, perhaps the lack of *CTH2* in -Fe would not simply increase ETC activities and

respiration, on the contrary, it would unbalance the ETC complexes including subunits without iron cofactor, thus reducing oxygen consumption and increasing ROS production. In fact, no higher oxygen consumption has been observed in -Fe in cells lacking *CTH2* in the presence of glucose (**Figure C3-1: B**). Also, the lack of *CTH2* in -Fe slightly increases complex II+III activity (**Figure C3-9: E; Figure C3-10: D**), suggesting an increase in ROS. On the other hand, if the complex IV integrity is maintained in -Fe, it could be beneficial under a rapid shift from iron deficiency to iron sufficiency to restore the ATP production and not to block the incoming electrons flow in complex I-III.

The protective role of Cth2 against oxidative stress has been shown, together with a decrease in mitochondrial membrane potential and diminished ROS production (Castells-Roca et al., 2016; Matsuto et al., 2017). Besides, the diauxic shift induces the iron regulon (Haurie et al., 2003). These authors suggested that cells respond during the diauxic shift to the exceptional need of iron, but the role of Cth2 here is not clear. Perhaps Cth2 could be beneficial in maintaining an efficient and coordinated ETC (and consequently, less ROS productive) under iron-limiting conditions. Interestingly, the H_2O_2 generated in respiring cells triggers the heme transfer from Ccp1 (cytochrome *c* peroxidase) to the catalase Cta1 for mitochondrial H_2O_2 detoxification (Kathiresan et al., 2014). In this line, as *CCP1* encodes for an ARE-containing mRNA strongly downregulated by Cth2 in -Fe (Puig et al., 2008), Cth2 could be helping in this heme transfer when expressed. Indeed, we have seen in Chapter 2 that *CCP1* mRNA translation is also repressed by Cth2 in -Fe (**Figure C2-8: A; Figure C2-9: A**).

In this chapter, we have shown a better complex IV functionality in -Fe in cells expressing *CTH2*, but we have not explored the Cth2-related molecular mechanism responsible of that. The fact that the entire core of complex IV genes belongs to the mitochondrial DNA could be the key. The mitochondrial genome encodes eight proteins: Cob1 (complex III); Cox1, Cox2 and Cox3 (complex IV); Atp6, Atp8 and Atp9 (complex V) and the ribosomal protein Var1. Except Var1, the rest of proteins (mitochondrial DNA polymerase, translational activators, other ribosomal proteins and ETC subunits, regulatory and assembly factors) are encoded by the nucleus (reviewed by Derbikova et al., 2018; Lindahl, 2019; Barros

and McStay, 2020). The intricate regulation of each mitochondrial subunit governed by the nucleus, adds more complexity to the regulation of the OXPHOS system. In the case of *COX1*, its transcript contains seven introns. Maturases encoded by open reading frames within *COX1* and *COB1* introns (Lazowska et al., 1980; Wenzlau et al., 1989) and several nuclear genes, including *MSS116* and *COX24*, are needed for *COX1* splicing (Séraphin et al., 1989; Huang et al., 2004; Barros et al., 2006; De Silva et al., 2017). Mss116 is also involved in the activation of *COX1* mRNA translation, together with Pet309, Cbp3, Mam33 and Mss51. Then, the Cox11 and Cox17 copper chaperones (Tzagoloff et al., 1990; Glerum et al., 1996; Hiser et al., 2000; Khalimonchuk et al., 2005) and the Cox10 and Cox15 heme synthases, install two unique heme centers (one heme *a* and one heme a_3:Cu_B) into Cox1 (Nobrega et al., 1990; Barros et al., 2001). Despite the numerous factors encoded by the nucleus for the *COX1* regulation, only two mRNAs (*COX15* and *CBP3*) contain AREs and have been described to be downregulated by Cth2 in -Fe (Puig et al., 2008). Interestingly, Mss51 besides activating *COX1* mRNA translation, is also required for the correct maturation of *COX1* pre-mRNA and the assembly of complex IV (Faye & Simon, 1983; Simon & Faye, 1984; Perez-Martínez et al., 2003; Perez-Martínez et al., 2009; García-Villegas et al., 2017). Mss51 is a heme-binding protein located in the mitochondrial inner membrane and regulated by heme/O_2 levels and oxidative stress. When heme levels are low or under oxidative stress (that forms disulfide bonds in Mss51 lowering the heme-binding affinity) *COX1* mRNA translation is inhibited (Soto et al., 2012; Soto & Barrientos, 2016). If Cth2 would have an oxidation-protective role related to mitochondrial respiration, it could enhance the *COX1* mRNA translation due to a better Mss51 functionality in -Fe compared to *cth2Δ* cells. Usually, translational activators are also involved in the complex assembly. If the assembly is impaired, the activator is not available to initiate a new round of mRNA translation. It has been shown with Cox1, when the coupling of complex IV assembly and *COX1* mRNA translation is impaired, Cox1 protein is rapidly degraded (Mick et al., 2007; Mick et al., 2010). Interactions between some translational activators of the *COX1*, *COX2* and *COX3* mRNAs (core complex IV) have been detected and suggest the co-regulation of the three subunits (Naithani et al., 2003).

Despite the interesting regulation of *COX1* by the heme-Mss51 protein, it is not known if Cth2 affects its function. Further studies are required to elucidate the molecular mechanisms of Cth2 in the maintenance of complex IV during iron starvation. How Cth2 affects mtDNA integrity, the transcription and translation of mitochondrial genes or the mitochondrial heme distribution could be important topics in future studies. The results of this chapter show the Cth2 role in the downregulation of apo-protein levels of some nuclear respiratory subunits. Under iron-sufficient conditions, Cth2 overexpression would diminish respiration. On the other hand, under iron limitation Cth2 could prevent the formation of non-functional ETC complexes and the ROS production like TTP does in mammals.

Chapter 4

Results

Chapter 4. Transcriptional regulation of the ribonucleotide reductase *RNR3* gene in long-term iron-deficient conditions

As previously introduced, the RNR enzyme catalyzes the rate-limiting step in the synthesis of dNTPs. This is an iron-dependent process that results prioritized through the action of Cth2 in response to iron starvation (Sanvisens et al., 2011). The RNR large subunit is an Rnr1 homodimer and sometimes an Rnr1-Rnr3 heterodimer. The *RNR3* gene is usually expressed at very low levels under normal growth conditions, but its promoter is strongly activated during DNA damage (Elledge & Davis, 1990). In fact, the *RNR3* promoter fused to different reporters has been widely used in studies about the regulation of the DNA damage or replication stress responses (Endo-Ichikawa et al., 1996*;* Ho et al., 1997), or about general aspects of the transcriptional and genome stability machineries (Li & Reese, 2000; Sharma et al., 2003; Zhang & Reese, 2007; Tomar et al., 2008; Minard et al., 2011; Ghosh & Pugh, 2011; Hendry et al., 2015), as well as being used as biosensor of genotoxic chemicals (Endo-Ichikawa et al, 1995; Ochi et al., 2011; Wei et al., 2013). Despite this, no clear physiological relevance of *RNR3* has been described upon these stresses. This work provides new evidence of an *RNR3* transcriptional induction with implications in cell growth taking place under severe iron-deficient conditions.

C4.1. Rnr3 is induced to the same extent under long-term iron-deficient and genotoxic/replication stress conditions

To explore the *RNR3* expression changes during the progress of iron starvation, we determined *RNR3* mRNA levels in wild-type BY4741 exponentially growing cells at different times of iron deficiency (-Fe) relative to *ACT1* mRNA levels. *RNR3* mRNA, similar to *CTH2*, displayed almost undetectable levels at 0 hours of -Fe (**Figure C4-1: A**). Both *CTH2* and *RNR3* were only expressed during iron deficiency, with a delayed induction in the case of *RNR3,* that showed the highest levels after 18 hours of iron scarcity (**Figure C4-1: A**). Although this experiment was performed in exponentially growing cultures, the cell viability was decreased to 75 % after 15 hours in -Fe (**Figure C4-1: B**). However, because the *ACT1* mRNA levels were also decreased after 18 hours of -Fe, not longer being a good gene of reference, 15 hours was the time chosen to study the long-term *RNR3*

upregulation observed in -Fe where, in the absence of normalization with *ACT1*, the peak of *RNR3* expression was observed (data not shown).

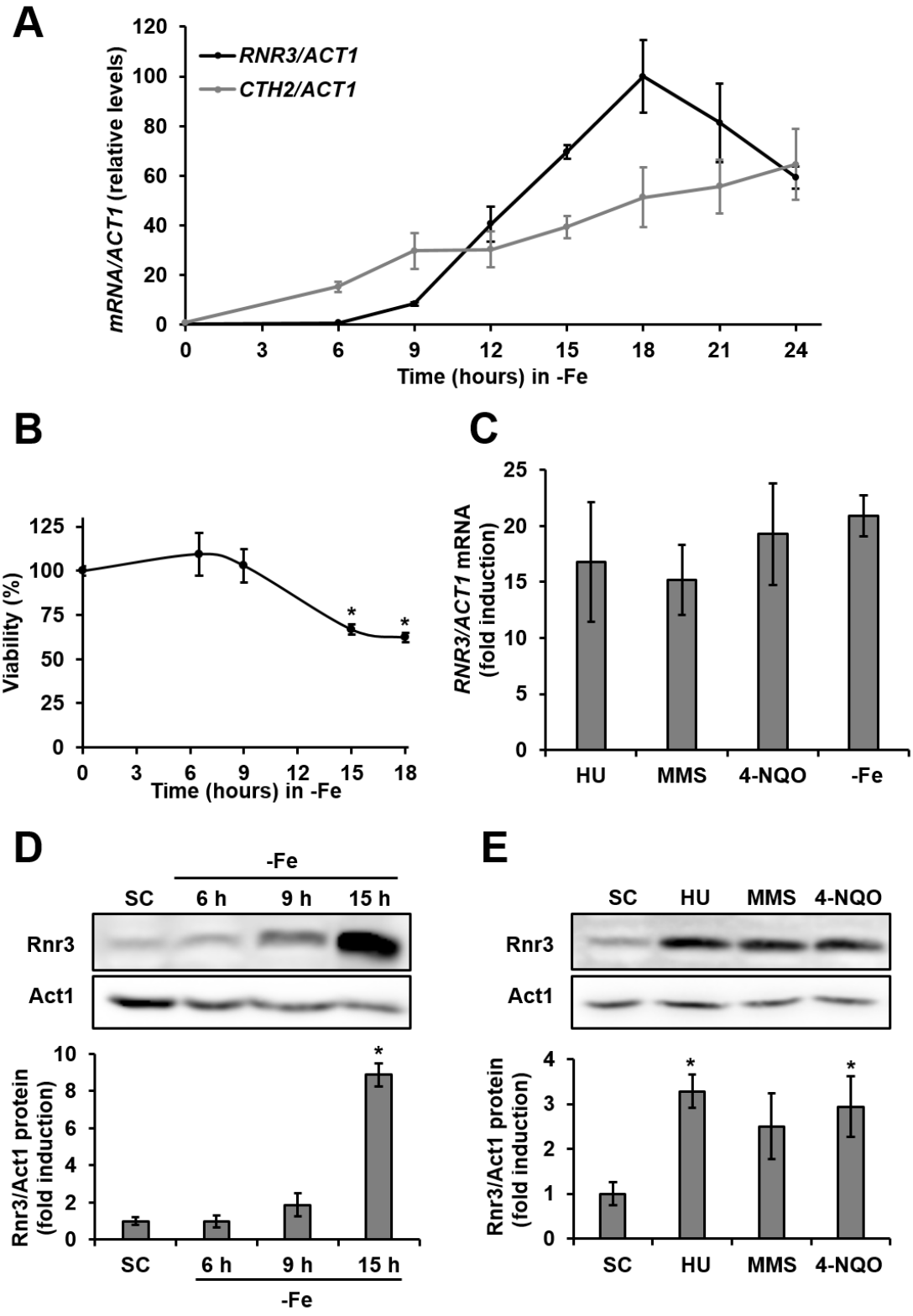

Figure C4-1. The *RNR3* levels are induced to the same extent under long-term iron deficiency, genotoxic stress and replication stress. (A) *RNR3/ACT1* and

CTH2/ACT1 mRNA levels of wild-type BY4741 cells were determined by RT-qPCR as described in Materials and Methods. Overnight cultures were reinoculated in SC for 6 hours (here indicated as 0 hours in -Fe) and SC with 100 μM BPS (-Fe, indicated times from 6 to 24 hours). Values are represented relative to *RNR3/ACT1* mRNA levels at 18 hours of -Fe. **(B)** The cell viability determination of wild-type BY4741 cells was performed as explained in section 1.5 of Materials and Methods from cells grown as in panel A. The percentages of cell viabilities at the different times of the iron deficiency were represented relative to the SC condition (0 hours in -Fe). **(C)** The *RNR3/ACT1* mRNA levels of wild-type BY4741 cells were determined from overnight cultures reinoculated in SC for 4 hours and then supplemented 1 hour with hydroxyurea 0.2 M (HU), methyl methanesulfonate 0.04 % (MMS) and 4-nitroquinoline N-oxide 0.2 mg/L (4-NQO), or overnight cultures reinoculated in SC for 6 hours (SC condition) and SC with 100 μM BPS (-Fe) for 15 hours. The *RNR3/ACT1* mRNA levels were represented as the fold-induction relative to the SC condition. **(D and E)** The Rnr3/Act1 protein levels were determined by Western blot. Cells were grown as described in panel C for SC, HU, MMS and 4-NQO **(D)** and SC and indicated -Fe times **(E)**. Protein quantifications were represented as the fold-induction relative to the SC condition. In all cases, mean values and standard deviations from at least two independent biological replicates are shown. An asterisk (*) indicates a significant difference (*p*-value <0.05) from two-tailed student's t-test compared to the SC condition (0 hours in -Fe).

As previously mentioned, the expression of *RNR3* was strongly increased under genotoxic or replication stress conditions. To compare these situations with iron starvation, we exposed wild-type BY4741 cells to the RNR inhibitor hydroxyurea (HU) and to the DNA-damaging agents methyl methanesulfonate (MMS) and 4-nitroquinoline N-oxide (4-NQO). A similar increase in *RNR3* mRNA levels (from 15 to 20-fold) was displayed under any of the conditions tested (**Figure C4-1: C**). Besides, an 8-fold increase in Rnr3 protein was observed after 15 hours in -Fe (**Figure C4-1: D**), higher than the ~2-fold increase observed earlier under iron deficiency or the ~3-fold increase under HU, MMS or 4-NQO exposure

(**Figure C4-1: D and E**). Taken together, these results demonstrate that Rnr3 is induced under long-term iron-deficient conditions to the same extent as in genotoxic and replication stress conditions.

C4.2. *RNR3* is transcriptionally activated in a Rad53/Dun1 checkpoint kinases-dependent manner under long-term iron deficiency

To determine if the *RNR3* induction under iron deficiency was caused by a transcriptional activation, we determined the RNA polymerase II recruitment to the *RNR3* promoter under iron sufficiency (+Fe) and deficiency (-Fe) relative to the recruitment to the *ACT1* promoter. The *FET3* promoter was used as a positive control of a gene transcriptionally activated when iron is scarce. We observed a higher recruitment of RNA Pol II to both *RNR3* and *FET3* promoters in -Fe compared to +Fe (**Figure C4-2**). This result suggests that the *RNR3* transcription is upregulated under iron deficiency.

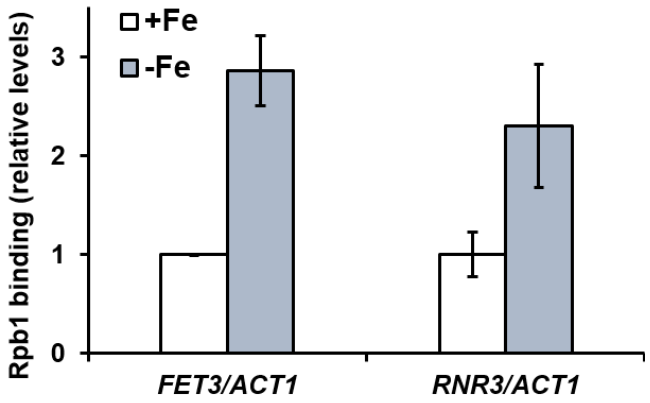

Figure C4-2. The RNA Pol II is recruited to the *RNR3* promoter under iron deficiency. The RNA polymerase II occupancy in *FET3* and *RNR3* promoters was determined relative to the *ACT1* promoter by ChIP as described in section 4.1.4 of Materials and Methods. Wild-type BY4741 overnight cultures were reinoculated in SC (+Fe) and in SC with 100 μM BPS (-Fe) for 6 hours. Mean values and standard deviations from two independent biological replicates are shown and represented relative to the +Fe situation in each case.

As previously introduced, the Mec1–Rad53–Dun1 checkpoint pathway is known to be required for the *RNR3* transcriptional activation in response to DNA

damage or replication blocking by dissociating the Crt1 repressor (Huang et al., 1998; Zhang & Reese, 2005; Sharma et al., 2007). In order to determine the implication of this pathway in the *RNR3* induction observed under long-term iron deficiency, we determined the β-galactosidase activity of a plasmid containing the *RNR3* promoter fused to the *lacZ* reporter in some checkpoint pathway mutants (**Figure C4-3**). The *RNR3-lacZ* β-galactosidase activity was highly induced in the wild-type W303 strain after 15 hours in -Fe compared to the +Fe condition, again indicating a transcriptional upregulation of *RNR3* under long-term iron deficiency (**Figure C4-3**). Importantly, this upregulation of activity in -Fe compared to +Fe was decreased in the *dun1Δ* and *rad53Δsml1Δ* mutant strains (**Figure C4-3**). The *SML1* gene was deleted to allow the *rad53Δ* viability. Nevertheless, the *sml1Δ* mutant alone not only did not show a decreased *RNR3-lacZ* activity, but it even showed an increased activity in -Fe (**Figure C4-3**). All these results together demonstrate the implication of the Rad53/Dun1 checkpoint kinases in the transcriptional upregulation of *RNR3* under long-term iron-deficient conditions.

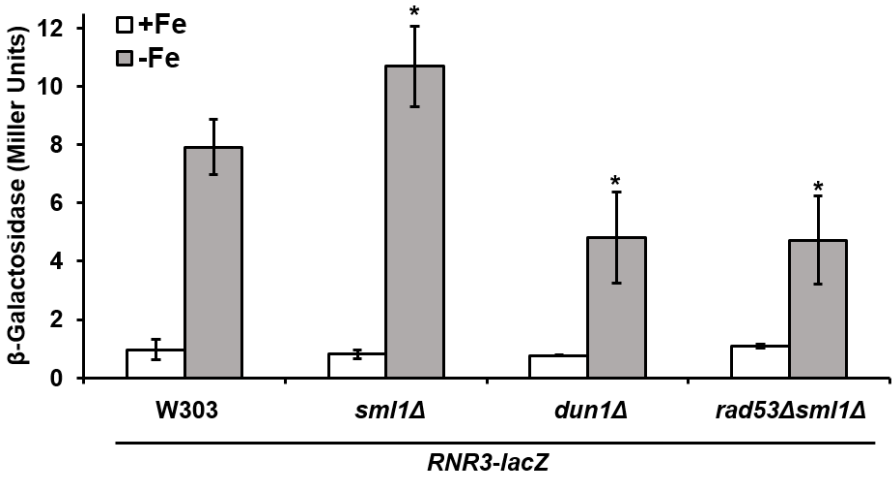

Figure C4-3. *RNR3* is transcriptionally induced in a Rad53 and Dun1 checkpoint kinases-dependent manner under long-term iron-deficient conditions. *RNR3-lacZ* β-galactosidase levels of wild type W303, *sml1Δ*, *dun1Δ* and *rad53Δsml1Δ* mutant cells transformed with *RNR3-lacZ* were determined from overnight cultures reinoculated in SC-Ura (+Fe) and in SC-Ura with 100 µM BPS (-Fe) for 15 hours. Mean values and standard deviations from three independent biological replicates are shown. An asterisk (*) indicates a significant difference (*p*-

value <0.05) from two-tailed student's t-test comparing the fold change in -Fe/+Fe levels of each mutant with the fold change in -Fe/+Fe levels of the wild-type W303.

C4.3. Cth2 induces the *RNR3* expression only when expressed under iron-deficient conditions

Cth2 was previously described to be important for the RNR assembly and production of dNTPs under iron starvation (Sanvisens et al., 2011). Therefore, we wanted to study a possible role of Cth1/Cth2 in the transcriptional induction of *RNR3* in -Fe. Again, the *RNR3-lacZ* β-galactosidase activity was highly induced in the wild-type BY4741 strain after 15 hours in -Fe, compared to the +Fe condition (**Figure C4-4: A**). This -Fe specific increment was slightly reduced in the *cth1Δ* mutant, drastically reduced in the *cth2Δ* mutant and even more decreased in the

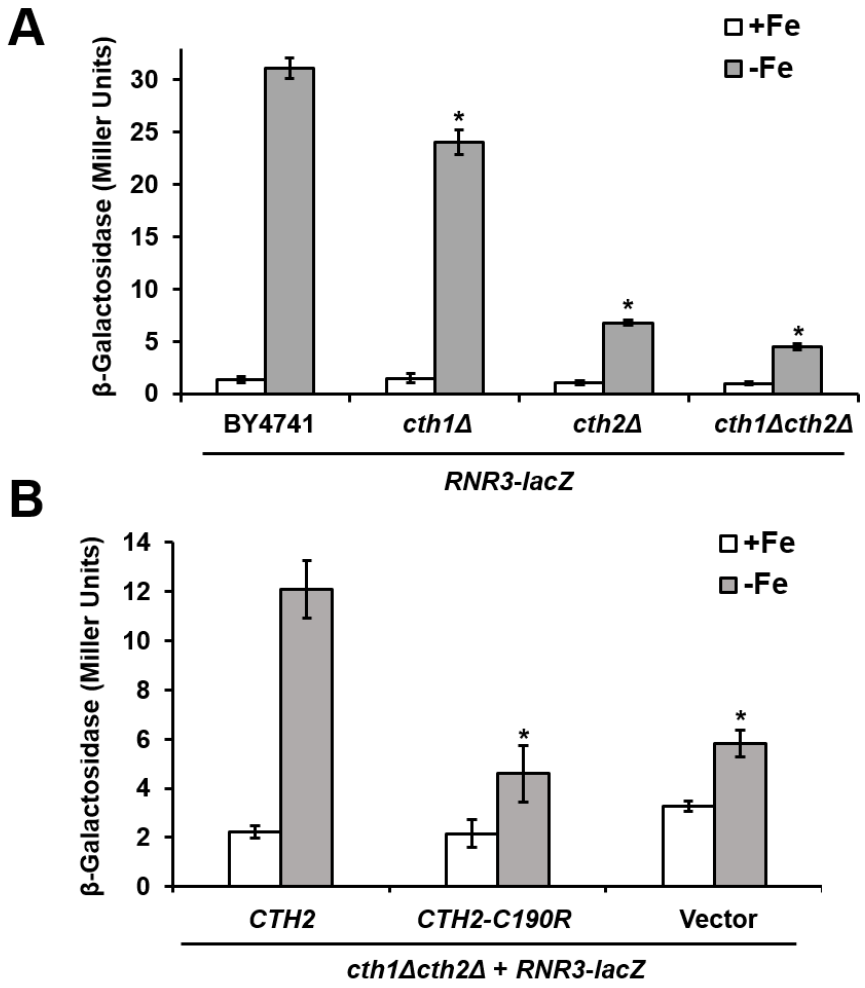

Figure C4-4. *RNR3* is transcriptionally induced in a Cth1, and mainly Cth2-TZF-dependent manner under long-term iron-deficient conditions. *RNR3-lacZ*

β-galactosidase levels of **(A)** wild-type BY4741, *cth1Δ*, *cth2Δ* and *cth1Δcth2Δ* mutant cells transformed with *RNR3-lacZ* and **(B)** *cth1Δcth2Δ* mutant cells co-transformed with *RNR3-lacZ* and either pRS415-*CTH2* (*CTH2*), pRS415-*CTH2-C190R* (*CTH2-C190R*) or pRS415 (Vector) were determined from overnight cultures reinoculated in SC-Ura (+Fe) and in SC-Ura with 100 μM BPS (-Fe) for 15 hours. Mean values and standard deviations from three independent biological replicates are shown. An asterisk (*) indicates a significant difference (*p*-value <0.05) from two-tailed student's t-test comparing the fold change in -Fe/+Fe levels of each mutant with the fold change in -Fe/+Fe levels of the wild-type BY4741 **(A)** and *CTH2* cells **(B)**.

cth1Δcth2Δ double mutant (**Figure C4-4: A**). Next, we wanted to determine more precisely the implication of the Cth2-TZFs in the induction of *RNR3* promoter in -Fe. The *cth1Δcth2Δ* background was co-transformed with the *RNR3-lacZ* plasmid and either the *CTH2* plasmid (*CTH2*), the TZF-mutated version (*CTH2-C190R*) or empty vector (Vector). The observed inducible activity in -Fe compared to +Fe in *CTH2* expressing cells was reduced to the same extent in both *CTH2-C190R* and Vector cells (**Figure C4-4: B**). This indicates that Cth2 has a significant TZF-dependent role in the *RNR3* transcriptional upregulation under long-term iron deficiency.

We wondered then whether a constitutive expression of *CTH2* in +Fe was sufficient to induce *RNR3* expression. We tested the *RNR3* and *CTH2* mRNA levels (**Figure C4-5: A and B**, respectively) in *cth1Δcth2Δ* cells expressing the wild-type version of *CTH2* (*CTH2*), the empty vector (Vector) and the *TEF2* promoter fusion with the *CTH2* coding sequence (*TEF-CTH2*). As expected from the β-galactosidase activity assays, the increase in *RNR3* mRNA levels in -Fe compared to +Fe in *CTH2* cells was also observed but to a much lower extent in Vector cells (**Figure C4-5: A**). Surprisingly, the *TEF-CTH2* expressing cells still showed the same low *RNR3* mRNA levels in +Fe and highly induced levels in -Fe (**Figure C4-5: A**), although the *CTH2* mRNA levels were increased by the *TEF2* promoter in both conditions (**Figure C4-5: B**). These results indicate that the Cth2-dependent *RNR3* upregulated expression only takes place under iron starvation.

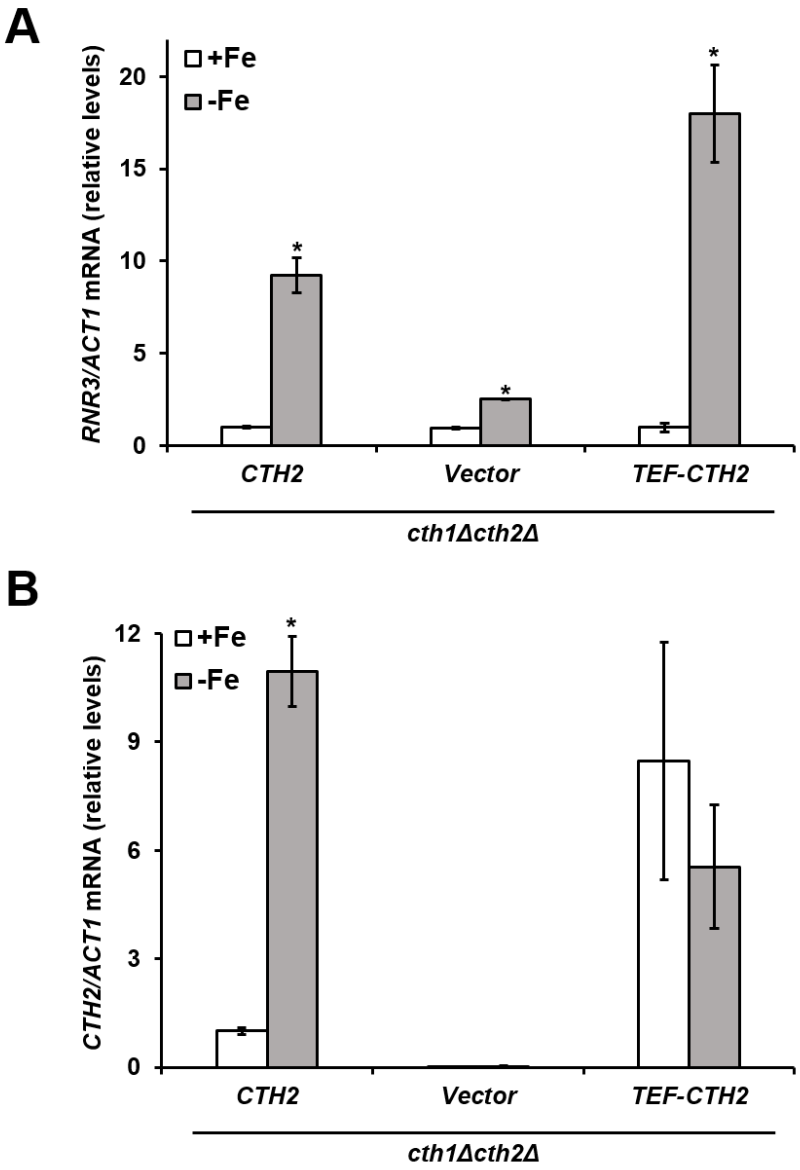

Figure C4-5. *RNR3* is not induced by Cth2 under iron sufficiency. The *RNR3/ACT1* **(A)** and *CTH2/ACT1* **(B)** mRNA levels of *cth1Δcth2Δ* mutant cells transformed with pRS416-*CTH2* (*CTH2*), pRS416 (Vector) or p416-*TEF-CTH2* (*TEF-CTH2*) were determined from overnight cultures reinoculated in SC-Ura with 10 μM FAS (+Fe, 6 hours) and in SC-Ura with 100 μM BPS (-Fe, 10 hours) by RT-qPCR as described in Materials and Methods. Mean values and standard deviations from three independent biological replicates are shown relative to *CTH2* in +Fe. An asterisk (*) indicates a significant difference (*p*-value <0.05) from two-tailed student's t-test comparing the -Fe to the +Fe situation in each case.

C4.4. Cth2 and Dun1 independently induce *RNR3* transcription under long-term iron deficiency

Here we have shown that the *RNR3* transcriptional induction under long-term iron deficiency is dependent on both Rad53/Dun1 and Cth2 (**Figure C4-3 and Figure C4-4**, respectively). Next, we wanted to test if these pathways act independently or not. The previously shown induction of *RNR3-lacZ* activity in -Fe compared to +Fe in the wild-type BY4741 was reduced to the same extent in both *dun1Δ* and *cth1Δcth2Δ* mutant strains (**Figure C4-6**). Importantly, the *RNR3-lacZ* induction in -Fe was even more drastically decreased in the *dun1Δcth1Δcth2Δ* mutant approaching the basal levels measured in +Fe (**Figure C4-6**). These results suggest that Cth2 and Dun1 have independent roles in the transcriptional induction of *RNR3* when iron is scarce.

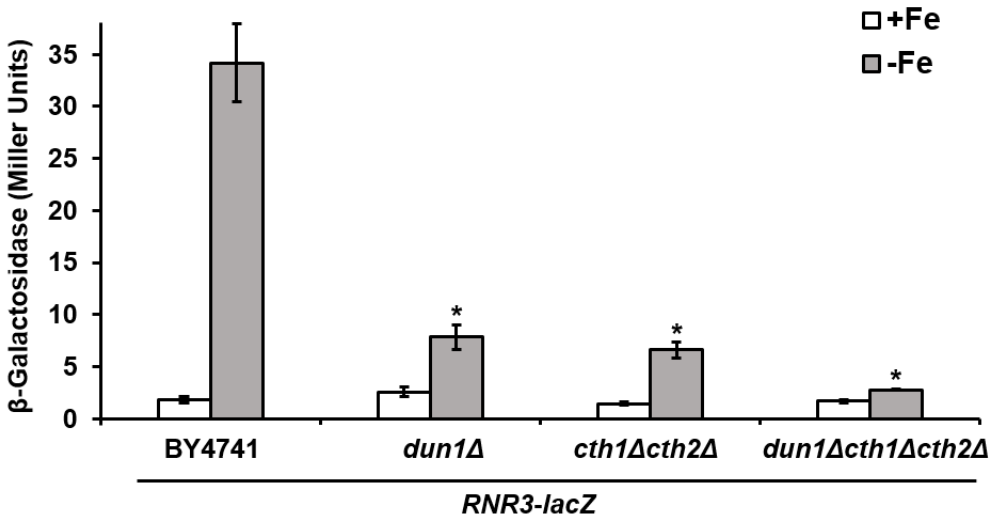

Figure C4-6. Cth2 and Dun1 independently induce the *RNR3* transcription under long-term iron-deficient conditions. *RNR3-lacZ* β-galactosidase levels of wild type BY4741, *dun1Δ*, *cth1Δcth2Δ* and *dun1Δcth1Δcth2Δ* mutant cells transformed with *RNR3-lacZ* were determined from overnight cultures reinoculated in SC-Ura (+Fe) and in SC-Ura with 100 μM BPS (-Fe) for 15 hours. Mean values and standard deviations from three independent biological replicates are shown. An asterisk (*) indicates a significant difference (*p*-value <0.05) from two-tailed student's t-test comparing the fold change in -Fe/+Fe levels of each mutant with the fold change in -Fe/+Fe levels of the wild-type BY4741.

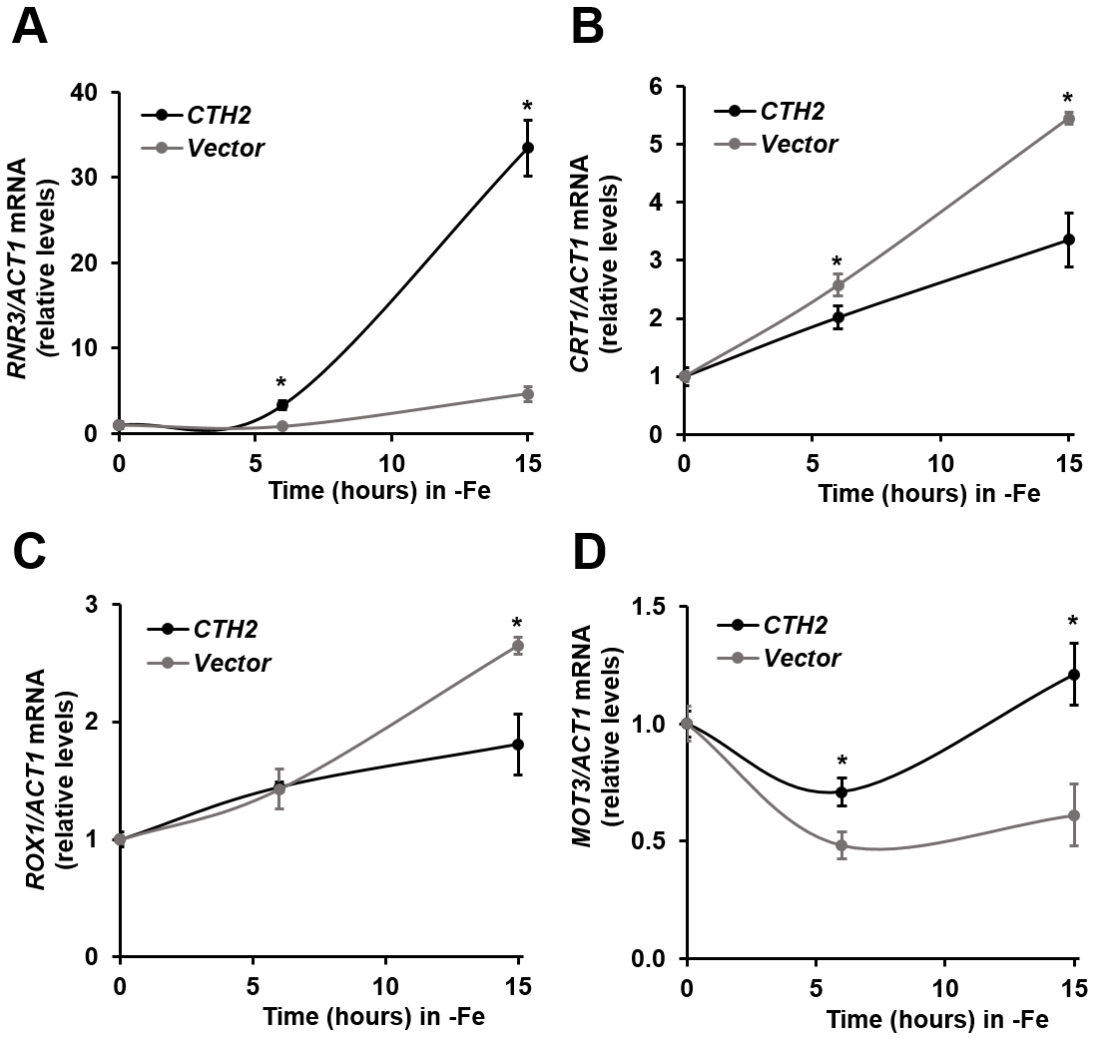

Figure C4-7. The mRNA levels of the *RNR3* transcriptional repressors *CRT1* and *ROX1* are decreased in a Cth2-dependent manner under long-term iron deficiency. The *RNR3/ACT1* **(A)**, *CRT1/ACT1* **(B)**, *ROX1/ACT1* **(C)** and *MOT3/ACT1* **(D)** mRNA levels of *cth1Δcth2Δ* mutant cells transformed with pRS416-*CTH2* (*CTH2*) and pRS416 (Vector) were determined from overnight cultures reinoculated in SC-Ura with 10 μM FAS for 6 hours (+Fe, here indicated as 0 hours in -Fe) and SC-Ura with 100 μM BPS (-Fe, 6 and 15 hours) by RT-qPCR as described in Materials and Methods. Mean values and standard deviations from at least two independent biological replicates are shown relative to the levels at 0 hours in -Fe. An asterisk (*) indicates a significant difference (p-value <0.05) from two-tailed student's t-test comparing the fold change -Fe/+Fe levels of the *CTH2* cells with the fold change -Fe/+Fe levels of the Vector cells.

C4.5. Cth2 partially promotes the *RNR3* transcriptional derepression through Crt1 regulation under long-term iron deficiency

As previously introduced, the role of Cth2 is to promote an ARE-mediated mRNA decay in order to facilitate the metabolic remodeling of cellular processes under iron starvation (Puig et al., 2005; Puig et al., 2008). However, the results above demonstrated a role of Cth2 in the transcriptional activation of *RNR3*. We wondered if Cth2 was promoting the AMD of any transcriptional repressor of the *RNR3* promoter. To study this possibility, we determined the mRNA levels of three well-known *RNR3* transcriptional repressors, namely Rox1, Mot3 and Crt1, all recruiting the Ssn6–Tup1 general repressor complex (Huang et al., 1998; Li & Reese, 2001; Zhang & Reese, 2004a; Klinkenberg et al., 2005; Klinkenberg et al., 2006). As expected, the *RNR3* mRNA levels were more induced in *CTH2* expressing cells compared to Vector cells especially after 15 hours in -Fe (**Figure C4-7: A**). Interestingly, the *CRT1* and *ROX1* mRNA levels were more incremented in Vector cells compared to *CTH2* cells especially after 15 hours in -Fe (**Figure C4-7: B and C**, respectively). On the contrary, the *MOT3* mRNA levels showed incremented levels in *CTH2* cells compared to Vector cells after 6 and 15 hours of iron deficiency, but the levels slightly fluctuated during the progress of the iron deficiency in both cases (**Figure C4-7: D**). These results suggest that the *RNR3* transcriptional repressors Crt1 and Rox1 could be negatively regulated in -Fe at the mRNA level in a Cth2-dependent manner.

In addition to these three repressors of *RNR3* promoter, other potential transcriptional repressors are described in the literature. We made a selection of those that were also described as possible Cth1/Cth2 targets (Puig et al., 2005; Puig et al., 2008) and/or contained ARE sequences in their 3'UTR mRNAs. Then, we measured if their mRNA levels were altered in a Cth2-dependent manner in -Fe (**Figure C4-8**). The paralogs *YOX1* and *YHP1* are homeobox transcriptional repressors (Horak et al., 2002). Yox1 has been described to bind the *RNR3* promoter, as well as other promoters of genes involved in DNA-damage responses (Horak et al., 2002; Aligianni et al., 2009). Besides, both *YOX1* and *YHP1* mRNAs contain one ARE each, at 15 and 230 nts after the translation termination codon, respectively. On the other hand, Hap4 is a transcriptional factor detected to bind

the *ROX1* promoter, one of the *RNR3* transcriptional repressors (Zhang et al., 2017). Besides, the *HAP4* mRNA (with 2 AREs at 274 and 302 nts after the translation termination codon) has been described as a Cth2-target (Puig et al., 2008). Despite that the mRNA levels of *YOX1*, *YHP1* and *HAP4* were decreased in the progression of the iron deficiency in *CTH2* expressing cells (**Figure C4-8: A, B and C**, respectively), they did not show differences at 15 hours in -Fe relative to +Fe between *CTH2* and Vector cells.

Another studied mechanism of repression of *RNR3* transcription involves the recruitment of histone deacetylases by the Ssn6–Tup1 repressor complex (Zhang & Reese, 2005). The triple histone deacetylase mutant *rpd3Δhos1Δhos2Δ* showed a reduced Crt1-dependent repression (Davie et al., 2002; Zhang & Reese, 2005). The *HOS1* mRNA is the only one containing an ARE (at 563 nts after the translation termination codon). Interestingly, the *HOS1* mRNA showed increased levels at 15 hours in -Fe in Vector cells compared to *CTH2* cells (**Figure C4-8: D**), suggesting a Cth2-dependent *HOS1* mRNA decay.

Another study using *RNR3-GFP* determined 150 mutants that showed an induction of *RNR3* expression in untreated and MMS treated cells (Hendry et al., 2015). Three of them were chosen because of the above-mentioned criteria: *RPA190*, *IRA2* and *DIA2* (**Figure C4-8: E, F and G** respectively). The *RPA190* (RNA polymerase I largest subunit) mRNA, with 2 AREs at 275 and 552 nts after the translation termination codon, is a Cth1-mRNA target (Puig et al., 2008). The *IRA2* and *DIA2* mRNAs, with no AREs, are possible Cth1 and Cth2-mRNA targets, respectively (Puig et al., 2008). However, their mRNA levels did not show significant changes between *CTH2* and Vector cells (**Figure C4-8: E, F and G** respectively).

The *CWP1* mRNA, with an ARE at 311 nts after the translation termination codon, was the last mRNA tested because when mutated together with other 6 genes (none with AREs) the *RNR3-GFP* was induced (Wei et al., 2013). Despite of its strongly decreased mRNA levels under iron deficiency, there were no differences between *CTH2* and Vector cells (**Figure C4-8: H**).

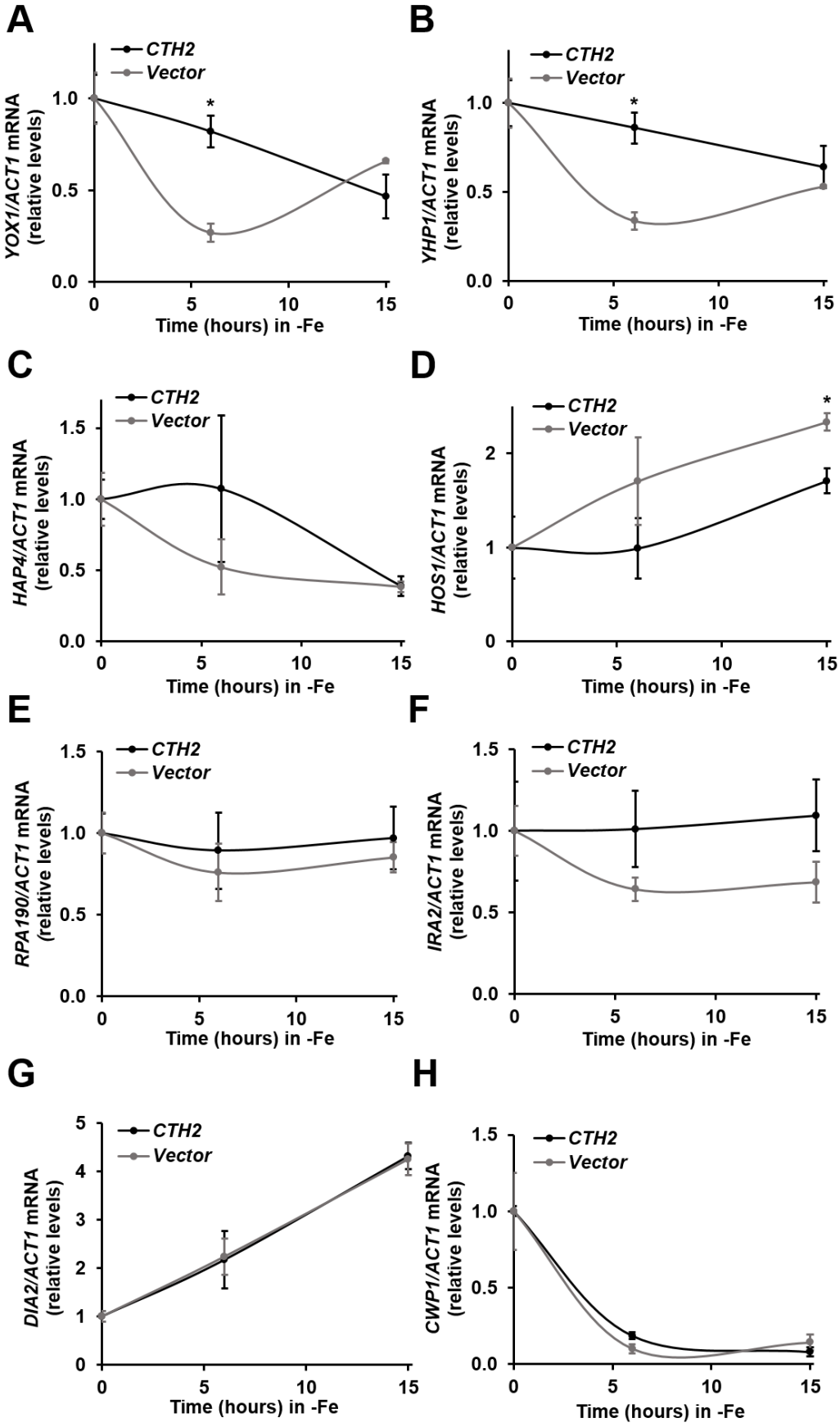

Figure C4-8. mRNA levels of other *RNR3* transcriptional repressors that are potential Cth2 mRNA targets. The *YOX1/ACT1* **(A)**, *YHP1/ACT1* **(B)**, *HAP4/ACT1*

(C), *HOS1/ACT1* **(D)**, *RPA190/ACT1* **(E)**, *IRA2/ACT1* **(F)**, *CWP1/ACT1* **(G)** and *DIA2/ACT1* **(H)** mRNA levels were determined as indicated in Figure C4-7.

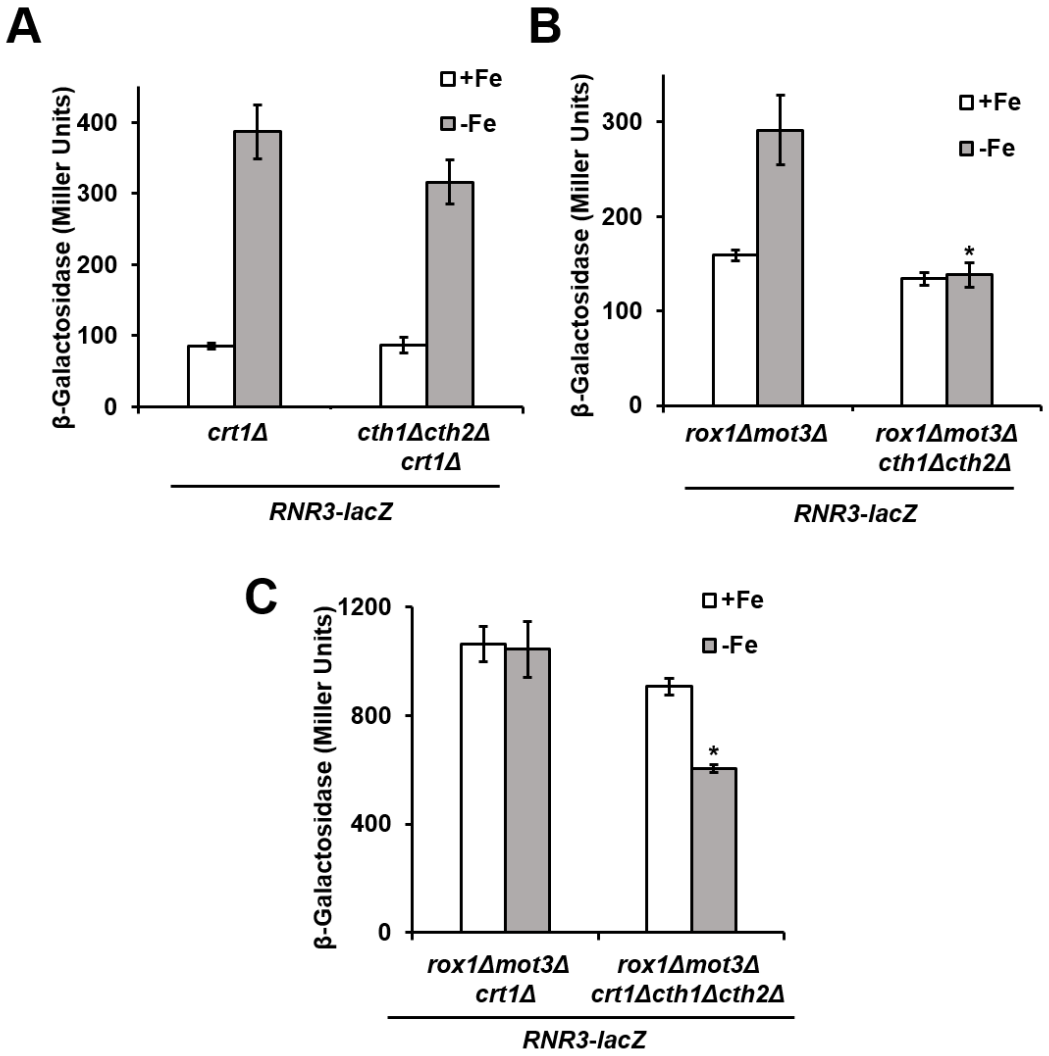

Figure C4-9. Cth2 partly induces the *RNR3* transcription through Crt1 regulation under long-term iron deficiency. *RNR3-lacZ* β-galactosidase levels of *crt1Δ* and *cth1Δcth2Δcrt1Δ* **(A)**, *rox1Δmot3Δ* and *rox1Δmot3Δcth1Δcth2Δ* **(B)**, *rox1Δmot3Δcrt1Δ* and *rox1Δmot3Δcrt1Δcth1Δcth2Δ* **(C)** mutant cells transformed with *RNR3-lacZ* were determined from overnight cultures reinoculated in SC-Ura (+Fe) and in SC-Ura with 100 μM BPS (-Fe) for 15 hours. Mean values and standard deviations from at least three independent biological replicates are shown. An asterisk (*) indicates a significant difference (*p*-value <0.05) from two-tailed student's t-test comparing the fold change in -Fe/+Fe levels of each mutant with the fold change in -Fe/+Fe levels of that mutant lacking *CTH1* and *CTH2*.

Once the list of Cth2-regulated *RNR3* repressors was reduced to Crt1, Hos1 (via Crt1–Ssn6–Tup1-dependent repression) and Rox1, several mutants, *crt1Δ*, *rox1Δmot3Δ* and *rox1Δmot3Δcrt1Δ* were generated in combination with the *cth1Δcth2Δ* mutant strain to test the *RNR3-lacZ* activity under iron sufficiency and deficiency (**Figure C4-9**). Although the -Fe/+Fe induction in the β-galactosidase activity has been considered, it should be noticed the higher basal activity levels in +Fe when any of these *RNR3*-promoter repressors was deleted (**Figure C4-9**). The *RNR3-lacZ* activity of the *crt1Δ* strain was induced in -Fe compared to +Fe, and importantly maintained almost intact this induction in the *crt1Δcth1Δcth2Δ* strain (**Figure C4-9: A**). However, the observed -Fe/+Fe induction in the *rox1Δmot3Δ* strain was completely lost in *rox1Δmot3Δcth1Δcth2Δ* cells (**Figure C4-9: B**). On the other hand, when the three repressors were mutated, *rox1Δmot3Δcrt1Δ* cells, there was no difference in the *RNR3-lacZ* activity levels between +Fe and -Fe conditions (**Figure C4-9: C**), probably because of a completely derepressed *RNR3*-promoter situation. However, the Cth1/Cth2 role was still present as the *rox1Δmot3Δcrt1Δcth1Δcth2Δ* strain showed diminished activity levels in -Fe (**Figure C4-9: C**). Together, these results suggest that Cth2 can promote the transcriptional derepression of *RNR3* possibly through the regulation of Crt1, although other mechanisms could be involved.

C4.6. Rnr3 is physiologically relevant under iron-deficient situations

No clear growth defects have been described with the unique deletion of *RNR3* in any of the stress conditions typically defined to induce its expression (DNA damage, genotoxic stress, replication stress). Here, we observed a remarkable growth defect in the *rnr3Δ* mutant strain in both liquid and solid iron-deficient media compared to the wild-type BY4741 (**Figure C4-10: B and C**, respectively). This situation is specific to the -Fe situation as the *rnr3Δ* cell growth was not affected in liquid nor solid iron-sufficient media compared to the wild-type (**Figure C4-10: A and C**, respectively). These results demonstrate a physiologically relevant role of Rnr3 under iron starvation.

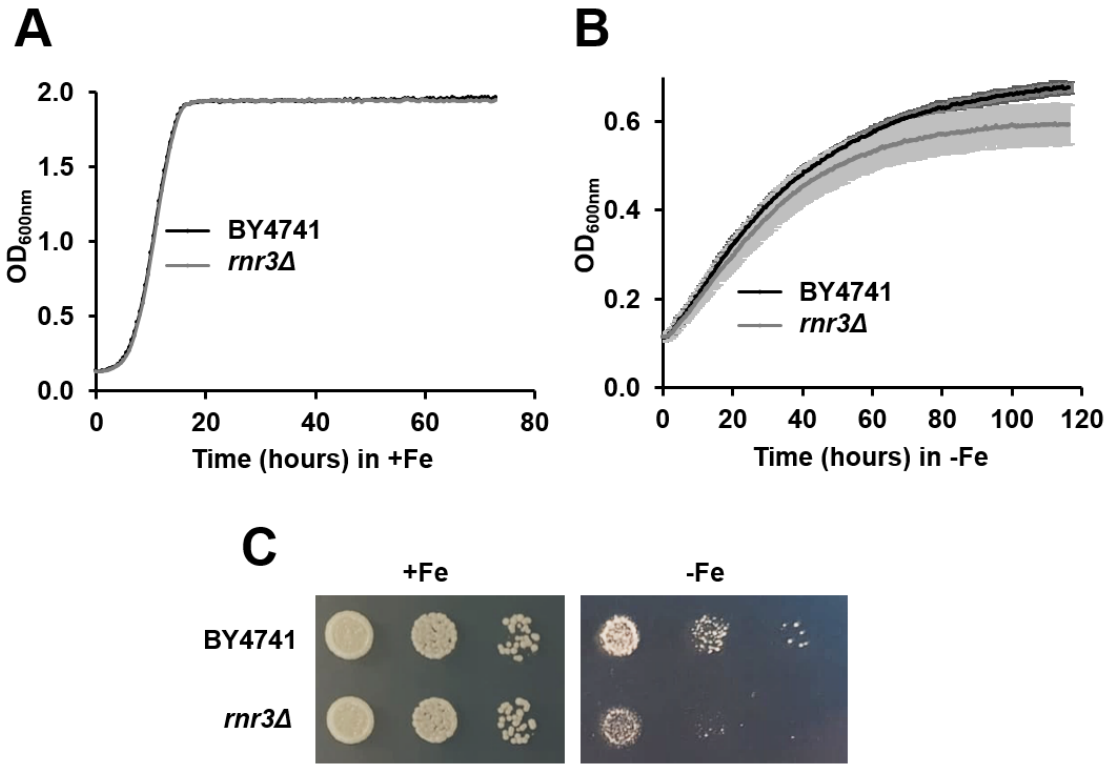

Figure C4-10. The *rnr3Δ* mutant shows growth defects under iron-deficient conditions. Cell growth analyses of wild-type BY4741 and *rnr3Δ* mutant cells in liquid media were performed from overnight cultures SC with 10 μM FAS (+Fe) **(A)** and SC with 1500 μM Ferrozine (-Fe) **(B)** and in solid media in SC (+Fe) and SC with 200 μM BPS (-Fe) **(C)** as explained in section 1.4 of Materials and Methods. Four independent experiments were performed in each case. Mean values of the growth curves (OD_{600} vs. time) were represented with standard deviations **(A and B)**.

Discussion

Chapter 4

Discussion of Chapter 4

The ribonucleotide reductase enzyme of *S. cerevisiae* harbors the essential oxo-diiron cofactor in the Rnr2 subunit. Despite this, all RNR subunits show iron-dependent regulations (Sanvisens et al., 2014; Pijuan et al., 2015; Ros-Carrero et al., 2020), and in the case of the regulation of Rnr2 and Rnr4, it includes the Cth2-dependent AMD under iron deficiency (Sanvisens et al., 2011). *RNR3* induction is known to occur in strains defective in ISC and CIA machineries in a Dun1-dependent manner (Stehling et al., 2012; Zhang et al., 2014). However, here we have shown that both Cth2 and Dun1, independently and to the same extent, induce *RNR3* expression under long-term iron-deficient conditions (**Figure C4-6**). This upregulation occurs at the transcriptional level, as higher RNA Pol II recruitment to the *RNR3* promoter has been observed (**Figure C4-2**). This is remarkable given that Rpb1 protein levels are reduced under iron-deficient conditions (Romero et al., 2019). The *RNR3* promoter induction results in higher mRNA and protein levels of Rnr3, comparable to those reached under genotoxic or replication stress conditions (**Figure C4-1: C, D and E**). And, importantly, the *RNR3* transcriptional upregulation led to sufficient protein levels to support a physiological role under iron starvation (**Figure C4-10**).

In response to DNA damage, the *RNR2/3/4* transcriptional repressor Crt1 is phosphorylated by Dun1 and then released from its target promoters (Huang et al., 1998; **Figure D4-1: A**). We believe that this is also the Dun1-related situation observed over *RNR3* transcription under iron deficiency (**Figure D4-1: B**): (i) Rad53 is more phosphorylated in strains defective in ISC and CIA machineries that induce the *RNR3* promoter (Stehling et al., 2012); (ii) *RNR3* mRNA levels are induced in a Dun1-dependent manner in a CIA-defective strain (Zhang et al., 2014); (iii) Rad53 and Dun1 kinases are required in the *RNR3* induction under long-term iron deficient-conditions (**Figure C4-3; Figure C4-6**). For these reasons, we decided to focus our efforts in elucidating the role of Cth2 in *RNR3* transcriptional induction under long-term iron deficiency.

In this chapter, we have described that the function of Cth2 in upregulating *RNR3* (i) depends on its TZF motif, (ii) predominates over the role of Cth1 and (iii) only takes place under iron deficiency (**Figure C4-4; Figure C4-5**). As Cth2 is an

mRNA-binding protein that promotes AMD, it is likely that Cth2 could downregulate the mRNA levels of an *RNR3* transcriptional repressor. The mRNA steady-state levels of *CRT1*, *ROX1* and *MOT3*, three well-known *RNR3* transcriptional repressors that act synergistically (Klinkenberg et al., 2006), showed that *CRT1* and *ROX1* (but not *MOT3*) mRNAs levels are increased in cells lacking *CTH2* compared to *CTH2*-expressing cells in -Fe (**Figure C4-7**). None of them has been described before as a potential Cth2 mRNA-target (Puig et al., 2005; Puig et al., 2008) and neither contains the canonical ARE 5′-UAUUUAUU-3′ / 5′-UUAUUUAU-3′ sequences within their 3'-UTRs. Despite this fact, *CRT1* and *ROX1* mRNA levels are clearly lowered by the presence of Cth2 after 15 hours in -Fe, when the highest *RNR3* expression takes place (**Figure C4-7: A, B and C**). Only in the case of *CRT1*, its mRNA is downregulated by Cth2 in the first 6 hours of -Fe (**Figure C4-7: B**). In fact, 6 hours in iron deficiency is the -Fe time used in the previous studies that characterized the possible Cth2 mRNA-targets (Puig et al., 2005; Puig et al., 2008). Despite the lack of Cth2-dependent regulation on *CRT1* and *ROX1* mRNAs found in these studies, and the lack of canonical AREs in their 3'-UTRs, an incomplete 5′-UAUUUAU-3′ ARE sequence is present at 551 nts in the 3'-UTR of *CRT1* mRNA. This suggests that *CRT1* mRNA could be a new direct Cth2 mRNA target in -Fe. On the other hand, the *ROX1* mRNA regulated by Cth2 only at long-term iron deficiency does not contain any ARE-like sequence and probably it is not a direct Cth2 target. Interestingly, it is possible that potential new mRNAs differentially regulated (directly or indirectly) by Cth2 would be better or only observed at long-term iron-deficient conditions.

In the case of *ROX1*, it is regulated by heme (and oxygen) as its transcription is activated by the heme-dependent proteins Hap1 and Hap4 (Zhang et al., 2017). Besides, *ROX1* has been described to be highly expressed upon oxidative stress (Castells-Roca et al., 2011; Liu & Barrientos, 2012). It is likely that Cth2 downregulates the *ROX1* mRNA levels indirectly. In fact, *HAP4* mRNA is a Cth2-target with 2 AREs (Puig et al., 2008). However, we did not see a Cth2-dependent downregulation of *HAP4* in our conditions (**Figure C4-8: C**). The possibility that Cth2 indirectly decreases *ROX1* mRNA levels under long-term iron deficiency via *HAP4* downregulation or other mechanisms that derepress *RNR3* expression

requires further studies. Interestingly, new mRNAs differentially regulated (directly or indirectly) by Cth2 could be detected in future expression studies performed at long-term iron-deficient conditions.

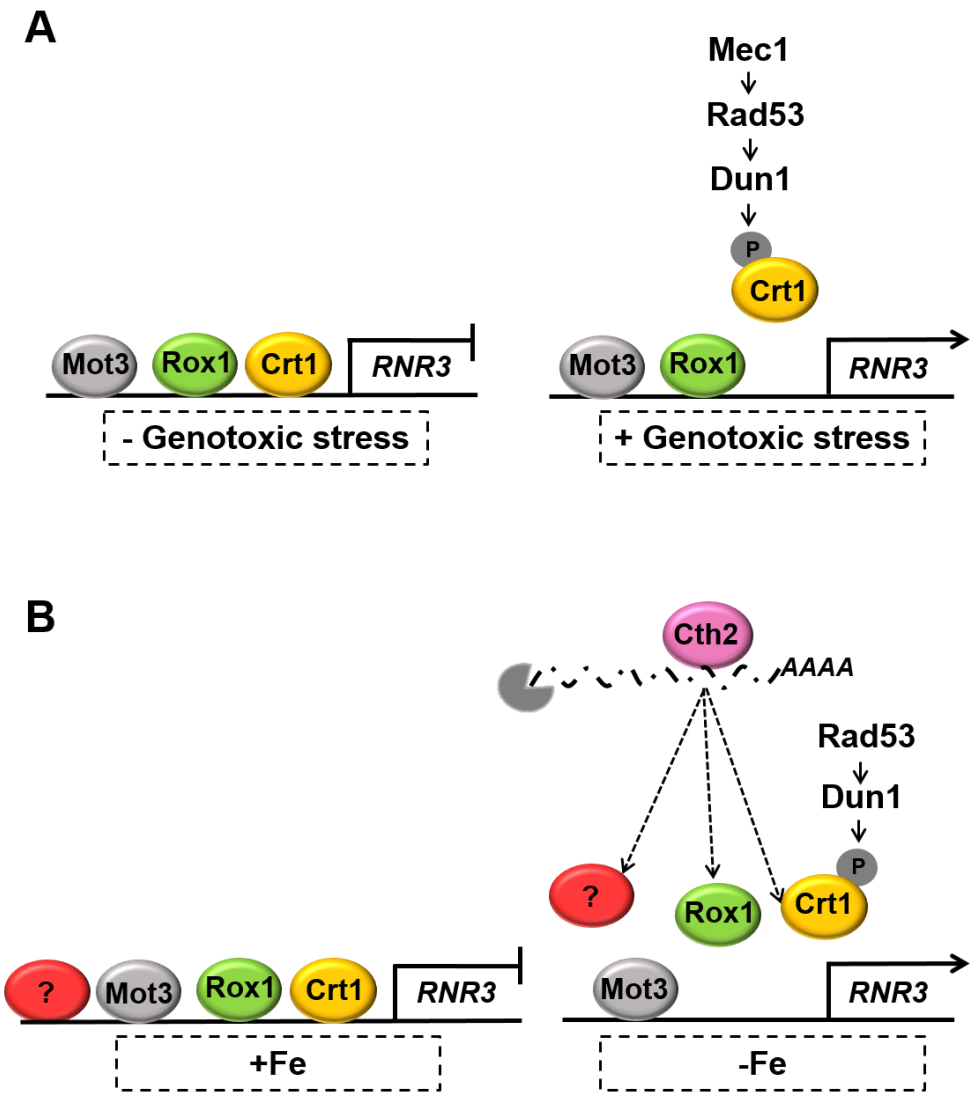

Figure D4-1. Proposed model for the *RNR3* transcriptional activation under long-term iron deficiency (B) compared to genotoxic stress (A).

In addition to *CRT1*, *ROX1* and *MOT3*, we tested the mRNA levels of other potential *RNR3* transcriptional repressors (**Figure C4-8**). We filtered those that have been described to potentially bind and repress *RNR3* promoter or derepress *RNR3* expression when mutated. Besides, they appear as possible Cth1/Cth2

targets (Puig et al., 2005; Puig et al., 2008) or if not, at least contain canonical AREs. Among them, only the ARE-containing *HOS1* mRNA showed increased levels in cells lacking *CTH2* compared to *CTH2*-expressing cells at long-term iron deficiency (**Figure C4-8: D**). Hos1 is a class I histone deacetylase that together with Rpd3 and Hos2 is recruited by the Ssn6–Tup1 repressor complex (Watson et al., 2000; Davie et al., 2002; Davie et al., 2003; Zhang & Reese, 2005). Ssn6–Tup1 is a general corepressor complex brought to target promoters by Crt1, Rox1 and Mot3 DNA-binding proteins, repressors of DNA damage- and hypoxia-inducible genes (Balasubramanian et al., 1993; Huang et al., 1998; Kastaniotis et al., 2000). The expression through the *RNR3* promoter was analyzed in several mutant strains of the three repressors and in combination with *cth1Δcth2Δ* deletions (**Figure C4-9**). The *RNR3* induction observed in the *crt1Δ* mutant under long-term iron deficiency was practically maintained in the *crt1Δcth1Δcth2Δ* strain (**Figure C4-9: A**). This was not the case when the *rox1Δmot3Δ* strain was compared to *rox1Δmot3Δcth1Δcth2Δ* (**Figure C4-9: B**). This would indicate that the Cth2-dependent *RNR3* upregulation occurs mainly through Crt1. However, when the three repressors are mutated, the Cth2-dependent role in *RNR3* induction is still present (**Figure C4-9: C**). These results using multiple mutant strains of *CRT1*, *ROX1* and *MOT3* can be difficult to interpret as they repress several other genes and act synergistically upon the *RNR3* promoter. The only *CRT1* deletion alone under normal conditions derepresses *RNR3* more than a wild-type strain under long-term iron deficiency; and the deletion of the three repressors probably derepresses *RNR3* completely. We cannot conclude that Cth2 only derepresses *RNR3* by these repressors. We propose a model of *RNR3* induction under long-term iron-deficient conditions (**Figure D4-1: B**) in which (i) Cth2 promotes the direct AMD of *CRT1* mRNA that, together with the Crt1 phosphorylation by Rad53–Dun1, derepresses the *RNR3* promoter; (ii) Cth2 indirectly downregulates *ROX1* (but not *MOT3*) mRNA levels by an unknow mechanism specific of the iron starvation; and (iii) probably other mechanisms directly or indirectly related with Cth2 could transcriptionally derepress *RNR3*. Further studies are required to elucidate the complex regulation of *RNR3* in -Fe. We consider essential to test if the observed lower *CRT1* and *ROX1* mRNA levels in a Cth2-dependent manner would result in diminished Crt1 and Rox1 protein levels and decreased *RNR3*-promoter binding.

On the other hand, the reason why Rnr3 is physiologically relevant specifically under long-term iron-deficient conditions is not known. The other only known condition that shows a negative phenotype in the *rnr3Δ* strain is under non-fermentable carbon sources or limiting concentrations of glucose (Corcoles-Saez et al., 2019). Interestingly, under these conditions the authors showed an *RNR3* upregulation and an *RNR1* downregulation important for mitochondrial function. However, they suggested that the physiological function of Rnr3 under glycerol growth was independent of its role in dNTP production (Corcoles-Saez et al., 2019). On the contrary, iron-deficient conditions are known to increase *RNR1* expression to optimize dNTP synthesis (Sanvisens et al., 2011; Ros-Carrero et al., 2020). *RNR1* upregulation was observed to occur in a Cth2- and Aft1-dependent manner during iron starvation (Sanvisens et al., 2011; Ros-Carrero et al., 2020). To know if this is also the case for *RNR3* regulation under long-term iron deficiency would require further investigation.

General Discussion

General Discussion

Iron deficiency is a nutritional stress to which yeast cells gradually respond. The acquisition of extracellular iron and its mobilization from the vacuole due to the activation of the iron regulon are the first steps. Then, the described metabolic remodeling response occurs mainly through Cth2. Iron is involved in an extraordinary number of cell processes that need to be progressively regulated to maintain iron homeostasis and survival. In this thesis, we have described that Cth2 specifically represses the translation of ARE-containing mRNAs (Chapter 2) before Gcn2 represses the global initiation of translation (Chapter 1). The Gcn2-dependent inhibition of general translation overlaps with the described TORC1 inhibition under iron deficiency (Romero et al., 2019). This suggests that cells try to face iron deficiency by promoting the Cth2-dependent specific metabolic remodeling (6-7 hours of -Fe in BY4741 strain) before repressing more general processes (9-11 hours in -Fe in BY4741 strain). In both cases, further studies would be required to elucidate the details of the molecular mechanisms already suggested to be involved in these translational regulations. Besides, similarly to Chapter 2, where specific mRNA and protein levels were used to determine translational efficiencies together with their distribution in polysome profiles, additional experiments detecting the global newly synthesized protein levels would corroborate our results in Chapter 1.

On the other hand, we have described new Cth2 functions taking place at longer exposures to iron-deficient conditions. We have shown that Cth2 contributes to the *RNR3* upregulation (Chapter 4) and cytochrome *c* oxidase function (Chapter 3) under long-term iron deficiency. Interestingly, these two novel roles of Cth2 only take place under iron starvation as Cth2 overexpression in +Fe did not induce *RNR3* or the complex IV activity of the ETC. Therefore, new Cth2-related functions could be described under more severe iron deficiencies. Most likely, after long periods of iron starvation, iron-related processes would be seriously compromised, as it has been shown with global translational inhibition after 12 hours of iron limitation regardless Gcn2 (Chapter 1). Besides, it is possible that ROS and DNA damage would accumulate more obviously during the progression of iron deficiency. The novel roles of Cth2 in derepressing *RNR3* and in

maintaining a more efficient ETC in -Fe could be decisive under these conditions, as DNA reparation and less ROS productive mitochondria would be indispensable for cell survival. However, there are several unexplored aspects of the Cth2-dependent regulation of respiration as well as in *RNR3* derepression (discussion of Chapters 3 and 4, respectively). Accurate ROS measurements would be needed to determine a possible role of Cth2 in reducing the oxidative stress generated by the ETC under iron deficiency. If this is the case, it could reduce *ROX1* expression as it is described to be highly induced upon oxidative stress (Castells-Roca et al., 2011; Liu & Barrientos, 2012). If demonstrated, this fact could partially explain the decreased *ROX1* mRNA levels (and therefore *RNR3* derepression) observed in a Cth2-dependent manner at long-term iron deficiency. It would correlate the ROS protective role of Cth2 in the ETC with a higher *RNR3* expression. As mentioned in the discussion of Chapter 4, Rnr3 is probably needed to optimize dNTP synthesis under long-term iron-deficient situations. But interestingly, Rnr3 is also the only RNR protein physically found in mitochondria (Sickmann et al., 2003; Reinders et al., 2006). To determine if Rnr3 has another mitochondria-related function, as Corcoles-Saez et al. (2019) suggested, further studies would be required.

Conclusions

1. During the progress of iron deficiency, global translation is gradually repressed at the initiation step.

2. When iron is scarce, Gcn2 kinase represses global translation initiation in a Gcn1-dependent manner by phosphorylating serine 51 of eIF2α, which causes the induction of *GCN4* translation.

3. In response to iron deficiency, Cth2 promotes the translational repression of ARE-containing mRNAs in a process that requires the integrity of both the TZF domain and the AREs.

4. Both the amino and the carboxy-terminal domains of Cth2 contribute to mRNA translational repression, whereas only the amino-terminal domain is responsible for mRNA decay under iron starvation.

5. The carboxy-terminal domain of Cth2 is physiologically relevant under iron deficiency.

6. Mitochondrial respiration is compromised under iron deficiency regardless of Cth2. However, the constitutive activation of the iron regulon represses respiration and diminishes growth capacity in non-fermentable media through Cth2.

7. The overexpression of Cth2 under iron sufficiency decreases not only oxygen consumption, but also multiple iron-dependent enzymatic activities, including Leu1, aconitase and complex II and III of the ETC.

8. The activity of complex IV of the ETC is unaffected by the overexpression of Cth2 under iron sufficiency and decreases under iron deficiency. However, Cth2 contributes to maintain a better functionality of complex IV when iron is scarce probably by increasing the Cox1 mRNA and apo-protein levels.

9. *RNR3* is transcriptionally induced under long-term iron-deficient conditions reaching mRNA and protein levels comparable to those under genotoxic or replication stress conditions. *RNR3* is physiologically relevant under iron-deficient conditions.

10. Rad53 and Dun1 checkpoint kinases are involved in the *RNR3* upregulation under long-term iron deficiency. Cth2 contributes to the upregulation of

RNR3, independently of Dun1, in a TZF-dependent manner and only under iron starvation.

References

Aligianni, S., Lackner, D. H., Klier, S., Rustici, G., Wilhelm, B. T., Marguerat, S., Codlin, S., Brazma, A., De Bruin, R. A. M., & Bähler, J. (2009). The fission yeast homeodomain protein Yox1p binds to MBF and confines MBF-dependent cell-cycle transcription to G1-S via negative feedback. *PLoS Genetics*, *5*, e1000626.

Anda, S., Zach, R., & Grallert, B. (2017). Activation of Gcn2 in response to different stresses. *PLoS ONE*, *12*, e0182143.

Anderson, C. P., Shen, M., Eisenstein, R. S., & Leibold, E. A. (2012). Mammalian iron metabolism and its control by iron regulatory proteins. *Biochimica et Biophysica Acta*, *1823*, 1468–1483.

Ashe, M. P., Long, S. K. De, & Sachs, A. B. (2000). Glucose depletion rapidly inhibits translation initiation in yeast. *Molecular Biology of the Cell*, *11*, 833–848.

Ast, T., Meisel, J. D., Patra, S., Wang, H., Grange, R. M. H., Kim, S. H., Calvo, S. E., Orefice, L. L., Nagashima, F., Ichinose, F., Zapol, W. M., Ruvkun, G., Barondeau, D. P., & Mootha, V. (2019). Hypoxia rescues frataxin loss by restoring iron sulfur cluster biogenesis. *Cell*, *177*, 1507–1521.

Atkinson, A., Smith, P., Fox, J. L., Cui, T., Khalimonchuk, O., & Winge, D. R. (2011). The LYR protein Mzm1 functions in the insertion of the Rieske Fe/S protein in yeast mitochondria. *Molecular and Cellular Biology*, *31*, 3988–3996.

Aye, Y., Li, M., Long, M. J. C., & Weiss, R. S. (2015). Ribonucleotide reductase and cancer: biological mechanisms and targeted therapies. *Oncogene*, *34*, 2011–2021.

Baccolo, G., Stamerra, G., Pellegrino, D., Orlandi, I., & Vai, M. (2018). Mitochondrial metabolism and aging in yeast. *International Review of Cell and Molecular Biology*, *340*, 1–33.

Balasubramanian, B., Lowry, C. V, & Zitomer, R. S. (1993). The Rox1 repressor of the *Saccharomyces cerevisiae* hypoxic genes is a specific DNA-binding protein with a high-mobility-group motif. *Molecular and Cellular Biology*, *13*, 6071–6078.

Barros, M. H., Carlson, C. G., Glerum, D. M., & Tzagoloff, A. (2001). Involvement of mitochondrial ferredoxin and Cox15p in hydroxylation of heme O. *FEBS Letters*, *492*, 133–138.

Barros, M. H., Myers, A. M., Driesche, S. Van, & Tzagoloff, A. (2006). *COX24* codes for a mitochondrial protein required for processing of the *COX1* transcript. *Journal of Biological Chemistry*, *281*, 3743–3751.

Barros, M. H., & Mcstay, G. P. (2020). Modular biogenesis of mitochondrial respiratory complexes. *Mitochondrion*, *50*, 94–114.

Bayeva, M., Khechaduri, A., Puig, S., Chang, H. C., Patial, S., Blackshear, P. J., & Ardehali, H. (2012). mTOR regulates cellular iron homeostasis through tristetraprolin. *Cell Metabolism*, *16*, 645–657.

Bayeva, M., Chang, H., Wu, R., & Ardehali, H. (2013). When less is more: novel mechanisms of iron conservation. *Trends in Endocrinology and Metabolism*, *24*, 569–577.

Bell, S. E., Sanchez, M. J., Spasic-boskovic, O., Santalucia, T., Gambardella, L., Burton, G. J., Murphy, J. J., Norton, J. D., Clark, A. R., & Turner, M. (2006). The RNA binding protein Zfp36l1 is required for normal vascularisation and post-transcriptionally regulates VEGF expression. *Developmental Dynamics*, *235*, 3144–3155.

Bellí, G., Molina, M. M., García-Martínez, J., Pérez-Ortín, J. E., & Herrero, E. (2004). *Saccharomyces cerevisiae* glutaredoxin 5-deficient cells subjected to continuous oxidizing conditions are affected in the expression of specific sets of genes. *Journal of Biological Chemistry*, *279*, 12386–12395.

Blaiseau, P. L., Lesuisse, E., & Camadro, J. M. (2001). Aft2p, a novel iron-regulated transcription activator that modulates, with Aft1p, intracellular iron use and resistance to oxidative stress in yeast. *Journal of Biological Chemistry*, *276*, 34221–34226.

Bouchez, C. L., Yoboue, E. D., de la Rosa Vargas, L. E., Salin, B., Cuvellier, S., Rigoulet, M., Duvezin-Caubet, S., & Devin, A. (2020). "Labile" heme critically regulates mitochondrial biogenesis through the transcriptional co-activator Hap4p in *Saccharomyces cerevisiae*. *The Journal of Biological Chemistry*, *295*, 5095–5109.

Brewer, B. Y., Malicka, J., Blackshear, P. J., & Wilson, G. M. (2004). RNA sequence elements required for high affinity binding by the zinc finger domain of tristetraprolin. *Journal of Biological Chemistry*, *279*, 27870–27877.

Brooks, S. A., Connolly, J. E., & Rigby, W. F. C. (2004). The role of mRNA turnover in the regulation of tristetraprolin expression: evidence for an extracellular signal-regulated kinase-specific, AU-Rich Element-dependent, autoregulatory pathway. *The Journal of Immunology*, *172*, 7263–7271.

Brooks, S. A., & Blackshear, P. J. (2013). Tristetraprolin (TTP): interactions with mRNA and proteins, and current thoughts on mechanisms of action. *Biochimica et Biophysica Acta*, *1829*, 666–679.

Carballo, E., Lai, W. S., & Blackshear, P. J. (1998). Feedback inhibition of macrophage tumor necrosis factor α production by tristetraprolin. *Science*, *281*, 1001–1006.

Carroll, J. S., Munchel, S. E., & Weis, K. (2011). The DExD/H box ATpase Dhh1 functions in translational repression, mRNA decay, and processing body dynamics. *Journal of Cell Biology*, *194*, 527–537.

Castells-Roca, L., Mühlenhoff, U., Lill, R., Herrero, E., & Bellí, G. (2011). The oxidative stress response in yeast cells involves changes in the stability of Aft1 regulon mRNAs. *Molecular Microbiology*, *81*, 232–248.

Castells-Roca, L., Pijuan, J., Ferrezuelo, F., Bellí, G., & Herrero, E. (2016). Cth2 protein mediates early adaptation of yeast cells to oxidative stress conditions. *PLoS ONE*, *11*, e0148204.

Chabes, A., Georgieva, B., Domkin, V., Zhao, X., Rothstein, R., & Thelander, L. (2003). Survival of DNA damage in yeast directly depends on increased dNTP levels allowed by relaxed feedback inhibition of ribonucleotide reductase. *Cell*, *112*, 391–401.

Chaparro, C. M., & Suchdev, P. S. (2019). Anemia epidemiology, pathophysiology, and etiology in low- and middle-income countries. *Annals of the New York Academy of Sciences*, *1450*, 15–31.

Chen, C. Y., Gherzi, R., Ong, S. E., Chan, E. L., Raijmakers, R., Pruijn, G. J. M., Stoecklin, G., Moroni, C., Mann, M., & Karin, M. (2001). AU binding proteins recruit the exosome to degrade ARE-containing mRNAs. *Cell*, *107*, 451–464.

Chen, O. S., Crisp, R. J., Valachovic, M., Bard, M., Winge, D. R., & Kaplan, J. (2004). Transcription of the yeast iron regulon does not respond directly to iron but rather to iron-sulfur cluster biosynthesis. *Journal of Biological Chemistry*, *279*, 29513–29518.

Chen, X. J., Wang, X., Kaufman, B. A., & Butow, R. A. (2005). Aconitase couples metabolic regulation to mitochondrial DNA maintenance. *Science*, *307*, 714–718.

Cherkasova, V. A., & Hinnebusch, A. G. (2003). Translational control by TOR and TAP42 through dephosphorylation of eIF2α kinase GCN2. *Genes and Development*, *17*, 859–872.

Chevtzoff, C., Yoboue, E. D., Galinier, A., Casteilla, L., Daignan-Fornier, B., Rigoulet, M., & Devin, A. (2010). Reactive oxygen species-mediated regulation of mitochondrial biogenesis in the yeast *Saccharomyces cerevisiae*. *Journal of Biological Chemistry*, *285*, 1733–1742.

Ciais, D., Bohnsack, M. T., & Tollervey, D. (2008). The mRNA encoding the yeast ARE-binding protein Cth2 is generated by a novel 3' processing pathway. *Nucleic Acids Research*, *36*, 3075–3084.

Clemens, M. J. (1997). PKR - A protein kinase regulated by double-stranded RNA. *International Journal of Biochemistry and Cell Biology*, *29*, 945–949.

Coller, J., & Parker, R. (2004). Eukaryotic mRNA decapping. *Annual Review of Biochemistry*, *73*, 861–890.

Coller, J., & Parker, R. (2005). General translational repression by activators of mRNA decapping. *Cell*, *122*, 875–886.

Corcoles-Saez, I., Ferat, J. L., Costanzo, M., Boone, C. M., & Cha, R. S. (2019). Functional link between mitochondria and Rnr3, the minor catalytic subunit of yeast ribonucleotide reductase. *Microbial Cell*, *6*, 286–294.

Cotruvo, J. A., & Stubbe, J. (2011). Class I Ribonucleotide reductases: metallocofactor assembly and repair in vitro and in vivo. *Annual Review of Biochemistry*, *80*, 733–767.

Courel, M., Lallet, S., Camadro, J.-M., & Blaiseau, P.-L. (2005). Direct activation of genes involved in intracellular iron use by the yeast iron-responsive transcription factor Aft2 without its Paralog Aft1. *Molecular and Cellular Biology*, *25*, 6760–6771.

Crawford, R. A., & Pavitt, G. D. (2019). Translational regulation in response to stress in *Saccharomyces cerevisiae*. *Yeast*, *36*, 5–21.

Crisp, R. J., Adkins, E. M., Kimmel, E., & Kaplan, J. (2006). Recruitment of Tup1p and Cti6p regulates heme-deficient expression of Aft1p target genes. *The EMBO Journal*, *25*, 512–521.

Daum, G., Böhni, P. C., & Gottfried, S. (1982). Import of proteins into mitochondria. Cytochrome b_2 and cytochrome *c* peroxidase are located in the intermembrane space of yeast mitochondria. *The Journal of Biological Chemistry*, *257*, 13028–13033.

Davie, J. K., Trumbly, R. J., & Dent, S. Y. R. (2002). Histone-dependent association of Tup1-Ssn6 with repressed genes in vivo. *Molecular and Cellular Biology*, *22*, 693–703.

Davie, J. K., Edmondson, D. G., Coco, C. B., & Dent, S. Y. R. (2003). Tup1-Ssn6 interacts with multiple class I histone deacetylases in vivo. *The Journal of Biological Chemistry*, *278*, 50158–50162.

De Silva, D., Poliquin, S., Zeng, R., Zamudio-Ochoa, A., Marrero, N., Perez-Martinez, X., Fontanesi, F., & Barrientos, A. (2017). The DEAD-box helicase Mss116 plays distinct roles in mitochondrial ribogenesis and mRNA-specific translation. *Nucleic Acids Research*, *45*, 6628–6643.

Decker, C. J., & Parker, R. (2012). P-bodies and stress granules: possible roles in the control of translation and mRNA degradation. *Cold Spring Harbor Perspectives in Biology*, *4*, a012286.

Deloche, O., De La Cruz, J., Kressler, D., Doère, M., & Linder, P. (2004). A membrane transport defect leads to a rapid attenuation of translation initiation in *Saccharomyces cerevisiae*. *Molecular Cell*, *13*, 357–366.

Derbikova, K. S., Levitsky, S. A., Chicherin, I. V, Vinogradova, E. N., & Kamenski, P. A. (2018). Activation of yeast mitochondrial translation: who is in charge? *Biochemistry (Moscow)*, *83*, 87–97.

DeRisi, J. L., Iyer, V. R., & Brown, P. O. (1997). Exploring the metabolic and genetic control of gene expression on a genomic scale. *Science*, *278*, 680–686.

Dever, T. E., Feng, L., Wek, R. C., Cigan, A. M., Donahue, T. F., & Hinnebusch, A. G. (1992). Phosphorylation of initiation factor 2α by protein kinase GCN2 mediates gene-specific translational control of *GCN4* in yeast. *Cell*, *68*, 585–596.

Dever, T. E., Kinzy, T. G., & Pavitt, G. D. (2016). Mechanism and regulation of protein synthesis in *Saccharomyces cerevisiae*. *Genetics*, *203*, 65–107.

Di Como, C. J., & Arndt, K. T. (1996). Nutrients, via the Tor proteins, stimulate the association of Tap42 with type 2A phosphatases. *Genes and Development*, *10*, 1904–1916.

Diaz, F., Enríquez, A., & Moraes, C. T. (2012). Cells lacking Rieske iron-sulfur protein have a reactive oxygen species-associated decrease in respiratory Complexes I and IV. *Molecular and Cellular Biology*, *32*, 415–429.

Dixon, D. A., Balch, G. C., Kedersha, N., Anderson, P., Zimmerman, G. A., Beauchamp, R. D., & Prescott, S. M. (2003). Regulation of cyclooxygenase-2 expression by the translational silencer TIA-1. *Journal of Experimental Medicine*, *198*, 475–481.

Dodd, M. S., Papineau, D., Grenne, T., Slack, J. F., Rittner, M., Pirajno, F., O'Neil, J., & Little, C. T. S. (2017). Evidence for early life in Earth's oldest hydrothermal vent precipitates. *Nature*, *543*, 60–64.

Domkin, V., Thelander, L., & Chabes, A. (2002). Yeast DNA damage-inducible Rnr3 has a very low catalytic activity strongly stimulated after the formation of a cross-talking Rnr1/Rnr3 complex. *Journal of Biological Chemistry*, *277*, 18574–18578.

Dubacq, C., Chevalier, A., Courbeyrette, R., Petat, C., Gidrol, X., & Mann, C. (2006). Role of the iron mobilization and oxidative stress regulons in the genomic response of yeast to hydroxyurea. *Molecular Genetics and Genomics*, *275*, 114–124.

Elledge, S. J., & Davis, R. W. (1990). Two genes differentially regulated in the cell cycle and by DNA-damaging agents encode alternative regulatory subunits of ribonucleotide reductase. *Genes and Development*, *4*, 740–751.

Endo-Ichikawa, Y., Kohno, H., Tokunaga, R., & Taketani, S. (1995). Induction in the gene *RNR3* in *Saccharomyces cerevisiae* upon exposure to different agents related to carcinogenesis. *Biochemical Pharmacology*, *50*, 1695–1699.

Endo-Ichikawa, Y., Kohno, H., Furukawa, T., Ueda, T., Ogawa, Y., Tokunaga, R., & Taketani, S. (1996). Requirement of multiple DNA-Protein interactions for inducible expression of *RNR3* gene in *Saccharomyces cerevisiae* in response to DNA damage. *Biochemical and Biophysical Research Communications*, *222*, 280–286.

Faye, G., & Simon, M. (1983). Analysis of a yeast nuclear gene involved in the maturation of mitochondrial RNA of the cytochrome oxidase subunit I. *Cell*, *32*, 77–87.

Fenger-Grøn, M., Fillman, C., Norrild, B., & Lykke-Andersen, J. (2005). Multiple processing body factors and the ARE binding protein TTP activate mRNA decapping. *Molecular Cell*, *20*, 905–915.

Forsburg, S. L., & Guarente, L. (1989). Identification and characterization of HAP4: a third component of the CCAAT-bound HAP2/HAP3 heteromer. *Genes & Development*, *3*, 1166–1178.

Foury, F., & Talibi, D. (2001). Mitochondrial control of iron Homeostasis. *The Journal of Biological Chemistry*, *276*, 7762–7768.

Galban, S., Martindale, J. L., Mazan-Mamczarz, K., Lopez de Silanes, I., Fan, J., Wang, W., Decker, J., & Gorospe, M. (2003). Influence of the RNA-binding protein HuR in pVHL-regulated p53 expression in renal carcinoma cells. *Molecular and Cellular Biology*, *23*, 7083–7095.

Garcia-Barrio, M., Dong, J., Ufano, S., & Hinnebusch, A. G. (2000). Association of *GCN1-GCN20* regulatory complex with the N-terminus of eIF2α kinase *GCN2* is required for *GCN2* activation. *The EMBO Journal*, *19*, 1887–1899.

García-Villegas, R., Camacho-Villasana, Y., Shing-Vázquez, M. Á., Cabrera-Orefice, A., Uribe-Carvajal, S., Fox, T. D., & Pérez-Martínez, X. (2017). The Cox1 C-terminal domain is a central regulator of cytochrome *c* oxidase biogenesis in yeast mitochondria. *Journal of Biological Chemistry*, *292*, 10912–10925.

Gari, K., María, A., Ortiz, L., Borel, V., Flynn, H., Skehel, J. M., & Boulton, S. J. (2012). MMS19 links cytoplasmic Iron-Sulfur assembly to DNA Metabolism. *Science*, *337*, 243–245.

Garre, E., Romero-Santacreu, L., De Clercq, N., Blasco-Angulo, N., Sunnerhagen, P., & Alepuz, P. (2012). Yeast mRNA cap-binding protein Cbc1/Sto1 is necessary for the rapid reprogramming of translation after hyperosmotic shock. *Molecular Biology of the Cell*, *23*, 137–150.

Garre, E., Pelechano, V., Sánchez del Pino, M., Alepuz, P., & Sunnerhagen, P. (2018). The Lsm1-7/Pat1 complex binds to stress-activated mRNAs and modulates the response to hyperosmotic shock. *PLoS Genetics*, *14*, e1007563.

Gebauer, F., & Hentze, M. W. (2004). Molecular mechanisms of translational control. *Nature Reviews Molecular Cell Biology*, *5*, 827–835.

Ghaemmaghami, S., Huh, W., Bower, K., Howson, R. W., Belle, A., Dephoure, N., O'Shea, E. K., & Weissman, J. (2003). Global analysis of protein expression in yeast. *Nature*, *425*, 737–741.

Ghosh, S., & Pugh, B. F. (2011). Sequential recruitment of SAGA and TFIID in a genomic response to DNA damage in *Saccharomyces cerevisiae*. *Molecular and Cellular Biology*, *31*, 190–202.

Gietz, R. D., & Woods, R. A. (2002). Transformation of yeast by lithium acetate/single-stranded carrier DNA/polyethylene glycol method. *Methods in Enzymology*, *350*, 87–96.

Glerum, D. M., Shtanko, A., & Tzagoloff, A. (1996). Characterization of *COX17*, a yeast gene involved in copper metabolism and assembly of cytochrome oxidase. *The Journal of Biological Chemistry*, *271*, 14504–14509.

Goossens, A., Dever, T. E., Pascual-Ahuir, A., & Serrano, R. (2001). The protein kinase Gcn2p mediates sodium toxicity in yeast. *Journal of Biological Chemistry*, *276*, 30753–30760.

Güldener, U., Heck, S., Fiedler, T., Beinhauer, J., & Hegemann, J. H. (1996). A new efficient gene disruption cassette for repeated use in budding yeast. *Nucleic Acids Research*, *24*, 2519–2524.

Güeldener, U., Heinisch, J., Koehler, G., Voss, D., & Hegemann, J. H. (2002). A second set of *loxP* marker cassettes for Cre-mediated multiple gene knockouts in budding yeast. *Nucleic Acids Research*, *30*, e23.

Gupta, M., & Outten, C. E. (2020). Iron-sulfur cluster signaling: The common thread in fungal iron regulation. *Current Opinion in Chemical Biology*, *55*, 189–201.

Hahn, C. K., & Lowrey, C. H. (2013). Eukaryotic initiation factor 2α phosphorylation mediates fetal hemoglobin induction through a post-transcriptional mechanism. *Blood*, *122*, 477–485.

Hahn, C. K., & Lowrey, C. H. (2014). Induction of fetal hemoglobin through enhanced translation efficiency of γ-globin mRNA. *Blood*, *124*, 2730–2734.

Han, A. P., Yu, C., Lu, L., Fujiwara, Y., Browne, C., Chin, G., Fleming, M., Leboulch, P., Orkin, S. H., & Chen, J. J. (2001). Heme-regulated eIF2α kinase (HRI) is required for translational regulation and survival of erythroid precursors in iron deficiency. *EMBO Journal*, *20*, 6909–6918.

Harding, H. P., Zhang, Y., & Ron, D. (1999). Protein translation and folding are coupled by an endoplasmic- reticulum-resident kinase. *Nature*, *397*, 271–274.

Haurie, V., Boucherie, H., & Sagliocco, F. (2003). The Snf1 protein kinase controls the induction of genes of the iron uptake pathway at the diauxic shift in *Saccharomyces cerevisiae*. *Journal of Biological Chemistry*, *278*, 45391–45396.

Hausmann, A., Samans, B., Lill, R., & Mühlenhoff, U. (2008). Cellular and mitochondrial remodeling upon defects in iron-sulfur protein biogenesis. *Journal of Biological Chemistry*, *283*, 8318–8330.

Hendry, J. A., Tan, G., Ou, J., Boone, C., & Brown, G. W. (2015). Leveraging DNA damage response signaling to identify yeast genes controlling genome stability. *G3 Genes|Genomes|Genetics*, *5*, 997–1006.

Herrero, E., Ros, J., Bellí, G., & Cabiscol, E. (2008). Redox control and oxidative stress in yeast cells. *Biochimica et Biophysica Acta*, *1780*, 1217–1235.

Hershey, J. W. B., Sonenberg, N., & Mathews, M. B. (2012). Principles of translational control: an overview. *Cold Spring Harbor Perspectives in Biology*, *4*, a011528.

Hinnebusch, A. G., & Fink, G. R. (1983). Positive regulation in the general amino acid control of *Saccharomyces cerevisiae*. *Proceedings of the National Academy of Sciences*, *80*, 5374–5378.

Hinnebusch, A. G. (2005). Translational regulation of Gcn4 and the general amino acid control of yeast. *Annual Review of Microbiology*, *59*, 407–450.

Hinnebusch, A. G., Ivanov, I. P., & Sonenberg, N. (2016). Translational control by 5′-untranslated regions of eukaryotic mRNAs. *Science*, *352*, 1413–1416.

Hiser, L., Di Valentin, M., Hamer, A. G., & Hosler, J. P. (2000). Cox11p is required for stable formation of the Cu_B and magnesium centers of cytochrome *c* oxidase. *Journal of Biological Chemistry*, *275*, 619–623.

Ho, Y., Mason, S., Kobayashi, R., Hoekstra, M., & Andrews, B. (1997). Role of the casein kinase I isoform, Hrr25, and the cell cycle-regulatory transcription factor, SBF, in the transcriptional response to DNA damage in *Saccharomyces cerevisiae*. *Proceedings of the National Academy of Sciences*, *94*, 581–586.

Horak, C. E., Luscombe, N. M., Qian, J., Bertone, P., Piccirrillo, S., Gerstein, M., & Snyder, M. (2002). Complex transcriptional circuitry at the G1/S transition in *Saccharomyces cerevisiae*. *Genes & Development*, *16*, 3017–3033.

Hortschansky, P., Haas, H., Huber, E. M., Groll, M., & Brakhage, A. A. (2017). The CCAAT-binding complex (CBC) in *Aspergillus* species. *Biochimica et Biophysica Acta - Gene Regulatory Mechanisms*, *1860*, 560–570.

Huang, M., Zhou, Z., & Elledge, S. J. (1998). The DNA replication and damage checkpoint pathways induce transcription by inhibition of the Crt1 repressor. *Cell*, *94*, 595–605.

Huang, H., Rowe, C. E., Mohr, S., Jiang, Y., Lambowitz, A. M., & Perlman, P. S. (2004). The splicing of yeast mitochondrial group I and group II introns requires a DEAD-box protein with RNA chaperone function. *Proceedings of the National Academy of Sciences*, *102*, 163–168.

Huch, S., & Nissan, T. (2014). Interrelations between translation and general mRNA degradation. *WIREs RNA*, *5*, 747–763.

Hudson, B. P., Martinez-Yamout, M. A., Dyson, H. J., & Wright, P. E. (2004). Recognition of the mRNA AU-rich element by the zinc finger domain of TIS11d. *Nature Structural and Molecular Biology*, *11*, 257–264.

Hueso, G., Aparicio-Sanchis, R., Montesinos, C., Lorenz, S., Murguía, J. R., & Serrano, R. (2012). A novel role for protein kinase Gcn2 in yeast tolerance to intracellular acid stress. *Biochemical Journal*, *441*, 255–264.

Huynh, N., Ou, Q., Cox, P., Lill, R., & King-Jones, K. (2019). Glycogen branching enzyme controls cellular iron homeostasis via Iron Regulatory Protein 1 and mitoNEET. *Nature Communications*, *10*, 5463.

Ihrig, J., Hausmann, A., Hain, A., Richter, N., Hamza, I., Lill, R., & Mühlenhoff, U. (2010). Iron regulation through the back door: Iron-dependent metabolite levels contribute to transcriptional adaptation to iron deprivation in *Saccharomyces cerevisiae*. *Eukaryotic Cell*, *9*, 460–471.

Jackson, R. J., Hellen, C. U. T., & Pestova, T. V. (2010). The mechanism of eukaryotic translation initiation and principles of its regulation. *Nature Reviews Molecular Cell Biology*, *10*, 113–127.

Jensen, L. T., & Culotta, V. C. (2002). Regulation of *Saccharomyces cerevisiae FET4* by oxygen and iron. *Journal of Molecular Biology*, *318*, 251–260.

Jiang, Y., & Broach, J. R. (1999). Tor proteins and protein phosphatase 2A reciprocally regulate Tap42 in controlling cell growth in yeast. *EMBO Journal*, *18*, 2782–2792.

Jordá, T., Romero, A. M., Perea-García, A., Rozès, N., & Puig, S. (2020). The lipid composition of yeast cells modulates the response to iron deficiency. *Biochimica et Biophysica Acta - Molecular and Cell Biology of Lipids*, *1865*, 158707.

Kastaniotis, A. J., Mennella, T. A., Konrad, C., Torres, A. N. A. M. R., & Zitomer, R. S. (2000). Roles of transcription factor Mot3 and chromatin in repression of the hypoxic gene *ANB1* in yeast. *Molecular and Cellular Biology*, *20*, 7088–7098.

Kathiresan, M., Martins, D., & English, A. M. (2014). Respiration triggers heme transfer from cytochrome *c* peroxidase to catalase in yeast mitochondria. *Proceedings of the National Academy of Sciences*, *111*, 17468–17473.

Kayikci, O., & Nielsen, J. (2015). Glucose repression in *Saccharomyces cerevisiae*. *FEMS Yeast Research*, *15*, fov068.

Khalimonchuk, O., Ostermann, K., & Rödel, G. (2005). Evidence for the association of yeast mitochondrial ribosomes with Cox11p, a protein required for the Cu_B site formation of cytochrome *c* oxidase. *Current Genetics*, *47*, 223–233.

Kispal, G., Csere, P., Prohl, C., & Lill, R. (1999). The mitochondrial proteins Atm1p and Nfs1p are essential for biogenesis of cytosolic Fe/S proteins. *EMBO Journal*, *18*, 3981–3989.

Kispal, G., Sipos, K., Lange, H., Fekete, Z., Bedekovics, T., Janáky, T., Bassler, J., Aguilar Netz, D. J., Balk, J., Rotte, C., & Lill, R. (2005). Biogenesis of cytosolic ribosomes requires the essential iron-sulphur protein Rli1p and mitochondria. *EMBO Journal*, *24*, 589–598.

Klinkenberg, L. G., Mennella, T. A., Luetkenhaus, K., & Zitomer, R. S. (2005). Combinatorial repression of the hypoxic genes of *Saccharomyces cerevisiae* by DNA binding proteins Rox1 and Mot3. *Eukaryotic Cell*, *4*, 649–660.

Klinkenberg, L. G., Webb, T., & Zitomer, R. S. (2006). Synergy among differentially regulated repressors of the ribonucleotide diphosphate reductase genes of *Saccharomyces cerevisiae*. *Eukaryotic Cell*, *5*, 1007–1017.

Knighton, L. E., Delgado, L. E., & Truman, A. W. (2019). Novel insights into molecular chaperone regulation of ribonucleotide reductase. *Current Genetics*, *65*, 477–482.

Kolberg, M., Strand, K. R., Graff, P., & Andersson, K. K. (2004). Structure, function, and mechanism of ribonucleotide reductases. *Biochimica et Biophysica Acta*, *1699*, 1–34.

Kramer, G., Cimadevilla, J. M., & Hardesty, B. (1976). Specificity of the protein kinase activity associated with the hemin controlled repressor of rabbit reticulocyte. *Proceedings of the National Academy of Sciences*, *73*, 3078–3082.

Kubota, H., Obata, T., Ota, K., Sasaki, T., & Ito, T. (2003). Rapamycin-induced translational derepression of *GCN4* mRNA involves a novel mechanism for activation of the eIF2α kinase *GCN2*. *Journal of Biological Chemistry*, *278*, 20457–20460.

Kumánovics, A., Chen, O. S., Li, L., Bagley, D., Adkins, E. M., Lin, H., Dingra, N. N., Outten, C. E., Keller, G., Winge, D., Ward, D. M., & Kaplan, J. (2008). Identification of *FRA1* and *FRA2* as genes involved in regulating the yeast iron regulon in response to decreased mitochondrial iron-sulfur cluster synthesis. *The Journal of Biological Chemistry*, *283*, 10276–10286.

Kumar, C., Igbaria, A., D'Autreaux, B., Planson, A. G., Junot, C., Godat, E., Bachhawat, A. K., Delaunay-Moisan, A., & Toledano, M. B. (2011). Glutathione revisited: a

vital function in iron metabolism and ancillary role in thiol-redox control. *EMBO Journal*, *30*, 2044–2056.

Lagunas, R. (1986). Misconceptions about the energy metabolism of *Saccharomyces cerevisiae*. *Yeast*, *2*, 221–228.

Lazowska, J., Jacq, C., & Sionimski, P. P. (1980). Sequence of introns and flanking exons in wild-type and *box3* mutants of cytochrome *b* reveals an interlaced splicing protein coded by an intron. *Cell*, *22*, 333–348.

Lee, H. N., Mostovoy, Y., Hsu, T. Y., Chang, A. H., & Brem, R. B. (2013). Divergence of iron metabolism in wild Malaysian yeast. *G3: Genes, Genomes, Genetics*, *3*, 2187–2194.

Levin, D. H., Singh Ranu, R., Ernst, V., & London, I. M. (1976). Regulation of protein synthesis in reticulocyte lysates: phosphorylation of methionyl $tRNA_f$ binding factor by protein kinase activity of translational inhibitor isolated from heme deficient lysates. *Proceedings of the National Academy of Sciences*, *73*, 3112–3116.

Li, B., & Reese, J. C. (2000). Derepression of DNA damage-regulated genes requires yeast $TAF_{II}s$. *EMBO Journal*, *19*, 4091–4100.

Li, B., & Reese, J. C. (2001). Ssn6-Tup1 regulates *RNR3* by positioning nucleosomes and affecting the chromatin structure at the upstream repression sequence. *Journal of Biological Chemistry*, *276*, 33788–33797.

Li, L., Bagley, D., Ward, D. M., & Kaplan, J. (2008). Yap5 is an iron-responsive transcriptional activator that regulates vacuolar iron storage in yeast. *Molecular and Cellular Biology*, *28*, 1326–1337.

Li, A., Jia, X., Ward, D. M., & Kaplan, J. (2011). Yap5 protein-regulated transcription of the *TYW1* gene protects yeast from high iron toxicity. *Journal of Biological Chemistry*, *286*, 38488–38497.

Li, H., Zhang, C., An, X., Stubbe, J., Lill, R., & Huang, M. (2017). The diferric-tyrosyl radical cluster of ribonucleotide reductase and cytosolic iron-sulfur clusters have distinct and similar biogenesis requirements. *The Journal of Biological Chemistry*, *292*, 11445–11451.

Li, H., & Outten, C. E. (2019). The conserved CDC motif in the yeast iron regulator Aft2 mediates iron-sulfur cluster exchange and protein-protein interactions with Grx3 and Bol2. *JBIC Journal of Biological Inorganic Chemistry*, *24*, 809–815.

Lill, R., Srinivasan, V., & Mühlenhoff, U. (2014). The role of mitochondria in cytosolic-nuclear iron-sulfur protein biogenesis and in cellular iron regulation. *Current Opinion in Microbiology*, *22*, 111–119.

Lill, R., Dutkiewicz, R., Freibert, S. A., Heidenreich, T., Mascarenhas, J., Netz, D. J., Paul, V. D., Pierik, A. J., Richter, N., Stümpfig, M., Srinivasan, V., Stehling, O., & Mühlenhoff, U. (2015). The role of mitochondria and the CIA machinery in the maturation of cytosolic and nuclear iron-sulfur proteins. *European Journal of Cell Biology*, *94*, 280–291.

Lindahl, P. A. (2019). A comprehensive mechanistic model of iron metabolism in: *Saccharomyces cerevisiae*. *Metallomics*, *11*, 1779–1799.

Liu, J., & Barrientos, A. (2012). Transcriptional regulation of yeast oxidative phosphorylation hypoxic genes by oxidative stress. *Antioxidants & Redox Signaling*, *19*, 1916–1927.

Lykke-Andersen, J., & Wagner, E. (2005). Recruitment and activation of mRNA decay enzymes by two ARE-mediated decay activation domains in the proteins TTP and BRF-1. *Genes and Development*, *19*, 351–361.

Maicher, A., Gazy, I., Sharma, S., Marjavaara, L., Grinberg, G., Shemesh, K., Chabes, A., & Kupiec, M. (2017). Rnr1, but not Rnr3, facilitates the sustained telomerase-dependent elongation of telomeres. *PLoS Genetics*, *13*, e1007082.

Maicher, A., & Kupiec, M. (2018). Rnr1's role in telomere elongation cannot be replaced by Rnr3: a role beyond dNTPs? *Current Genetics*, *64*, 547–550.

Mannargudi, M. B., & Deb, S. (2017). Clinical pharmacology and clinical trials of ribonucleotide reductase inhibitors: is it a viable cancer therapy? *Journal of Cancer Research and Clinical Oncology*, *143*, 1499–1529.

Mao, Y., & Chen, C. (2019). The Hap complex in yeasts: structure, assembly mode, and gene regulation. *Frontiers in Microbiology*, *10*, 1645.

Martínez-Garay, C. A., de Llanos, R., Romero, A. M., Martínez-Pastor, M. T., & Puig, S. (2016). Responses of *Saccharomyces cerevisiae* strains of different origins to elevated iron concentrations. *Applied and Environmental Microbiology*, *82*, 1906–1916.

Martínez-Pastor, M. T., & Estruch, F. (1996). Sudden depletion of carbon source blocks translation, but not transcription, in the yeast *Saccharomyces cerevisiae*. *FEBS Letters*, *390*, 319–322.

Martínez-Pastor, M., Vergara, S. V, Puig, S., & Thiele, D. J. (2013a). Negative feedback regulation of the yeast *CTH1* and *CTH2* mRNA binding proteins is required for adaptation to iron deficiency and iron supplementation. *Molecular and Cellular Biology*, *33*, 2178–2187.

Martínez-Pastor, M. T., de Llanos, R., Romero, A. M., & Puig, S. (2013b). Post-transcriptional regulation of iron homeostasis in *Saccharomyces cerevisiae*. *International Journal of Molecular Sciences*, *14*, 15785–15809.

Martínez-Pastor, M. T., Perea-García, A., & Puig, S. (2017). Mechanisms of iron sensing and regulation in the yeast *Saccharomyces cerevisiae*. *World Journal of Microbiology and Biotechnology*, *33*, 75.

Martins, T. S., Pereira, C., Canadell, D., Vilaça, R., Teixeira, V., Moradas-Ferreira, P., de Nadal, E., Posas, F., & Costa, V. (2018). The Hog1p kinase regulates Aft1p transcription factor to control iron accumulation. *Biochimica et Biophysica Acta - Molecular and Cell Biology of Lipids*, *1863*, 61–70.

Marton, M. J., Aldana, C. R. V. D. E., Qiu, H., Chakraburtty, K., & Hinnebusch, A. G. (1997). Evidence that GCN1 and GCN20, translational regulators of *GCN4*, function on elongating ribosomes in activation of eIF2α kinase GCN2. *Molecular and Cellular Biology*, *17*, 4474–4489.

Matsuo, R., Mizobuchi, S., Nakashima, M., & Miki, K. (2017). Central roles of iron in the regulation of oxidative stress in the yeast *Saccharomyces cerevisiae*. *Current Genetics*, *63*, 895–907.

Mazan-Mamczarz, K., Galbán, S., De Silanes, I. L., Martindale, J. L., Atasoy, U., Keene, J. D., & Gorospe, M. (2003). RNA-binding protein HuR enhances p53 translation in response to ultraviolet light irradiation. *Proceedings of the National Academy of Sciences*, *100*, 8354–8359.

Means, R. T. (2020). Iron deficiency and iron deficiency anemia: implications and impact in pregnancy, fetal development, and early childhood parameters. *Nutrients*, *12*, 447.

Melamed, D., Pnueli, L., & Arava, Y. (2008). Yeast translational response to high salinity: global analysis reveals regulation at multiple levels. *RNA*, *14*, 1337–1351.

Mészáros, B., Erdös, G., & Dosztányi, Z. (2018). IUPred2A: context-dependent prediction of protein disorder as a function of redox state and protein binding. *Nucleic Acids Research*, *46*, W329–W337.

Mick, D. U., Wagner, K., Laan, M. Van Der, Frazier, A. E., Perschil, I., Pawlas, M., Meyer, H. E., Warscheid, B., & Rehling, P. (2007). Shy1 couples Cox1 translational regulation to cytochrome *c* oxidase assembly. *The EMBO Journal*, *26*, 4347–4358.

Mick, D. U., Vukotic, M., Piechura, H., Meyer, H. E., Warscheid, B., Deckers, M., & Rehling, P. (2010). Coa3 and Cox14 are essential for negative feedback regulation of *COX1* translation in mitochondria. *The Journal of Cell Biology*, *191*, 141–154.

Minard, L. V., Williams, J. S., Walker, A. C., & Schultz, M. C. (2011). Transcriptional regulation by Asf1: new mechanistic insights from studies of the DNA damage response to replication stress. *Journal of Biological Chemistry*, *286*, 7082–7092.

Muckenthaler, M. U., Rivella, S., Hentze, M. W., & Galy, B. (2017). A red carpet for iron metabolism. *Cell*, *168*, 344–361.

Mugler, C. F., Hondele, M., Heinrich, S., Sachdev, R., Vallotton, P., Koek, A. Y., Chan, L. Y., & Weis, K. (2016). ATPase activity of the DEAD-box protein Dhh1 controls processing body formation. *ELife*, *5*, e18746.

Mühlenhoff, U., Molik, S., Godoy, J. R., Uzarska, M. A., Richter, N., Seubert, A., Zhang, Y., Stubbe, J., Pierrel, F., Herrero, E., Lillig, C. H., & Lill, R. (2010). Cytosolic monothiol glutaredoxins function in intracellular iron sensing and trafficking via their bound iron-sulfur cluster. *Cell Metabolism*, *12*, 373–385.

Mühlenhoff, U., Hoffmann, B., Richter, N., Rietzschel, N., Spantgar, F., Stehling, O., Uzarska, M. A., & Lill, R. (2015). Compartmentalization of iron between mitochondria and the cytosol and its regulation. *European Journal of Cell Biology*, *94*, 292–308.

Murray, D. B., Haynes, K., & Tomita, M. (2011). Redox regulation in respiring *Saccharomyces cerevisiae*. *BBA - General Subjects*, *1810*, 945–958.

Naithani, S., Saracco, S. A., Butler, C. A., & Fox, T. D. (2003). Interactions among *COX1*, *COX2*, and *COX3* mRNA-specific translational activator proteins on the inner surface of the mitochondrial inner membrane of *Saccharomyces cerevisiae*. *Molecular Biology of the Cell*, *14*, 324–333.

Narasimhan, J., Staschke, K. A., & Wek, R. C. (2004). Dimerization is required for activation of eIF2 kinase Gcn2 in response to diverse environmental stress conditions. *Journal of Biological Chemistry*, *279*, 22820–22832.

Ngoc, L. V., Wauquier, C., Soin, R., Bousbata, S., Twyffels, L., Kruys, V., & Gueydan, C. (2014). Rapid proteasomal degradation of posttranscriptional regulators of the TIS11/tristetraprolin family is induced by an intrinsically unstructured region independently of ubiquitination. *Molecular and Cellular Biology*, *34*, 4315–4328.

Nobrega, M. P., Nobrega, F. G., & Tzagoloff, A. (1990). *COX10* codes for a protein homologous to the ORF1 product of *Paracoccus denitrificans* and is required for the synthesis of yeast cytochrome oxidase. *The Journal of Biological Chemistry*, *265*, 14220–14226.

Nordlund, P., & Reichard, P. (2006). Ribonucleotide reductases. *Annual Review of Biochemistry*, *75*, 681–706.

Ochi, Y., Sugawara, H., Iwami, M., Tanaka, M., & Eki, T. (2011). Sensitive detection of chemical-induced genotoxicity by the *Cypridina* secretory luciferase reporter assay, using DNA repair-deficient strains of *Saccharomyces cerevisiae*. *Yeast*, *28*, 265–278.

Ojeda, L., Keller, G., Muhlenhoff, U., Rutherford, J. C., Lill, R., & Winge, D. R. (2006). Role of glutaredoxin-3 and glutaredoxin-4 in the iron regulation of the Aft1 transcriptional activator in *Saccharomyces cerevisiae*. *The Journal of Biological Chemistry*, *281*, 17661–17669.

Pakos-Zebrucka, K., Koryga, I., Mnich, K., Ljujic, M., Samali, A., & Gorman, A. M. (2016). The integrated stress response. *EMBO Reports*, *17*, 1374–1395.

Pavitt, G. D. (2018). Regulation of translation initiation factor eIF2B at the hub of the integrated stress response. *Wiley Interdisciplinary Reviews: RNA*, *9*, c1491.

Pedro-Segura, E., Vergara, S. V., Rodríguez-Navarro, S., Parker, R., Thiele, D. J., & Puig, S. (2008). The Cth2 ARE-binding protein recruits the Dhh1 helicase to promote the decay of succinate dehydrogenase *SDH4* mRNA in response to iron deficiency. *Journal of Biological Chemistry*, *283*, 28527–28535.

Perez-Martinez, X., Broadley, S. A., & Fox, T. D. (2003). Mss51p promotes mitochondrial Cox1p synthesis and interacts with newly synthesized Cox1p. *EMBO Journal*, *22*, 5951–5961.

Perez-Martinez, X., Butler, C. A., Shingu-Vazquez, M., & Fox, T. D. (2009). Dual functions of Mss51 couple synthesis of Cox1 to assembly of cytochrome *c* oxidase in *Saccharomyces cerevisiae* mitochondria. *Molecular Biology of the Cell*, *20*, 4524–4530.

Philpott, C. C., Leidgens, S., & Frey, A. G. (2012). Metabolic remodeling in iron-deficient fungi. *Biochimica et Biophysica Acta - Molecular Cell Research*, *1823*, 1509–1520.

Piecyk, M., Wax, S., Beck, A. R. P., Kedersha, N., Gupta, M., Maritim, B., Chen, S., Gueydan, C., Kruys, V., Streuli, M., & Anderson, P. (2000). TIA-1 is a translational silencer that selectively regulates the expression of TNF-α. *The EMBO Journal*, *19*, 4154–4163.

Pijuan, J., María, C., Herrero, E., & Bellí, G. (2015). Impaired mitochondrial Fe-S cluster biogenesis activates the DNA damage response through different signaling mediators. *Journal of Cell Science*, *128*, 4653–4665.

Poor, C. B., Wegner, S. V., Li, H., Dlouhy, A. C., Schuermann, J. P., Sanishvili, R., Hinshaw, J. R., Riggs-Gelasco, P. J., Outten, C. E., & He, C. (2014). Molecular mechanism and structure of the *Saccharomyces cerevisiae* iron regulator Aft2. *Proceedings of the National Academy of Sciences*, *111*, 4043–4048.

Protchenko, O., & Philpott, C. C. (2003). Regulation of intracellular heme levels by *HMX1*, a homologue of heme oxygenase, in *Saccharomyces cerevisiae*. *The Journal of Biological Chemistry*, *278*, 36582–36587.

Prouteau, M., Daugeron, M. C., & Séraphin, B. (2008). Regulation of ARE transcript 3′ end processing by the yeast Cth2 mRNA decay factor. *EMBO Journal*, *27*, 2966–2976.

Puig, S., Lau, M., & Thiele, D. J. (2004). Cti6 is and Rpd3-Sin3 histone deacetylase-associated protein required for growth under iron-limiting conditions in *Saccharomyces cerevisiae*. *Journal of Biological Chemistry*, *279*, 30298–30306.

Puig, S., Askeland, E., & Thiele, D. J. (2005). Coordinated remodeling of cellular metabolism during iron deficiency through targeted mRNA degradation. *Cell*, *120*, 99–110.

Puig, S., Andrés-Colás, N., García-Molina, A., & Peñarrubia, L. (2007). Copper and iron homeostasis in *Arabidopsis*: responses to metal deficiencies, interactions and biotechnological applications. *Plant, Cell and Environment*, *30*, 271–290.

Puig, S., Vergara, S. V., & Thiele, D. J. (2008). Cooperation of two mRNA-binding proteins drives metabolic adaptation to iron deficiency. *Cell Metabolism*, *7*, 555–564.

Puig, S., Ramos-Alonso, L., Romero, A. M., & Martínez-Pastor, M. T. (2017). The elemental role of iron in DNA synthesis and repair. *Metallomics*, *9*, 1483–1500.

Pujol-Carrión, N., Belli, G., Herrero, E., Nogues, A., & de la Torre-Ruiz, M. A. (2006). Glutaredoxins Grx3 and Grx4 regulate nuclear localization of Aft1 and the oxidative stress response in *Saccharomyces cerevisiae*. *Journal of Cell Science*, *119*, 4554–4464.

Pullmann, R., Kim, H. H., Abdelmohsen, K., Lal, A., Martindale, J. L., Yang, X., & Gorospe, M. (2007). Analysis of turnover and translation regulatory RNA-binding protein expression through binding to cognate mRNAs. *Molecular and Cellular Biology*, *27*, 6265–6278.

Qi, M.-Y., Wang, Z.-Z., Zhang, Z., Shao, Q., Zeng, A., Li, X.-Q., Li, W.-Q., Wang, C., Tian, F.-J., Li, Q., Zou, J., Qin, Y.-W., Brewer, G., Huang, S., & Jing, Q. (2012). AU-Rich-Element-dependent translation repression requires the cooperation of tristetraprolin and RCK/P54. *Molecular and Cellular Biology*, *32*, 913–928.

Radhakrishnan, A., Chen, Y. H., Martin, S., Alhusaini, N., Green, R., & Coller, J. (2016). The DEAD-Box protein Dhh1p couples mRNA decay and translation by monitoring codon optimality. *Cell*, *167*, 122–132.

Ramos-Alonso, L., Romero, A. M., Soler, M. À., Perea-García, A., Alepuz, P., Puig, S., & Martínez-Pastor, M. T. (2018a). Yeast Cth2 protein represses the translation of ARE-containing mRNAs in response to iron deficiency. *PLoS Genetics*, *14*, e1007476.

Ramos-Alonso, L., Wittmaack, N., Mulet, I., Martínez-Garay, C. A., Fita-Torró, J., Lozano, M. J., Romero, A. M., García-Ferris, C., Martínez-Pastor, M. T., & Puig, S.

(2018b). Molecular strategies to increase yeast iron accumulation and resistance. *Metallomics*, *10*, 1245–1256.

Ramos-Alonso, L., Romero, A. M., Polaina, J., Puig, S., & Martínez-Pastor, M. T. (2019). Dissecting mRNA decay and translation inhibition during iron deficiency. *Current Genetics*, *65*, 139–145.

Ranu, R. S., & London, I. M. (1976). Regulation of protein synthesis in rabbit reticulocyte lysates: Purification and initial characterization of the cyclic 3':5'-AMP independent protein kinase of the heme regulated translational inhibitor. *Proceedings of the National Academy of Sciences*, *73*, 4349–4353.

Reinders, J., Zahedi, P., Pfanner, N., Meisinger, C., & Sickmann, A. (2006). Toward the complete yeast mitochondrial proteome: multidimensional separation techniques for mitochondrial proteomics. *Journal of Proteome Research*, *5*, 1543–1554.

Richardson, D. R., Kalinowski, D. S., Lau, S., Jansson, P. J., & Lovejoy, D. B. (2009). Cancer cell iron metabolism and the development of potent iron chelators as anti-tumour agents. *BBA - General Subjects*, *1790*, 702–717.

Rietzschel, N., Pierik, A. J., Bill, E., Lill, R., & Mühlenhoff, U. (2015). The basic leucine zipper stress response regulator Yap5 senses high-iron conditions by coordination of [2Fe-2S] clusters. *Molecular and Cellular Biology*, *35*, 370–378.

Rigby, W. F. C., Roy, K., Collins, J., Rigby, S., Connolly, J. E., Bloch, D. B., & Brooks, S. A. (2005). Structure/function analysis of Tristetraprolin (TTP): p38 stress-activated protein kinase and lipopolysaccharide stimulation do not alter TTP function. *The Journal of Immunology*, *174*, 7883–7893.

Rolfes, R. J., & Hinnebusch, A. G. (1993). Translation of the yeast transcriptional activator *GCN4* is stimulated by purine limitation: implications for activation of the protein kinase GCN2. *Molecular and Cellular Biology*, *13*, 5099–5111.

Romero, A. M. (2018). Tesis doctoral: Identificación y caracterización de nuevos procesos implicados en la respuesta a deficiencia de hierro en *Saccharomyces cerevisiae*. Universitat de València.

Romero, A. M., Jordá, T., Rozès, N., Martínez-Pastor, M. T., & Puig, S. (2018a). Regulation of yeast fatty acid desaturase in response to iron deficiency. *Biochimica et Biophysica Acta - Molecular and Cell Biology of Lipids*, *1863*, 657–668.

Romero, A. M., Martínez-Pastor, M., Du, G., Solé, C., Carlos, M., Vergara, S. V, Sanvisens, N., Wohlschlegel, J. A., Toczyski, D. P., Posas, F., de Nadal, E., Martínez-Pastor, M. T., Thiele, D. J., & Puig, S. (2018b). Phosphorylation and proteasome recognition of the mRNA-binding protein Cth2 facilitates yeast adaptation to iron deficiency. *MBio*, *9*, e01694-18.

Romero, A. M., Ramos-Alonso, L., Montellá-Manuel, S., García-Martínez, J., de la Torre-Ruiz, M. Á., Pérez-Ortín, J. E., Martínez-Pastor, M. T., & Puig, S. (2019). A genome-wide transcriptional study reveals that iron deficiency inhibits the yeast TORC1 pathway. *Biochimica et Biophysica Acta - Gene Regulatory Mechanisms*, *1862*, 194414.

Romero, A. M., Ramos-Alonso, L., Alepuz, P., Puig, S., & Martínez-Pastor, M. T. (2020). Global translational repression induced by iron deficiency in yeast depends on the Gcn2/eIF2α pathway. *Scientific Reports*, *10*, 233.

Ros-Carrero, C., Ramos-Alonso, L., Romero, A. M., Bañó, M. C., Martínez-Pastor, M. T., & Puig, S. (2020). The yeast Aft1 transcription factor activates ribonucleotide reductase catalytic subunit *RNR1* in response to iron deficiency. *BBA - Gene Regulatory Mechanisms*, *1863*, 194522.

Roy, B., & Jacobson, A. (2013). The intimate relationships of mRNA decay and translation. *Trends in Genetics*, *29*, 691–699.

Rutherford, J. C., Jaron, S., Ray, E., Brown, P. O., & Winge, D. R. (2001). A second iron-regulatory system in yeast independent of Aft1p. *Proceedings of the National Academy of Sciences*, *98*, 14322–14327.

Rutherford, J. C., Jaron, S., & Winge, D. R. (2003). Aft1p and Aft2p mediate iron-responsive gene expression in yeast through related promoter elements. *Journal of Biological Chemistry*, *278*, 27636–27643.

Rutherford, J. C., Ojeda, L., Balk, J., Mühlenhoff, U., Lill, R., & Winge, D. R. (2005). Activation of the iron regulon by the yeast Aft1/Aft2 transcription factors depends on mitochondrial but not cytosolic iron-sulfur protein biogenesis. *Journal of Biological Chemistry*, *280*, 10135–10140.

Salahudeen, A. A., Thompson, J. W., Ruiz, J. C., Ma, H. W., Kinch, L. N., Li, Q., Grishin, N. V., & Bruick, R. K. (2009). An E3 ligase possessing an iron-responsive hemerythrin domain is a regulator of iron homeostasis. *Science*, *326*, 722–726.

Sánchez, E., Lobo, T., Fox, J. L., Zeviani, M., Winge, D. R., & Fernández-Vizarra, E. (2013). LYRM7 / MZM1L is a UQCRFS1 chaperone involved in the last steps of mitochondrial Complex III assembly in human cells. *BBA - Bioenergetics*, *1827*, 285–293.

Sanvisens, N., & Puig, S. (2011). Causes and consequences of nutritional iron deficiency in living organisms. *Edited by Merkin TC: Nova Science Publishers*, 245–276.

Sanvisens, N., Bañó, M. C., Huang, M., & Puig, S. (2011). Regulation of ribonucleotide reductase in response to iron deficiency. *Molecular Cell*, *44*, 759–769.

Sanvisens, N., de Llanos, R., & Puig, S. (2013). Function and regulation of yeast ribonucleotide reductase: cell cycle, genotoxic stress, and iron bioavailability. *Biomedical Journal*, *36*, 51–58.

Sanvisens, N., Romero, A. M., An, X., Zhang, C., de Llanos, R., Martínez-Pastor, M. T., Bañó, M. C., Huang, M., & Puig, S. (2014). Yeast Dun1 kinase regulates ribonucleotide reductase inhibitor Sml1 in response to iron deficiency. *Molecular and Cellular Biology*, *34*, 3259–3271.

Sanvisens, N., Romero, A. M., Zhang, C., Wu, X., An, X., Huang, M., & Puig, S. (2016). Yeast Dun1 kinase regulates ribonucleotide reductase small subunit localization in response to iron deficiency. *The Journal of Biological Chemistry*, *291*, 9807–9817.

Sato, T., Chang, H.-C., Bayeva, M., Shapiro, J. S., Ramos-Alonso, L., Kouzu, H., Jiang, X., Liu, T., Yar, S., Sawicki, K. T., Chen, C., Martínez-Pastor, M. T., Stumpo, D. J., Schumacker, P. T., Blackshear, P. J., Ben-Sahra, I., Puig, S., & Ardehali, H. (2018). mRNA-binding protein tristetraprolin is essential for cardiac response to iron deficiency by regulating mitochondrial function. *Proceedings of the National Academy of Sciences*, *115*, E6291–E6300.

Seraphin, B., Simon, M., Boulet, A., & Faye, G. (1989). Mitochondrial splicing requires a protein from a novel helicase family. *Nature*, *337*, 84–87.

Shakoury-Elizeh, M., Tiedeman, J., Rashford, J., Ferea, T., Demeter, J., Garcia, E., Rolfes, R., Brown, P. O., Botstein, D., & Philpott, C. C. (2004). Transcriptional remodeling in response to iron deprivation in *Saccharomyces cerevisiae*. *Molecular Biology of the Cell*, *15*, 1233–1243.

Shakoury-Elizeh, M., Protchenko, O., Berger, A., Cox, J., Gable, K., Dunn, T. M., Prinz, W. A., Bard, M., & Philpott, C. C. (2010). Metabolic response to iron deficiency in *Saccharomyces cerevisiae*. *The Journal of Biological Chemistry*, *285*, 14823–14833.

Sharma, V. M., Li, B., & Reese, J. C. (2003). SWI/SNF-dependent chromatin remodeling of *RNR3* requires TAF_{II}s and the general transcription machinery. *Genes and Development*, *17*, 502–515.

Sharma, V. M., Tomar, R. S., Dempsey, A. E., & Reese, J. C. (2007). Histone deacetylases RPD3 and HOS2 regulate the transcriptional activation of DNA damage-inducible genes. *Molecular and Cellular Biology*, *27*, 3199–3210.

Shaw, G., & Kamen, R. (1986). A conserved AU sequence from the 3' untranslated region of GM-CSF mRNA mediates selective mRNA degradation. *Cell*, *46*, 659–668.

Shenton, D., Smirnova, J. B., Selley, J. N., Carroll, K., Hubbard, S. J., Pavitt, G. D., Ashe, M. P., & Grant, C. M. (2006). Global translational responses to oxidative stress

impact upon multiple levels of protein synthesis. *The Journal of Biological Chemistry*, *281*, 29011–29021.

Shi, Y., Vattem, K. M., Sood, R., An, J. I. E., Liang, J., Stramm, L., & Wek, R. C. (1998). Identification and characterization of pancreatic eukaryotic initiation factor 2 α-subunit kinase, PEK, involved in translational control. *Molecular and Cellular Biology*, *18*, 7499–7509.

Sickmann, A., Reinders, J., Wagner, Y., Joppich, C., Zahedi, R., Meyer, H. E., Schonfisch, B., Perschil, I., Chacinska, A., Guiard, B., Rehling, P., Pfanner, N., & Meisinger, C. (2003). The proteome of *Saccharomyces cerevisiae* mitochondria. *Proceedings of the National Academy of Sciences*, *100*, 13207–13212.

Sikorski, R. S., & Hieter, P. (1989). A system of shuttle vectors and yeast host strains designed for efficient manipulation of DNA in *Saccharomyces cerevisiae*. *Genetics*, *122*, 19–27.

Simon, M., & Faye, G. (1984). Steps in processing of the mitochondrial cytochrome oxidase subunit I pre-mRNA affected by a nuclear mutation in yeast. *Proceedings of the National Academy of Sciences*, *81*, 8–12.

Sipos, K., Lange, H., Fekete, Z., Ullmann, P., Lill, R., & Kispal, G. (2002). Maturation of cytosolic iron-sulfur proteins requires glutathione. *Journal of Biological Chemistry*, *277*, 26944–26949.

Sonenberg, N., & Hinnebusch, A. G. (2009). Regulation of translation initiation in eukaryotes: mechanisms and biological targets. *Cell*, *136*, 731–745.

Sood, R., Porter, A. C., Olsen, D., Cavener, D. R., & Wek, R. C. (2000). A mammalian homologue of GCN2 protein kinase important for translational control by phosphorylation of eukaryotic initiation factor-2α. *Genetics*, *154*, 787–801.

Soto, I. C., & Barrientos, A. (2016). Mitochondrial cytochrome *c* oxidase biogenesis is regulated by the redox state of a heme-binding translational activator. *Antioxidants & Redox Signaling*, *24*, 281–298.

Soto, I. C., Fontanesi, F., Myers, R. S., Hamel, P., & Barrientos, A. (2012). A heme-sensing mechanism in the translational regulation of mitochondrial cytochrome *c* oxidase biogenesis. *Cell Metabolism*, *16*, 801–813.

Spriggs, K. A., Stoneley, M., Bushell, M., & Willis, A. E. (2008). Re-programming of translation following cell stress allows IRES-mediated translation to predominate. *Biology of the Cell*, *100*, 27–38.

Srinivasan, V., Pierik, A. J., & Lill, R. (2014). Crystal structures of nucleotide-free and glutathione-bound mitochondrial ABC transporter Atm1. *Science*, *343*, 1137–1140.

Stehling, O., Vashisht, A. A., Mascarenhas, J., Jonsson, Z. O., Sharma, T., Netz, D. J. A., Pierik, A. J., Wohlschlegel, J. A., & Lill, R. (2012). MMS19 assembles iron-sulfur proteins required for DNA metabolism and genomic integrity. *Science*, *337*, 195–200.

Stehling, O., Wilbrecht, C., & Lill, R. (2014). Mitochondrial iron-sulfur protein biogenesis and human disease. *Biochimie*, *100*, 61–77.

Sweet, T., Kovalak, C., & Coller, J. (2012). The dead-box protein Dhh1 promotes decapping by slowing ribosome movement. *PLoS Biology*, *10*, e1001342.

Tan, F. E., & Elowitz, M. B. (2014). Brf1 posttranscriptionally regulates pluripotency and differentiation responses downstream of Erk MAP kinase. *Proceedings of the National Academy of Sciences*, *111*, E1740–E1748.

Taylor, G. A., Carballo, E., Lee, D. M., Lai, W. S., Thompson, M. J., Patel, D. D., Schenkman, D. I., Gilkeson, G. S., Broxmeyer, H. E., Haynes, B. F., & Blackshear, P. J. (1996). A pathogenetic role for TNFα in the syndrome of cachexia, arthritis, and autoimmunity resulting from Tristetraprolin (TTP) deficiency. *Immunity*, *4*, 445–454.

Tchen, C. R., Brook, M., Saklatvala, J., & Clark, A. R. (2004). The stability of tristetraprolin mRNA is regulated by mitogen-activated protein kinase p38 and by tristetraprolin itself. *Journal of Biological Chemistry*, *279*, 32393–32400.

Thompson, J. W., Salahudeen, A. A., Chollangi, S., Ruiz, J. C., Brautigam, C. A., Makris, T. M., Lipscomb, J. D., Tomchick, D. R., & Bruick, R. K. (2012). Structural and molecular characterization of iron-sensing hemerythrin-like domain within F-box and leucine-rich repeat protein 5 (FBXL5). *The Journal of Biological Chemistry*, *287*, 7357–7365.

Tiedje, C., Ronkina, N., Tehrani, M., Dhamija, S., Laass, K., Holtmann, H., Kotlyarov, A., & Gaestel, M. (2012). The p38/MK2-driven exchange between tristetraprolin and HuR regulates AU-Rich Element-dependent translation. *PLoS Genetics*, *8*, e1002977.

Tomar, R. S., Zheng, S., Brunke-Reese, D., Wolcott, H. N., & Reese, J. C. (2008). Yeast Rap1 contributes to genomic integrity by activating DNA damage repair genes. *EMBO Journal*, *27*, 1575–1584.

Tomar, R. S., Psathas, J. N., Zhang, H., Zhang, Z., & Reese, J. C. (2009). A novel mechanism of antagonism between ATP-dependent chromatin remodeling complexes regulates *RNR3* expression. *Molecular and Cellular Biology*, *29*, 3255–3265.

Tzagoloff, A., Capitanio, N., Nobrega, M. P., & Gatti, D. (1990). Cytochrome oxidase assembly in yeast requires the product of *COX11*, a homolog of the *P. denitrificans* protein encoded by ORF3. *The EMBO Journal*, *9*, 2759–2764.

Ueta, R., Fukunaka, A., & Yamaguchi-iwai, Y. (2003). Pse1p mediates the nuclear import of the iron-responsive transcription factor Aft1p in *Saccharomyces cerevisiae*. *The Journal of Biological Chemistry*, *278*, 50120–50127.

Ueta, R., Fujiwara, N., Iwai, K., & Yamaguchi-iwai, Y. (2007). Mechanism underlying the iron-dependent nuclear export of the iron-responsive transcription factor Aft1p in *Saccharomyces cerevisiae*. *Molecular Biology of the Cell*, *18*, 2980–2990.

Ueta, R., Fujiwara, N., Iwai, K., & Yamaguchi-Iwai, Y. (2012). Iron-induced dissociation of the Aft1p transcriptional regulator from target gene promoters is an initial event in iron-dependent gene suppression. *Molecular and Cellular Biology*, *32*, 4998–5008.

Valenzuela, L., Aranda, C., & González, A. (2001). TOR modulates *GCN4*-dependent expression of genes turned on by nitrogen limitation. *Journal of Bacteriology*, *183*, 2331–2334.

Vashisht, A. A., Zumbrennen, K. B., Huang, X., Powers, D. N., Durazo, A., Sun, D., Bhaskaran, N., Persson, A., Uhlen, M., Sangfeit, O., Spruck, C., Leibold, E. A., & Wohlschlegel, J. A. (2009). Control of iron homeostasis by an iron-regulated ubiquitin ligase. *Science*, *326*, 718–721.

Vergara, S. V., Puig, S., & Thiele, D. J. (2011). Early recruitment of AU-Rich Element-containing mRNAs determines their cytosolic fate during iron deficiency. *Molecular and Cellular Biology*, *31*, 417–429.

Wach, A., Brachat, A., Alberti-Segui, C., Rebischung, C., & Philippsen, P. (1997). Heterologous *HIS3* marker and GFP reporter modules for PCR-targeting in *Saccharomyces cerevisiae*. *Yeast*, *13*, 1065–1075.

Warringer, J., Hult, M., Regot, S., Posas, F., & Sunnerhagen, P. (2010). The HOG pathway dictates the short-term translational response after hyperosmotic shock. *Molecular Biology of the Cell*, *21*, 3080–3092.

Watson, A. D., Edmondson, D. G., Bone, J. R., Mukai, Y., Yu, Y., Du, W., Stillman, D. J., & Roth, S. Y. (2000). Ssn6–Tup1 interacts with class I histone deacetylases required for repression. *Genes & Development*, *14*, 2737–2744.

Wei, T., Zhang, C., Xu, X., Hanna, M., Zhang, X., Wang, Y., Dai, H., & Xiao, W. (2013). Construction and evaluation of two biosensors based on yeast transcriptional response to genotoxic chemicals. *Biosensors and Bioelectronics*, *44*, 138–145.

Weider, M., Machnik, A., Klebl, F., & Sauer, N. (2006). Vhr1p, a new transcription factor from budding yeast, regulates biotin-dependent expression of *VHT1* and *BIO5*. *Journal of Biological Chemistry*, *281*, 13513–13524.

Wenzlau, J. M., Saldanha, R. J., Butow, R. A., & Perlman, P. S. (1989). A latent intron-encoded maturase is also an endonuclease needed for intron mobility. *Cell*, *56*, 421–430.

Yamaguchi-Iwai, Y., Dancis, A., & Klausner, R. D. (1995). AFT1: a mediator of iron regulated transcriptional control in *Saccharomyces cerevisiae*. *The EMBO Journal*, *14*, 1231–1239.

Yamaguchi-Iwai, Y., Stearman, R., Dancis, A., & Klausner, R. D. (1996). Iron-regulated DNA binding by the AFT1 protein controls the iron regulon in yeast. *The EMBO Journal*, *15*, 3377–3384.

Yamaguchi-Iwai, Y., Ueta, R., Fukunaka, A., & Sasaki, R. (2002). Subcellular localization of Aft1 transcription factor responds to iron status in *Saccharomyces cerevisiae*. *Journal of Biological Chemistry*, *277*, 18914–18918.

Yamamoto, Y., & Izawa, S. (2013). Adaptive response in stress granule formation and bulk translational repression upon a combined stress of mild heat shock and mild ethanol stress in yeast. *Genes to Cells*, *18*, 974–984.

Yan, G., Shen, X., & Jiang, Y. (2006). Rapamycin activates Tap42-associated phosphatases by abrogating their association with Tor complex 1. *EMBO Journal*, *25*, 3546–3555.

Yang, R., Wek, S. A., & Wek, R. C. (2000). Glucose limitation induces *GCN4* translation by activation of Gcn2 protein kinase. *Molecular and Cellular Biology*, *20*, 2706–2717.

Yang, J., Yan, R., Roy, A., Xu, D., Poisson, J., & Zhang, Y. (2015). The I-TASSER suite: protein structure and function prediction. *Nature Methods*, *12*, 7–8.

Yao, R., Zhang, Z., An, X., Bucci, B., Perlstein, D. L., Stubbe, J., & Huang, M. (2003). Subcellular localization of yeast ribonucleotide reductase regulated by the DNA replication and damage checkpoint pathways. *Proceedings of the National Academy of Sciences*, *100*, 6628–6633.

Yarunin, A., Panse, V. G., Petfalski, E., Dez, C., Tollervey, D., & Hurt, E. C. (2005). Functional link between ribosome formation and biogenesis of iron-sulfur proteins. *EMBO Journal*, *24*, 580–588.

Yoboue, E. D., Augier, E., Galinier, A., Blancard, C., Pinson, B., Casteilla, L., Rigoulet, M., & Devin, A. (2012). cAMP-induced mitochondrial compartment biogenesis: role of glutathione redox state. *Journal of Biological Chemistry*, *287*, 14569–14578.

Zhang, L., & Guarente, L. (1995). Heme binds to a short sequence that serves a regulatory function in diverse proteins. *The EMBO Journal*, *14*, 313–320.

Zhang, L., & Hach, A. (1999). Molecular mechanism of heme signaling in yeast: the transcriptional activator Hap1 serves as the key mediator. *Cell Mol. Life Sci.*, *56*, 415–426.

Zhang, Z., & Reese, J. C. (2004a). Redundant mechanisms are used by Ssn6-Tup1 in repressing chromosomal gene transcription in *Saccharomyces cerevisiae*. *Journal of Biological Chemistry*, *279*, 39240–39250.

Zhang, Z., & Reese, J. C. (2004b). Ssn6-Tup1 requires the ISW2 complex to position nucleosomes in *Saccharomyces cerevisiae*. *EMBO Journal*, *23*, 2246–2257.

Zhang, Z., & Reese, J. C. (2005). Molecular genetic analysis of the yeast repressor Rfx1/Crt1 reveals a novel two-step regulatory mechanism. *Molecular and Cellular Biology*, *25*, 7399–7411.

Zhang, H., & Reese, J. C. (2007). Exposing the core promoter is sufficient to activate transcription and alter coactivator requirement at *RNR3*. *Proceedings of the National Academy of Sciences*, *104*, 8833–8838.

Zhang, H., Kruk, J. A., & Reese, J. C. (2008). Dissection of coactivator requirement at *RNR3* reveals unexpected contributions from TFIID and SAGA. *Journal of Biological Chemistry*, *283*, 27360–27368.

Zhang, Y., Liu, L., Wu, X., An, X., Stubbe, J., & Huang, M. (2011). Investigation of *in vivo* diferric tyrosyl radical formation in *Saccharomyces cerevisiae* Rnr2 protein. *The Journal of Biological Chemistry*, *286*, 41499–41509.

Zhang, Y., Li, H., Zhang, C., An, X., Liu, L., Stubbe, J., & Huang, M. (2014). Conserved electron donor complex Dre2–Tah18 is required for ribonucleotide reductase metallocofactor assembly and DNA synthesis. *Proceedings of the National Academy of Sciences*, *111*, E1695–E1704.

Zhang, T., Bu, P., Zeng, J., & Vancura, A. (2017). Increased heme synthesis in yeast induces a metabolic switch from fermentation to respiration even under conditions of glucose repression. *Journal of Biological Chemistry*, *292*, 16942–16954.

Zhang, X., Zhang, D., Sun, W., & Wang, T. (2019a). The adaptive mechanism of plants to iron deficiency via iron uptake, transport, and homeostasis. *International Journal of Molecular Sciences*, *20*, 2424.

Zhang, S., Macias-Garcia, A., Ulirsch, J. C., Velazquez, J., Butty, V. L., Levine, S. S., Sankaran, V. G., & Chen, J. J. (2019b). HRI coordinates translation necessary for protein homeostasis and mitochondrial function in erythropoiesis. *ELife*, *8*, e46976.

Zwietering, M. H., Jongenburger, I., Rombouts, F. M., & Van't Riet, K. (1990). Modeling of the bacterial growth curve. *Applied and Environmental Microbiology*, *56*, 1875–1881.